

Departamento de Inmunología, Microbiología y Parasitología
Immunologia, Mikrobiologia eta Parasitologia Saila
Department of Immunology, Microbiology and Parasitology

PhD thesis

Study of the *Aspergillus fumigatus* host-
pathogen interaction using
transcriptomic techniques and mutant
strains generation

Xabier Guruceaga Sierra

Leioa, February 2021

Supervisors

Dr. Aitor Rementeria Ruiz

Dr. Andoni Ramirez Garcia

CONTRIBUCIONES CIENTÍFICAS

Los resultados que se presentan en esta Tesis Doctoral han sido presentados a la comunidad científica de diferentes maneras durante el periodo de realización de la misma. Se han publicado 3 artículos en revistas indexadas (un artículo original y dos artículos de revisión) y se ha especificado las siete comunicaciones a congresos internacionales de las más de treinta comunicaciones a congresos tanto nacionales como internacionales presentadas durante el periodo de la tesis.

Publicaciones

Perez-Cuesta U., Aparicio-Fernandez L., Guruceaga X., Martin-Souto L., Abad-Diaz-de-Cerio A., Antoran A., Buldain I., Hernando F. L., Ramirez-Garcia A., & Rementeria A. (2020). **Melanin and pyomelanin in *Aspergillus fumigatus*: from its genetics to host interaction.** *International Microbiology*, 23, 55–63. <https://doi.org/10.1007/s10123-019-00078-0>

Guruceaga X., Perez-Cuesta U., De Cerio A. A. D., Gonzalez O., Alonso R. M., Hernando F. L., Ramirez-Garcia A & Rementeria A. (2020). **Fumagillin, a mycotoxin of *Aspergillus fumigatus*: biosynthesis, biological activities, detection, and applications.** *Toxins*, 12(7), 1–26. <https://doi.org/10.3390/toxins12010007>

Guruceaga X., Ezpeleta G., Mayayo E., Sueiro-Olivares M., Abad-Diaz-De-Cerio A., Urizar J. M. A., Liu H. G., Wiemann P., Bok J. W., Filler S. G., Keller N. P., Hernando F. L., Ramirez-Garcia A., & Rementeria A. (2018). **A possible role for fumagillin in cellular damage during host infection by *Aspergillus fumigatus*.** *Virulence*, 9(1), 1548–1561. <https://doi.org/10.1080/21505594.2018.1526528>

Congresos

Guruceaga X., Ezpeleta G., Arbizu-Delgado A., Abad-Diaz de Cerio A., Mayayo E., Liu H., Wiemann P., Filler S.G., Keller N.P., Hernando F.L., Ramirez-Garcia A., Rementeria A. ***Aspergillus fumigatus* fumagillin as possible virulence factor.** 20th Congress of the International Society for Human and Animal Mycology (ISHAM). Ámsterdam (Países Bajos). 2018. Oral

X. Guruceaga, U. Perez-Cuesta, A. Pellon, B. Uribe, O. Gonzalez, N. P. Keller, F.L. Hernando, J. Anguita, R.M. Alonso, A. Ramirez-Garcia & A. Rementeria. **The role of *Aspergillus fumigatus* fumagillin in fungal virulence.** 9th Trends in Medical Mycology (TIMM). Niza (Francia). 2019. Poster

X. Guruceaga, U. Perez-Cuesta, A. Martin-Vicente, A.C.O. Souza, A.V. Nywening, Q. Al Abdallah, W. Ge, F.L. Hernando, J. Fortwendel, A. Ramirez-Garcia & A. Rementeria. **Phenotypic characterization of *Aspergillus fumigatus* *maiA* deficient strain.** 9th Trends in Medical Mycology (TIMM). Niza (Francia). 2019. Poster

Guruceaga X., Ezpeleta G., Arbizu-Delgado A., Abad-Diaz de Cerio A., Hernando F.L., Ramirez-Garcia A. & Rementeria A. **Whole genome transcriptomic analysis of *Aspergillus fumigatus* during the co-incubation with the murine macrophages cell line RAW 264.7.** 8th Advances Against Aspergillosis (AAA). Lisboa (Portugal). 2018. Poster

Guruceaga X., Ezpeleta G., Etxenagusia S., Ramirez-Garcia A., Abad-Diaz de Cerio A., Aguirre J.M., Mayayo E., Hernando F.L. & Rementeria A. **Study of the alterations in gene expression during an *Aspergillus fumigatus* murine intranasal infection from a transcriptomic point of view.** 8th Trends in Medical Mycology (TIMM). Belgrado (Serbia). Poster

Guruceaga X., Ezpeleta G., Arbizu-Delgado A., Ramirez-Garcia A., Hernando F.L., & Rementeria A. **Transcriptomic study during the *in vitro* contact between *Aspergillus fumigatus* and the human pulmonary epithelial cell line (A549).** 8th Trends in Medical Mycology (TIMM). Belgrado (Serbia). Poster

Guruceaga X., Ezpeleta G., Etxenagusia S., Balmaseda-Rubina A., Fernandez-Molina J., Sueiro-Olivares M., Ramirez-Garcia A., Abad-Diaz de Cerio A., Garaizar J., Hernando F.L. & Rementeria A. **Effect of microarray expression data normalization for the choice of differentially expressed genes of *Aspergillus fumigatus* during an intranasal infection.** 7th Trends in Medical Mycology (TIMM). Lisboa (Portugal). Poster

Contenido

Introducción.....	- 13 -
1.1 El género <i>Aspergillus</i>	- 13 -
1.2 <i>Aspergillus fumigatus</i>	- 15 -
1.2.1 Biología y ecología	- 15 -
1.2.2 Conidios de <i>A. fumigatus</i>	- 17 -
1.2.3 Germinación de los conidios de <i>A. fumigatus</i>	- 18 -
1.2.4 Biopelículas de <i>A. fumigatus</i>	- 19 -
1.3 La infección fúngica invasiva	- 21 -
1.3.1 Contexto epidemiológico general	- 21 -
1.3.2 Aspergilosis.....	- 22 -
1.3.3 Aspergiloma.....	- 23 -
1.3.4 Aspergilosis broncopulmonar alérgica	- 24 -
1.3.5 Aspergilosis invasiva	- 24 -
1.4 Factores de virulencia de <i>Aspergillus fumigatus</i>	- 29 -
1.4.1 Termotolerancia	- 30 -
1.4.2 Pared celular.....	- 31 -
1.4.3 Mecanismos de evasión a la respuesta inmunológica	- 32 -
1.4.4 Melanina.....	- 34 -
1.4.5 Toxinas.....	- 37 -
1.5 Estudio de los factores de virulencia.....	- 47 -
1.5.1 Estudios transcriptómicos	- 47 -
1.5.2 Generación de cepas mutantes de <i>A. fumigatus</i>	- 51 -
1.5.3 Método clásico	- 51 -
1.5.4 Generación de cepas mutantes utilizando el sistema CRISPR-Cas	- 52 -
Objetivo / Aim of the study	- 59 -
Resultados / Results	- 63 -

Chapter 1: A possible role for fumagillin in cellular damage during host infection by *Aspergillus fumigatus*

1. Introduction	67 -
2. Material & Methods	68 -
2.1 <i>Aspergillus fumigatus</i> strains, media and growth conditions.....	68 -
2.2 Obtention of the complemented strain $\Delta fmaA::fmaA$	68 -
2.3 Animal infection.....	70 -
2.4 Histological study.....	71 -
2.5 RNA isolation	71 -
2.6 Microarray selection and hybridization	71 -
2.7 Microarray expression data analysis.....	72 -
2.8 Gene ontology analysis	72 -
2.9 Microarray data confirmation by reverse transcription quantitative PCR ...	72 -
2.10 ⁵¹ Cr release cytotoxic assay	73 -
2.11 Fumagillin detection.....	73 -
3. Results	74 -
3.1 Survival of animals after <i>Aspergillus</i> infection, selection of doses and progression of fungal burden in the lung.....	74 -
3.2 Genes differentially expressed during the progression of lung infection after intranasal exposure to <i>A. fumigatus</i> conidia.....	76 -
3.3 RT-qPCR verification of microarray data.	81 -
3.4 Fumagillin production is associated with cytotoxicity in an <i>in vitro</i> infection model of a pneumocyte cell line.	83 -
4 Discussion	85 -
5. Supplementary material	92 -

Chapter 2: Fumagillin as new virulence factor of the pathogenic mold *Aspergillus fumigatus*

1. Introduction	107 -
2. Material & Methods	108 -
2.1 <i>Aspergillus fumigatus</i> strains, media and growth conditions.....	108 -
2.2 <i>Aspergillus fumigatus</i> phenotypic characterization	109 -
2.3 Determination of fumagillin by UHPLC in RPMI samples	110 -
2.4 Cell lines.....	111 -
2.5 Isolation and culture of BMMs	111 -
2.6 <i>Aspergillus fumigatus</i> fumagillin secretion ability.....	111 -
2.7 Cell lines fumagillin absorption ability.....	112 -
2.8 Cellular electron transport chain activity	112 -
2.9 Wound healing assay.....	113 -
2.10 Flow cytometry assays.....	113 -
2.11 Phagocytosis assay and fungal behavior	114 -
2.12 Animal infection	115 -
2.13 Statistics.....	116 -
2.14 Ethical issues.....	116 -
3. Results	117 -
3.1 Characterization of <i>A. fumigatus</i> strains: phenotype and ability to produce fumagillin	117 -
3.2 Different fumagillin absorption ability in cell lines.....	117 -
3.3 Fumagillin promotes a decrease in cellular activity and a delay in proliferation in lung epithelial cells	120 -
3.4 Fumagillin reduces cellular activity and viability of macrophages.	122 -

3.5 The inability to produce fumagillin affects <i>A. fumigatus</i> germination and phagocytosis.....	- 124 -
3.6 The capacity to produce fumagillin increase mortality rate and fungal load in a mouse model of invasive aspergillosis	- 127 -
4. Discussion	- 130 -

Chapter 3: Association between *A. fumigatus maiA* gene, cell wall and virulence

1. Introduction	- 137 -
2. Matherial & Methods	- 139 -
2.1 <i>Aspergillus fumigatus</i> strains, media and growth conditions.....	- 139 -
2.2 Cell lines.....	- 139 -
2.3 Phagocytosis assays and fungal behavior against RAW 264.7 cell line	- 139 -
2.4 Endocytosis assays and fungal behavior against A549 cell line.....	- 139 -
2.5 RAW 264.7 ability to produced ROS and RNS against <i>A. fumigatus</i>	- 140 -
2.6 Cellular electron transport chain activity	- 141 -
2.7 RNA isolation	- 141 -
2.8 Microarray selection and hybridization.....	- 142 -
2.9 Microarray expression data analysis	- 142 -
2.10 Microarray data confirmation by RT-qPCR.....	- 142 -
2.11 Gene ontology analysis.....	- 142 -
2.12 Gene target selection criteria.....	- 142 -
2.13 Generation of the $\Delta maiA$ mutant strain using CRISPR-Cas technology....	- 143 -
2.14 Mutant strains PCR confirmation	- 145 -
2.15 Determination of the pyomelanin production	- 145 -
2.16 Fungal susceptibility to H ₂ O ₂ oxidative agent.....	- 146 -

2.17 Quantification of cell wall glucan content.....	- 146 -
2.18 <i>A. fumigatus</i> stress response: spotting assay and radial growth.	- 147 -
2.19 Scanning electron microscopy	- 148 -
2.20 Murine model of invasive pulmonary aspergillosis.....	- 148 -
3. Results	- 150 -
3.1 Different <i>A. fumigatus</i> behaviour against macrophages and lung epithelial cell lines	- 150 -
3.1.1 Study of co-incubation between <i>A. fumigatus</i> and macrophages	- 150 -
3.1.2 Study of co-incubation between <i>A. fumigatus</i> and epithelial cells	- 151 -
3.2 <i>A. fumigatus</i> gene expression in response to the co-incubation with RAW 264.7 macrophages or A549 epithelial cell line	- 152 -
3.3 Go enrichment analysis of the most up/down-regulated DEGs and comparison between different infection models.....	- 155 -
3.4 Δ <i>maiA</i> disruption mutant strain genetic manipulation strategy.....	- 158 -
3.5 The <i>maiA</i> gene is essential for Phe/Tyr degradation pathway.....	- 158 -
3.6 The <i>maiA</i> gene affects germination, cell-wall composition and cellular homeostasis in <i>A. fumigatus</i>	- 160 -
3.7 The Δ <i>maiA</i> hyphae present an unstructured morphology.....	- 162 -
3.8 The <i>maiA</i> gene has a direct impact in the virulence of <i>A. fumigatus</i>	- 163 -
4. Discussion	- 166 -
5. Supplementary material	- 175 -
Discusión general	- 195 -
Conclusiones / Conclusions.....	- 211 -
Referencias / Reference.....	- 217 -

Introducción



1. Introducción

1.1 El género *Aspergillus*

En 1729 el biólogo italiano Pier Antonio Micheli, autor de la obra "*Nova Plantarum Genera*", que supuso el inicio de la micología como ciencia, describió por primera vez el género *Aspergillus*. Su nombre le fue asignado por la similitud que la estructura del conidióforo del hongo guardaba con el "*Aspergillum*", conocido en castellano como aspersorio, que es un útil utilizado en ciertos momentos de la liturgia cristiana para dispersar agua bendita. Sin embargo, no fue hasta mediados del siglo XIX cuando se describió este género fúngico como patógeno y por tanto capaz de causar infecciones tanto en humanos como en animales (Kenneth, Dorothy and Fennell, 1965).

Actualmente, el género *Aspergillus* se clasifica dentro de la división *Ascomycota*, clase *Eurotiomycetes*, orden *Eurotiales*, familia *Trichocomaceae*. Este género está compuesto por más de 300 especies (Samson *et al.*, 2014; Vidal-Acuña *et al.*, 2018) y, utilizando caracteres tanto macro como microscópicos, inicialmente se clasificó en subgéneros y secciones (Kenneth, Dorothy and Fennell, 1965). De hecho, no se otorgó ninguna nomenclatura concreta hasta que en 1985 Gams y colaboradores (Gams *et al.*, 1985) siguiendo las directrices del "*International Code of Botanical Nomenclature*" (ICBN) asignaron nombre a esos subgéneros y secciones. A partir de este momento, la clasificación del género *Aspergillus* ha sido objeto de constantes modificaciones. En el año 2008, Peterson y colaboradores clasificaron las especies del género en 5 subgéneros y 16 secciones, entendiendo las secciones como grupos de especies estrechamente relacionados (Vidal-Acuña *et al.*, 2018). Posteriormente, en 2012 el género se volvió a reorganizar en 8 subgéneros y 18 secciones (Samson & Varga 2012) y en 2014 se propuso reducir a 4 el número de subgéneros (*Aspergillus*, *Circundati*, *Fumigati* y *Nidulantes*) y aumentar a 20 el número de secciones (Houbraken, de Vries and Samson, 2014; Hubka *et al.*, 2015). Actualmente, este género sigue en continua revisión a través de ensayos filogenéticos basados en estudios moleculares.

Lo que caracteriza a este género fúngico es que está compuesto de hongos filamentosos capaces de formar una estructura especializada llamada conidióforo, encargada de la generación de esporas o conidios implicados en la reproducción asexual. Estos conidióforos surgen como hifas erectas y aseptadas que surgen del micelio vegetativo (**Fig. 1**). En la zona apical, estas hifas se engrosan dando lugar a una vesícula sobre la que las fiálides (células conidiogénicas) emergen. Las fiálides se caracterizan por ser células con forma de matraz capaces de formar cadenas de conidios que se caracterizan por su alta hidrofobicidad y su pequeño tamaño. Además, cuando los conidios se acumulan en masas sobre las colonias pueden observarse pigmentaciones específicas de las especies que forman el género.

Finalmente hay que destacar que en muchas de las especies que conforman este género, entre la vesícula y las fiálides se encuentran otras células denominadas métulas. Cuando el conidióforo está formado tanto por métulas como por fiálides, este se denomina biseriado, mientras que cuando hay ausencia de métulas el conidióforo recibe el nombre de uniseriado (**Fig. 1**).

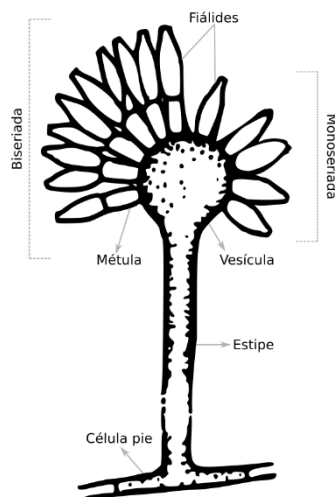


Figura 1. Diagrama de la estructura del conidióforo del género *Aspergillus* (modificado de Guarro *et al.*, 2010).

Cuando se habla de hongos filamentosos, el tipo de reproducción que estos llevan a cabo es un factor determinante para su clasificación. El género *Aspergillus* agrupa tanto a hongos que poseen reproducción asexual (anamorfos) como a hongos que

poseen reproducción sexual (teleomorfos). Históricamente, este género se ha considerado dentro de los deuteromicetes, también llamados hongos imperfectos, ya que únicamente se conocía la morfología de la fase anamorfa (Carlile et al., 2001). Sin embargo, en los últimos años se están comenzando a conocer las fases teleomorfas de diferentes especies consideradas anamorfias. Estos descubrimientos dificultan la nomenclatura de estos hongos, ya que, como ocurre con otros géneros fúngicos, a esas especies se les comenzaba a asignar dos nombres, uno para referirse a la forma anamorfa y otro para la teleomorfa, como ocurre por ejemplo con las dos especies más conocidas de este género *Emericella nidulans*/*Aspergillus nidulans* (teleomorfa/anamorfa) ó *Neosartorya fumigata*/*Aspergillus fumigatus* (teleomorfa/anamorfa). Esta forma dual de nomenclatura permitida por el ICBN, causaba confusión. Por ello, bajo la iniciativa “*One fungus = One name*”, comenzó a verse reflejada la necesidad de establecer un único nombre para cada especie de hongo, intentando desligar la terminología micológica del antiguo sistema ICBN (Taylor, 2011). Posteriormente, en el simposio “*One fungus = which name*” celebrado en Amsterdam (Holanda) en abril del 2012, se propuso en el caso de *Aspergillus*, el uso del nombre de la fase anamorfa para denominar a las especies pertenecientes a dicho género (Hawksworth et al., 2011).

1.2 *Aspergillus fumigatus*

1.2.1 Biología y ecología

Aspergillus fumigatus es una especie del género *Aspergillus* que se caracteriza por presentar un crecimiento filamentosos rápido y producir colonias de un color verde grisáceo característico. Este hongo haploide de reproducción asexual es un gran productor de conidios en forma de elipse. El conidióforo de *A. fumigatus* se caracteriza por ser uniseriado con una vesícula que tiene un diámetro variable de entre 10-26 µm y una célula pie de 6-10 µm de diámetro (Latgé, 1999; Samson et al., 2007; Latgé and Chamilos, 2019).

En 2009, Celine M. O’Gorman y colaboradores describieron por primera vez la fase teleomorfa de *A. fumigatus*, que como anteriormente se ha explicado, se denomina *N. fumigata*. Tal y como la describen en su publicación, se trata de una fase

heteroalélica (con dos alelos por cada locus) y presenta un cleistotecio o ascocarpo de un diámetro variable entre 150 y 480 μm rodeado de micelio. El ascocarpo

inicialmente es de un color blanco amarillento que con el tiempo se oscurece hacia un color grisáceo amarillento. En su interior presenta ocho ascosporas de forma esférica rodeadas de una cresta ecuatorial, que tienen un diámetro de 0.3-1 μm . Hay que destacar que *N. fumigata* tarda en desarrollar las estructuras anteriormente descritas seis meses en condiciones *in vitro*, mientras que la fase anamorfa (*A. fumigatus*) tarda en torno a 5-7 días en generar el conidióforo y las esporas asexuales (O'Gorman, Fuller and Dyer, 2009) (Fig. 2). Estos autores en una publicación reciente, trabajando con 131 cepas aisladas de muestras de suelo de los diferentes continentes, han demostrado que la capacidad de reproducción sexual de este hongo es universal y que no depende de la cepa utilizada (Swilaiman *et al.*, 2020).

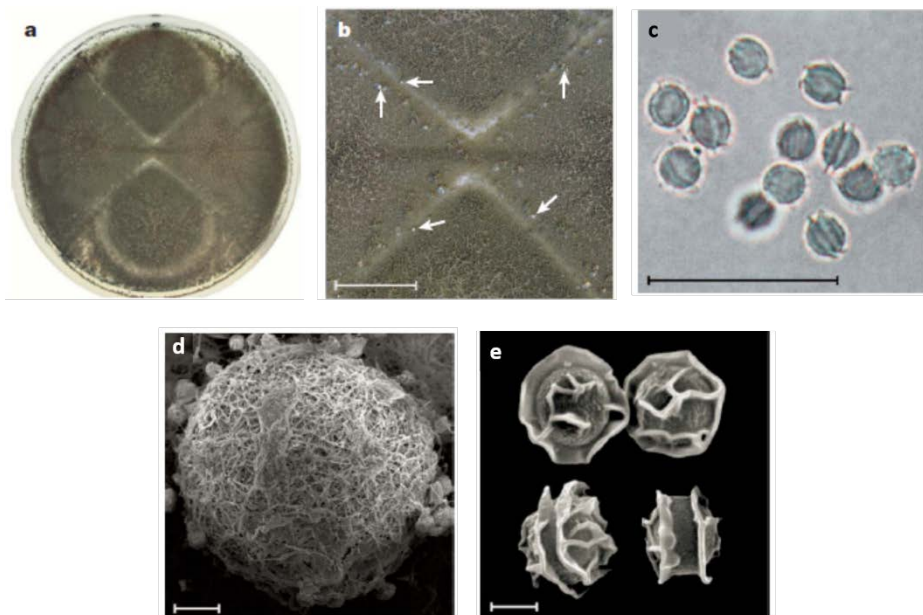


Figura 2. *Neosartorya fumigata* sp. nov. **A)** Cultivo en Agar avena incubado durante 6 meses a 30 °C, resultado de cruzar por pares los aislamientos de *A. fumigatus* AfRB2 x AfIR956. **B)** Cleistotecio (Flechas blancas) dispuestos a lo largo de las cruces de intersección de las colonias opuestas (escala 1 cm). **C)** Ascosporas observadas al microscopio óptico (escala 20 μm). **D)** Micrografía electrónica de barrido donde se muestra el cleistotecio junto con las hifas entrelazadas (escala 100 μm). **E)** Micrografía electrónica de barrido de las ascosporas de *N. fumigata* (escala 2 μm). (modificado de O'Gorman *et al.*, 2009).

Desde el punto de vista ecológico, podemos decir que *A. fumigatus* es un hongo filamentosamente saprófito que juega un papel ecológico muy importante como

descomponedor de materia orgánica, reciclando de este modo el carbono y nitrógeno (Debeaupuis *et al.*, 1997; Latgé, 1999; Tekaia and Latgé, 2005). *A. fumigatus* es un hongo que se ha encontrado de forma ubicua, desde muestras de aire y suelo a nivel mundial, hasta incluso en muestras de la Estación Espacial Internacional (Chazalet *et al.*, 1998; Pöggeler, 2002; Nierman *et al.*, 2005; Pringle *et al.*, 2005). Esta ubicuidad le viene dada por su gran capacidad adaptativa, ya que es capaz de colonizar un abanico enorme de ambientes gracias por una parte a su diversidad metabólica y por otra a una serie de características físicas que le permiten resistir de manera eficaz a una gran cantidad estreses ambientales y que describiremos con detalle más adelante.

1.2.2 Conidios de *A. fumigatus*

Como hemos indicado anteriormente, *A. fumigatus* es un hongo que se reproduce por conidios asexuales y sus conidióforos esporulan de manera abundante, generando por tanto una gran cantidad de estas formas de dispersión. Sus conidios se caracterizan por tener un tamaño pequeño (2-3 μm) y ser altamente hidrofóbicos, dos características que les permiten mantenerse en suspensión durante largos periodos de tiempo y dispersarse por el aire de manera muy efectiva (Latgé, 1999; Bayry *et al.*, 2014). Además, la pared celular de los conidios no solo está dotada de varias hidrofobinas, sino que presenta también una capa de melanina que, entre otras funciones, hace que estos conidios sean termotolerantes (son capaces de permanecer viables en un amplio rango de temperaturas), sean capaces de persistir viables en condiciones de deshidratación, e incluso mantengan su viabilidad tras su exposición a la radiación ultravioleta (O’Gorman, 2011; Krijgsheld *et al.*, 2013).

Basándonos en lo anteriormente descrito, es lógico pensar que los conidios de *A. fumigatus* pueden entrar en contacto con el ser humano de manera frecuente a través de las vías respiratorias, del sistema digestivo, de la piel, de los ojos y de los oídos. La inhalación es la ruta de acceso más frecuente de este hongo y se estima que una persona inhala diariamente alrededor de 100 conidios y que la concentración de estos, tanto en ambientes exteriores como en interiores, es de 1-100 conidios/ m^3 (Kwon-Chung and Sugui, 2013), pudiendo incluso alcanzar concentraciones de 10^8 conidios por m^3 en algunos ambientes (Wéry, 2014; Latgé and Chamilos, 2019).

El pequeño tamaño de estas esporas asexuales, permite al hongo traspasar las defensas de la cavidad nasal y el tracto respiratorio superior y alcanzar los alveolos pulmonares con facilidad (Hope, Walsh and Denning, 2005). Una vez que los conidios alcanzan los alveolos, podemos describir tres escenarios posibles en función del estado inmunológico de la persona que los ha inhalado (Latgé, 1999): **1)** En individuos inmunocompetentes, la inhalación de estos conidios rara vez tiene efecto, ya que se eliminan de forma eficaz por los mecanismos innatos del sistema inmunológico. **2)** Si la persona que inhala los conidios es inmunocompetente pero presenta hipersensibilidad, tras la inhalación de estos puede desarrollar una respuesta alérgica pudiendo causar sinusitis alérgica, un cuadro clínico de asma o en el peor de los casos de aspergilosis broncopulmonar alérgica (ABPA, por sus siglas en inglés *Allergic Bronchopulmonary Aspergillosis*). **3)** Si el paciente que inhala los conidios presenta una inmunodepresión, los conidios pueden superar las defensas inmunológicas y establecerse en el pulmón donde los conidios pueden germinar y por ende comenzar una colonización/invasión del tejido pulmonar (Dagenais and Keller, 2009), pudiendo causar un cuadro clínico severo conocido como aspergilosis invasiva (IA por sus siglas en inglés *Invasive Aspergillosis*) (Osherov, 2007).

1.2.3 Germinación de los conidios de *A. fumigatus*

Como ya se había explicado anteriormente los conidios son las formas de resistencia y dispersión de *A. fumigatus* originados en la reproducción asexual de este hongo filamentoso, y por tanto la germinación de estos es un fenómeno cuya primera etapa implica romper la dormancia/letargo que estos sufren. Este primer paso de activación se consigue cuando los conidios detectan que están expuestos a una situación favorable donde pueda haber agua, sales inorgánicas, aminoácidos y/o azúcares fermentables (Osherov and May, 2001; Thanh, Rombouts and Nout, 2005).

Posteriormente, el conidio entra en una fase conocida como *swelling* o hinchamiento que se caracteriza porque estos comienzan a experimentar un crecimiento isotrópico. Durante esta fase, se duplica el diámetro de los conidios debido a que estos comienzan a absorber agua, y, en consecuencia, se produce una reducción de la viscosidad citoplasmática (Van Leeuwen *et al.*, 2010). Este proceso de *swelling* ocurre al mismo

tiempo que se activa la expresión de genes necesarios para diferentes actividades metabólicas como pueden ser la respiración o la biosíntesis de proteínas, DNA y RNA (Mirkes, 1974; Osherov and May, 2001).

El siguiente estadio en el proceso germinativo se produce cuando se establece una polaridad celular a partir de la cual se comienza a formar un tubo germinal que crece de manera polarizada (Barhoom and Sharon, 2004; Harris and Momany, 2004). Durante este periodo, lo que se conoce como maquinaria morfogenética, que incluye: el citoesqueleto celular, el sistema de tráfico vesicular, las rutas de señalización y endocitosis (proteínas Rho, GTPasas...), el polarisoma y los complejos Arp2/3, se localizan en el sitio de crecimiento polarizado (D'Enfert, 1997; Momany, 2002; Harris and Momany, 2004; Harris, 2006). Por otra parte, en esa zona de polarización también ocurre un cambio en la composición de la membrana plasmática ya que aparecen en ella dominios ricos en esteroides (Van Leeuwen *et al.*, 2008). Finalmente, el proceso genera un aumento tanto de longitud como de velocidad de crecimiento de los tubos germinales y del área de la punta de la hifa (Köhli *et al.*, 2008; Taheri-Talesh *et al.*, 2008) para formar en última instancia un micelio complejo (Glass *et al.*, 2004).

A pesar de que se han descrito de manera bastante detallada las diferentes etapas y los diferentes hitos de la germinación de *A. fumigatus*, todavía no se conocen bien los aspectos moleculares que orquestan todo este proceso.

1.2.4 Biopelículas de *A. fumigatus*

Las biopelículas son comunidades de microorganismos adheridos a una superficie que están a su vez, embebidos en una matriz extracelular producida por el propio microorganismo. Este tipo de crecimiento en comunidades microbianas es el más prevalente de los crecimientos microbianos en la naturaleza (Kuhn *et al.*, 2002).

La mayoría de los estudios sobre la formación de biopelículas fúngicas se han efectuado con la especie *Candida albicans*. La estructura de las biopelículas producidas por esta levadura muestran dos capas celulares distintas: una capa basal fina, constituida esencialmente por levaduras, y una segunda capa más gruesa y menos compacta formada por hifas (Baillie and Douglas, 1999). En el caso de

A. fumigatus, al tratarse de un hongo filamentoso, la formación de la biopelícula viene derivada de la germinación de los conidios y la posterior adherencia y entrecruzamiento que sufren las hifas entre sí para formar una estructura compleja embebida en una matriz extracelular hidrofóbica que actúa a modo de pegamento (Beauvais *et al.*, 2007).

La composición de la matriz extracelular, y su producción *in vivo* se ha estudiado mediante ensayos inmunohistoquímicos y de microscopía electrónica, detectándose que está formada por tres polisacáridos principalmente: α -1,3-glucano, galactomanano y galactosaminogalactano (Loussert *et al.*, 2010) a diferencia de las de *C. albicans*, rica en β -1,3-glucano, y de *Saccharomyces cerevisiae*, rica en α -1,2-1,6 manano (Beauvais *et al.*, 2007; Latgé and Chamilos, 2019).

Además, se ha demostrado por microscopía electrónica que la melanina es también uno de los principales componentes de esta matriz extracelular. Sin embargo, aunque se han descrito anticuerpos anti-melanina capaces de reaccionar con los conidios pigmentados (Youngchim, Hay and Hamilton, 2005; Nosanchuk, Stark and Casadevall, 2015), estos no son capaces de reaccionar frente a la melanina de la matriz extracelular que embebe la biopelícula de este hongo (Loussert *et al.*, 2010). Además, se presupone que hay otras proteínas, metabolitos y monosacáridos que forman parte de la matriz extracelular pero que no se han podido detectar (Loussert *et al.*, 2010).

Finalmente, cabe destacar que la matriz extracelular que rodea la biopelícula de *A. fumigatus* juega un papel esencial en la patogénesis de la IA ya que interviene en la adherencia de las hifas al tejido pulmonar infectado, confiere al hongo resistencia a los antifúngicos, e interviene en la resistencia del hongo al sistema inmunológico del hospedador (Seidler, Salvenmoser and Müller, 2008; Ramage *et al.*, 2012; Pierce *et al.*, 2013; Kernien *et al.*, 2018).

1.3 La infección fúngica invasiva

1.3.1 Contexto epidemiológico general

Las infecciones fúngicas invasivas (IFI) se han convertido en un problema de relevancia creciente desde el inicio de la década de los 1980. En esos primeros años, se produjo un incremento generalizado de los casos de infección fúngica tanto invasiva como superficial. Estos casos estaban ligados fundamentalmente con la aparición de la infección por el virus de la inmunodeficiencia humana (VIH). Durante este periodo, las IFI más prevalentes en el mundo occidental fueron la candidiasis diseminada, la criptocosis meníngea o la neumonía por *Pneumocystis jirovecii*, estando todas ellas asociadas con el déficit de inmunidad celular provocado por la infección por el VIH.

Afortunadamente, durante la década de los 1990, la disponibilidad clínica de nuevos fármacos antifúngicos, como el fluconazol, y la implantación y generalización de la triple terapia antirretroviral, supuso un cambio en la epidemiología descrita, al favorecer el control de la infección por el VIH y la disminución del número de casos de infecciones fúngicas, al menos en el mundo occidental, pero quedando aún hoy en día un largo camino por recorrer en los países con menos recursos económicos.

A pesar de los avances descritos, a finales de dicha década se observó un nuevo giro epidemiológico en la dinámica de las IFI. La mejora de las técnicas en los procedimientos médicos y quirúrgicos asociados a los trasplantes (de órgano sólido - o de precursores hematopoyéticos) junto con el uso de fármacos inmunosupresores empleados para evitar el rechazo y la enfermedad injerto contra huésped, con una posología óptima y con menores efectos adversos e interacciones farmacológicas, permitieron incrementar la supervivencia de los pacientes receptores de trasplantes. Sin embargo, también supuso un aumento del número absoluto de IFI que comenzaron a ser un problema clínico añadido importante en el manejo de estos pacientes. Este hecho auspició una revolución en la terapia antifúngica existente hasta el momento con la aparición de nuevos triazoles (posaconazol y voriconazol), la mejora de algunos fármacos antifúngicos ya existentes (anfotericina B liposómica) o el descubrimiento de nuevas familias de fármacos, como fue el caso de las equinocandinas (anidulafungina, caspofungina y micafungina). El desarrollo y la

puesta en marcha de todos estos hitos han tenido una gran relevancia en el arsenal antifúngico y las guías terapéuticas actuales (Aguado *et al.*, 2011; Pappas *et al.*, 2016).

1.3.2 Aspergilosis

Se conocen como aspergilosis a aquellas infecciones oportunistas producidas por diferentes especies del género *Aspergillus*. No obstante, las producidas por *A. fumigatus* son las más frecuentemente descritas, seguidas por aquellas producidas por *A. flavus*, *A. niger*, *A. terreus* y otras especies de mucha menor incidencia (Nicolle, Benet and Vanhems, 2011). Concretamente en España, un estudio llevado a cabo en el año 2013, en el cual se estudia la población de hongos filamentosos y su resistencia a los fármacos antifúngicos, reveló una prevalencia de 1,6 casos por cada millón de habitantes, siendo *Aspergillus* el género más frecuente, ya que especies de este género se identificaron en el 86.3% de los casos. Tal y como se muestra en la **Fig. 3**, *A. fumigatus* fue la especie más prevalente (56.11%) seguido de *A. flavus* (9.75%), *A. terreus* (9.38%), *A. tubingensis* (7.94%), *A. niger* (7.58%), *A. nidulans* (2.89%) y otras especies de menor incidencia (6.35%) (Alastruey-Izquierdo *et al.*, 2013).

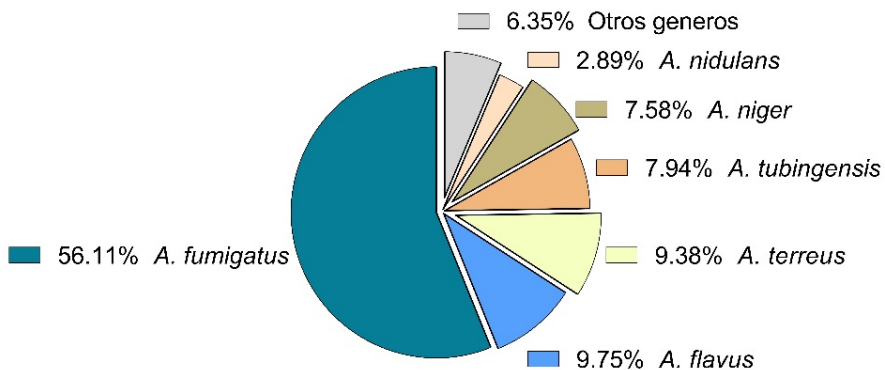


Figura 3. Prevalencia de las especies del género *Aspergillus* según el estudio FILPOP (Alastruey-Izquierdo *et al.*, 2013).

Dentro del término aspergilosis se recogen patologías que van desde la alergia a la IA, siendo la aspergilosis broncopulmonar alérgica (ABPA), el aspergiloma y la IA las patologías más graves causadas por especies de este género (Kousha, Tadi and Soubani, 2011). Como se ha comentado anteriormente, en general los individuos adquieren los conidios por inhalación a través de las vías respiratorias, siendo los pulmones el principal órgano afectado. No obstante, la patología que estos conidios

puedan generar depende del estado inmunológico del individuo y de sus enfermedades de base (Abad *et al.*, 2010) (Fig. 4).

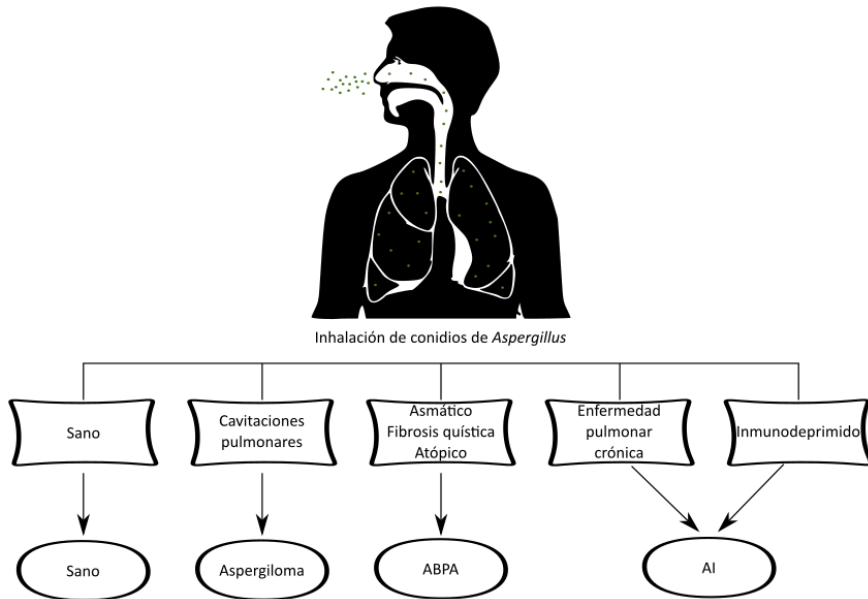


Figura 4. Esquema de las AI según el estado inmunológico del paciente.

1.3.3 Aspergiloma

El aspergiloma se define como la colonización persistente por *Aspergillus* de cavitaciones previamente formadas tras sufrir tuberculosis, sarcoidosis, enfisema pulmonar o bronquiectasias entre otras muchas causas. Concretamente, la tuberculosis es el principal factor de predisposición (90%) para desarrollar aspergiloma (Latgé and Chamilos, 2019). Este crecimiento fúngico consiste en una masa de hifas fúngicas (también llamada bola fúngica) entremezcladas que puede presentar cantidades variables de restos mucosos y celulares. Si en la localización donde se encuentra la bola fúngica, hay una cantidad de aire, el hongo puede desarrollar también conidióforos (Latgé and Chamilos, 2019).

Hay una cantidad considerable de pacientes que resultan asintomáticos. No obstante, cuando los síntomas aparecen, cabe destacar que la hemoptisis (expectoración de sangre proveniente de los pulmones o bronquios provocado por alguna lesión de las vías respiratorias) es el síntoma más común (50-90% de los pacientes). Esta hemoptisis se produce cuando la bola fúngica rompe de manera mecánica los vasos más cercanos

a su localización y puede ser de gravedad variable, incluso fatal para el paciente en el peor de los casos (Denning *et al.*, 2015; Kosmidis and Denning, 2015; Patterson *et al.*, 2016; Van De Veerdonk *et al.*, 2017; Alastruey-Izquierdo *et al.*, 2018). Finalmente hay que destacar que la bola fúngica también puede localizarse en la cavidad maxilar o en alguna otra zona sinusal (Grosjean and Weber, 2007), pero este tipo de casos no suelen ser preocupantes ya que se puede eliminar de manera sencilla mediante cirugía endoscópica sinusal (Pagella *et al.*, 2007).

1.3.4 Aspergilosis broncopulmonar alérgica (ABPA)

La ABPA se define como una enfermedad de hipersensibilidad pulmonar debida a la exposición ambiental a alérgenos de *A. fumigatus*. Normalmente, esta patología se observa en individuos atópicos que, o bien sufren fibrosis quística (Price *et al.*, 2015), o bien presentan una predisposición genética a ABPA (Agarwal *et al.*, 2013; Kosmidis and Denning, 2015; Vacher, Niculita-Hirzel and Roger, 2015). Además, cabe destacar que prácticamente la totalidad de los pacientes que padecen ABPA, sufren enfermedad asmática crónica (Latgé and Chamilos, 2019). Para el desarrollo de ABPA, *A. fumigatus* crece de manera saprofita colonizando el tracto bronquial y causando una inflamación persistente generada por la producción de inmunoglobulina E (IgE) en el hospedador causando una obstrucción bronquial (Zmeili and Soubani, 2007). Entre los síntomas más comunes se encuentran; fiebre crónica, tos, sibilancias, infiltrados pulmonares, eosinofilia y presencia de esputo con sangre y mocos marrones (Latgé and Chamilos, 2019).

1.3.5 Aspergilosis invasiva (IA)

Esta patología se define como una infección nosocomial que afecta principalmente a pacientes inmunodeprimidos y que presenta tasas de mortalidad variables dependiendo de la enfermedad de base del paciente y de los órganos que se vean afectados. En el caso de pacientes sometidos a trasplante de hígado o bazo, esta enfermedad puede alcanzar el 85-100% de mortalidad. Por otra parte, en aquellos pacientes con leucemia severa y receptores de trasplantes hematopoyéticos la mortalidad puede alcanzar el 50% (Lortholary *et al.*, 2011; Azie *et al.*, 2012; Brown *et al.*, 2012; Montagna *et al.*, 2014; Robin *et al.*, 2019). La obstrucción pulmonar crónica

es un factor que también predispone al desarrollo de la IA así como el uso de tratamientos de esteroides y el uso continuado de antibióticos para el tratamiento de infecciones del tracto respiratorio (Ledoux *et al.*, 2020), lo cual relaciona la enfermedad con el microbioma pulmonar, pero esta relación todavía no es concluyente (Briard *et al.*, 2019).

Existen diversas localizaciones desde las que se pueden desarrollar la IA, entre ellas son relativamente frecuentes la aspergilosis traqueo-bronquial, sinusal y cutánea. No obstante, la aspergilosis pulmonar invasiva (IPA, por sus siglas en inglés *Invasive Pulmonary Aspergillosis*) es la presentación más común de las enfermedades invasivas producidas por hongos del género *Aspergillus* (Muñoz, Guinea and Bouza, 2006). La IPA se caracteriza porque los conidios germinan dentro de los pulmones generando hifas que crecen produciendo daño tisular, hemorragia pulmonar y obstrucción vascular (Zaas & Alexander 2009). Finalmente, tras la ruptura de los vasos sanguíneos pulmonares, el hongo puede diseminarse de manera hematogena pudiendo alcanzar cualquier órgano y es entonces cuando hablaremos de aspergilosis diseminada. Entre los órganos que puede verse infectados, el cerebro suele ser el más afectado (50% de los casos), produciéndose abscesos, hemorragias y meningitis cerebrales que cursan con una mortalidad del 90% (Muñoz, Guinea and Bouza, 2006). Además, el hongo también puede diseminarse hacia el tracto gastrointestinal, hígado, bazo, corazón, ojos, huesos o articulaciones (Montejo 2002).

El primer caso de IA en humanos fue descrito en 1951, y desde entonces, esta ha sido la enfermedad más frecuente causada por un hongo filamentoso y la segunda causa de infección fúngica por detrás de las infecciones producidas por levaduras del género *Candida* (Latgé, 1999). Desde entonces y como ocurre con otros hongos, el resultado del aumento del número de casos de VIH, del desarrollo de fármacos para quimioterapia, del aumento de trasplantes de órgano sólido y el aumento de la utilización de fármacos inmunosupresores para el tratamiento de diferentes patologías, se ha traducido en un aumento significativo del número de pacientes inmunodeprimidos y por tanto también del número de casos de IA descritos (Lumbreras and Gavalda, 2003; Maschmeyer, Haas and Cornely, 2007).

1.3.5.1 Diagnóstico de la aspergilosis pulmonar invasiva

El diagnóstico precoz de la IPA supone un reto importante, ya que ser capaces de diagnosticar y anticipar el inicio de una terapia antifúngica se convierte en un factor clave para asegurar la supervivencia del paciente. Debido a que en muchas ocasiones la sintomatología es inespecífica (tos seca, fiebre constante, dolor en el pecho y dificultad respiratoria), al grado de inmunosupresión de los pacientes y a las enfermedades de base de estos, el diagnóstico de la enfermedad suele ser complicado y tardío (Denning, 1998). El método de referencia para diagnosticar la IPA todavía sigue siendo el cultivo microbiológico y la observación de las hifas del hongo mediante examen histopatológico o mediante observación directa. Estas técnicas presentan una baja sensibilidad y no pueden llevarse a cabo en todos los casos, de ahí que se hable de las dificultades diagnósticas de la IPA (Barnes and Marr, 2006). A este hecho hay que sumarle que las muestras que se toman para el diagnóstico suelen ser, por lo general, muestras de esputo que pueden tener presencia de conidios ambientales en ellas ya que el hongo se transmite por el aire. La obtención de muestras estériles mediante técnicas invasivas (biopsia) no está recomendada debido al delicado estado de los pacientes (Singh and Paterson, 2005; Del Bono, Mikulska and Viscoli, 2008). Por tanto, el diagnóstico clásico mediante cultivo microbiológico, es una técnica que no es capaz de diferenciar entre colonización e invasión (Singh and Paterson, 2005), por ello siempre debe realizarse de manera conjunta de la histología para confirmar la existencia de estructuras fúngicas (Ascioglu *et al.*, 2002).

Las pruebas radiológicas son otra opción diagnóstica. La imagen de la IPA obtenida mediante radiografía de tórax es heterogénea y poco útil en las primeras etapas de la enfermedad. Los hallazgos habituales que se pueden observar son densidades rodeadas, infiltrados pleurales que sugieren infarto pulmonar y cavitaciones (Pagani and Libshitz, 1981; Kuhlman, Fishman and Siegelman, 1985). Por otra parte, cuando la tomografía axial computarizada se ha combinado con imágenes de alta resolución ha permitido detectar lesiones pulmonares como nódulos múltiples y el signo del halo de manera más precoz en pacientes con IPA, agilizando y facilitando el diagnóstico de la enfermedad (Caillot *et al.*, 1997, 2001). Una técnica más novedosa llamada tomografía por emisión de positrones, en la cual se utiliza la ¹⁸F-fluorodeoxyglucosa, ha supuesto

una mejoría en la detección de lesiones ocultas en los pulmones causadas por candidiasis diseminadas y por IPA (Bryant and Cerfolio, 2006; Chamilos, Macapinlac and Kontoyiannis, 2008; Hot *et al.*, 2011; Ankrah *et al.*, 2019).

Otra forma diferente de realizar el diagnóstico de la enfermedad es mediante la detección directa de algunos de sus antígenos como puede ser la detección de galactomanano (GM) o del (1-3)- β -glucano. El GM es un componente de la pared celular de los hongos del género *Aspergillus* y se puede detectar en suero, en lavados broncoalveolares y en orina, ya que es uno de los principales exoantígenos liberados por estos hongos (Latgé, 1999; Latgé and Chamilos, 2019; Ledoux *et al.*, 2020). La detección se realiza utilizando un anticuerpo monoclonal de rata que reconoce el GM mediante un ensayo ELISA (Platelia^R *Aspergillus*, Bio-Rad Laboratories) (Klont, Mennink-Kersten and Verweij, 2004; Wheat and Walsh, 2008). Esta técnica presenta sus limitaciones ya que no puede ser aplicado sobre líquido cefalorraquídeo, líquido pleural o directamente en tejido biopsiado (Ledoux *et al.*, 2020). Además, la detección de GM no es específica de *Aspergillus* ya que presenta reactividad cruzada con otros hongos (*Fusarium spp.*, *Paecilomyces spp.*, *Penicillium spp.*, *Acremonium spp.*, *Alternaria spp.*, *Wangiella dermatitidis.*, *Histoplasma capsulatum* y *Blastomyces dermatitidis* (Miceli and Maertens, 2015). Finalmente destacar que los datos de sensibilidad, especificidad, así como los valores predictivos de este método son variables en función de la cohorte estudiada por los diferentes grupos de investigación que se dedican a ello (Ledoux *et al.*, 2020). Por otra parte, la detección en suero de (1-3)- β -glucano presente en la pared celular del hongo es una técnica que también puede ser utilizada. Este método se realiza por ensayo de coagulación o bien por ensayo colorimétrico (Obayashi *et al.*, 2008; Senn *et al.*, 2008). Este método diagnóstico también puede presentar falsos positivos tanto por reactividad cruzada con otros hongos, dado que es un componente frecuente en las paredes celulares de los mismos, como si el paciente ha tenido un consumo continuado de antibióticos β -lactámicos (Del Bono, Mikulska and Viscoli, 2008).

Otra aproximación diagnóstica, en este caso detectando el ADN del hongo, es la PCR. En los últimos años se han estandarizado y publicado diversos protocolos (Barnes *et al.*, 2018; Patterson and Donnelly, 2019). Esta técnica se puede hacer partiendo de

suero, plasma o lavado broncoalveolar presentando un valor diagnóstico similar a la detección de GM (White *et al.*, 2015; Barnes *et al.*, 2018). Además, se puede realizar tras extracción de ADN de biopsias, tejidos fijados en parafina y fijados en formalina, aunque partiendo de tejidos fijados existen problemas de inhibición de la reacción por degradación del ADN o por acumulación de inhibidores (Salehi *et al.*, 2016). Existen kits comerciales que presentan una alta sensibilidad (>90%) y altos valores predictivos negativos (Torelli *et al.*, 2011; Chong *et al.*, 2015; Denis *et al.*, 2018; Rath and Steinmann, 2018; Cruciani *et al.*, 2019). Por otra parte, se han publicado diversos estudios donde se observa reactividad cruzada con *Penicillium spp.*, *Fusarium spp.*, y *Rhizopus oryzae* (Torelli *et al.*, 2011; Chong *et al.*, 2015; Moura, Cerqueira and Almeida, 2018).

1.3.5.2 Tratamiento de la aspergilosis invasiva

La consecuencia de un diagnóstico tardío de la enfermedad es que los pacientes que la padecen o no llegan a recibir tratamiento o lo empiezan a recibir en un estadio muy avanzado de la misma. Durante las últimas dos décadas se han realizado enormes avances en el desarrollo de nuevas terapias antifúngicas. Históricamente, se consideraba la anfotericina B desoxicolato como único tratamiento frente a la enfermedad (Denning *et al.*, 1994). Posteriormente, una nueva presentación oral de itraconazol fue considerada como una opción válida para el tratamiento de las aspergilosis crónicas (Denning, 2001). Pero la realidad es que durante las últimas décadas se han realizado diversos ensayos clínicos evaluando la efectividad de compuestos como el isavuconazol, voriconazol, anfotericina B liposomal, caspofungina y anidulafungina entre otros (Herbrecht *et al.*, 2002, 2010, 2015; Cornely *et al.*, 2007, 2010; Viscoli *et al.*, 2009; Marr *et al.*, 2015; Maertens *et al.*, 2016). Estos estudios midieron la supervivencia de las diferentes cohortes tras 12 semanas de tratamiento, y en el mejor de los casos se obtuvo una supervivencia cercana al 70% mientras que en el peor fue del 50%.

El tratamiento de elección actualmente es el voriconazol, pero hay que destacar que hay muchos estudios en los cuales se realizan comparaciones de la efectividad de unos fármacos frente a otros (Cornely *et al.*, 2007; Ullmann *et al.*, 2007; Maertens *et al.*,

2016) o diferentes dosificaciones del mismo fármaco (Cornely *et al.*, 2007). De todos estos estudios se puede concluir que dependiendo de la enfermedad de base del paciente o del uso que se quiera dar al fármaco (si se va a usar en profilaxis o como terapia de un cuadro avanzado de la enfermedad) unos fármacos antifúngicos tienen ventajas sobre otros y viceversa. Por ejemplo, en un estudio doble ciego donde se comparó la supervivencia de la cohorte en la semana 6 y 12 de tratamiento, se concluyó que tanto voriconazol como isavuconazol presentaron la misma eficacia pero que en pacientes con riesgo de afección hepática, el isavuconazol era una mejor alternativa al voriconazol (Maertens *et al.*, 2016).

Toda esta cantidad de estudios y de elecciones terapéuticas sumado a una realidad como es el retraso diagnóstico y la alta tasa de mortalidad de la enfermedad de los pacientes infectados, llama a reflexionar sobre la necesidad de encontrar nuevas dianas moleculares tanto diagnósticas como terapéuticas. Para ello es necesario realizar estudios enfocados a comprender los genes y proteínas involucradas en el proceso de infección por estos hongos, y en este caso, y por ser el agente etiológico más prevalente del grupo, de *A. fumigatus*.

1.4 Factores de virulencia de *Aspergillus fumigatus*

La capacidad que tiene *A. fumigatus* de sobrevivir y crecer en un amplio rango de condiciones ambientales, la eficacia que presenta para dispersarse por el aire, las características físicas de sus conidios, así como los mecanismos que dispone para adaptarse al huésped, son algunas de las características que hacen que este hongo sea el agente etiológico más prevalente causante de las IA (Kwon-Chung and Sugui, 2013). La importancia de este hongo como causante de infecciones se ve reflejada en la gran cantidad de revisiones publicadas sobre la biología, patogenicidad y la identificación de nuevos factores de virulencia (Lalgé, 1999; Brakhage and Langfelder, 2002; Banerjee and Kurup, 2003; Rementeria *et al.*, 2005; Tekaia and Lalgé, 2005; Hohl and Feldmesser, 2007; Askew, 2008; Dagenais and Keller, 2009; Abad *et al.*, 2010; Kwon-Chung and Sugui, 2013; Lalgé and Chamilos, 2019; Perez-Cuesta *et al.*, 2020). Por otra parte, hay una gran cantidad de trabajos en los cuales, para demostrar la relación de un gen o genes con la virulencia del hongo, se realizan diferentes manipulaciones

genéticas de las cepas delecionándose, sobreexpresándose o silenciándose dichos genes y generando así cepas mutantes cuya virulencia se compara con la de una cepa salvaje (WT de sus siglas en inglés *Wild Type*). (Bertuzzi *et al.*, 2014; Guruceaga *et al.*, 2018; Souza *et al.*, 2019; Martin-Vicente *et al.*, 2020; Scott *et al.*, 2020).

En las siguientes líneas se recoge un resumen de los principales factores de virulencia de *A. fumigatus* descritos en la bibliografía, haciendo especial hincapié y profundizando en aquellos que tienen relación directa en el desarrollo de la presente tesis doctoral.

1.4.1 Termotolerancia

Aspergillus fumigatus es un hongo termófilo capaz de crecer en un amplio rango de temperaturas, pudiendo sobrevivir incluso a temperaturas de 75°C (Beffa *et al.*, 1998; Ryckeboer *et al.*, 2003). Partiendo de este hecho, parece lógico pensar que las proteínas que facilitan al hongo la adaptación a estas temperaturas pueden contribuir directamente en la virulencia del hongo (Bhabhra and Askew, 2005). Genes como *thtA*, *afpmt1*, *kre2/afmnt1*, *cgrA* y *hsp1/aspf12* han sido relacionados con la termotolerancia de este patógeno (Abad *et al.*, 2010), no obstante, de todos ellos, solo la proteína Hsp1/Asp f 12 parece estar relacionada con la patogénesis. De hecho, esta proteína alergénica ha sido descrita como uno de los principales antígenos durante la IA (Kumar *et al.*, 1993; Ramirez-Garcia *et al.*, 2018).

A pesar de que hay varios estudios transcriptómicos en donde se estudia la expresión de los genes del hongo cuando crece a diferentes temperaturas (30 °C vs. 37 °C; 30 °C vs. 48 °C) todavía no se ha encontrado una relación directa entre ningún gen/proteína implicado en el proceso de adaptación a la temperatura y la patogénesis del hongo. Estos estudios han detectado grupos de genes sobre expresados en alguna temperatura comparándola con la otra, pero no han profundizado en la función que cumple esa sobreexpresión en la biología de *A. fumigatus* (Nierman *et al.*, 2005; Sueiro-Olivares *et al.*, 2015).

1.4.2 Pared celular

La pared celular de *A. fumigatus* está formada principalmente por polisacáridos, proteínas, lípidos, melanina y otros pigmentos (Gastebois *et al.*, 2009). Alguna de las funciones que cumple es mantener la estructura celular, mediar en la adherencia a las superficies, actuar como “filtro molecular” permitiendo el tráfico selectivo entre la célula y el exterior, y participar en la generación de matrices extracelulares que, como hemos indicado, son la base para el desarrollo de biopelículas (Lee and Sheppard, 2016). Además, hay que destacar que la pared celular es una estructura dinámica cuya composición varía acorde a las variaciones ambientales (Latgé and Chamilos, 2019).

Los conidios de *A. fumigatus* presentan una pared celular con dos capas. La capa exterior, también denominada capa *rodlet*, está formada principalmente por melanina e hidrofobinas que confieren al conidio de una alta hidrofobicidad. Por otro lado, la capa está formada principalmente por α -(1,3)-glucano (14%), β -(1,3)-glucano (13%), galactomanano (13%) y quitina/quitosano (0.5%) (Lee and Sheppard, 2016). Tradicionalmente esta capa está organizada por β -(1,3)-glucanos ramificados y unidos entre sí y a quitina y galactomanano, formado así el núcleo rígido de la pared celular, mientras que los α -(1,3)-glucanos y los mananos actúan a modo de cemento rellenando la estructura (Fontaine *et al.*, 2000; Henry, Latgé and Beauvais, 2012; Latgé and Chamilos, 2019) (**Fig. 5**). Sin embargo, estudios recientes realizados por resonancia magnética nuclear sugieren, en cambio, que el núcleo de la pared está formado por los α -(1,3)-glucanos asociados a la quitina mientras que los β -(1,3)-glucanos son los que rellenarían los poros (Kang *et al.*, 2018). Un reciente estudio publicado por Valsecchi y colaboradores (Valsecchi *et al.*, 2020) propone la presencia de este compuesto, α -(1,3)-glucano, justo por debajo de la capa *rodlet*.

Por otra parte, hay que destacar que la composición de la pared celular de las hifas difiere a la de los conidios. Principalmente, la capa interna está compuesta por β -(1,3)-glucano (30%), quitina/quitosano (17%), galactomanano (5%), galatosaminogalactano (4%) y β -(1,3;1-4)-glucanos (3%). Por el contrario, la capa externa está formada por α -(1,3)-glucano (42%), galactosaminogalactano (4%) y galactomanano (1,4%) (Lee and Sheppard, 2016) **Fig. 5**.

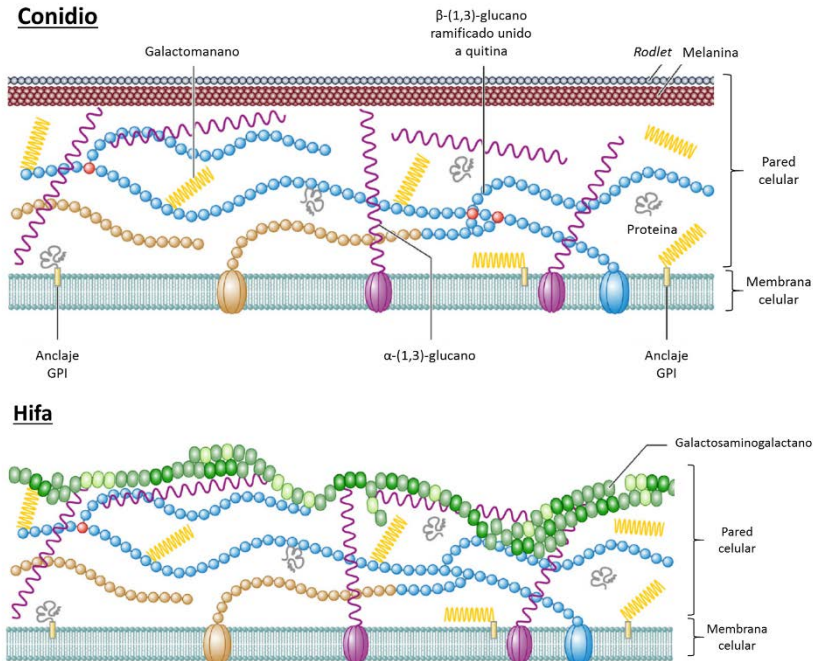


Figura 5. Representación esquemática de la pared celular tanto del conidio como de la hifa de *A. fumigatus*. Obsérvese que, aunque el núcleo de polisacáridos de la pared celular de ambos morfotipos se mantiene, existen diferencias en la composición de las superficies. Mientras que la pared celular del conidio está formada por *rodlet* y melanina, la de la hifa está compuesta principalmente por galactosaminogalactano. (Modificada de Latgé and Chamilo, 2019).

Finalmente, hay que destacar que su composición varía en función de la posición celular en la hifa (apical, sub-apical o distal) y en función de los estímulos ambientales que reciba (pH, presencia de fármacos antifúngicos, hipoxia, presencia de microbiota etc...) (Loussert *et al.*, 2010; Latgé and Beauvais, 2014). Dada esta plasticidad y el descubrimiento del reconocimiento del hongo por parte de las células del sistema inmunológico a través de los receptores, como Dectina-1, que reconocen los β -(1,3)-glucanos (Brown and Gordon, 2001), es más que evidente que esta estructura celular supone un factor de virulencia importante para el hongo. Su capacidad de cambiar tanto de composición como de estructura en función de los estímulos que reciba el hongo, permite a este una alta capacidad de adaptación a diferentes ambientes.

1.4.3 Mecanismos de evasión a la respuesta inmunológica

Están descritos varios genes y moléculas relacionadas con estructuras de la superficie de *A. fumigatus* que activan y/o interactúan con el sistema inmunológico del huésped

(Osherov 2007). Entre todas ellas podemos destacar las denominadas proteínas hidrofóbicas o hidrofobinas. Hasta la fecha se conoce que el genoma de *A. fumigatus* codifica para hidrofobinas según los siguientes genes; *rodA* (Afu5g09580), *rodB* (Afu1g175250), *rodC* (Afu8g07060), *rodD* (Afu5g01490), *rodE* (Afu8g05890), *rodF* (Afu5g03280) y *rodG* (Afu2g14661). De todas estas hidrofobinas, solo RodA y RodB están bien caracterizadas, mientras que el resto se han anotado como adhesinas mediante predicción bioinformática y todavía deben ser estudiadas (Chaudhuri *et al.*, 2011; Cerqueira *et al.*, 2014).

Las hidrofobinas son las responsables de dotar de hidrofobicidad a los conidios y les ayudan a dispersarse por el aire y a adherirse a las superficies sólidas (Linder *et al.*, 2005; Aimanianda *et al.*, 2009; Latgé and Chamilos, 2019), y al epitelio respiratorio (Thau *et al.*, 1994). Parece además que estas proteínas podrían conferir al hongo resistencia a las células del huésped (Paris, Debeaupuis, *et al.*, 2003). Como hemos indicado, estas proteínas se sitúan formando parte de lo que se denomina la capa *rodlet* de los conidios, que exclusivamente está codificadas por el gen *rodA* y ayudan a enmascarar el reconocimiento del hongo por parte del sistema inmunológico (Aimanianda *et al.*, 2009). La hidrofobina RodA, es una proteína que se caracteriza por estar compuesta de 8 residuos de cisteína capaces de formar puentes de disulfuro y organizar las proteínas en una configuración fibrilar que confiere a la pared celular de los conidios resistencia al agua (Valsecchi *et al.*, 2019). Esta proteína necesita de una estructura tridimensional adecuada ya que el plegamiento de RodA es esencial para la correcta formación de la capa *rodlet* (Valsecchi *et al.*, 2017). Por otra parte, se han realizado estudios originando una mutación en la proteína que impide la formación de puentes de disulfuro de RodA, y esta proteína mutante activa las células dendríticas y en consecuencia la secreción de citocinas inflamatorias, mientras que la estructura nativa evita esa respuesta. Por su parte, RodB, es una proteína que se sobreexpresa en condiciones *in vivo* y cuando el hongo crece formando biopelículas (Valsecchi *et al.*, 2017) lo cual convierte a esta proteína en otro posible factor de virulencia.

Además de las hidrofobinas, para la evasión de la respuesta inmunológica, el genoma de *A. fumigatus* cuenta con 5 genes que codifican catalasas: *catA*, *catB/cat1*, *catC*, *catE* y *cat2*. La catalasa codificada por el gen *catA*, se encuentra expresada en el

conidio del hongo mientras que las codificadas por los genes *catB/cat1* y *cat2* aparecen cuando la hifa de *A. fumigatus* ya está formada (Calera *et al.*, 1997; Paris, Wysong, *et al.*, 2003). Estas enzimas son oxidoreductasas que catalizan la descomposición del peróxido de hidrógeno en oxígeno y agua y cobran especial importancia cuando las ubicamos en el contexto de la colonización del sistema respiratorio, dado que los macrófagos y las células polimorfonucleares son las responsables de defender al huésped frente al conidio y las hifas respectivamente (Schaffner, Douglas and Braude, 1982). Para ello, una de las estrategias que siguen las células del sistema inmunológico es la producción de especies reactivas de oxígeno (ROS por sus siglas en inglés *Reactive Oxygen Species*) (Diamond and Clark, 1982). De ahí la importancia que supone para el hongo contar, entre su arsenal de enzimas, con catalasas capaces de neutralizar el efecto de las ROS y por qué se consideran factores de virulencia. Esto se ha confirmado en estudios llevados a cabo mediante generación de cepas mutantes de delección en los cuales se silenciaron las catalasas CatA, CatB y Cat2. En estos estudios se concluyó que el enzima CatA producida por el conidio no es un factor de virulencia, mientras que las catalasas formadas en la fase micelial (CatB y Cat2) tiene un papel fundamental en la degradación *in vitro* del peróxido de hidrógeno y en proteger al hongo durante infecciones experimentales en un modelo de rata (Paris, Wysong, *et al.*, 2003).

1.4.4 Melanina

La melanina es uno de los principales pigmentos que puede ser sintetizado por los hongos. Concretamente, los hongos pueden sintetizar tres tipos diferentes de melaninas: DOPA melanina, dihidroxinaftaleno-melanina (melanina-DHN) y una forma de melanina extracelular y soluble en agua conocida como piomelanina. Estos pigmentos son metabolitos secundarios formados por complejos polímeros fenólicos o indólicos y *A. fumigatus* es capaz de producir los dos últimos, melanina-DHN y piomelanina (Bayry *et al.*, 2014).

1.4.4.1 Melanina-DHN

Los genes encargados en la biosíntesis de este tipo de melanina están ubicados en el cromosoma 2 del hongo y cubren en torno a 19 kb del genoma. Estos genes se

encuentran asociados y agrupados en lo que se denomina un *cluster* biosintético que en este caso está formado por 6 genes (*abr1*, *abr2*, *ayg1*, *arp1*, *arp2* y *pksP/alb1*) (Tsai et al., 1998). En 1998, Langfelder y colaboradores complementaron una cepa del hongo blanca, que habían producido por mutagénesis espontánea tras exposición a radiación ultravioleta, con el gen *pksP/alb1* y la cepa resultante volvió a presentar el color verde grisáceo característico de este hongo (Langfelder *et al.*, 1998). Por este motivo, el gen es conocido como *alb1* ya que la cepa deficiente en él es albina (Tsai *et al.*, 1998). Posteriormente, se fueron realizando mutantes de cada uno de los genes de la ruta y en cada uno se presentó una coloración específica en función del paso de biosíntesis interrumpido por la mutación (Tsai *et al.*, 1997, 1998) tal y como se puede observar en la **Fig. 6**.

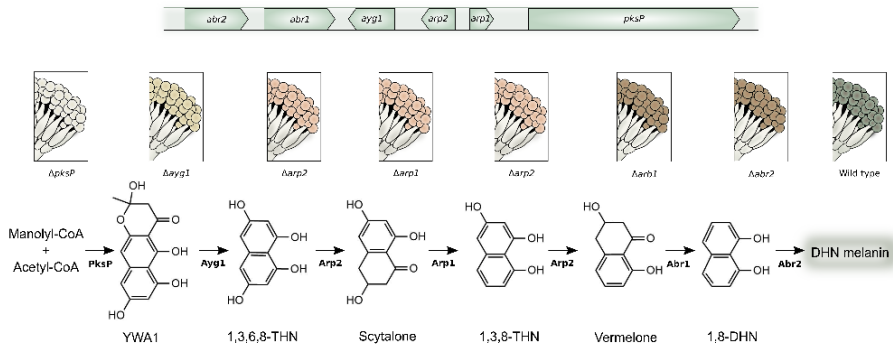


Figura 6. Organización genómica del *cluster* biosintético de la melanina-DHN así como la ruta metabólica que da lugar al pigmento. Además, la imagen muestra los cambios de color que *A. fumigatus* sufre en cada una de las mutaciones de delección de los genes implicados en cada caso (Extraído de Perez-Cuesta *et al.*, 2020).

La melanina es un pigmento asociado a la virulencia de *A. fumigatus* ya que forma parte de la capa *rodlet* externa de la pared celular de los conidios, así como de la estructura de las biopelículas que este hongo puede generar. Este pigmento protege al conidio frente a los estreses ambientales como la desecación (Gow, Latgé and Munro, 2017) y evita el daño celular causado por la radiación ultravioleta (UVA y UVB) así como la radiación ionizante (Eisenman and Casadevall, 2012; Braga *et al.*, 2015). Además, la melanina protege al hongo frente a la predación por amebas en el suelo (Hillmann *et al.*, 2015) y esta capacidad se relaciona con la protección frente a la fagocitosis, así como frente a enzimas líticas y estrés oxidativo (Jahn *et al.*, 2002; Heinekamp *et al.*, 2013; Perez-Cuesta *et al.*, 2020).

Por otra parte, la melanina además de ser un factor de virulencia por sí misma, interviene en el correcto funcionamiento de otros factores de virulencia como pueden ser las hidrofobinas y adhesinas (Pihet *et al.*, 2009) e interviene también, como hemos indicado, en la formación de biopelículas (Beauvais and Latgé, 2015).

1.4.4.2 Piomelanina

La piomelanina es un pigmento soluble en agua de color marrón oscuro que, a diferencia de la melanina, no tiene una ruta biosintética propia. Su producción se da por polimerización de un sub-producto derivado de la degradación de la L-fenilalanina. Esta degradación está mediada por un *cluster* de seis genes localizados en el cromosoma 2 de *A. fumigatus* (*hppD*, *hmgX*, *hmgA*, *fahA*, *maiA*, y *hmgR*) tal y como se puede observar en la **Fig. 7**. Cuando se acumula Homogentisato (HGA), un compuesto intermediario de la ruta de degradación, este por transformación oxidativa de manera espontánea pasa a benzoquinona acetato que polimeriza a piomelanina. Hay que destacar que la síntesis de piomelanina está asociada a la germinación de los conidios y depende directamente de sensores de superficie del hongo (*Wsc1*, *Wsc3* y *MidA*) que detectan L-fenilalanina (Phe), L-tirosina (Tyr) u otros estreses de integridad celular y que transmiten la señal a las Rho GTPasas y MAP kinasas (*Bck1*, *Mkk2* y *MpkA*) activando finalmente el *cluster* (Valiante *et al.*, 2009).

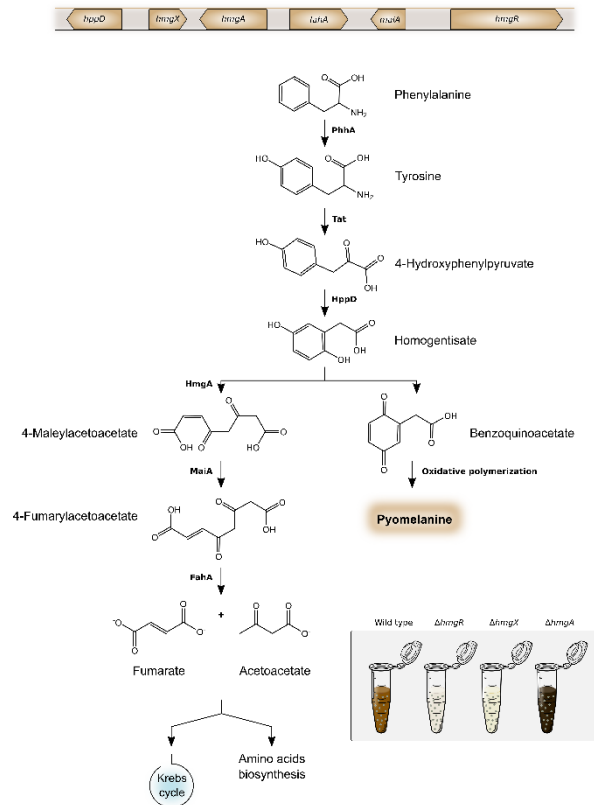


Figura 7. Organización genómica del *cluster* de genes de degradación de la L-fenilalanina, así como de su ruta metabólica de degradación de este aminoácido. La figura incluye la acumulación de piomelanina en los sobrenadantes de los cultivos de cada uno de los mutantes de delección obtenidos en genes del este *cluster* (Extraído de Perez-Cuesta *et al.*, 2020).

Entre las funciones que cumple la piomelanina se puede destacar que parece proteger a las hifas jóvenes del estrés oxidativo (Schmaler-Ripcke *et al.*, 2009). Además, hay estudios que demuestran que cuando se somete al hongo a estreses de pared (tanto mecánicos como químicos) se observa un aumento de la expresión de la degradación de Tyr y un aumento de la producción del pigmento (Valiante *et al.*, 2009; Jain *et al.*, 2011) pudiendo actuar por tanto la piomelanina como un factor de protección de la pared celular.

1.4.5 Toxinas

Los hongos filamentosos producen, como consecuencia de su complejo metabolismo secundario, un gran abanico de moléculas de bajo peso molecular denominadas metabolitos secundarios (SM) (Guruceaga *et al.*, 2020). Estos SM se caracterizan por

ser moléculas bioactivas, no esenciales para el crecimiento del organismo, pero que cumplen una función importante ayudando a este a adaptarse a las condiciones medioambientales. Entre otras funciones, los SM intervienen en la mejora de la competitividad con otros microorganismos y con la respuesta inmunológica durante el proceso de infección, suponen una de las defensas del hongo para sobrevivir en su nicho ecológico e intervienen en la comunicación y virulencia (Bennett and Bentley, 1989; Raffa and Keller, 2019). La especie *A. fumigatus*, concretamente, tiene el potencial genético de producir 226 SM (Frisvad *et al.*, 2009).

Los genes responsables de la síntesis de estos compuestos normalmente se encuentran asociados y agrupados en *clusters* genes (Nierman *et al.*, 2005; Bignell *et al.*, 2016; Keller, 2019). En el genoma de *A. fumigatus* se han detectado entre 26-36 *cluster* de genes con capacidad de biosíntesis de SM (Bignell *et al.*, 2016; Lind *et al.*, 2017, 2018). Aquellos SM que presentan una actividad tóxica, se conocen como micotoxinas, y en los últimos años se han publicado diversas revisiones sobre la producción de micotoxinas por especies del género *Aspergillus* (Kamei and Watanabe, 2005; Keller *et al.*, 2006; Arias *et al.*, 2018; Shankar *et al.*, 2018; Keller, 2019; Raffa and Keller, 2019; Raffa, Osheroov and Keller, 2019; Romsdahl and Wang, 2019).

Una de estas toxinas es la fumigacina, destacada por afectar a los macrófagos (Mitchell, Slight and Donaldson, 1997), al metabolismo de lipoproteínas de baja densidad (Shinohara, Hasumi and Endo, 1993), e inducir ciliostasis y lisis de células epiteliales (Amitani *et al.*, 1995). Otra toxina producida por *A. fumigatus* que ha sido estudiada es la ribotoxina, capaz de interactuar con la subunidad 28S del RNA ribosomal de las células del huésped inhibiendo la síntesis de proteínas (Kao and Davies, 1995, 1999). Por otra parte, también se conoce la mitogilina o Asp F 1, que está directamente relacionada con los procesos alérgicos y es uno de los antígenos predominantes durante la aspergilosis alérgica (Arruda *et al.*, 1990). *A. fumigatus* también es capaz de producir una hemolisina (codificada por el gen *aspHS*) que como su nombre indica presenta un efecto hemolítico sobre los eritrocitos además de efecto citotóxico frente a macrófagos y células endoteliales (Yokota, Kamaguchi and Sakaguchi, 1977). Finalmente hay que destacar que este hongo es capaz de producir

toxinas que producen efecto neurológico, como son la fumitremorgina A y B (Yamazaki, Fujimoto and Kawasaki, 1980).

Además de las anteriores, la gliotoxina, una toxina pertenece a la familia de las piperazinas, es producida por *A. fumigatus* pero también por otros hongos filamentosos como pueden ser *Eurotium chevalieri*, *Gliocladium fimbriatum* y algunas especies de los géneros *Trichoderma* y *Penicillium* (Scharf *et al.*, 2012). Su estructura se descubrió en 1958 (Bell *et al.*, 1958) y se comenzaron a realizar estudios para comprender su función y los efectos que produce. Se ha detectado que presenta efectos inmunosupresores, afecta a la capacidad fagocítica de los macrófagos, produce la activación de los mastocitos, induce citotoxicidad de las células T y puede causar apoptosis de los monocitos (Mullbacher and Eichner, 1984; Eichner *et al.*, 1986; Yamada, Kataoka and Nagai, 2000; Stanzani *et al.*, 2005). Por otra parte, también está descrito que esta toxina inhibe en los neutrófilos la captación de energía vía NADPH suprimiendo la capacidad oxidativa y fagocítica de estos y además reduce el movimiento ciliar de las células epiteliales y provoca daño celular de las mismas (Amitani *et al.*, 1995; Tsunawaki *et al.*, 2004; Watanabe *et al.*, 2004; Orciuolo *et al.*, 2007). Finalmente cabe destacar que hay dos publicaciones en las cuales se ha detectado la presencia de la toxina en tejido pulmonar y suero de ratones y paciente que sufren IPA, llegando a cuantificar niveles de 166-785 ng/ml de toxina en ellos (Richard, Dvorak and Ross, 1996; Lewis *et al.*, 2005).

Entre las toxinas que *A. fumigatus* puede producir, se va a prestar especial atención a la fumagilina a continuación por tener especial relación con el tema de la presente tesis doctoral

1.4.5.1 Fumagilina

La fumagilina es una micotoxina producida por *A. fumigatus* y sus características, biosíntesis, dianas y usos han sido revisados recientemente (Guruceaga *et al.*, 2020). Esta toxina fue aislada por primera vez en el año 1949 por Hanson y colaboradores (Hanson and Eble, 1949). Desde un punto de vista químico, esta es una molécula de bajo peso molecular (458,4 g/mol) y su estructura se compone de un ácido decatetranodioico conectado a un ciclohexano mediante un enlace éster. El

ciclohexano a su vez posee un grupo metoxy, un grupo epoxi y una cadena alifática derivada de un terpeno que a su vez contiene otro grupo epoxi. Estos epóxidos son los responsables de conferir inestabilidad a la molécula (**Fig. 8**). Así mismo, esta molécula presenta una baja solubilidad en agua (3,3 mg/L), pero puede ser disuelta en solventes orgánicos como puede ser el etanol o el DMSO.

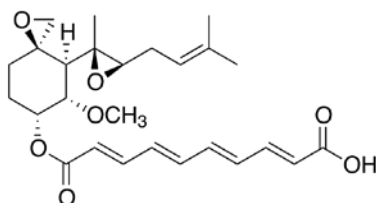


Figura 8. Estructura química de la fumagilina (Extraído de Guruceaga *et al.*, 2020).

La parte ácida de la molécula es muy interesante desde el punto de vista cromatográfico, ya que es la responsable de que esta micotoxina tenga capacidad de absorber la luz ultravioleta en un rango de longitud de onda que varía desde 335nm hasta 350 (Garret and Eble, 1954) siendo el pico de absorción característico el que se muestra en la **Fig. 9**.

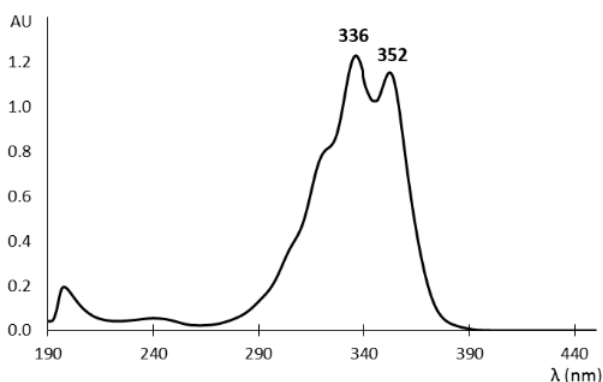


Figura 9. Espectro de absorción de la fumagilina a pH 2 (Extraído de Guruceaga *et al.*, 2020)

1.4.5.2 Biosíntesis de la molécula

La información genética necesaria para llevar a cabo la producción de la micotoxina por parte de *A. fumigatus*, se encuentra recogida en lo que se denomina un *supercluster* de genes. Este *supercluster*, localizado en el cromosoma 8 del hongo, contiene los genes necesarios para la producción de tres micotoxinas: fumitremorgina

B, pseurotina A y fumagilina (Perrin *et al.*, 2007; Wiemann *et al.*, 2013). Dentro del *supercluster*, el *cluster* de genes de biosíntesis de la fumagilina se le conoce con el nombre de *cluster fma* y está formado por 15 genes (Afu8g00370-Afu8g00520) tal y como se muestra en la **Fig. 10**.



Figura 10. Esquema del cluster *fma* de producción de fumagilina de la cepa de *A. fumigatus* Af293. Verde: genes implicados en la ruta de biosíntesis; Azul: gen regulador; Gris y Negro: otros genes relacionados con la biosíntesis de fumagilina; Blanco: genes no relacionados con la biosíntesis de la micotoxina (Extraído de Guruceaga *et al.*, 2020).

A diferencia de otros cluster biosintéticos de otros metabolitos, se ha detectado que el *cluster fma* se encuentra entrelazado con el *cluster* de biosíntesis de pseurotina A, ya que se encuentran genes de la biosíntesis de la segunda micotoxina dentro de el mismo (Wiemann *et al.*, 2013a). Además, investigaciones llevadas a cabo por dos grupos de investigación en los cuales se desarrollaron cepas mutantes de delección de los genes del *cluster*, describieron como el gen regulador de la biosíntesis *fumR/fapR*(Afu8g00420) regula tanto la biosíntesis de fumagilina como de pseurotina A (Dhingra *et al.*, 2013; Wiemann *et al.*, 2013a). A pesar de que tras la delección de varios de los genes del cluster se observó que la micotoxina no se formaba, la delección de *fumR* supuso un silenciamiento de la expresión de las rutas biosintéticas tanto de la fumagilina como de la pseurotina A (**Tabla 1**)

Tabla1. Lista de genes/proteínas involucrados en la biosíntesis de la fumagilina

	Nombres del gen	Nombre de la proteína	UniProtKB^d	Fenotipo del mutante
Afu8g00370	<i>fma-PKS</i>	Fma- <i>PKS</i>	Q4WAY3	No productor de fumagilina Producción de fumagilol
Afu8g00380	<i>fma-AT</i>	Fma- <i>AT</i>	Q4WAY4	No productor de fumagilina Producción de fumagilol
Afu8g00390 /00400	<i>fmaD</i>	Fma- <i>MT</i>	A0A067Z9B 6	No productor de fumagilina Producción de dimetil-fumagilina
Afu8g00410	<i>metAP</i>	MAP2-1/MetAP2-1	Q4WAY7	
Afu8g00420	<i>fumR</i>	FumR	Q4WAY8	<i>Cluster</i> de genes de fumagilina y pseurotina silenciados
Afu8g00430		EthD domain-containing protein	Q4WAY9	
Afu8g00440	<i>psoF</i>	PsoF	Q4WAZ0	No productor de pseurotina
Afu8g00460	<i>fpaI</i>	Methionine aminopeptidase	Q4WAZ1	
Afu8g00470	<i>fmaE</i>	Fma- <i>ABM</i>	Q4WAZ2	No productor de fumagilina Acumulación de pre-fumagilina
Afu8g00480	<i>fmaF</i>	Fma- <i>C6H</i>	Q4WAZ3	No productor de fumagilina Acumulación de 6-demethoxy-fumagilina
Afu8g00490	<i>af490</i>	Fma- <i>KR</i>	Q4WAZ4	Muy baja producción de fumagilina m
Afu8g00500		Acetate-CoA ligase, putative	Q4WAZ5	
Afu8g00510	<i>fmaG</i>	Fma- <i>P450</i>	Q4WAZ6	No productor de fumagilina, Acumulación de β -trans-bergamoteno
Afu8g00520	<i>fma-TC</i>	Fma- <i>TC</i>	M4VQY9	No productor de fumagilina

1.4.5.3 Ruta biosintética de la fumagilina

La ruta biosintética de producción de la toxina ha sido descrito por tres grupos de investigación (Dhingra *et al.*, 2013; Lin *et al.*, 2013, 2014; Wiemann *et al.*, 2013a). Esta ruta de biosíntesis necesita de dos componentes principales para poder generar la fumagilina: un sesquiterpeno y un poliquetido derivado del ácido tetraenoico. Estos se producen independientemente por dos vías diferentes (Lin *et al.*, 2013, 2014) y posteriormente se unen por esterificación. El resumen de la ruta biosintética se puede observar en la **Fig. 11**.

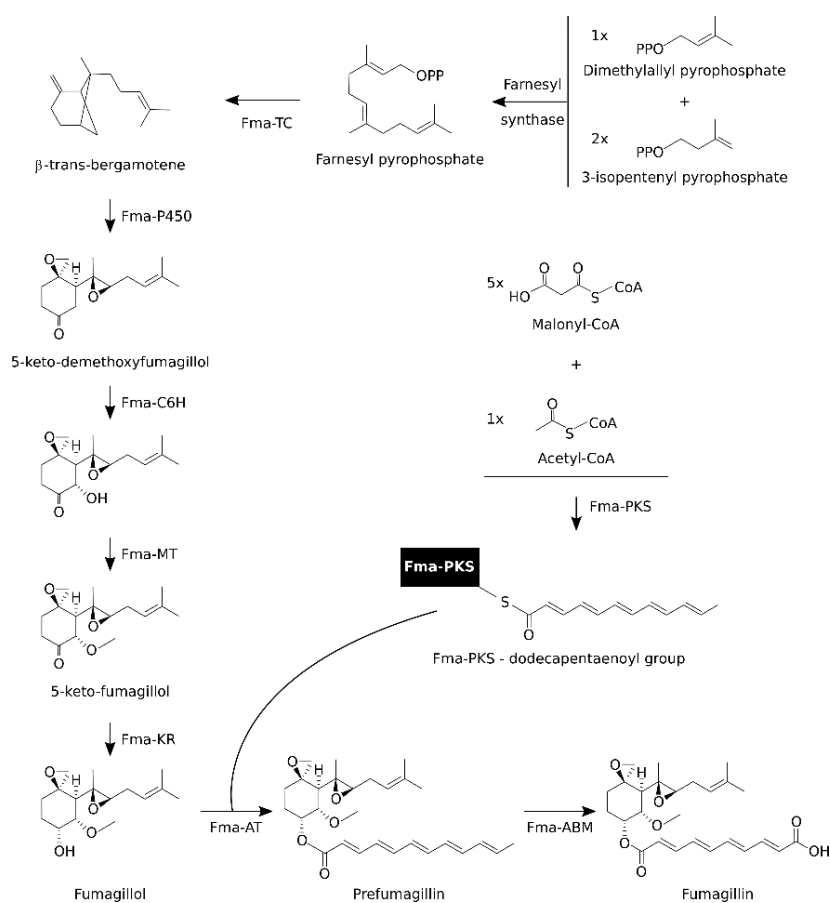


Figura 11. Ruta biosintética de la fumagilina (Extraído de Guruceaga *et al.*, 2020).

1.4.5.4 Regulación del *cluster* genético de biosíntesis de la fumagilina

Anteriormente ya se ha apuntado en varias ocasiones que los hongos filamentosos en general y más concretamente *A. fumigatus* cuentan con mecanismos de adaptación y respuesta a los diferentes estreses ambientales que les rodean (Lind *et al.*, 2016). El caso de los SM no iba a ser diferente, y los estreses externos al hongo como puede ser la temperatura, el pH, las fuentes de carbono y nitrógeno presentes, etc. también modulan el metabolismo secundario, pero no se conoce con precisión la manera en que influyen sobre la producción de los SM (Guruceaga, Perez-Cuesta, *et al.*, 2020).

Centrando la atención exclusivamente en la regulación génica del *cluster* biosintético de la fumagilina, se ha descrito como FumR regula la expresión de los *cluster fma* y pseurotina A (Dhingra *et al.*, 2013; Wiemann *et al.*, 2013a). Por otra parte, se ha descrito en diversos estudios como existe un regulador, LaeA, que controla de manera general la regulación del metabolismo secundario y en consecuencia también regula a FumR (Bok and Keller, 2004; Jin *et al.*, 2005; Keller *et al.*, 2006; Perrin *et al.*, 2007; Bayram *et al.*, 2008; Amaike and Keller, 2009). Realizando estudios de delección del gen *laeA*, se ha descubierto que esta metiltransferasa reguladora controla la expresión de al menos el 9,5% del genoma total del hongo y del 20%-40% de los genes implicados en la biosíntesis de SM (Perrin *et al.*, 2007). Por tanto, se podría concluir que el *cluster* biosintético *fma* está regulado directamente por el factor de transcripción FumR que a su vez está regulado por la metiltransferasa LaeA.

1.4.5.5 Metionin-aminopeptidasas como diana celular de fumagilina

Las Metionin-aminopeptidasas (MetAP) son una familia de enzimas proteolíticas intracelulares que llevan a cabo una función muy importante realizando modificaciones post-transcripcionales y co-traduccionales de las proteínas sintetizadas (Mauriz *et al.*, 2010). Además, cumplen una función esencial en la síntesis de las nuevas proteínas ya que controlan la hidrólisis de la metionina inicial (iMet) localizada en el extremo N-terminal de estas (Mauriz *et al.*, 2010; Vetro *et al.* 2004). La correcta escisión de la iMet es necesaria para que se expongan correctamente los

residuos de glicina y permitir la correcta asociación de esta con las membranas celulares u otras proteínas (Vetro *et al.*, 2004).

Existen dos tipos de estas enzimas, MetAP1 y MetAP2 (Arfin *et al.*, 1995). A pesar de que ambas cumplen la misma actividad enzimática, presentan distinta especificidad por los sustratos. MetAP2 es la única responsable del procesamiento N-terminal de las proteínas sintetizadas de *novo*, mientras que MetAP1 realiza la misma actividad en la mayoría de las proteínas (Chang, Teichert and Smith, 1992; Chen, Vetro and Chang, 2002). Estructuralmente son parecidas, con pequeñas diferencias en el dominio de inserción helical de la superficie (Walker and Bradshaw, 1999; Lowther and Matthews, 2000; Catalano *et al.*, 2001). Hay que destacar que no siempre se expresan ambos tipos de MetAP simultáneamente, las Eubacterias únicamente expresan MetAP1, las Arqueobacterias solo MetAP2 y las células eucariotas ambos tipos (Datta *et al.*, 1989; Ray *et al.*, 1992; Bradshaw, Brickey and Walker, 1998; Endo *et al.*, 2002).

Aunque la proteína MetAP1 es muy interesante, clásicamente se ha estudiado más la MetAP2 por su capacidad de inhibir la angiogénesis y la proliferación celular. En 1990 Ingber y colaboradores de una manera poco ortodoxa descubrieron la relación entre la MetAP2 y su capacidad de inhibir la proliferación celular. En sus estudios, algunos cultivos de células endoteliales se contaminaron con lo que identificaron como *A. fumigatus* Fresenius y observaron que alrededor del hongo había una zona de inhibición en gradiente de las células que no correspondía con la toxicidad producida por otros hongos cuando contaminaban los cultivos celulares. Hicieron estudios sobre el fenómeno observado utilizando medios condicionados donde había crecido el hongo y fueron capaces de aislar la fracción activa en la cual, finalmente, identificaron a la fumagilina como el compuesto responsable. Tras purificar la fumagilina observaron que esta era capaz de inhibir completamente la proliferación endotelial, la angiogénesis y el proceso de neovascularización inducida por los tumores (Ingber *et al.*, 1990).

No fue hasta 1997 cuando Sin y colaboradores usando un análogo de la fumagilina, conocido como TNP-470, descubrieron que la diana celular de la fumagilina es la enzima MetAP2, la cual se inactiva irreversiblemente cuando la fumagilina se une

covalentemente a su sitio activo. Para llegar a esta conclusión utilizaron modelos mutantes de delección de *S. cerevisiae* para MetAP1 y MetAP2. Al poner en contacto las cepas con la fumagilina observaron que solo las que expresaban MetAP2 se veían afectadas, siendo por tanto esta proteína la diana de la toxina (Sin *et al.*, 1997). Un año más tarde fueron Liu y colaboradores los que definieron que el sitio de unión fumagilina-MetAP2 en la histidina 231 donde se forma una unión covalente entre el anillo C3 del grupo epóxido de la micotoxina y el imidazol localizado en ese residuo de histidina (Liu *et al.*, 1998). Esta unión irreversible (Sin *et al.*, 1997; Lowther and Matthews, 2000) la podemos observar en la **Fig. 12**.

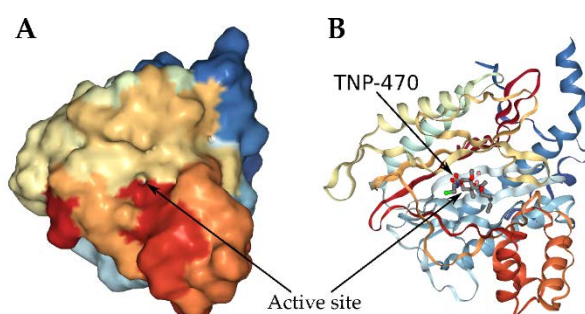


Figura 12. Representación 3D de la enzima MetAP2 humana. A) Vista frontal de la enzima donde se observa el sitio de unión de la toxina. B) Vista del análogo TNP-470 uniéndose a la MetAP2 en la histidina 231. Azul: Extremo N-terminal; Rojo: Extremo C-terminal. (Extraído de Guruceaga *et al.*, 2020).

1.4.5.6 Aplicaciones de la fumagilina

Desde que se descubrió la toxina en los años 90 esta ha sido utilizada con diferentes fines. Quizá desde el punto de vista biomédico el uso como antiangiogénico y antitumoral sea lo más destacado. Diversos estudios han probado la fumagilina y su derivado AGM-1470 en diferentes modelos de rata, de ratón y de embrión de pollo con diferentes tipos de cáncer y tumores con este propósito (Kusaka *et al.*, 1991; Sawanyawisuth *et al.*, 2007; Hou *et al.*, 2009; Kidoikhammouan *et al.*, 2019).

Por otra parte, su uso como tratamiento ante la microsporidiosis también ha sido ampliamente estudiado. El tratamiento de colmenas de abejas melíferas con fumagilina para evitar la infección de las abejas por los patógenos fúngicos del género *Microsporidia* así como diversos estudios de toxicidad de la toxina frente a las abejas han sido publicados en los últimos años (Katznelson and Jamieson, 1952; Bailey, 1953;

Hartwig, 1971; Fries, 1993; Webster, 1994; Williams *et al.*, 2008; Huang *et al.*, 2013). Además, también se ha utilizado como tratamiento frente a la microsporidiosis intestinal humanas producida por el patógeno *Enterocytozoon bieneusi* (Conteas *et al.*, 2000; Champion *et al.*, 2010; Bukreyeva *et al.*, 2017). Además se ha probado su efecto frente a diferentes protozoos parásitos como *Plasmodium falciparum* y *Leishmania donavani* (Zhang *et al.*, 2002), *Entamoeba histolytica*, *Trypanosoma brucei* y *Dictyostelium discoideum* (Hillmann *et al.*, 2015).

Finalmente cabe destacar que se ha estudiado la utilidad de esta micotoxina como tratamiento frente al SIDA, dada su capacidad para detener el ciclo celular de las células (Watanabe *et al.*, 2006) y como tratamiento frente a la obesidad dada su actividad antiangiogénica, ya que la adipogénesis se encuentra relacionada con el proceso de angiogénesis (Cao, 2007; Lijnen, Frederix and Van Hoef, 2010; Scroyen, Christiaens and Lijnen, 2010).

1.5 Estudio de los factores de virulencia

1.5.1 Estudios transcriptómicos

La secuenciación de genomas completos ha permitido entender la biología de los organismos estudiando las secuencias de nucleótidos que los componen. El producto final de los genes son las proteínas, pero para llegar a ellas hay un primer paso que es lo que se denomina transcripción, donde la información de los genes codificada en el ADN se transcribe a ARN mensajero (ARNm). En este punto se llega a una correlación directa en la cual la ausencia de un ARNm implica la ausencia de proteína, en cambio la presencia de ARNm no siempre implica que la proteína se vaya a traducir (Brazma and Vilo, 2000). Aun así, los estudios transcriptómicos permiten comprender de una manera global los genes que se están transcribiendo en una condición determinada. La mayoría de estos estudios suelen llevarse a cabo utilizando principalmente tres técnicas: RT-qPCR, microarrays de expresión y/o secuenciación de ARNs (como RNA-seq) (Breakspear and Momany, 2007).

1.5.1.1 RT-qPCR

La reacción en cadena de la polimerasa, conocida comúnmente por sus siglas PCR, fue la revolución de la biología molecular y, a partir de ella, se han desarrollado diferentes variantes. La PCR a tiempo real o cuantitativa (qPCR) es una modificación de la misma utilizada por primera vez en 1992 por Higuchi y colaboradores. Esta técnica se ha usado con diferentes objetivos y utilidades como el genotipado (Alker, Mwapasa and Meshnick, 2004; Cheng, Zhang and Li, 2004; Gibson, 2006), la determinación del número de copias de un gen en células cancerosas (Frorl *et al.*, 2005) o la cuantificación de la carga viral en muestras de pacientes (Ward *et al.*, 2004).

La combinación de la qPCR con la retrotranscripción (RT-qPCR) genera una nueva técnica con la cual se puede cuantificar la cantidad de ARNm presente en una muestra. La pandemia por el virus SARS-CoV-2 ha logrado dar fama mundial a esta técnica, ya que la detección de la carga viral en las muestras de los pacientes se realiza mediante RT-qPCR (Guruceaga, Sierra, *et al.*, 2020). No obstante, otra utilidad que guarda más relación con el presente trabajo es la de cuantificar el ARNm y, por tanto, los niveles de expresión de los genes de un organismo en una condición determinada. Esta cuantificación de la expresión es normalmente, sin embargo, una cuantificación relativa donde se compara la expresión de un gen en dos condiciones determinadas: infección vs. control, tratado vs. no tratado, enfermo vs. sano, etc.

1.5.1.2 Microarrays de expresión

La tecnología de los microarray está basada en la capacidad que tienen las secuencias de ADN o de ARN de unirse a una secuencia complementaria de la misma naturaleza. La gran ventaja que presenta este sistema frente a otras técnicas convencionales de hibridación de nucleótidos (Northern-blot, Southern-Blot, RT-qPCR, PCR...) es que permiten el análisis de genomas completos en un mismo experimento.

Un microarray de expresión consiste en una superficie sólida sobre la que se adhieren moléculas de ADN complementario (ADNc), que son moléculas de ADN de doble cadena en donde una de sus hebras es totalmente complementaria al ARN mensajero (ARNm) a partir del cual se ha sintetizado. La muestra sometida a estudio se marcará

o bien de manera enzimática o bien de manera fluorescente (la más común) y se incubará con el microarray. Los transcritos de ARNm presentes en la muestra, que previamente se habrán retrotranscrito a ADNc, hibridarán con su secuencia complementaria, que es la que se encuentra fijada en la superficie sólida, emitiendo una señal de fluorescencia que será medida por un detector. Finalmente, y tras un complejo tratamiento de datos, se realiza una cuantificación relativa de la muestra en dos condiciones. La información que se obtiene de este tipo de experimentos nos indica que genes de la muestra estudiada presentan sobre- o infra-expresión con respecto a la condición control (Sugui *et al.*, 2008; Sueiro-Olivares *et al.*, 2015; Guruceaga *et al.*, 2018).

1.5.1.3 RNA-seq

La aparición de técnicas de secuenciación de segunda generación ha dado lugar a la aparición del RNA-seq, una técnica donde se secuencian de manera masiva y paralela de todos los ARNm presentes en una muestra con un elevado rendimiento y un coste relativamente bajo permitiendo el mapeo y cuantificación de transcriptomas (Wang, Gerstein and Snyder, 2009).

A diferencia de los microarrays, mediante los cuales solo podemos medir los transcritos incluidos/representados en el sistema, el RNA-seq permite cuantificar todos los transcritos presentes en la muestra (Marioni *et al.*, 2008). Las secuencias de los ARNm obtenidas por esta técnica son generalmente cortas (alcanzando un máximo de 250 pb) pero el procesamiento en paralelo de millones de lecturas permite alcanzar una alta cobertura del transcriptoma estudiado (Mardis, 2008). De esta manera, esta técnica proporciona información sobre la estructura de los transcritos, la existencia de fenómenos de corte/empalme no descritos, y la detección de variantes genómicas en regiones codificantes (Mardis, 2008). Por el contrario, el procesamiento de todos los datos generados mediante esta técnica supone un reto bioinformático muy grande (Wang, Gerstein and Snyder, 2009).

1.5.1.4 Interpretación de los datos transcriptómicos

Comprender los procesos genéticos subyacentes a la interacción entre un patógeno y su huésped es una pieza clave para profundizar en el conocimiento de la infección. En el caso de *A. fumigatus* el estudio de esta relación es fundamental para entender mejor la AI y por tanto mejorar los diagnósticos, los tratamientos y la prevención de la enfermedad.

Los estudios de expresión realizados mediante RT-qPCR son estudios sencillos desde el punto de vista de interpretación porque están centrados en un gen concreto o en un grupo de genes. Por el contrario, el análisis transcriptómico que hay que realizar tras la utilización de un microarray de expresión o la realización de un ensayo de ARN-seq supone realizar el tratamiento de cantidades ingentes de datos de expresión.

Los ensayos transcriptómicos utilizando microarrays de expresión en *A. fumigatus* durante la primera década del siglo XXI se basaban en la descripción general de los genes diferencialmente expresados en la comparación de dos condiciones y en la descripción de las principales funciones biológicas o metabólicas implicadas en esa comparación, y en ningún caso, se profundizaba ni se buscaba un sentido biológico a los genes detectados en ellos y por qué presentaban ese patrón de expresión. De esta manera se ha comparado el transcriptoma de *A. fumigatus* creciendo a diferentes temperaturas (Nierman *et al.*, 2005), en presencia de fármacos antifúngicos (da Silva Ferreira *et al.*, 2006), comparando diferentes estadios de la germinación de la hifa (Sugui *et al.*, 2008) o incluso en contacto con células humanas (Morton *et al.*, 2011; Oosthuizen *et al.*, 2011). Hoy en día en cambio, la tendencia de este tipo de estudios ha cambiado y es complicado encontrar estudios transcriptómicos en los cuales no se seleccione un gen o grupo de genes para profundizar en el motivo de su patrón de expresión y buscar el sentido biológico a la implicación de ese gen o genes en las condiciones estudiadas (Bertuzzi *et al.*, 2014; Guruceaga *et al.*, 2018b; Furukawa *et al.*, 2020).

1.5.2 Generación de cepas mutantes de *A. fumigatus*

Para estudiar en profundidad el papel biológico de nuevos genes o nuevos factores de virulencia, hay un proceso esencial que es la generación de cepas mutantes. La disrupción de genes de interés basándose en el proceso de recombinación homóloga es la principal estrategia para estudiar la virulencia de *A. fumigatus*.

1.5.3 Método clásico

La técnica de generación de mutantes de disrupción en *A. fumigatus* consiste en la sustitución del gen diana por un gen que porte un marcador mediante recombinación homóloga. Para ello la estrategia clásica que se ha utilizado hasta el momento ha consistido en construir un constructo genético, llamado *cassete* de delección, que porta un gen marcador (normalmente un gen que confiera resistencia a un antimicrobiano) flanqueado en sus extremos 5' y 3' por regiones de 1 kb homólogas a la del gen diana.

El proceso de transformación del hongo supone realizar un paso inicial en el cual se tiene que eliminar la pared celular del hongo para facilitar que este incorpore ADN exógeno que en este caso es el *cassete* de delección. Estas células sin pared celular son las que se conocen como protoplastos y se incuban con el *cassete* de delección con el objetivo que las células lo incorporen y por recombinación homóloga este se inserte en su genoma. La inserción es dirigida por las regiones flanqueantes insertadas en los extremos del gen de resistencia, sustituyendo así al gen diana. El último paso de la transformación consiste en seleccionar las colonias mutantes añadiendo el antimicrobiano elegido como marcador de tal manera que solo aquellos protoplastos que hayan insertado el *cassete* de delección tengan la capacidad de crecer. Finalmente se debe comprobar que todas aquellas colonias resultantes capaces de crecer en presencia del antimicrobiano tienen insertado el *cassete* sustituyendo al gen diana y no en otra parte del genoma.

En los hongos en general, y también en *A. fumigatus*, el procedimiento de generación de cepas mutantes presenta una baja eficiencia porque cuentan en su genoma con la información necesaria para producir una kinasa dependiente de ADN conocida como Ku70-Ku80 encargada de la reparación del ADN evitando las pérdidas de material

genético en el genoma del hongo y que por tanto interfiere en los procesos de mutación. Para evitar este sistema de recombinación no homologa, Goldman y colaboradores (da Silva Ferreira *et al.*, 2006) desarrollaron una cepa mutante para la subunidad 80 de la proteína dimérica, inutilizando de esta manera el complejo y generando una cepa de *A. fumigatus* (\DeltaakuB^{KU80}) que ha servido como base para diversos estudios de generación de mutantes ya que en ella la eficiencia de transformación aumenta considerablemente.

1.5.4 Generación de cepas mutantes utilizando el sistema CRISPR-Cas

1.5.4.1 CRISPR-Cas como sistema de defensa en bacterias

La tecnología CRISPR-Cas (*Clustered Regularly Interspaced Palindromic Repeats-Caspase*) que hoy en día está tan de moda, realmente es una estrategia de defensa inmunitaria presente en procariontes con el que las bacterias generan memoria inmunitaria para defenderse de los bacteriófagos.

En 1987, Ishino y colaboradores describieron por primera vez la presencia de repeticiones palindrómicas en el genoma de *Escherichia coli*. No obstante, no fue hasta 2005 cuando descubrieron que esas secuencias se encontraban en un porcentaje elevado de genomas bacterianos y de arqueas (Mojica *et al.*, 2005). Finalmente, en 2007 relacionaron los genes Cas con las secuencias CRISPR concluyendo que este sistema era un mecanismo de inmunidad bacteriana frente a fagos (Barrangou *et al.*, 2007).

Este sistema funciona en tres etapas que comienza después de que la bacteria sufra una infección por un fago. A partir de ese momento la bacteria incorpora al locus CRISPR una secuencia procedente del fago llamado protoespaciador, posteriormente la bacteria expresa el CRISPR-ARN (crRNA) y el ARN transactivador (tracrRNA). Todo ello con el objetivo de que cuando la bacteria sufra posteriores infecciones por fagos, esta al contar en su genoma con una secuencia crRNA complementaria al fago, puede unirse al tracrRNA formando la secuencia guía (gRNA) que se une al genoma del fago

atrayendo hasta a ese punto a la nucleasa Cas con lo que se forma la ribonucleoproteína (RNP) con la unión de gRNA y Cas. La enzima Cas de esta RNP escindirá únicamente secuencias complementarias que contengan un motivo PAM (*Protospacer Adjacent Motif*) o una secuencia adyacente al genoma del fago, pero ausente en el locus CRISPR bacteriano (Mojica *et al.*, 2009) (**Fig. 13**).

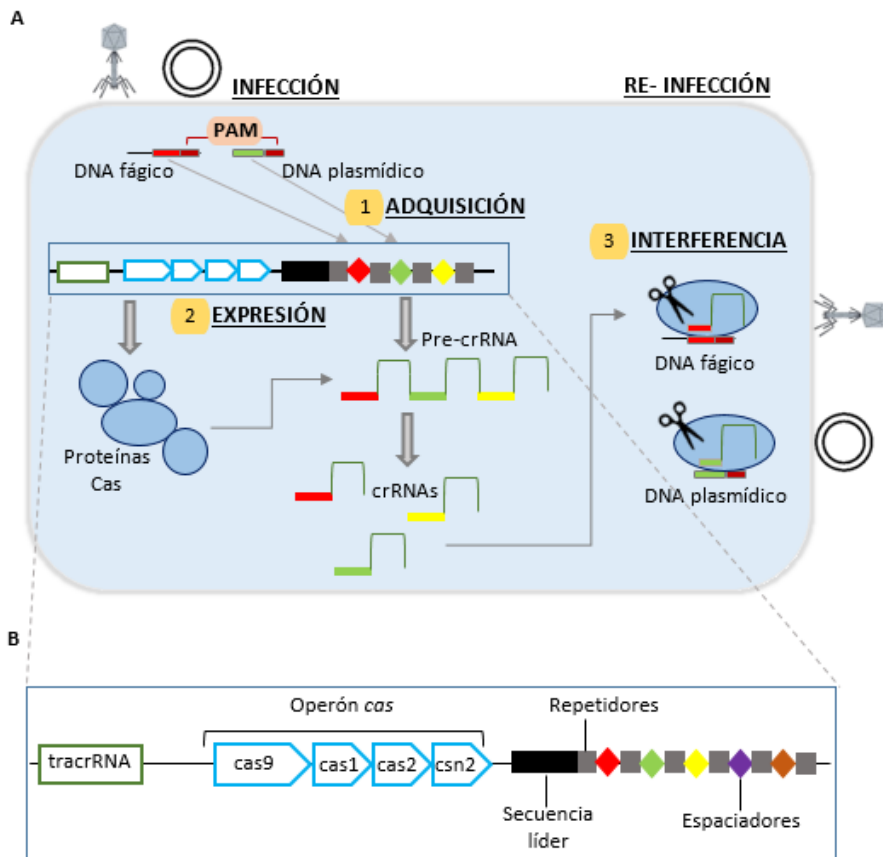


Figura 13. Estructura y actividad del sistema CRISPR-Cas9 **A)** Mecanismo de inmunidad bacteriana mediado por CRISPR-Cas9. Se muestran las etapas de adquisición de CRISPRs, biogénesis o expresión de crRNA e interferencia de DNA. El objetivo final de dicho sistema es la defensa frente a bacteriófagos y plásmidos invasores. **B)** Estructura del locus CRISPR-Cas9. Las proteínas Cas1, Cas2 y Csn2 se encargan de escindir el material genético invasor que posteriormente será incluido en el locus CRISPR como secuencia espaciadora entre las secuencias de repetición y finalmente se transcribirán en crRNAs. Por otro lado, tracrRNA se encarga de desencadenar el procesamiento del pre-crRNA así como de activar la guía del crRNA para dar lugar a la escisión generada por la endonucleasa Cas9.

1.5.4.2 CRISPR-Cas9 como herramienta para editar genomas

Tras descubrir como el sistema CRISPR-Cas funcionaba en bacterias como sistema primitivo de defensa frente a fagos (Charpentier and Marraffini, 2014), la ciencia vio la oportunidad de poder aplicar estos principios como herramienta genómica. Se ha demostrado que las secuencias guías pueden ser sustituidas *in vitro* por secuencias de interés sintetizadas según las necesidades, con el único objetivo de guiar a la enzima Cas a una región concreta del genoma donde interesa escindir la secuencia de nucleótidos (Jinek *et al.*, 2012, 2013). Para ello, purificaron la enzima Cas9 de *Streptococcus thermophilus* y de *S. pyogenes*, y la fusionaron *in vitro* con un gRNA formada por crRNA y tracrRNA sintetizados a la carta (Jinek *et al.*, 2012, 2013). Esto supuso la revolución de la ingeniería genética ya que únicamente con el diseño de crRNAs dirigidos a las zonas de interés del genoma, formaran la guía utilizando un tracrRNA que puede ser siempre el mismo, y estos a su vez la RNP con una Cas9 purificada que tampoco variará. Además, existe la posibilidad de poder hacer funcionar diferentes guías de manera simultánea en una célula (Cong *et al.*, 2013) produciendo varios cortes a la vez.

Por todo ello, en los últimos 7 años la tecnología CRISPR-Cas ha sido utilizada para modificar genéticamente plantas (Jiang *et al.*, 2013), insectos (Bassett *et al.*, 2013), ratones (Seruggia *et al.*, 2015), conejos (Honda *et al.*, 2015), cerdos (Whitworth *et al.*, 2014), monos (Niu *et al.*, 2014) y células humanas (Liang *et al.*, 2015).

1.5.4.3 CRISPR-Cas9 en hongo filamentosos

Dentro de los hongos filamentosos, *A. fumigatus* es el hongo filamentoso que más frecuentemente se aísla en pacientes con IFI, y es por ello que es el hongo filamentoso en el que más se está estudiando sus factores de virulencia y sobre el que más se ha investigado el sistema CRISPR-Cas con el objetivo de producir cepas delecionadas de algunos de sus genes. Inicialmente esta tecnología llegó para poner solución a la baja eficiencia de transformación que se obtiene con la estrategia clásica de mutación, pero las primeras veces que se utilizó no fue muy eficiente. No obstante, esta técnica, que se lleva utilizando desde 2015 (Fuller *et al.*, 2015) fue mejorada entre 2017-2018

en dos publicaciones en donde se asentaron las bases para la generación de manera muy eficiente de cepas mutantes de *A. fumigatus* (Al Abdallah, Ge and Fortwendel, 2017; Umeyama *et al.*, 2018).

La principal ventaja que presenta la realización de mutantes mediante la tecnología CRISPR-Cas es que para la construcción del cassette de delección se añade una cola con microhomología de 40 pares de bases frente a los 1000 pares de bases que se utilizan con la metodología clásica. Además, la posibilidad de guiar mediante el crRNA a la Cas9 a la zona de corte hace que la eficiencia de transformación utilizando esta técnica sea elevada. Al Abdallah y colaboradores mostraron eficiencias de entorno al 90% cuando se utiliza la cepa \DeltaakuB^{KU80} y de entorno al 75% utilizando la cepa salvaje *Af293* cuando silenciaron el gen *pksP* (Afu2g17600) involucrado en la síntesis de melanina y cuyo mutante da lugar a colonias albinas (Al Abdallah, Ge and Fortwendel, 2017).

Objetivos / Aim of the study



2. Objetivo / Aim of the study

Dado que la virulencia del hongo patógeno *Aspergillus fumigatus* es multifactorial y poligénica, los estudios transcriptómicos de genoma completo son una buena opción para profundizar en el conocimiento del proceso de patogénesis que lleva a cabo este hongo, combinándolos con la utilización de mutantes para el estudio de genes seleccionados. Por ello, el objetivo principal de este proyecto de tesis doctoral es estudiar el transcriptoma del hongo, mediante la utilización del microarray de expresión de genoma completo AWAFLUGE, en tres modelos de infección experimental con el objetivo de detectar y seleccionar genes o grupos de genes que tomen especial protagonismo en estas situaciones, así como de estudiar su actividad mediante el desarrollo de mutantes de delección/disrupción.

Para lograr este objetivo principal se han planteado los siguientes objetivos parciales:

1. Desarrollar una infección intranasal experimental en modelo de ratón inmunosuprimido para estudiar el transcriptoma del hongo durante las primeras 96 horas post-infección.
2. Estudiar el transcriptoma del hongo durante el primer contacto con dos de los tipos celulares presentes en el pulmón, macrófagos y células epiteliales, utilizando modelos de infección in vitro.
3. Profundizar en el estudio del efecto de la fumagilina como factor de virulencia durante el proceso infeccioso mediante el uso de esta micotoxina comercial y de mutantes de delección no productores de la misma.
4. Estudiar el efecto del gen *maiA* como nuevo factor de virulencia, dentro de los genes seleccionados en estudios previos de infección, mediante el uso de un mutante de disrupción.

Since the virulence of *Aspergillus fumigatus* is multifactorial and poligenic, the combination of the whole genome transcriptomic studies with the development of mutant strains of those genes selected, are a suitable approach to deepen our understanding of the pathogenesis process carried out by this fungus. Therefore, the aim of this project is to study the fungal transcriptome, by using the AWAFUGE whole genome expression microarray in three experimental infection models in order to detect genes or clusters of genes that take an important role in these situations, as well as to study their activity through the development of deletion/disruption mutant strains.

To achieve this main objective, the following partial objectives have been set:

1. To develop an experimental intranasal infection in an immunosuppressed murine model to study the *A. fumigatus* transcriptome during the first 96 hours post-infection.
2. To study the fungal transcriptome during the first contact with two of the cell types usually present in the lung, macrophages and epithelial cells, using *in vitro* infection models.
3. To deepen the study of the effect of the fumagillin as a virulence factor during the infectious process using this commercial mycotoxin and non-producing deletion mutant strains of *A. fumigatus*.
4. To study the effect of the *maiA* gene as a new virulence factor, among all the genes selected in previous infection studies, through the use of a disruption mutant.

Resultados



3.Resultados / Results

Dada la gran variedad de experimentos y la complejidad/cantidad de resultados obtenidos en el presente proyecto de tesis doctoral, estos van a ser divididos en tres capítulos. Además, con el objetivo de contextualizar los resultados cada capítulo constara de una breve introducción, un apartado de material y métodos, los resultados obtenidos y una breve discusión. El objetivo de esta distribución es facilitar al lector la comprensión de los resultados y de los experimentos que se han realizado para obtenerlos.

Due to the great variety of experiments done and the complexity/quantity of the results obtained in this Doctoral Thesis project, the results are going to be divided in three chapters. Moreover, with the aim to contextualize the results, each chapter will be composed by several sections: brief introduction, material and methods, results and brief discussion. The only proposed of this distribution is to make easy to the reader the understanding of the results and the experiments done to obtained them.

Chapter 1

A possible role for fumagillin in cellular damage during host infection by *Aspergillus fumigatus*



Results published in:

Guruceaga, X., Ezpeleta, G., Mayayo, E., Sueiro-Olivares, M., Abad-Diaz-De-Cerio, A., *et al.*, (2018) A possible role for fumagillin in cellular damage during host infection by *Aspergillus fumigatus*. *Virulence* 9: 1548–1561.

1. Introduction

The lung is the main target organ of the *A. fumigatus* and is where this fungus can cause a broad spectrum of disease, ranging from allergic responses to invasive pulmonary aspergillosis. In the bronchial tree, the combined action of the ciliated epithelium (Escobar *et al.*, 2016) and the alveolar immune cells (Philippe *et al.*, 2003) attempt to eliminate any infection potentially produced by this aetiological agent. Faced with this type of response, the fungus deploys a series of multifactorial activities including its virulence mechanisms to develop the infection, to invade tissues and to evade the immune response (Tekaiia & Latgé 2005; Osheroov 2007; Abad *et al.*, 2010; Slesiona *et al.*, 2012). In this context of host-pathogen interaction when it is necessary to know the fungal gene expression patterns in order to improve the knowledge of which genes are involved in the infection process.

There are some studies in the bibliography that have identified *A. fumigatus* protein expression patterns during host-pathogen interaction. In these studies they have identified up-regulated proteins such as allergens (Singh *et al.*, 2010), immunogenic proteins (Kumar *et al.*, 2011), new putative diagnostic targets (Virginio *et al.*, 2014) and toxins/secondary metabolites (Bignell *et al.*, 2016) among others. In addition to these findings, studies of the changes in gene expression during encounters with host tissues or in stress conditions have presented genes encoding proteins possibly involved in virulence (Oosthuizen *et al.*, 2011; Barker *et al.*, 2012; Irmer *et al.*, 2015; Sueiro-Olivares *et al.*, 2015).

It is known that a large number of modifications in the gene expression pattern are observed during the first few hours after conidia break their dormancy, most of these genes being related to fungal growth and metabolism, but not specifically to virulence (Oda *et al.*, 2016). Up to date, only a few transcriptomic experiments have been performed using *A. fumigatus* directly isolated from bronchoalveolar lavage from intranasal infection models (McDonagh *et al.*, 2008; Bertuzzi *et al.*, 2014). In consequence, the aim of this study was to describe the modifications in gene expression of *A. fumigatus* during pulmonary infection once conidia have settled in

the lung. To perform this study, a microarray analysis of *A. fumigatus* gene expression during a murine intranasal infection model was performed. In this analysis, we detected the overexpression of many of the genes involved in the fumagillin production. Furthermore, an *A. fumigatus* $\Delta fmaA$ (fumagillin null) mutant caused significantly less damage than the wild-type strain to a pulmonary epithelial cell line *in vitro*, suggesting a role for fumagillin in inducing cellular injury.

2. Material & Methods

2.1 *Aspergillus fumigatus* strains, media and growth conditions

The Af293 strain of *A. fumigatus* was grown on potato dextrose agar (Cultimed, Castellar de Vallés, Spain) at 28°C for seven days to obtain conidia for infection. After harvesting and cleaning twice with a saline-Tween solution (0.9% NaCl, 0.02% Tween 20) (SS-Tw20), the number of conidia was calculated using a haemocytometer and their viability tested by plating them onto potato dextrose agar (Cultimed) and expressed as a percentage. Furthermore, the previously published (Wiemann *et al.*, 2016) deletion mutants strains $\Delta fmaA$ (fumagillin⁻ pseurotin⁺) and $\Delta psoA$ (fumagillin⁺ pseurotin⁻), and their correspondent wild type (Wt) strain *A. fumigatus* CEA17 were used for the fumagillin ⁵¹Cr release assays and HPLC detection assays. We have also produced the complemented strain of the mutant strain $\Delta fmaA$ ($\Delta fmaA::fmaA$) as we explain in the next section. All the strains were maintained on glucose minimal medium agar (GMM) for seven days at 37°C as previously described (Fortwendel *et al.*, 2009).

2.2 Obtention of the complemented strain $\Delta fmaA::fmaA$

The extraction of DNAs from fungi and bacteria, restriction enzyme digestion, gel electrophoresis, blotting, hybridization, and probe preparation were performed by standard methods (Sambrook *et al.*, 1989; Bok *et al.*, 2004). The plasmid pJW165 for $\Delta fmaA$ complementation was generated by standard techniques. Pfu Ultra II Fusion

HS DNA polymerase (Agilent, Santa Clara, USA) was used to amplify a 3 kb fragment by *fmacomhygF* and *fmacomhygR* primers (**Table S1**), which includes *fmaA* wild type gene with its own promoter and terminator from *A. fumigatus* CEA10. This 3kb amplicon was also used as a template for Southern hybridization probe. The PCR product was inserted into the *HindIII* site of the plasmid pUG2-8 (Alexander *et al.*, 1998), which contains a hygromycin B (*hygB*) resistance gene. The *fmaA* gene in pJW165 was confirmed by sequencing before transformation as the previously published transformation method (Bok *et al.*, 2004). First, hyphae were obtained after incubating the fungus for 16 h at 37°C, 250 rpm in 100 ml of yeast peptone dextrose broth (YPD) at a concentration of 5×10^7 conidia/ml. Then, cells were harvested by filtration through Miracloth (Merck, Darmstadt, Germany), and washed with sterile H₂O. Next, fungal cell walls were enzymatically degraded using 2 g of lysing enzymes Vinotaste[®]Pro (Lamothe Abiet) in 40 ml of OM buffer (pH 5.6; 1.2 M MgSO₄, 0.1 M NaH₂PO₄) for 2-3 h at 37°C, 90 rpm. After the incubation, cold Trapping buffer (0.6 M sorbitol, 0.1 M Tris-HCl pH 7.5) was added little by little, without letting the phases mix. Samples were centrifuged in a swinging bucket rotor for 20 min at 4,000 g and 4°C, being fungal protoplasts recovered from the OM/ST interface. A volume of cold STC buffer (1.2 M sorbitol, 0.01 M Tris-HCl pH 7.5, 0.05 M CaCl₂) was added to protoplasts suspension, and centrifuged for 20 min at 1,500 g and 4°C. Protoplast pellet were gently resuspended in 10 ml of STC buffer, centrifuged again as mentioned before, and resuspended in 500 µl of STC buffer to count and adjust them to 10^8 protoplasts/ml microscopically.

Once the protoplast suspension was ready, 100 µl were gently mixed with 25 µl containing deletion cassettes or with STC for negative controls. Next, 200 µl of cold PTC buffer (0.1 ml of 1 M Tris-HCl pH 7.5, 0.1 ml of 1 M CaCl₂, 9.8 ml of PEG 60%) were added, mixed by slight inversion, and incubated 10 min in ice. After repeating this step one more time, 800 µl of temperate PTC buffer were added, mixed, and incubated 10 min at room temperature. Then, 675 µl of STC buffer were added to achieve a final volume of 2 ml. Finally, transformation reaction volume was distributed in four Petri dishes, adding 500 µl in each, containing molten agar (1 M sucrose, 0.2 % [w/v] yeast extract, 0.2 % [w/v] casaminoacids and 30% [w/v] agar). Cultures were incubated

overnight at 37°C to let the fungus recover from the process, and, the next day, 150 mg/ml of hygromycin B were added to the plates diluted in molten agar. The growth of mutant colonies was monitored daily.

Those transformants that grew at least twice in presence of hygromycin B (150 µg/ml) were confirmed first by PCR and then by Southern hybridization (**Fig. S1**). We also confirmed the restoration of fumagillin production in the complemented strain TJW199.14 (data not shown).

2.3 Animal infection

First of all, an assay to select the suitable *A. fumigatus* dose was performed. For that, 1×10^6 , 1×10^7 and 1×10^8 resting conidia of *A. fumigatus* Af293 strain per mouse were intranasally administered and survival rates studied.

Once the suitable dose was selected, three independent animal infections were carried out. For each one, ten female BALB/c mice between 16-20 g were used. Mice were kept in the General Animal Unit Service of the University of the Basque Country (UPV/EHU), with water and food *ad libitum*, handled in biological safety cabinets, and kept in sterilized cages with negative-pressure ventilation and filters. All the mice were immunosuppressed by the administration of 150 mg/Kg cyclophosphamide (Sigma-Aldrich, Madrid, Spain) intraperitoneally four days and 100 mg/Kg the day before infection. Eight mice were infected by exposing them intranasally to a 20 µl SS-Tw20 solution containing 1×10^7 resting conidia of *A. fumigatus*. The other two animals received 20 µl of SS-Tw20 without conidia and were used as controls. After infection, two animals were euthanized daily, minimizing mice suffering. Controls were euthanized on the fifth day. Subsequently, the pair of lungs of each mouse were extracted and divided into two halves. One half was used for histological diagnosis and colony forming units (CFUs) counting onto Sabouraud glucose agar with chloramphenicol plates (Cultimed). The other half was pooled with the half of the lungs of the other mouse euthanized the same day to isolate total RNA, which was kept at -80 °C into RNAlater until use (Qiagen, Valencia, CA and the USA).

2.4 Histological study

Lungs removed from mice were fixed with 10% formalin, and subsequently embedded in paraffin. After this, consecutive slices four micrometers in thickness were obtained and stained with haematoxylin-eosin (H.E.) and Grocott's silver methenamine (G.M.S.) to carry out a classic fungus histology study.

2.5 RNA isolation

Mice lung tissues conserved in RNAlater were broken and homogenized by blunt crushing in a bag (Deltalab, Barcelona, Spain), that contained 2 ml of diethylpyrocarbonate (DEPC) sterile water. The resulting material was centrifuged at 13,000 g for 3 minutes, and the pellet obtained was ground three times in the presence of liquid nitrogen using an agate mortar. Finally, total RNA was isolated using the RNeasy Plant Mini Kit (Qiagen) following the manufacturer's protocol, and the RNA quantity and integrity verified on a 2100 Bioanalyzer (Agilent Technologies, Santa Clara, CA, USA). For transcriptomic studies, microarray analysis and RT-qPCR confirmation, three independent RNA samples for each time point, each of them obtained from an independent infection, were studied.

2.6 Microarray selection and hybridization

The Agilent Whole *A. fumigatus* Genome Expression 44K v.1 (AWAFUGE) microarray was used to analyze the transcriptome profiles from each sample (Sueiro-Olivares *et al.*, 2015). From each time point studied, starting at a maximum of 100 ng per sample, RNA was labeled using the "Low Input Quick Amp WT Labeling kit, One-Color" kit (Agilent Technologies, Santa Clara, CA, USA). Then, cDNA was transcribed using T7 RNA polymerase in the presence of Cy3-CTP, and hybridized using the SureHyb hybridization chambers (Agilent Technologies) following the ozone barrier slide covers Agilent protocol. Finally, microarray slides were scanned using a GenePix 4100A scanner (Axon Instruments), and images were analyzed using the associated GenePix Pro 6.0 software (Molecular Devices).

2.7 Microarray expression data analysis

The raw intensity data obtained from each microarray was processed following the conventional scheme, using the limma library under the Bioconductor package (Schmyth *et al.*, 2004; Lopez-Romero 2011). After subtracting the background and normalizing the data set using the normexp and quantile routines, respectively, expression levels were compared using an ANOVA test with a Benjamini-Hochberg correction. The statistical significance level was fixed at 0.05. Results were expressed as \log_2 fold change, in the case of the DEGs the \log_2 fold change represents the statistical difference of expression between the first day of infection and the third and fourth days. A negative or positive value indicated down or up-regulation relative to the first day post-infection, respectively.

2.8 Gene ontology (GO) analysis

The GO enrichment of differentially expressed genes was performed using the GO Slim Mapper tool available in the *Aspergillus* Genome Database (available at <http://www.aspergillusgenome.org>). Most of them were ascribed to one of the three GO domains (Cellular Component, Molecular Function, and Biological Process), regardless of their expression pattern.

2.9 Microarray data confirmation by reverse transcription quantitative PCR

A subset of 43 genes among the total of DEGs were verified by RT-qPCR. To avoid false positives due to mouse RNA remaining in the samples, *A. fumigatus* specific primers were designed using Primer Quest Tool (available at <https://eu.idtdna.com/site>) (**Table S1**). RT-qPCR experiments and subsequent data analysis were performed following the methodology (Sueiro-Olivares *et al.*, 2015). Base on the microarrays expression results, four genes that presented stable expression level during all the experiment were selected as Housekeeping candidates (Afu2g02920, Afu3g013950, Afu3g14500 and Afu7g01580). Furthermore we added a mouse housekeeping gene

with the aim to evaluate the amount of mice RNA present in the samples (NM_019468.2).

2.10 ⁵¹Cr release cytotoxic assay

The amount of epithelial cell injury induced by conidia and hyphae was quantified by the release of ⁵¹Cr. Briefly, A549 pulmonary epithelial cell line were grown to confluence in 96-well plates containing detachable wells. The cells were incubated overnight with 1 μCi (0.037 MBq) Na₂⁵¹CrO₄ (ICN Biomedicals, Irvine, CA) per well. The following day, the unincorporated tracer was aspirated and the wells were rinsed twice with prewarmed Hanks balanced salt solution. Next, epithelial cells were incubated with 10⁵ spores per well in 100 μL tissue culture medium using either wild type *A. fumigatus* or the deletion mutant strains and the complementary strain generated in this study.

After 20 h of incubation, the upper 50% of the medium was aspirated from each well and then the wells were manually detached from one another. The amount of ⁵¹Cr in the aspirates and in the wells was determined by gamma counting. To measure the spontaneous release of ⁵¹Cr, uninfected epithelial cells exposed to medium alone were processed in parallel as control. For the initial screen of the mutants, each strain was tested in duplicate in 3 separate experiments. The percentage of specific release of ⁵¹Cr was calculated as previously described (Lopez-Bezerra & Filler 2004).

2.11 Fumagillin detection

For fumagillin analysis, co-incubation of cells and fungal strains were carried out as described in the cell damage assay above and samples from the 24 h time points were processed as follows. A549 pulmonary epithelial cells were incubated with 10⁵ conidia of either the WT or the *ΔfmaA* per well in 100 μL tissue culture medium for 24 h. As controls, cells without conidia, conidia without cells, and only media were used under the same conditions. Cells/germinated conidia and media were separated by centrifugation. Cells/germinated conidia were washed twice and resuspended in 500 μL media. Both, cells and supernatant were extracted with an equal amount of ethyl

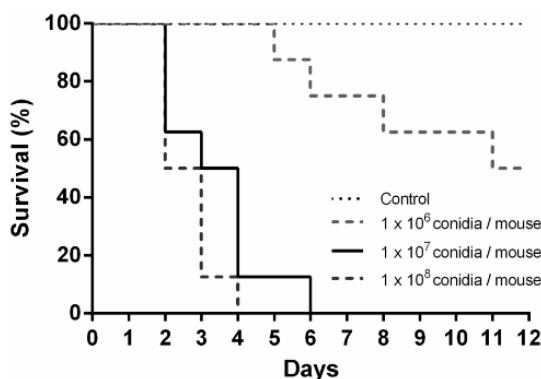
acetate, respectively. Ethyl acetate was evaporated and samples were resuspended in methanol and filtered through 0.2 μm polyvinylidene fluoride filters before high performance liquid chromatography (HPLC) photodiode array (PDA) analysis. The samples were separated on a ZORBAX Eclipse XDB-C18 column (Agilent, 4.6 mm by 150 mm with a 5 μm particle size) using a binary gradient of 0.5% (v/v) formic acid (FA) as solvent A and 0.5 % (v/v) FA in acetonitrile (ACN) as solvent B delivered by a Flexar Binary Liquid Chromatography (LC) Pump (PerkinElmer) coupled to a Flexar LC Autosampler (Perkin Elmer) and a Flexar PDA Plus Detector (PerkinElmer). The PDA was set to 340 nm which is the absorption maximum for fumagillin. Identification of fumagillin was performed using Chromera Manager (PerkinElmer) by comparison to UV peak patterns and retention time of standards, as described by (Wiemann *et al.*, 2014). The fumagillin showed a peak detected at 14.5 min.

3. Results

3.1 Survival of animals after *Aspergillus* infection, selection of doses and progression of fungal burden in the lung.

Three doses of *A. fumigatus* conidia were tested in a leukopenic mouse model of invasive aspergillosis to find the most appropriate one for transcriptomic studies.

Fig. 14 summarizes the survival results obtained with each dose of conidia used. The



selected infective dosage was 1×10^7 conidia per mouse, as it resulted in a 90% mortality after four days of infection.

Figure 14. Survival analysis of immunosuppressed mice intranasally infected with *Aspergillus fumigatus*. Mice were immunosuppressed with two intraperitoneal doses of cyclophosphamide, 150 mg/Kg and 100 mg/Kg, four days and one day before infection, respectively. Animals were infected with 1×10^6 , 1×10^7 and 1×10^8 *A. fumigatus* resting conidia/animal. Non-infected animals were used as controls. (Extracted from (Guruceaga *et al.*, 2018)).

The fungal burden in infected mice was determined by colony forming units (CFU) and histological analysis. Among all organs analyzed, CFUs were only detected in lungs, which showed a progressive decrease in the total number of CFUs recovered over time (data not shown). However, the histological evidence revealed a clear progression of the disease (**Fig. 15**). Specifically, the percentage of lung parenchyma occupied by fungal lesions in each lung sample increased approximately from 5% to 75% during the infection timeline. After the first day, the pathological findings showed most of the conidia around the edge of the airways with small areas of the lung containing germlings (**Fig. 15A**). Over the subsequent days, a rapid progression in the infection process occurred. On the second day post infection, a substantial amount of invasive hyphae were visible, concurrent with the beginning of tissue necrosis (**Fig. 15B**). On the third day, apparent histological necrosis, together with small foci of vascular congestion and hemorrhage, and both arterial and venous angioinvasion obstructing the vascular lumen were seen (**Fig. 15C**). By the fourth day, hyphae had invaded a significant area of lung tissue, encompassing nearly 75% of the parenchyma (**Fig. 15D**). These findings are theoretically compatible with severe respiratory failure and subsequent acute respiratory distress-like syndrome, and death. In no case mice reach this point and always ethical statements were followed. Furthermore, the observed lack of a significant inflammatory response was probably caused by the correct immunosuppression supplied to mice. Finally it is important to highlight that the reduced in the number of CFUs observed could be due to the *A. fumigatus* mycelia ability to hold together being therefore very difficult a correct CFUs stimulation.

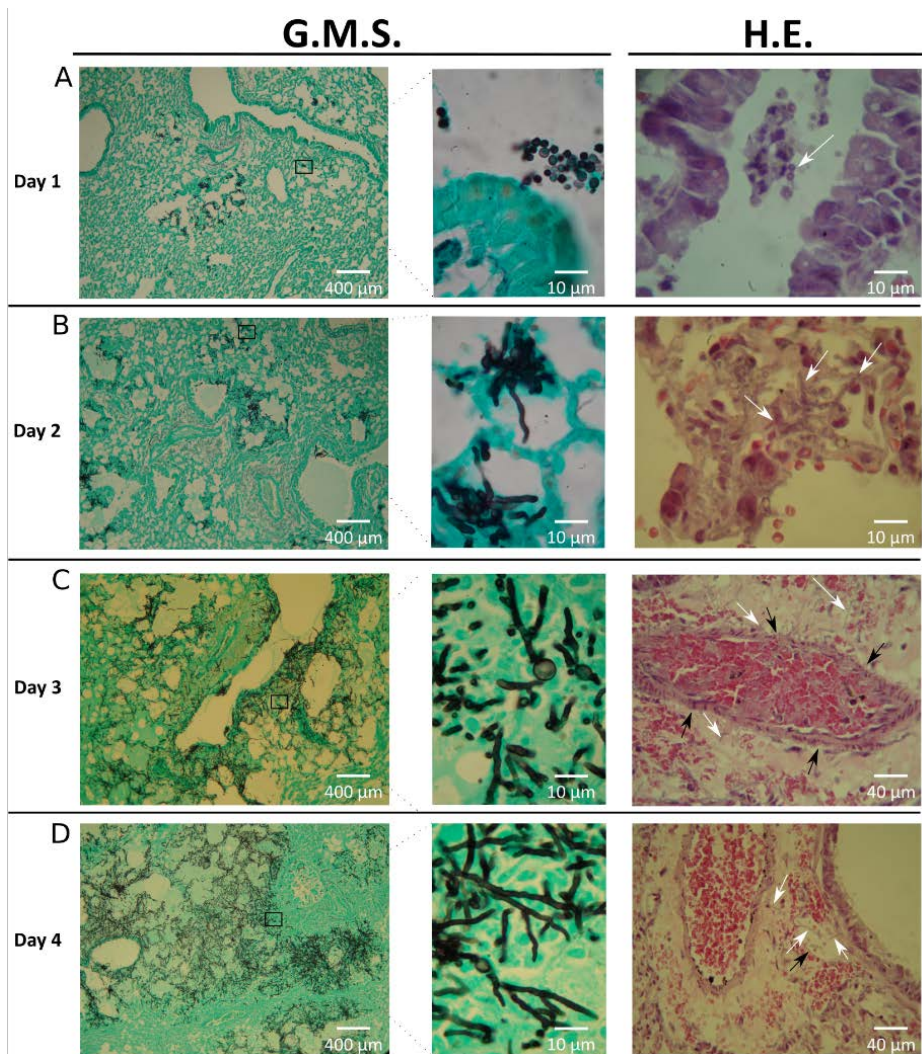


Figure 15. Histology of infected lungs. To study the fungal progression and the subsequent tissue damage, lung slices were stained with Grocott's methenamine silver (G.M.S.) and haematoxylin-eosin (H.E.). White arrows show: (A) conidia in the lumen airways, (B and C) hyphae in lung parenchyma, (D) hyphae in lung parenchyma and inside venous vessels. Black arrows show vascular walls: (C) arterial and (D) venous vessels. (Extracted from (Guruceaga *et al.*, 2018))

3.2 Genes differentially expressed during the progression of lung infection after intranasal exposure to *A. fumigatus* conidia.

Of the 9,630 *A. fumigatus* genes represented in the AWAFUGE microarray, only 103 were statistically differentially expressed genes (DEGs) ($p < 0.05$) on day 3 and 4 (72 and 96 h) compared to the first day post infection (24 h).

Among these, 18 genes were down-regulated during infection, ten of them detected on both the third and fourth day (**Table S2**). More than 70% of DEGs were not associated with any GO term (**Fig. 16A, 16B and 16C**). In fact, regarding the concrete function of each down-regulated DEG, 61% (11 out of 18) codify for hypothetical proteins. The rest of the genes encoded two pectin lyases (Afu5g10170 and Afu5g10380), one C6 transcription factor (Afu5g00950), one a dehydrogenase involved in the biosynthesis of the ergot alkaloid fumigaclavine, (*fgaDH* gene, Afu2g18000) (Wallwey *et al.*, 2010), one oxidase (Afu3g09500), one acetyltransferase (Afu1g09260) and an ankyrin repeat protein (Afu7g08610) (**Table S2**).

More numerous than the former group of genes were 85 genes found to be up-regulated (**Table S3**). Of these, 41 genes were up-regulated at 72 h post-intranasal exposition, 78 genes at 96 h and 33 genes on both days, compared with 24 h. In the GO enrichment study of biological process of this group of genes, more variability in the categories than down-regulated genes were observed in spite of the fact that more than 40% of annotations were also unknown (**Fig. C16**). Around 20% of the up-regulated DEGs were related to fungal structural components such as cytosol, nucleus, cell wall and plasma membrane, while only 5% were related to mitochondria. Interestingly, 20% of the DEGs were predicted to be involved in molecular lytic functions (hydrolase and peptidase activities) and around 15% in secondary metabolism (**Fig. 16D, 16E and 16F**).

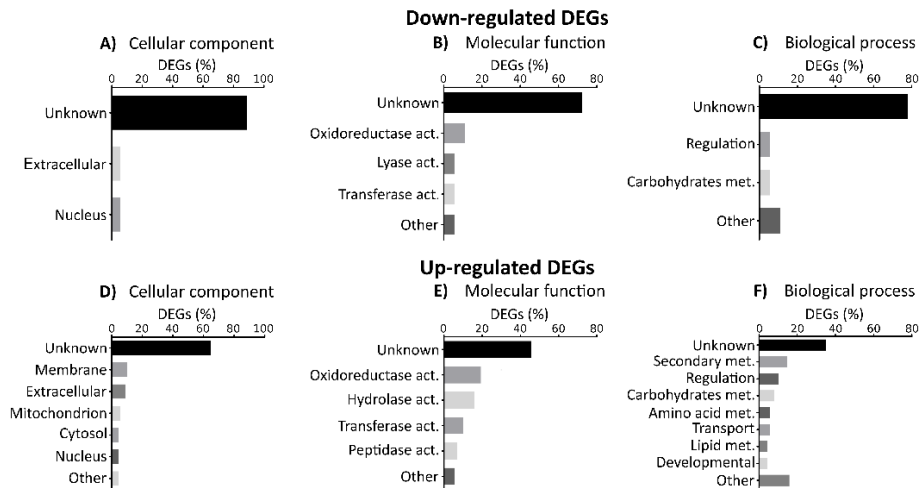


Figure 16. Gene ontology enrichment of differential expressed genes (DEGs). Percentage of down-regulated and up-regulated genes belonging to one of GO categories: (A and D) cellular components, (B and E) molecular functions and (C and F) biological process. The graphics only included the most representative groups (>4%). (Extracted from (Guruceaga *et al.*, 2018))

Remarkably, the up-regulated DEGs group contained 14 genes (out of 21) of the intertwined fumagillin/pseurotin gene cluster (Table 2). These included the fumagillin/pseurotin transcription factor FumR (Wiemann *et al.*, 2013; Dhingra *et al.*, 2013), four fumagillin biosynthetic genes, one of the two non-canonical methionine aminopeptidase encoding genes located inside the supercluster region, implicated to convey fumagillin resistance (*metAP*; Afu8g00410), five pseurotin biosynthetic genes and three genes of unknown function. Additional DEGs included genes codifying for hydrolytic enzymes such as DppIV (Afu4g09320), DppV (Afu2g00930), the allergens Asp f 1 (Afu5g02330) and Asp f 5 or elastinolytic metalloproteinase Mep (Afu8g07080) and the chitinase ChiB1 (Afu8g01410), among others (Table S2).

Table 2. Results of Differential Expressed Genes (DEGs) detected using microarray technologies versus expression data using specific primers in RT-qPCR.

Product description ^b	Systematic Name ^c	Standard Name ^d	Fold Change ^a			
			Day3 vs Day1		Day4 vs Day1	
			AWAFUGE	RT-qPCR	AWAFUGE	RT-qPCR
Fumagillin/Pseurotin pathway						
Polyketide synthase	Afu8g00370	<i>fma-PKS / fmaB</i>		6.28	5.66	7.10
O-methyltransferase	Afu8g00390	<i>fmaD</i>	6.37	7.97	5.71	8.46
Hypothetical protein	Afu8g00400		7.8	15.90	6.84	16.23
Methionine aminopeptidase. type II	Afu8g00410	<i>metAP / fpall</i>	4.53	5.03	4.09	4.88
C6 finger transcription factor	Afu8g00420	<i>fumR / fapR</i>	4.28	5.48		5.52
Hypothetical protein	Afu8g00430		7.21	9.52	6.97	9.61
Steroid monooxygenase	Afu8g00440	<i>psoF</i>	5.22	8.63	4.89	9.05
Phytanoyl-CoA dioxygenase family protein	Afu8g00480	<i>fmaF</i>	4.63	11.24	4.65	11.56
Acetate-CoA ligase	Afu8g00500		5.03	9.95	4.68	10.36
Cytochrome P450 oxidoreductase OrdA-like	Afu8g00510	<i>fmaG</i>	5.87	11.07	5.02	10.92
α/β hydrolase	Afu8g00530	<i>psoB</i>	5.41	8.30	5.29	8.47
Methyltransferase	Afu8g00550	<i>psoC</i>	7.09	10.12	6.90	10.70
Cytochrome P450 oxidoreductase	Afu8g00560		4.61	ND	4.46	ND
Glutathione S-transferase like	Afu8g00580	<i>elfB / psoE</i>	5.06	9.48	4.96	9.87
Lytic enzymes						
Secreted dipeptidyl peptidase DppV	Afu2g09030	<i>dppV</i>	3.47	3.25	3.92	3.83
Vacuolar carboxypeptidase Cps1	Afu3g07040	<i>cps1</i>			2.82	3.43
Extracellular dipeptidyl-peptidase Dpp4	Afu4g09320	<i>dppIV</i>			3.50	0.63
Extracellular lipase	Afu5g02040		3.93	3.20	4.21	3.97
Major allergen and cytotoxin Asp f 1	Afu5g02330	<i>aspf1</i>			4.64	4.09
Lipase	Afu7g04020		5.64	3.62	5.95	4.90
Class V chitinase ChiB1	Afu8g01410	<i>chiB1</i>			3.50	5.17
Elastinolytic metalloproteinase Mep	Afu8g07080	<i>Mep</i>			3.88	3.59
Others						
Acetyltransferase. GNAT family family	Afu1g09260		-3.40	1.43	-3.05	4.12

Hypothetical protein	Afu1g10450		-3.39	-0.41	-3.39	-0.23
Methionine aminopeptidase, type II	Afu2g01750		3.60	2.37	4.10	3.02
4-hydroxyphenylpyruvate dioxygenase	Afu2g04200	<i>hppD</i>			4.21	4.87
Maleylacetoacetate isomerase MaiA	Afu2g04240	<i>maiA</i>			3.72	3.79
Hypothetical protein	Afu2g16440		-3.35	0.58	-3.66	0.73
Short chain dehydrogenase/ oxidoreductase CpoX2	Afu2g18000	<i>fgaDH</i>	-3.43	1.01	-3.31	-0.17
Hypothetical protein	Afu3g00410				-3.47	0.06
MFS sugar transporter	Afu3g03700		3.39	2.31	3.77	3.65
C6 sexual development transcription factor NosA	Afu4g09710	<i>rosA</i>			3.87	6.59
C6 transcription factor	Afu5g00950		-3.71	1.26	-4.09	0.72
Hypothetical protein	Afu5g08800		3.99	4.82		
Pectin lyase	Afu5g10170				-3.79	-4.50
Pectin lyase	Afu5g10380				-3.57	-3.31
C6 transcription factor	Afu5g14290		4.36	1.16		
Aldehyde dehydrogenase	Afu7g01000				4.11	7.86
Indoleamine 2,3-dioxygenase	Afu7g02010		4.19	5.94	5.72	8.21
Defensin domain protein	Afu7g05180		5.06	6.71	4.81	4.21
Integral membrane protein Pth11-like	Afu7g06620		3.41	4.72	3.38	4.41

^aThis value represents the difference of the fold change in log₂ obtained for each gene between days of infection compared in each case. A negative or positive value indicated down or up-regulation relative to the first day post-infection respectively. AWAFUGE: data obtained with Agilent Whole *A. fumigatus* Genome Expression 44K v.1; RT-qPCR: data obtained with RT-qPCR using the *A. fumigatus* specific primers designed.

^bProduct description of the genes found on the microarray following RefSeq nomenclature.

^cSystematic name of the gene following AspGD nomenclature.

^dGene name following AspGD nomenclature (<http://www.aspergillusgenome.org>), except fumagillin/pseurotin pathway that also included the nomenclature published by (Wiemann *et al.*, 2013).

3.3 RT-qPCR verification of microarray data.

Since traces of mouse RNA in analyzed microarray samples could remain and lead to bias due to cross-hybridization phenomena, a RT-qPCR confirmation assay was designed to estimate the accuracy of the obtained microarray results. Forty-one genes were confirmed by RT-qPCR, including most of those related to the production of fumagillin and pseurotin (**Fig. 17**), the hydrolytic enzymes, a few transcription factors and some metabolic enzymes detected on the microarray. The analysis revealed that 90% of the genes selected exhibited the same expression pattern as the microarray (**Table 2**). In addition, the genes selected as fungal housekeeping (Afu2g02920, Afu3g013950, Afu3g14500 and Afu7g01580) did not vary in their expression, and none of the *Aspergillus* specific primers showed RT-qPCR amplifications in the non-infected mouse RNA samples (data not shown).

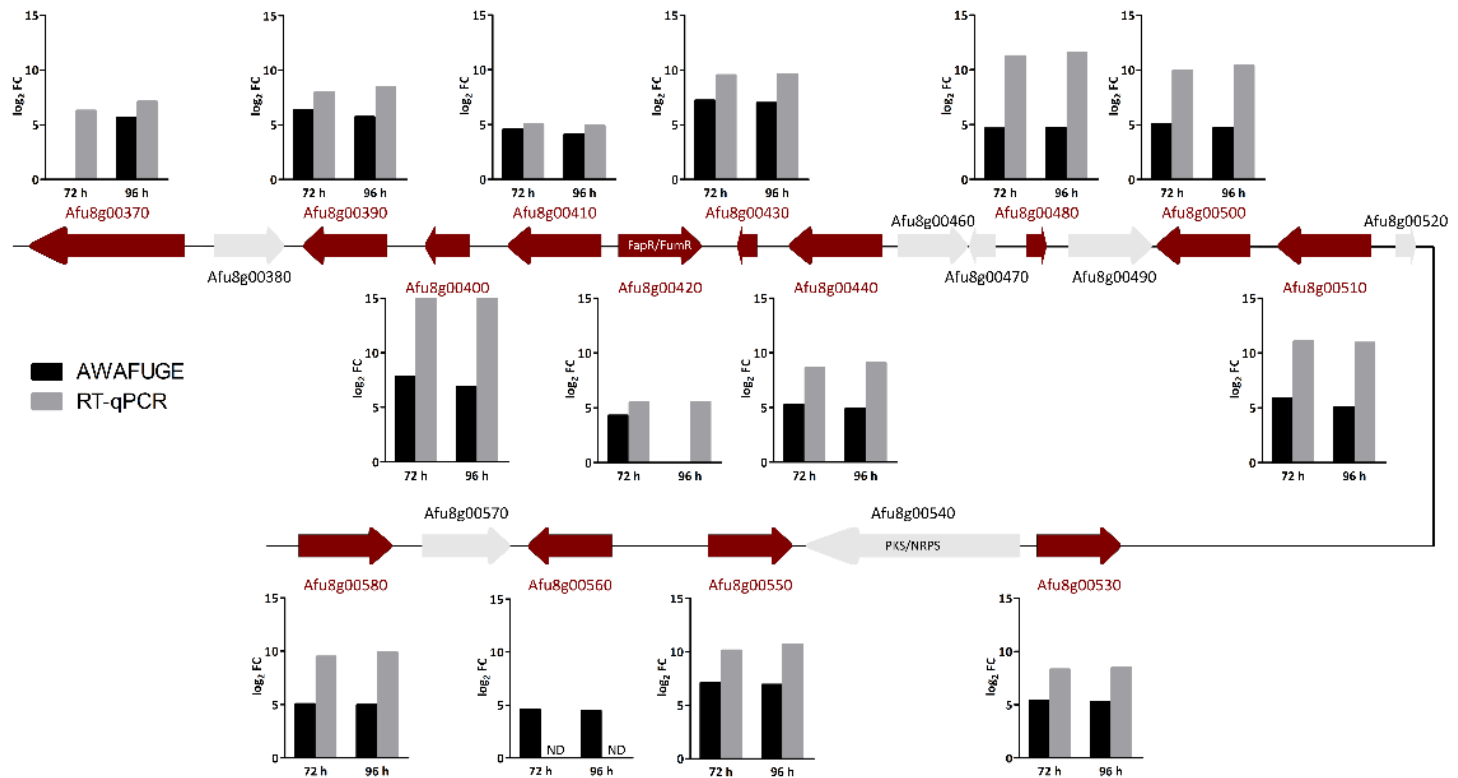


Figure 17. Schematic representation of the intertwined fumagillin/pseurotin gene cluster. Red arrows indicate the up-regulated DEGs relative to the first day post-infection. Graphics represent the log₂ fold change (FC) obtained by AWAfUGE microarray and RT-qPCR assays. FumR is the transcription factor that regulates fumagillin and pseurotin production. PKS/NRPS regulates pseurotin production. ND: Not determined by RT-qPCR. (Extracted from (Guruceaga *et al.*, 2018))

3.4 Fumagillin production is associated with cytotoxicity in an *in vitro* infection model of a pneumocyte cell line.

The observation that over half of the fumagillin/pseurotin cluster genes were significantly upregulated during infection led us to query if either metabolite could be elucidating/ causing a host response. To address a possible role of either metabolite in host cell damage, we analyzed the interactions with the A549 pulmonary epithelial cell line of Wt strain of *A. fumigatus*, $\Delta fmaA$ strain, which still produces pseurotin, and a new pseurotin mutant strain, $\Delta psoA$, which still produces fumagillin (Wiemann *et al.*, 2013).

First, the extent of epithelial cell injury was assessed by the ^{51}Cr release method and the cytotoxic effect of each mutant was compared with the WT strain (**Fig. 18A**). After 20 h of infection, the $\Delta fmaA$ strain caused significantly less epithelial cell injury than the wild-type strain, while the damage caused by $\Delta psoA$ strain was similar to that of the WT. In a separate set of experiments, complementing the $\Delta fmaA$ strain with an intact copy of *fmaA* was found to restore its capacity to damage the epithelial cells (**Fig. 18B**).

Next, we determined whether fumagillin was detected in association with A549 cells during co-incubation with *A. fumigatus*. For the WT strain, fumagillin could be detected in the absence and in presence of epithelial cells, while no fumagillin was detected from samples using the $\Delta fmaA$ strain, the cell and media controls only (**Fig. 18C**). Interestingly, in presence of epithelial cells, fumagillin was only detectable in the cell lysate but not in the media (**Fig. 18C**) while, in the absence of cells, fumagillin was detected in media when the *A. fumigatus* WT was grown. These data suggest a localization of fumagillin inside to A549 cells during co-incubation with *A. fumigatus*.

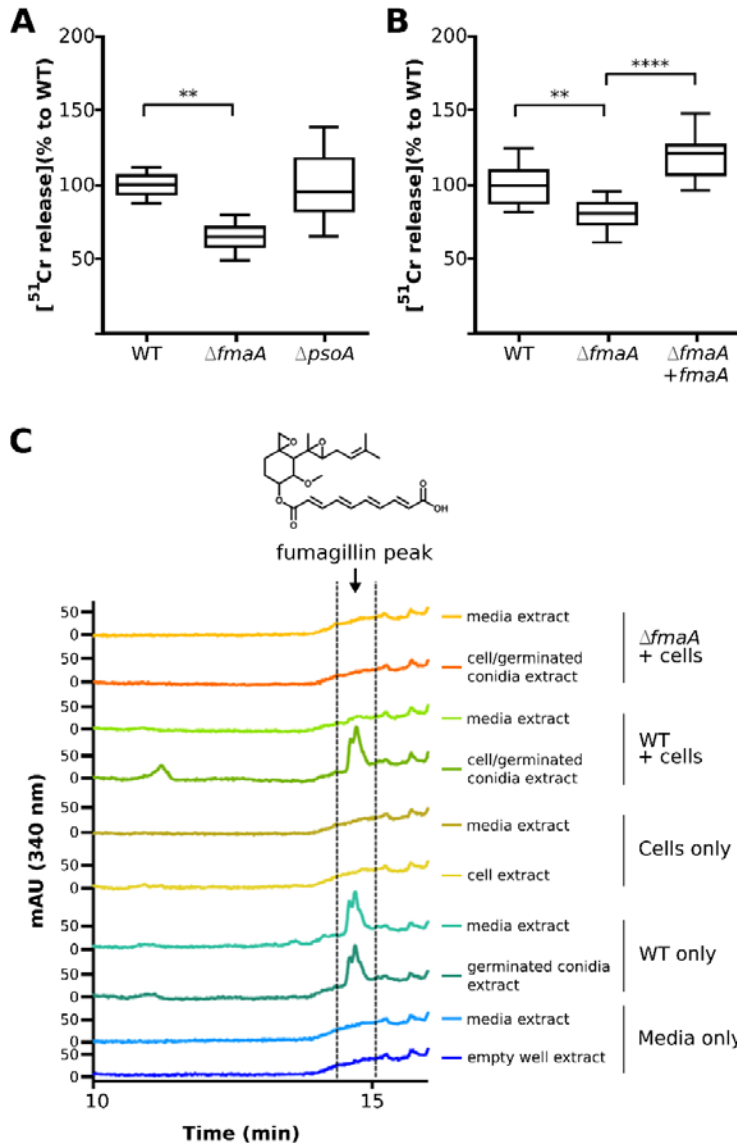


Figure 18. Cell damage and fumagillin production during co-incubation of *A. fumigatus* with A549 cells. (A and B) Extent of *A. fumigatus*-induced damage to the A549 pulmonary epithelial cell line. The indicated strains of *A. fumigatus* were incubated with A549 cells for 20h, and the extent of epithelial cell damage was determined using a ^{51}Cr release assay. Results in (A) are a box-whisker plot of three independent experiments, each performed in duplicate. Results in (B) are from three independent experiments, each performed in triplicate. ** $p < 0.01$; **** $p < 0.0001$. (C) HPLC chromatograms of indicated sample fractions from A549 cells co-incubated with *A. fumigatus* conidia after 24 h and respective controls (cells without *A. fumigatus* conidia, conidia without cells and media only). Samples were prepared as described in Material and Methods. The wavelength of the shown chromatograms was set to 340 nm, which is the absorption maximum for fumagillin detected at 14.5 min. Fumagillin was absent in the $\Delta fmaA$ mutant. (Extracted from (Guruceaga *et al.*, 2018))

4 Discussion

Fair interpretation of host-pathogen interactions and invasive aspergillosis pathogenesis requires a rigorous understanding of gene expression changes that occur during the disease progression with follow up on protein or metabolite production. Therefore, in this work, we focused on these alterations during invasive lung aspergillosis after an intranasal exposure to *A. fumigatus* conidia using a murine model with a focus on gene expression and metabolite bioactivity of the fumagillin/pseurotin gene cluster. In this way, this study might contribute to the understanding of the primary mechanisms used by *A. fumigatus* to develop an infection once conidia have entered and settled in the murine lung.

During the lung infection process, our pathological study revealed that pulmonary aspergillosis progressed daily. At the beginning of the infection, *Aspergillus* conidia were detected inside the airways, distributed into small infection loci filled with fungal germlings eliciting a low or no inflammatory response. After 24 h, vigorous growth and spread of the fungal cells occurred, including hyphae formation, causing severe respiratory tissue disruption and blood vessel angioinvasion. This progression is consistent with observations made by other studies (Ibrahim-Granet *et al.*, 2010). Concurrent with the invasion process, genes that showed differential expression between the moment when the fungus invades tissue and penetrates blood vessels (72 and 96 h post infection) compared to the beginning of the infection (24 h) were analyzed.

Of the whole genome, only 103 genes - approximately 1% of total *A. fumigatus* genes were detected as differentially expressed. Other studies reported that transcriptional changes during the initiation of invasive aspergillosis involve more than 1,000 genes. However, in those studies, the authors compared fungal growth *in vivo* (during infection) vs. *in vitro* (on culture media) (McDonagh *et al.*, 2008; Bertuzzi *et al.*, 2014). Therefore, the interpretation of these results and the subsequent conclusions have to be taken with caution, since transcriptomic studies depend on the experimental design, the time points studied and the type of reference sample used (Cairns *et al.*,

2010). Our study was designed so that the first day of infection was used as reference, this was to avoid comparisons with *in vitro* conditions which may have led to differences connected to the culture conditions but not to the infectious process. In this way, we try to explain the transcriptomic changes during the progression of the infection, and we ignore the adaptive process (first 24 h).

To avoid biased interpretations due to cross-hybridization with traces of mouse RNA that could remain in some samples, we confirmed the result of the most relevant genes identified after microarray analysis by RT-qPCR using fungal-specific primers. Our results support the utility of the microarray data as an initial screening tool to point out the most relevant genes during infection progression. In fact, 92% of the genes identified by microarray analysis could be confirmed by specific RT-qPCR. This assessment is particularly critical because most of the detected genes in our study have been implicated in lung invasive aspergillosis previously (da Silva Ferreira *et al.*, 2006; Oosthuizen *et al.*, 2011; Rokas *et al.*, 2012).

As observed in other studies, we found that many of the differentially regulated genes encoded for hypothetical proteins (61% of the down-regulated genes - 11 genes - and 21% - 18 genes - of the up-regulated genes). Thus, these proteins may play an important role during the initial stages of lung infection as well as during the progression of the lung infection.

Of the few down-regulated DEGs with putative functions, two encoded pectin lyases, which are essential for the degradation of pectins during plant infection. Other authors describe *A. fumigatus* as a microorganism better adapted to plant decomposition than to human infection (van de Veerdonk *et al.*, 2017), so these genes might show a high basal expression, which drop dramatically during host infection.

Most of the DEGs showed significant increase in expression during the progression of the infectious disease. Among them, the 14 (out of 21) genes belonging to the intertwined fumagillin/pseurotin biosynthetic cluster were notable, including the essential transcription factor FumR (Afu8g00420) critical for the production of both metabolites (Dhingra *et al.*, 2013; Wiemann *et al.*, 2013). Our transcriptome data

showed that *fumR* expression was early with increases of expression of the *fma/pso* biosynthetic gene cluster with invasion time. Although several *A. fumigatus* secondary metabolites such as gliotoxin (Dagenais *et al.*, 2009) and endocrocin (Berthier *et al.*, 2013) have been shown to contribute to *A. fumigatus* virulence or interactions with immune cells, no studies have addressed any effects of either fumagillin or pseurotin in this regard. However the anti-angiogenic effects of fumagillin are well known (Laschke & Menger 2012; Kanno *et al.*, 2015), reducing the proliferation of endothelial cells and blood vessel formation (Ingber *et al.*, 1990; Kusaka *et al.*, 1991; Yoshida *et al.*, 1997; Chiang *et al.*, 2008; Ito 2013). Angiogenesis has been proposed as a host response to thrombosis and necrosis caused by *A. fumigatus* angioinvasion, in order to compensate for hypoxia and to achieve higher levels of effector molecules at the infection site (Ben-Ami *et al.*, 2013). Additionally, this mycotoxin promotes epithelial cell damage and slower beating of ciliary cells (Killough *et al.*, 1952; Sin *et al.*, 1997; Lin *et al.*, 2013; Jean-Michel Molina *et al.*, 2016). Purified fumagillin was shown to inhibit the immune response of larvae of the wax moth *Galleria mellonella* (Fallon *et al.*, 2011). In contrast, pseurotin, which has been poorly studied, had anti-inflammatory properties (Shi *et al.*, 2015).

To examine any possible effect of fumagillin production by *A. fumigatus* on host cells, we compared the extent of damage to a pulmonary epithelial cell line following incubation with either the Wt strain, a known non-fumagillin producer mutant, $\Delta fmaA$, or a known non-pseurotin producer mutant, $\Delta psoA$, of *A. fumigatus*. Importantly, we found that the fungus does produce fumagillin in Wt cell cultures and that the $\Delta fmaA$ mutant caused less epithelial cell damage than the wild-type strain. Our results also showed that this toxin is undetectable in the supernatant of infected cultures, indicating that it is retained on cell surface or inside the cells, thus being able to exert its toxic function. In addition, fumagillin added to A549 pulmonary epithelial cells culture disappeared progressively from the media, decreasing the concentration up to 80% in 20 h compared with controls without cells (data not shown). Moreover, it is highlighting that fumagillin was detected by HPLC in *in vitro* assays at 24 h, while transcriptomic data of *in vivo* infections showed up-regulation at 72 h compared with 24 h. Therefore, although fumagillin seems to be produced in the early stages of

infection, the expression of the fumagillin gene cluster increases as the infection progresses so their production seems to be also increased. However, animal infections with the abovementioned mutant and complemented strains will be necessary in a near future to deepen into the knowledge about this mycotoxin. In the next chapter of this doctoral thesis, other complementary studies on the effect of fumagillin on different cell lines cultures, and the effect of the loss of the fumagillin production capacity on the development of experimental infections *in vivo*.

Other up-regulated DEGs encoded putative lytic enzymes, which may be related to the invasion and subsequent destruction of the lung parenchyma. It is well known that *A. fumigatus* produces a wide range of proteases and hydrolytic enzymes to degrade the lung and liberate nutrients to enable fungal growth (Bertuzzi *et al.*, 2014; Krappmann 2016; van de Veerdonk *et al.*, 2017). However, more information is required to understand which proteases and enzymes have a role in providing nutrients to *A. fumigatus* in the human lungs (van de Veerdonk *et al.*, 2017). Regarding this group of genes in our study, two important lipase encoding genes were identified (Afu5g02040 and Afu7g04020). Lipases seems to be important molecules in the host-pathogen interaction processes (Asif *et al.*, 2006). Additionally, four of the major extracellular proteases secreted by *A. fumigatus* (DppIV, DppV, Mep or Asp f 5, and the ribotoxin Asp f 1) were also found overexpressed at the onset of our infection model. Some of them, are well-known allergens and virulence factors. In fact, the expression of Asp f 1 is greater when the transcriptomic data obtained from mice infection models are compared to *in vitro* assays (Arruda *et al.*, 1992; Gravelat *et al.*, 2008). In addition to these findings, the detection of another gene that encodes a major chitinase (chiB1), which is related to autolytic functions (Jaques *et al.*, 2003; Alcazar-Fuoli *et al.*, 2011), could indicate a partial cell wall lysis allowing the hyphal elongation during progression of invasion. Finally, it is remarkable that many of the proteins codified by these genes, such as DppV, chitinase, Asp f 5 or Asp f 1, have been previously reported as secreted antigens related to infection and are of interest for medical applications (Ramirez-Garcia *et al.*, 2018).

Furthermore, two of the six genes of the tyrosine degradation cluster (*hppD* and *maiA*) and an aldehyde dehydrogenase (Afu7g01000), a gene that is overexpressed in the presence of L-tyrosine (Schamler-Ripcke *et al.*, 2009), were DEGs, with a higher expression on the final day of infection. Interestingly, pyomelanin is derived by degradation of L-tyrosine present in the lungs of immunosuppressed patients, and has been reported to protect swollen conidia and young hyphae from reactive oxygen intermediates (Heinekamp *et al.*, 2012). Therefore, our results suggest that *A. fumigatus* could synthesize pyomelanin during lung infection to protect fungal cells during progression of invasion, and ensure an efficient dispersion. This aspect will be studied in the last chapter of this Doctoral Thesis.

In conclusion, this study suggests that gene expression and pathological changes are correlated during the development of invasive lung aspergillosis. The up-regulation of genes encoding lytic enzymes and fumagillin biosynthetic enzymes could promote angiogenesis, epithelial destruction, and lung parenchymal architecture disruption (**Fig. 19**). To our knowledge, this is the first study to propose fumagillin may be an important contributor during early stages of infection. This strategy may allow the fungus to evade some host defense mechanisms and promote fungal invasion in order to reach other organs and tissues.

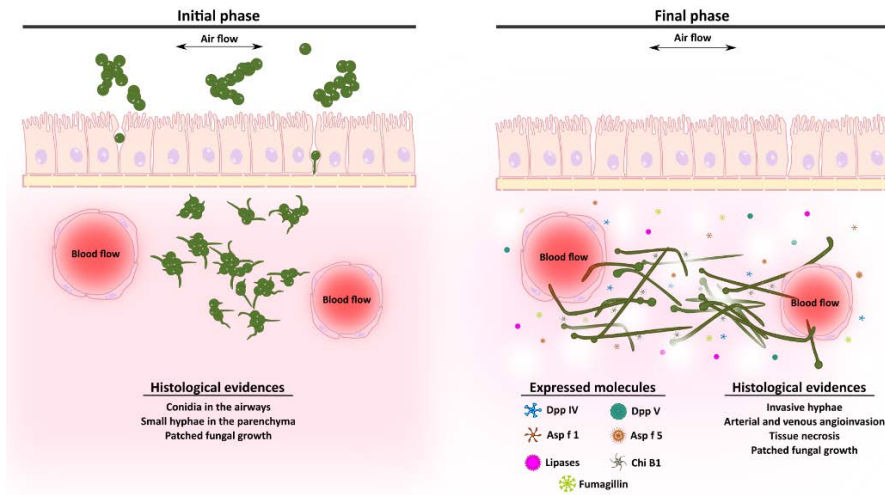


Figure 19. Scheme of the development of an *Aspergillus fumigatus* intranasal infection in a murine model. In the initial stages of the infection (1st and 2nd days), fungal conidia colonize the lung tissue and start to germinate invading the parenchyma. By contrast, during the final phase of the infection (3rd and 4th days), which are associated with angioinvasion and tissue necrosis, the fungus continues growing and forming invasive hyphae and increasing the expression of genes related to virulence such as lytic enzymes and fumagillin (Extracted from (Guruceaga *et al.*, 2018))

5. Supplementary material

Table S1. List of primers used in this study

Target ^a	Symbol ^b	Primer name ^c	Sequence (5'->3') ^d	Tm ^e
Polyketide synthase (fma-PKS)	AFUA_8G00370	8g00370F	GCCATCGATTTGATAACCT	59.00
		8g00370R	GACGCTTGACGTCTGTAGT	59.12
O-methyltransferase	AFUA_8G00390	8g00390F	CTTTGAGGAGGGAGTTGAGC	59.01
		8g00390R	TGTCTCATCCGACCAGTCAT	59.05
Hypothetical protein	AFUA_8G00400	8g00400F	ATCGAAAAGCTCCAGACGTT	57.54
		8g00400R	TCTTCTTCGTTTCCAGCGT	57.77
Methionine aminopeptidase type II (metAP)	AFUA_8G00410	8g00410F	TTCCCGAACAACCTCTATCC	58.98
		8g00410R	TTGTGAGGTGACGTTTCTC	58.85
C6 transcription factor (fumR)	AFUA_8G00420	8g00420F	CCTCCTCGTTACAGGTCGAT	59.16
		8g00420R	CGGTTGACTCGTATGGACAC	59.01
Hypothetical protein	AFUA_8G00430	8g00430F	GCCAAACTACATGCGAAGAA	58.92
		8g00430R	TCCGACGTAAGTCACGAAA	59.32
Monooxygenase	AFUA_8G00440	8g00440F	TCGAAAGGGTGATTGCCAAA	58.01
		8g00440R	AGAGAGATACACGCGGAAGA	57.96
Phytanoyl-CoA dioxygenase	AFUA_8G00480	8g00480F	TCTGGTTCCAACGTGACTGA	58.88
		8g00480R	CATGTGAGGCGCCGAATAAT	58.77
Acetate CoA ligase	AFUA_8G00500	8g00500F	AGGGGTCAAGAAGGGTGATG	59
		8g00500R	AACAGCTCCCAGACGATTGA	59.02
Cytochrome P450 oxidoreductase OrdA-like	AFUA_8G00510	8g00510F	CCCTGATCCGAGCGAAATTG	59.06
		8g00510R	TCTCGTTGCCCTGGTCATCT	59.02
Alpha/beta hydrolase	AFUA_8G00530	8g00530F	ATCCTCGGCGTTCTCAAGAA	59.1
		8g00530R	CAAGTATTCGTCGCGTCTG	59
Defensin domain protein	AFUA_7G05180	7g05180F	TCCACCTGCAACAACGTCT	59.48
		7g05180R	CATCAATCACCTCGTCGCTG	59.07
Extracelular lipase	AFUA_5G02040	5g02040F	GCAACATTTCATACCCGGACA	58.84
		5g02040R	TCTGGGCTAATGTGGCTGAA	59.01

Extracelular lipase	AFUA_7G04020	7g04020F	TGGCCATCTACCCGAAAAGT	59.01
		7g04020R	ACAAGTGACCTCATGACCGT	58.95
Methionine aminopeptidase. type II	AFUA_2G01750	2g01750F	TTTTCTCGCCGGTATCTCGA	58.90
		2g01750R	AACCCTTCACGTCAACAAGC	58.98
Secreted dipeptidyl peptidase DppV	AFUA_2G09030	2g09030F	CGTCAAATGCTGGGAGTACG	59
		2g09030R	AATTGATCATGAACCCGCCG	58.98
Elastinolytic metalloproteinase Mep	AFUA_8G07080	8g07080F	ACCTCTAACGTACACCAGC	59.11
		8g07080R	AACACCTCGTACAGCATGGA	59.03
Allergen and cytotoxin Asp f 1	AFUA_5G02330	5g02330F	CACGCCATCAAATTCGGAA	59.19
		5g02330R	TCCTTGGGTTTCTTCGAGTCA	58.96
Dipeptidyl-peptidase DppIV	AFUA_4G09320	4g09320F	CTACACCAAGCAATACCGGC	58.99
		4g09320R	CGGTGCGAATTTTCATCGACT	59
Vacuolar carboxypeptidase Cps1	AFUA_3G07040	3g07040F	GGCAGCATCGATATTGTGCT	58.77
		3g07040R	GATGATCTCGCCATGATGC	58.91
C6 transcription factor	AFUA_5G14290	5g14290F	AACGTGCAAGCCCTGTTAAG	59.05
		5g14290R	CCATGCATGAAGAAGGGACG	58.98
C6 sexual development transcription factor NosA	AFUA_4G09710	4g09710F	ACCTTTT CAGCATGACCCTCA	58.93
		4g09710R	CGATAGGTGTGGGCGAATTG	59.06
Class V chitinase ChiB1	AFUA_8G01410	8g01410F	CGGGAGTCTTCGAACAGAGT	59.12
		8g01410R	GCCATTGCGCAGGTTATCAT	59.33
C6 transcription factor	AFUA_5G00950	5g00950F	CCTCCTTTTCGTAGCCAAGC	58.91
		5g00950R	TTGTCCAGATGATCGCCGTA	58.89
Pectin lyase	AFUA_5G10170	5g10170F	CGTCACCATCTCCAACAACG	59.21
		5g10170R	AGTCCAGTAGTGCTTGCCAT	59.01
Pectin lyase	AFUA_5G10380	5g10380F	GAACAAATCCCTGATCGGCC	58.97
		5g10380R	GGTTGATGTCCGTGATAGCG	58.79
Hypothetical protein	AFUA_5G08800	5g08800F	GTCATCAAACCGCCCTCATC	58.98
		5g08800R	ACTTGTGGCAGGCAGATAGT	59.01
Hypothetical protein	AFUA_3G00410	3g00410F	ACGTCTCCTTGAGCAAAGA	58.95
		3g00410R	TATACTGTTCGCGGCATCT	58.96

Ankyrin repeat protein	AFUA_7G08610	7g08610F	CAGCAAAGGTCGATTCAGG	58.91
		7g08610R	TTCAGCCGTAAGTTCGCC	59.13
Aryl-alcohol oxidase; vanillyl-alcohol oxidase	AFUA_3G09500	3g09500F	CTTTGGCCCTGTTATCGAGC	58.98
		3g09500R	ATCCGCTTCTCCCACTTGA	59.02
Acetyltransferase. GNAT family	AFUA_1G09260	1g09260F	ACTGTGGTCTCCTCGTCTTG	59.04
		1g09260R	TGTGCGAGGATGTCAAATGC	59.20
Short chain dehydrogenase/oxidoreductase CpoX2	AFUA_2G18000	2g18000F	GCCTGCGCCTATTTCACTAC	59.06
		2g18000R	ATTGGCGTGTGTGACTCC	59.05
Xylosidase/glycosyl hydrolase	AFUA_2G00930	2g00930F	GGGGCTCCGTATACACTGAA	58.88
		2g00930R	CCCAGCGAGACAGTAGCATA	58.97
Aldehyde dehydrogenase	AFUA_7G01000	7g01000F	CTATGACAAGTTCCTGGCGC	58.99
		7g01000R	ATCCGGTCAAATTCACCTG	58.82
Maleylacetoacetate isomerase MaiA	AFUA_2G04240	2g04240F	AATCCTCCGGTACAGTCCC	58.80
		2g04240R	GATGGTCACGGTTCTTTGG	58.83
4-Hydroxyphenylpyruvate dioxygenase	AFUA_2G04200	2g04200F	TATGCAGCGACGAACAATGG	58.99
		2g04200R	CTAAAGTGTGCGTGGTCTCG	58.94
Indoleamine 2,3-dioxygenase family protein	AFUA_7G02010	7g02010F	GCCGCTTATTCGCTCTCAA	58.99
		7g02010R	GTTGTCGTAACCAAGCCCT	58.40
Methyltransferase SirN-like	AFUA_8G00550	8g00550F	ACGTTGAAGGCGAGTTGTTG	59.06
		8g00550R	ATGGGCGAAATAGGTGATGC	58.39
Glutathione S-transferase elfB	AFUA_8G00580	8g00580F	CGACCAGTGCCGAACAATAG	59
		8g00580R	TTCGCGAATATCCAGGTGCA	58.97
Hypothetical protein	AFUA_1G10450	1g10450F	AGGGACCAGATGACGAGTTG	59.10
		1g10450R	ATCCCTTCCATGAGCGTGA	59.09
Hypothetical protein	AFUA_2G16440	2g16440F	GTTGGGCAATGTATCGACC	58.98
		2g16440R	GAGGAAGCCATGTCCGTCTA	58.89
Integral membrane protein Pth11-like	AFUA_7G06620	7g06620F	TCATCGGCGAGTACTCATCC	59.05
		7g06620R	ACTGTCTTTGAAGCGGGAGA	58.95
MFS sugar transporter	AFUA_3G03700	3g03700F	TCAGTTTAGTTGCTCCCATTGC	59.18
		3g03700R	ACCGATTCCCAACAGTATACGA	58.97

<i>fmaA</i> complementation	AFUA_8g00520	fmacomhygF	GGCATCTTTAAGCTTGAACCACTG	64.10
		fmacomhygR	CAGATACTCGG GATCTACGAAAGCTTGACGAGTCT CCAAGATGGCG	64.70
Alpha/beta hydrolase	AFUA_2G02920	H_AlphBet_F	ACTGGTCGTGACACTGTTGG	59.62
		H_AlphBet_R	CGCATTGGGATGCTAGACT	58.90
Mis12-Mtw1 family protein	AFUA_3G13950	H_Mis12_F	GCTCTCGAATTGGTTTGAC	59.68
		H_Mis12_R	ATGTTTTTCGGGTTTCGGTTT	60.57
Isochorismatase family protein	AFUA_3G14500	H_Isochor_F	GAAGAACGACGGAGTGGTAAG	62
		H_Isochor_R	CTCAGGTAGGTCCAAGTCATAAAT	62
Molybdopterin synthase small subunit CnxG	AFUA_7G01580	H_Molybdop_F	ACCAGTCTTCCAAATCCACTAC	62
		H_Molybdop_R	TAGGAAATCAAAGAGCTGGAC	62
Glucose-6-phosphate 1-dehydrogenase 2	NM_019468.2	MmF	CCTTTGGTACTGAGGGTCGT	59.03
		MmR	ATCCATTGGCAGCTTCTCT	59.08

^aProduct description of the genes chosen to verificate the microarray data following RefSeq nomenclature.

^bSystematic name of the gene following AspGD nomenclature.

^cF: Forward; R: Reverse

^dSequence of each primer.

^eTm: Melting temperature of each primer.

Table S2. Results of 18 DEGs down-regulated detected after microarrays analysis.

Product description ^b	Systematic Name ^c	Standard Name ^d	Fold Change ^a	
			Day3 vs Day1	Day4 vs Day1
Hypothetical protein	Afu3g14390		-4.72	-5.17
Hypothetical protein	Afu8g06300		-3.98	-2.94
C6 transcription factor	Afu5g00950		-3.71	-4.09
Hypothetical protein	Afu7g07140		-3.57	-4.08
Hypothetical protein	Afu1g12475		-3.53	-3.67
Short chain dehydrogenase/ oxidoreductase CpoX2	Afu2g18000	<i>fgaDH</i>	-3.43	-3.31
Acetyltransferase. gNAT family family	Afu1g09260		-3.4	-3.05
Hypothetical protein	Afu1g10450		-3.39	-3.39
Hypothetical protein	Afu8g01795		-3.39	-3.21
Hypothetical protein	Afu2g16440		-3.35	-3.66
Aryl-alcohol oxidase vanillyl-alcohol oxidase	Afu3g09500		-4.64	
Hypothetical protein	Afu4g08310		-3.73	
Hypothetical protein	Afu5g14850		-3.49	
Hypothetical protein	Afu6g03330		-3.41	
Ankyrin repeat protein	Afu7g08610		-3.37	
Pectin lyase	Afu5g10170			-3.79
Pectin lyase	Afu5g10380			-3.57
Hypothetical protein	Afu3g00410			-3.47

^aThis value represents the difference of the fold change in log2 obtained for each gene between days of infection compared in each case. Negative values indicated down-regulation relative to the first day post-infection. Data obtained with Agilent Whole *A. fumigatus* genome Expression 44K v.1.

^bProduct description of the genes found on the microarray following RefSeq nomenclature.

^cSystematic name of the gene following AspgD nomenclature.

^dGene name following AspgD nomenclature (<http://www.aspergillusgenome.org>).

Table S3. Results of the 85 DEGs up-regulated detected after microarrays analysis.

Product description ^b	Systematic Name ^c	Standard Named ^d	Fold Change ^a	
			Day3 vs Day1	Day4 vs Day1
Indoleamine 2,3-dioxygenase family protein	Afu7g02010		4.19	5.72
Hypothetical protein	Afu8g00400		7.80	6.84
Hypothetical protein	Afu8g00430		7.21	6.97
Methyltransferase SirN-like	Afu8g00550	<i>psoC</i>	7.09	6.90
O-methyltransferase	Afu8g00390	<i>fmaD</i>	6.37	5.71
Cytochrome P450 oxidoreductase OrdA-like	Afu8g00510	<i>fmaG</i>	5.87	5.02
Lipase	Afu7g04020		5.64	5.95
α/β hydrolase	Afu8g00530	<i>psoB</i>	5.41	5.29
Steroid monooxygenase	Afu8g00440	<i>psoF</i>	5.22	4.89
Glutathione S-transferase	Afu8g00580	<i>elfB / psoE</i>	5.06	4.96
Defensin domain protein	Afu7g05180		5.06	4.81
Acetate-CoA ligase	Afu8g00500		5.03	4.68
Hypothetical protein	Afu6g01870		4.97	4.65
Phytanoyl-CoA dioxygenase family protein	Afu8g00480	<i>fmaF</i>	4.63	4.65
Cytochrome P450 oxidoreductase	Afu8g00560		4.61	4.46
Methionine aminopeptidase, type II	Afu8g00410	<i>metAP/ fpall</i>	4.53	4.09
GTP-binding protein EsdC	Afu7g01930	<i>esdC</i>	4.26	3.78
IgE-binding protein	Afu6g00430		4.18	4.02
DUF124 domain protein	Afu3g08610		4.18	3.34
ThiJ/Pfpl family protein	Afu5g02670		4.13	4.02
Secreted antimicrobial peptide	Afu8g00710		4.04	4.28
Plasma membrane protein Pth11-like	Afu7g06130		4.02	3.71
β -D-glucoside glucohydrolase	Afu7g06140	<i>exg13</i>	4.01	4.10
Hypothetical protein	Afu6g13740		3.96	3.12
Extracellular lipase	Afu5g02040		3.93	4.21
Hypothetical protein	Afu5g00700		3.92	4.32

Hypothetical protein	Afu2g08820		3.75	3.60
Hypothetical protein	Afu8g00910		3.68	3.45
Methionine aminopeptidase, type II	Afu2g01750		3.60	4.10
Hypothetical protein	Afu3g13080		3.48	4.45
Secreted dipeptidyl peptidase DppV	Afu2g09030	<i>dppV</i>	3.47	3.92
Hypothetical protein	Afu1g09030		3.45	4.00
Integral membrane protein Pth11-like	Afu7g06620		3.41	3.38
MFS sugar transporter	Afu3g03700		3.39	3.77
Cytochrome P450 monooxygenase	Afu6g02210			4.28
Aldehyde dehydrogenase	Afu7g01000			4.11
H ⁺ /nucleoside cotransporter	Afu6g13190			4.10
Citrate synthase Cit1	Afu6g03590	<i>mcsA</i>		4.05
Fumarate reductase Osm1	Afu8g05530	<i>osm1</i>		3.97
Glycerol kinase	Afu6g08470			3.89
Elastinolytic metalloproteinase Mep	Afu8g07080	<i>mep</i>		3.88
3-methylcrotonyl-CoA carboxylase beta subunit (MccB), putative	Afu5g08940			3.20
C6 transcription factor	Afu5g14290		4.36	
C6 finger transcription factor	Afu8g00420	<i>fumR / fapR</i>	4.28	
Hypothetical protein	Afu5g08800		3.99	
MFS myo-inositol transporter	Afu4g01560		3.95	
Hypothetical protein	Afu4g12700		3.64	
Hypothetical protein	Afu5g00590		3.35	
LaeA-like methyltransferase	Afu2g04380		3.00	
Polyketide synthase	Afu8g00370	<i>fma-PKS</i>		5.66
Major allergen and cytotoxin Asp f 1	Afu5g02330	<i>aspf1</i>		4.64
N.O-diacetyl muramidase	Afu6g10130			4.4
Stress responsive A/B barrel domain protein	Afu4g10610			4.39
4-hydroxyphenylpyruvate dioxygenase	Afu2g04200	<i>hppD</i>		4.21
Hypothetical protein	Afu1g02290			3.91
C6 sexual development transcription factor NosA	Afu4g09710	<i>rosA</i>		3.87

NAD-dependent formate dehydrogenase AciA/Fdh	Afu6g04920	<i>fdh</i>	3.82
Hypothetical protein	Afu2g17630		3.75
Maleylacetoacetate isomerase MaiA	Afu2g04240	<i>maiA</i>	3.72
Succinyl-CoA, 3-ketoacid-coenzyme A transferase (ScoT). putative	Afu6g12250		3.61
DUF614 domain protein	Afu1g14190		3.58
NAD+ dependent glutamate dehydrogenase	Afu2g06000		3.53
Class V chitinase ChiB1	Afu8g01410	<i>chiB1</i>	3.50
Extracellular dipeptidyl-peptidase DppIV	Afu4g09320	<i>dppIV</i>	3.50
Fg-GAP repeat protein	Afu1g04130		3.49
Hypothetical protein	Afu5g10930		3.48
Carbon-nitrogen family hydrolase	Afu4g02790		3.47
WSC domain protein	Afu3g07050	<i>wsc2</i>	3.45
DUF895 domain membrane protein	Afu1g00440		3.39
Homoserine acetyltransferase family protein	Afu1g15350		3.38
Hypothetical protein	Afu1g15160		3.38
Hypothetical protein	Afu5g02320		3.33
MFS transporter	Afu2g17840		3.25
Isovaleryl-CoA dehydrogenase IvdA	Afu5g08930		3.23
Aspartate aminotransferase	Afu1g04160		3.22
Zinc-dependent alcohol dehydrogenase	Afu1g14390		3.20
MFS transporter	Afu1g01812		3.20
Short chain dehydrogenase/reductase family oxidoreductase	Afu5g09290		2.98
Oxidoreductase. short-chain dehydrogenase/reductase family	Afu5g14340		2.95
Hypothetical protein	Afu3g11450		2.94
Succinate dehydrogenase subunit Sdh1	Afu3g07810	<i>sdh1</i>	2.90
Oxidoreductase. 2-nitropropane dioxygenase family. putative	Afu2g09850		2.82
Vacuolar carboxypeptidase Cps1	Afu3g07040	<i>cps1</i>	2.82

Hypothetical protein	Afu2g14450	2.73
Sterol carrier protein	Afu4g06380	2.65

^aThis value represents the difference of the fold change in log₂ obtained for each gene between days of infection compared in each case. Negative values indicated down-regulation relative to the first day post-infection. Data obtained with Agilent Whole *A. fumigatus* genome Expression 44K v.1.

^bProduct description of the genes found on the microarray following RefSeq nomenclature.

^cSystematic name of the gene following AspgD nomenclature.

^dGene name following AspgD nomenclature (<http://www.aspergillusgenome.org>).

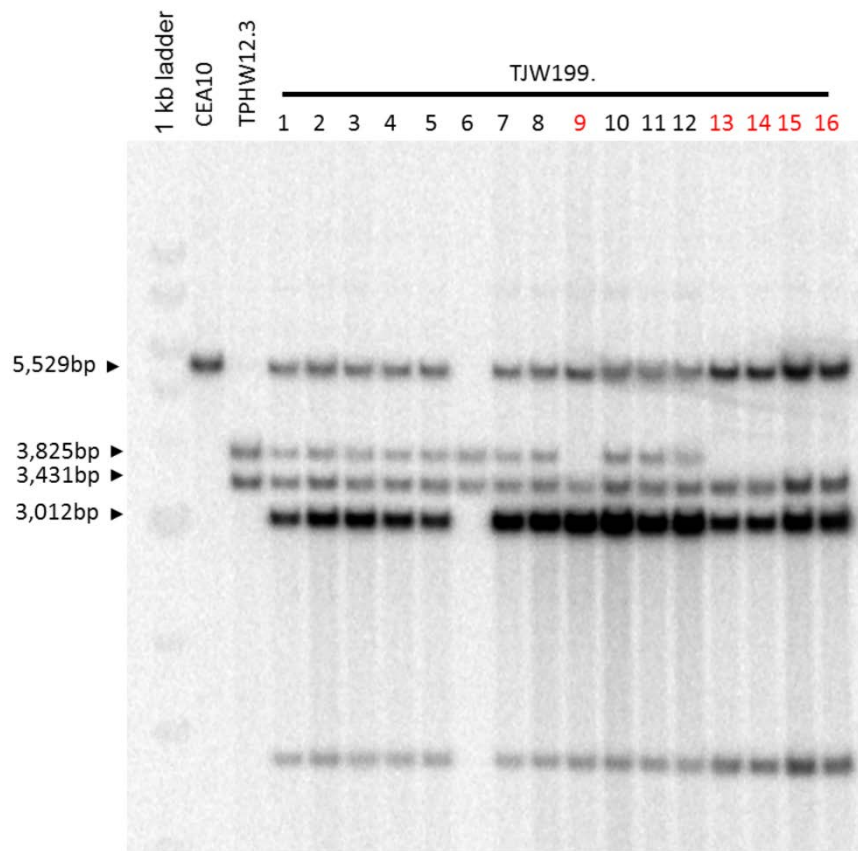


Figure S1. Southern blot analysis of $\Delta fmaA$ complemented mutants. The indicated strains had genomic DNA purified and digested with *HindIII*. CEA10, wild-type control; TPHW12.3, $\Delta fmaA$; TJW199, transformants for complementation of TPHW12.3. The Wt shows the expected band of 5,529 bp, $\Delta fmaA$ shows the expected 3,431 and 3,825 bp bands. The complemented transformants 1, 2, 3, 4, 5, 7, 8, 10, 11 and 12 were excluded since they can be possible heterokaryons (of complemented mutant and $\Delta fmaA$) even if it shows the expected 3,012 bp band. The complemented strain number 6 was also excluded due to *fmaA* deletion background. The transformants 9, 12, 13, 14, 15 and 16 were chosen as complemented. One of them, TJW199.14 was used for the subsequent experiments. Those complemented mutants may have both homologous (native locus) and heterologous integration of the wild type copy of *fmaA*.

Chapter 2

Fumagillin as new virulence factor of the pathogenic mold *Aspergillus fumigatus*



1. Introduction

In the field of the infection, all those biological characteristics that allow *A. fumigatus* to colonize and/or infect the respiratory tract are known as virulence factors. Within them, it is worth mentioning the fungal cell wall and the proteins involved in its formation, the resistance of the conidia to ultraviolet radiation and dryness, the mechanisms to evade the immune response, and the production of proteases and toxins, among others (Abad *et al.*, 2010). In fact, *A. fumigatus* genome counts with a great variety of biosynthetic clusters (Bignell *et al.*, 2016; Keller, 2019) that provide the fungus with a very complex and productive secondary metabolism, including the production of toxins (Raffa and Keller, 2019; Venkatesh and Keller, 2019; Drott *et al.*, 2020). Among them, gliotoxin, which is an immunosuppressive molecule that interferes with the phagocytosis and cytotoxic response of T cells causing apoptosis of monocytes. This toxin is one of the most studied (Mullbacher and Eichner, 1984; Eichner *et al.*, 1986; Yamada, Kataoka and Nagai, 2000; Stanzani *et al.*, 2005). Other important toxins produced by *A. fumigatus* are aflatoxin (Pepeljnjak *et al.*, 2004), fumitremorgine A and B (Yamazaki, Fujimoto and Kawasaki, 1980; Liu, Yang and Meng, 1996), hemolysin and mitogillin (Arruda *et al.*, 1990).

A previous transcriptomic study, included in the previous chapter, demonstrated that most of the *fma* cluster, in charge of fumagillin production, was overexpressed by fungal cells in the lungs of immunosuppressed mice intranasally infected (Guruceaga *et al.*, 2018). In the same study, a non-fumagillin producer mutant strain caused significant less cellular damage than the wild type *in vitro*, demonstrating a potential relevance of this toxin in virulence (Guruceaga *et al.*, 2018).

Given these previous data and the need to improve the study of the implication of secondary metabolites in virulence (Latgé and Chamilos, 2019), the aim of the present chapter was to study the implication of this molecule in the pathogenesis of *A. fumigatus*. For this purpose, we carried out a batch of assays using the commercial toxin to understand its effect over epithelial cells and macrophages and we also

deepened into the real role of the toxin on the fungal virulence using a non-fumagillin producer strain ($\Delta fmaA$) and mice infections.

2. Material & Methods

2.1 *Aspergillus fumigatus* strains, media and growth conditions

In this chapter, the \DeltaakuB^{ku80} strain of *A. fumigatus* was used as wild type (Wt) strain during this study. In contrast, we used the previously published (Wiemann *et al.*, 2013) deletion mutant strain $\Delta fmaA$ (that is non-fumagillin producer strain) and its complemented strain $\Delta fmaA::fmaA$ (Guruceaga *et al.*, 2018). The maintenance of these strains and the collection of conidia and the adjustment of their concentration for subsequent studies will be carried out as indicated in **Section 2.2.1** of the previous chapter.

2.2 *Aspergillus fumigatus* phenotypic characterization

The phenotype study of the mutant *A. fumigatus* strains used in this work ($\Delta fmaA$ and $\Delta fmaA::fmaA$) was evaluated following the spotting assay protocol described by Martin-Vicente and co-workers (Martin-Vicente *et al.*, 2018). Briefly, we seeded 5 μ l drops containing suspensions of fresh conidia (10^4 , 10^3 and 10^2 conidia respectively) of each strain in a GMM agar plate supplemented with 80 μ g/ml of congo red (CR), 40 μ g/ml calcofluor white (CW) and 0.0125% of sodium lauryl sulfate (SDS) as structural stress agents and NaCl (1M), KCl (1M) and sorbitol (1.2M) as osmotic stress agents following the scheme represented in **Fig 20**.

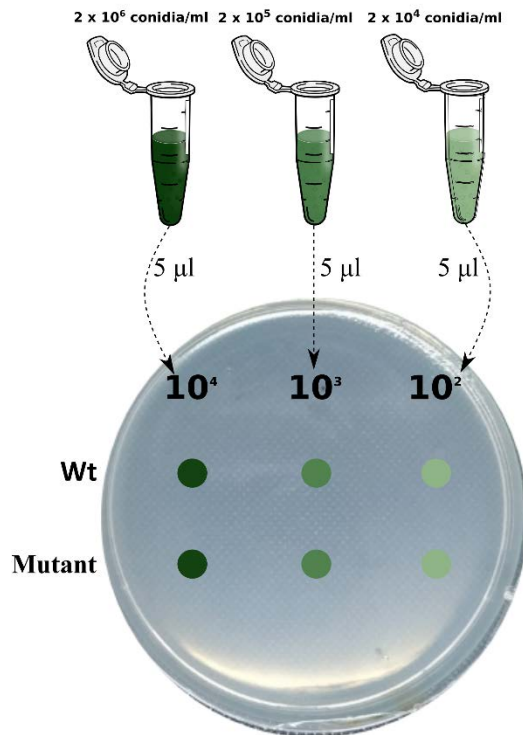


Figure 20. Spotting assay procedure scheme. In this assay the GMM medium was supplemented with different stressors. Each green point represent a drop of 5 μ l from the correspondent dilution tube.

2.3 Determination of fumagillin by UHPLC (Ultra high performance liquid chromatography) in RPMI samples

Quantitative analysis of fumagillin was carried out using an Acquity Ultra Performance Liquid Chromatography (UPLC) system (Waters, Milford, MA, USA) coupled to a photodiode array (PDA) detector. The chromatographic separation was performed on an Acquity BEH C18 column (2.1 x 50 mm, 1.7 μ m) from Waters. The mobile phases used were a 50 mM ammonia/ammonium buffer (pH 10) as the aqueous mobile phase (A) and acetonitrile as the organic modifier (B). A flow rate of 0.40 ml/min was used with an elution gradient as follows: 0-0.5 min, 20 % B; 0.5-5.5 min, linear change from 20% to 95% B; 5.5–6.5 min, 95 % B; 6.5–7.0 min, from 95% to 20% B. During the chromatographic analysis, the column was thermostated at 35°C and samples were kept at 4°C in the auto sampler. Wavelengths of 336 and 280 nm were employed for fumagillin and diclofenac (internal standard, IS), respectively. System control, data collection, and data processing were accomplished using Empower 2 software.

Prior to the chromatographic analysis, a solid phase extraction (SPE) procedure was applied to the RPMI samples, to each 500 μ l of RPMI sample was spiked with 37.5 μ l of 20 mg/ml IS solution in methanol and 465 μ l of phosphate buffer (100 mM, pH 12). After vortex mixing the solution was transferred to Oasis MAX cartridges (30 mg, 1 cm³) from Waters. The cartridges had been previously activated with 1 ml methanol and conditioned with 1 ml phosphate buffer (100 mM, pH 12). Once the sample was loaded, the cartridges were washed with 1 ml phosphate buffer (100 mM, pH 12):methanol (55:45) followed by 5 minutes drying at high vacuum, and then 1 ml of 3.5% formic acid solution in methanol was used for eluting the analyte. Subsequently, 500 μ l of aqueous mobile phase were added to 500 μ l of the eluate and after centrifugation, the solution was transferred to autosampler vials and injected into the UHPLC system for analysis. For the quantification of fumagillin, a calibration curve in RPMI was built with a linear range between 25-1500 μ g/l.

2.4 Cell lines

Two different cell lines obtained from the American Type Culture Collection (ATCC, Manassas, VA, USA) were used in this study. On the one hand, we used the murine macrophages RAW 264.7 cell line, to study the cell line sensitivity to the fumagillin (MTT and flow cytometry), the toxin absorption assays and to performed the phagocytosis assays. On the other hand, we employed the human alveolar epithelia A549 cell line to study also its sensitivity to the fumagillin and the toxin absorption assays, and to the scratch assays. The cell cultures were maintained in RPMI 1640 medium supplemented with 10% heat-inactivated FBS, 200 mM L-glutamine, 100 U/ml penicillin and 0.1 mg/ml streptomycin (RPMI complete), and incubated at 37°C, 5% CO₂ and 95% of humidity (cell culture atmosphere). Cell line passages were used only when the viability of the cells was higher than 90%. Cell lines viability was calculated staining an aliquot with trypan blue and counting in a Bürker counting chamber. All culture media components were obtained from Sigma Aldrich (St. Louis, MO, USA).

2.5 Isolation and culture of BMMs

Mouse bone marrow-derived macrophages (BMMs) were generated following the method publish by Pellon and coworkers (Pellon *et al.*, 2018) perform with 8-12 week-old C57Bl/6 mice instead of rats. Briefly, BMMs were obtained flushing out mice femurs and tibias using RPMI complete. After that, the homogenized was filtered through a 70 µm-nylon mesh (ThermoFisher, Waltham, MA, USA) and then centrifuged at 400 rpm for 5 minutes Ammonium chloride potassium lysis buffer was used in order to remove red blood cells from the samples. Finally, the remaining cells were incubated in 100 mm × 15 mm Petri dishes during 7 days in presence of RPMI complete supplemented with 30 ng/ml of M-CSF (Miltenyi Biotec, Bergisch Gladbach, GE). Fresh medium was added after 3 days of culture.

2.6 *Aspergillus fumigatus* fumagillin secretion ability

To study the skill of each fungal strain, used in this chapter, to produced fumagillin we seeded 5 × 10⁶ conidia/ml of each strain in 2 ml of RPMI complete using 6-well plates

(ThermoFisher, Waltham, MA, USA). The plates were incubated in the same conditions that cell lines, at 37°C, 5% CO₂ and 95% of humidity. After 48 hours of incubation, we centrifuge an aliquot of 1 ml at 14.000 rpm during 5 minutes and the supernatant was transferred to a light safe microtube and kept in ice until its measurement by UHPLC. Each assay was done using four independent conidia batches of each strain harvested just before to the assay start point. In order to save commercial fumagillin we planned two assays being the total measures done eight for each fungal strain and two standards of 0.2 µg/ml from the commercial fumagillin as control.

2.7 Cell lines fumagillin absorption ability

To study the absorption of fumagillin for the cells, we seeded 1 x 10⁶ and 3 x 10⁶ cells/ml of the RAW 264.7 and A549 cell lines, respectively, in a final volume of 2 ml of RPMI complete medium using 6-well plates. After 1 hour of incubation to allow cell attachment we replaced the culture media with 2 ml of fresh RPMI complete supplemented with 1 µg/ml of fumagillin (SigmaAldrich, St. Louis, Mo, USA). Aliquots of 500 µl were collected after 8, 20 and 24 hours of cell exposition in light safe microtubes and processed as we explain before until its measurement by UHPLC. The assays were done by triplicate in three independent days..

2.8 Cellular electron transport chain activity

The electron chain activity in contact with different concentration of fumagillin performed by MTT assay. Briefly, we seeded 8 x 10⁴ cells per well (RAW 264.7 or A549) in a 96-well plates (ThermoFisher, Waltham, MA, USA) with 150 µl of RPMI complete. After 2 hours of incubation to allow cell attachment we replace the culture medium with 150 µl of the fresh RPMI complete supplemented with different concentrations of fumagillin (0, 0.5, 1 and 2 µg/ml) and the cells were incubated using the conditions abovementioned of the cell culture atmosphere. After 24 hours of incubation, we eliminated the medium and we added 150 µl/well of fresh RPMI complete supplemented with 0.5 mg/ml of MTT (SigmaAldrich, St. Louis, MO, USA) and the plate was incubated during 4 hours to allow the reduction of the tetrazolium dye MTT to formazan crystals that are purple and insoluble. Finally, we replaced MTT solution and

we added 150 μ l of DMSO in order to dissolve formazan crystals and after 15 minutes the absorbance was measured at 560 nm using the microplate reader Synergy™ HT (BioTek, Winooski, VT, USA). The results were expressed as percentage of metabolic activity, all the experiments were carried out by triplicate, and each experiment was done at least with three technical replicates per condition studied.

2.9 Wound healing assay

In order to evaluate the inhibitory capacity of the fumagillin over the epithelial cell line A549 we performed a scratch injury assay. Briefly, in a 24 well plate were seeded 1.5×10^5 cells per well and, after incubating for 24 hours, confluent monolayers were obtained. Using a 1,000 μ l pipette tip, a vertical and a horizontal scratch was done, and then washed twice with PBS to remove the floating cells. Fresh RPMI complete containing 0.5, 1 or 2 μ g/ml of fumagillin was added to the cultures. We used as control a cell culture with this fresh medium without fumagillin. Images were taken from one field of view down between the intersection of the two scratches at 24 and 48 hours after fumagillin addition, using a Nikon Eclipse TE2000-U (Nikon, Minato, Tokio, Japan) inverted microscope. Finally, the percentage of scratch reduction was calculated and normalized to the untreated control. The assays were done by triplicate in three independent days.

2.10 Flow cytometry assays

The flow cytometry assays were carried out in the general services from the University of the Basque Country (sGiker, UPV/EHU). The cytometer used for all the experiments was the Beckman Coulter Gallios equipped with three solid lasers (Beckman Coulter, Brea, CA, USA).

Cell proliferation assays of A549 or RAW 264.7 cell lines in presence and absence of the fumagillin concentration indicated below, were developed using the fluorescent dye CFSE (Invitrogen, Carlsbad, CA, USA). Cells were stained using 2 μ M of CFSE in PBS during 30 minutes at 37°C and 5% CO₂. After the incubation period, cells were washed twice in RPMI complete. Finally, we seeded 1×10^5 cells/well (both A549 and RAW 264.7) in a 6-well plates. At time 0 hours, the just stained cells were analyzed in the

flow cytometer (517 nm) alongside a group control of cells without staining. The study was extended during 72 hours and daily samples were analyzed by flow cytometry. For that, the cells were detached from each well and suspended in RPMI. The flow cytometer was set up to analyzed 10.000 events from each sample exciting the sample at 492 nm and measuring the fluorescence at 517 nm.

On the other hand, we carried out parallel live and death assays in contact with fumagillin using the Propidium Iodide Ready Flow™ Reagent (Invitrogen, Carlsbad, CA, USA). The concentration of cells per well, the detached protocol and the number of cells analyzed in each run was the same as the proliferation assay, except that the sample was excited at 535 nm and the emission was at 617 nm following the manufacturer's instructions.

The concentration of fumagillin used in the flow cytometry assays were 0.5 µg/ml, 1 µg/ml and 2 µg/ml in a total volume of 2 ml of RPMI. All assays were done by triplicate in three independent days.

2.11 Phagocytosis assay and fungal behavior

To understand the behavior of the fungal strains in contact with the murine macrophages cell line RAW 264.7 and the BMMs isolated, we seeded 2×10^5 cells/ml in 500 µl of RPMI complete using 24-well plates (ThermoFisher, Waltham, MA, USA) which contained 12 mm-diameter cover slips (ThermoFisher, Waltham, MA, USA). After an overnight incubation, immune cells were co-culture with *A. fumigatus* conidia of each strain (Wt, $\Delta fmaA$, $\Delta fmaA::fmaA$) at a multiplicity of infection of 10 (ten conidia per immune cell). In parallel, we seeded the same number of each fungal strain conidia but in this case without cells, acting as control. At each incubation time (2, 4, 6 and 8 hours), we removed the coverslip to a new plate in order to calculate the phagocytosis (%), fungal germination (%) and hyphal branching (%) in co-culture and fungal germination (%) and hyphal branching (%) without cells. For that, a minimum of 500 cell (conidia/hyphae) were count using the invert microscope Nikon Eclipse TE2000-U (Nikon, Minato, Tokio, Japan). Furthermore, we developed the same

abovementioned phagocytic assay but adding heat inactivated conidia (121°C during 30 minutes) of each *A. fumigatus* strain in RPMI complete.

On the other hand, in order to calculate the hyphae length of the fungal strains after 6 and 8 hours both in with and without the immune cells, a Calcofluor white (CW) stain was performed. For that, the coverslip of each time study was washed with PBS, stained with 100 µl of a CW solution (20 mg/ml) and then we incubated the samples at room temperature during 20 minutes in dark. Finally, we washed the coverslips with PBS and they were mounted in order to be observed with the fluorescence microscope Eclipse Ni microscope (Nikon, Minato, Japan). Ten random photographs using the Nikon Ds-Fi2 camera (Nikon, Minato, Japan) of a high hyphae density zone were captured. Image analysis was carried out using ImageJ software (<http://imagej.nih.gov/ij/>). All the experiments explained in this section were done by triplicate in three independent days.

2.12 Animal infection

A total of 30 Swiss mice of 25-35 g divided in two independent infections of three independent groups were infected (one group per each fungal strain). Mice were kept in the General Animal Unit Service of the University of the Basque Country (UPV/EHU), with water and food *ad libitum*, handled in biological safety cabinets, and kept in sterilized cages with negative-pressure ventilation and filters. All mice were immunosuppressed by the administration of 100 mg/Kg cyclophosphamide (Sigma-Aldrich, St Louis, MO, USA) each three days, starting four days before infection. Each infection group was composed by five mice that were infected intranasally using a 20 µl SS-T solution containing 1×10^7 resting conidia of *A. fumigatus* Wt, *Δfma* or *Δfma::fma* strains respectively.

Mice were monitored each 24 hours in order to study the weight evolution and quantified the suffering score derived from the infection process using a scale 0-10 in which we evaluate different aspects of animal suffering (**Table S1**) following the recommendations of experts from our institution animal facility and the ethical committee members. Those mice that reached the critical suffer score were

euthanized minimizing mice suffering and were considered as die animals due to the *A. fumigatus* infection.

The *post mortem* dissection of the mice corpse were done in order to obtain the different organs of the animals. We extracted the lungs in order to study the fungal burden of each one. Organs were first weighed and then were processed as is described in **Section 2.4** of chapter 1 to determinate the lung fungal load by counting the Colony Forming Units (CFUs).

2.13 Statistics

All the statistical analysis of this study were performed using the GraphPad Prism 7 software (GraphPad Software Inc., CA, USA). As mentioned above, all studies have been performed with at least three independent biological replicates in triplicate and the statistically significant differences were established in $p < 0.05$. All data present in this study followed a normal distribution. T-test or ANOVA were used to study differences between conditions depending if we compared punctual data or multiple comparison respectively.

2.14 Ethical issues

The Ethics Committee for Animal Welfare (CEBA) of the University of the Basque Country (UPV/EHU) (reference number CEBA/36-P03-01/2010/REMENTERIA RUIZ and CEBA/36-P03-03/2010/REMENTERIA RUIZ) approved all the animal experimental procedures carried out in this study.

3. Results

3.1 Characterization of *A. fumigatus* strains: phenotype and ability to produce fumagillin

Monitoring the possible effects of the mutations in the phenotype of the resulting strain is an essential step to understand the effect of the mutation done. For that, a phenotypic characterization following the spot dilution protocol was performed, the results showed that there is not any significant difference between Wt and $\Delta fmaA$ fungal strains under the different structural and osmotic stresses tested (**Fig. 21A**).

Later, the fungal strains ability to secrete fumagillin was studied by UHPLC using as internal control a fixed concentration of toxin (0.2 $\mu\text{g/ml}$). As it is observed in **Fig. 21B**, the $\Delta fmaA$ strain was no able to produce fumagillin in the *in vitro* conditions assayed. In contrast, the Wt strain produced an average concentration of fumagillin of 0.43 $\mu\text{g/ml}$, registering the most variable secretion results. The strain $\Delta fmaA::fmaA$ secreted an average concentration of fumagillin of 0.25 $\mu\text{g/ml}$ but, it is highlighting that the concentration of fumagillin secreted was higher than the produced by the Wt strain in 25% of the assays performed.

3.2 Different fumagillin absorption ability in cell lines

A toxin fulfill its cellular effect as long as it is able to join to its cellular target. It was monitored the fumagillin disappearance in the cultures in contact with macrophage (RAW 264.7) and lung epithelium (A549) cell lines during 24 hours of exposition by UHPLC. The results showed that 10% of the fumagillin added to the medium disappeared spontaneously and gradually during the time studied with any contact with cells (control), maybe due to a light or temperature degradation processes. In contrast, in those wells in which the RAW 264.7 cell line was in presence of fumagillin it was detected a higher progressive loss of concentration in the culture medium than control, with a total loss of 23.5% of the initial concentration of fumagillin after 24 hours of exposition. The contact fumagillin-A549 cell line showed a very stronger fumagillin lost than control or the other cell line, since 8 to 24 hours of exposition

reaching a total loss toxin concentration of 93.5% of fumagillin. All the results are summarized in the **Fig. 21C**.

Finally it is important to highlight that using the above explained UHPLC method we were able to detect a minimum of 0.1 µg/ml of fumagillin in a reliably way, using the chemical toxin.

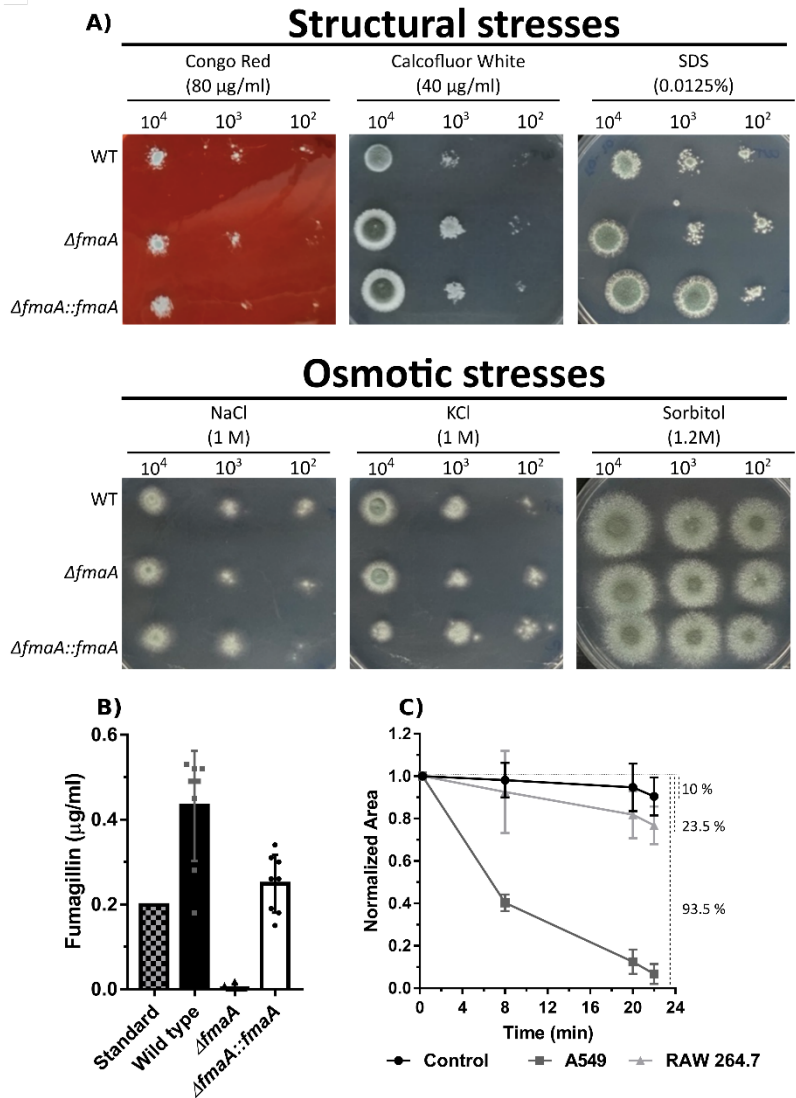


Figure 21. Phenotypic characterization of the mutant strains **A)** Spot dilution assay of the three fungal strains (Wt, $\Delta fmaA$ and $\Delta fmaA::fmaA$) growing in presence of 80 µg/ml of congo red, 40 µg/ml of calcofluor white, 0.0125% of SDS, 1M of NaCl, 1M of KCl and 1.2M of Sorbitol. **B)** Ability of the *A. fumigatus* strains to secrete fumagillin after 48 hours of incubation in RPMI complete and measured by UHPLC taking as internal control a standard (0.2 µg/ml) of commercial fumagillin. **C)** Fumagillin absorption ability of each cell line. The experiment was carried out during 24 hours of exposition with UHPLC measures at 8, 20 and 24 hours after inoculation of 1 µg/ml of fumagillin. (Black) Control; fumagillin during 24 hours in wells with RPMI complete without cells. (Light grey) Fumagillin-RAW 264.7. (Dark grey) Fumagillin-A549. On the right edge of the graph is represented (discontinuous lines) the total loss of fumagillin concentration after 24 hours of exposition and in comparison with 1 µg/ml of fumagillin that was the initial concentration.

3.3 Fumagillin promotes a decrease in cellular activity and a delay in proliferation in lung epithelial cells

To evaluate the effect of fumagillin over the electron transport chain (ETC) activity of lung epithelial A549 cell line, a MTT reduction assay was performed (**Fig. 22A**). This ETC activity was lower in those cells that grew in contact with any of the fumagillin concentrations tested than cells growing with no presence of fumagillin. In contrast, the propidium iodide staining measured by flow cytometry (**Fig. 22B**), detected a cell viability of about 75% and showed no differences between cells in contact with any of the fumagillin concentrations tested and the control cells.

The proliferation and migration ability of the A549 cell line in presence of the toxin was also studied using the wound healing assay. This assay showed the inability of the epithelium to close the gap caused in the monolayer with a pipette tip after 24 hours of incubation with all the fumagillin concentrations tested, being the results even more significant after 48 hours of incubation (**Fig. 22C**). At this end time, a wound closure of around 20% in the cultures in contact with the mycotoxin was measured, while control cells closed completely the wound.

Finally, the cell proliferation by flow cytometry previous staining with CFSE was also evaluated in presence of fumagillin. In this way, a similar delay of cell proliferation was detected after 48 hours of exposition to all the fumagillin concentration tested (**Fig. 22D**). In contrast, after 72 hours a marked fumagillin concentration dependent effect was detected. At this time, in both control and treated cells, two peaks of fluorescence that correspond to two different generations of cells were observed. The overlay graph of the proliferation with the different concentrations of fumagillin used (**Fig. 22E**) demonstrates that while the percentage of cells corresponding to the first generation did not significantly change in relation to the treatment, the concentration of fumagillin was determinant in the second generation of cells. In fact, an 8% less

cells were detected in this phase when the cells grew during 72 hours with 2 µg/ml of fumagillin than with 0.5 µg/ml.

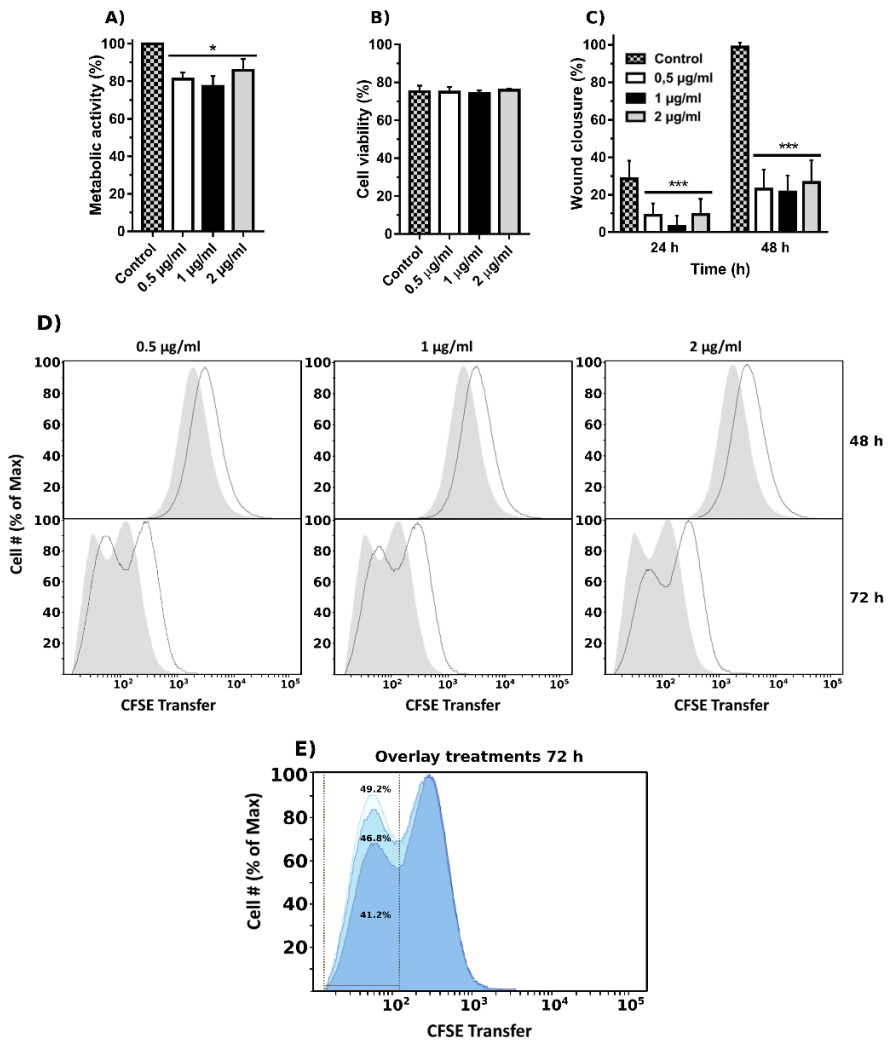


Figure 22. Fumagillin effect over A549 cell line. A) Electron transport chain activity of the cell cultures growing in presence of different fumagillin concentration during 24 hours. Results are expressed relative to the cells growing without fumagillin. **B)** Cell viability of the A549 cells measured by flow cytometry previous stain with propidium iodide. **C)** Wound healing assay in which we monitored the ability of the A549 culture to close the gap in presence of fumagillin during 24 hours and 48 hours of toxin exposition. **D)** CFSE analysis of the A549 cell line in presence of 0.5, 1 and 2 µg/ml of fumagillin during 72 hours. The percentage of cells normalized versus the CFSE transferred at 48 hours and 72 hours is plot. Grey area represented the control cells without fumagillin while black line represent the results of the cells after exposition to the mycotoxin. **E)** Last panel shows the overlay results obtained at 72 hours with the three concentration of fumagillin tested. * $p < 0.05$ *** $p < 0.0001$

3.4 Fumagillin reduces cellular activity and viability of macrophages.

Similarly to what we observed with epithelial cells, the ETC activity of the macrophages RAW 264.7 cell line was significantly lower when they grew in presence of 1 µg/ml and 2 µg/ml of fumagillin than control without mycotoxin and even with 0.5 µg/ml (**Fig. 23A**). On the other hand, the assay using propidium iodide and flow cytometry showed a significant reduction of cell viability in presence of all the fumagillin concentrations used (**Fig. 23B**).

The proliferation analysis showed a slight delay in cell proliferation after 48 and 72 hours of toxin exposition in comparison with the control cells without fumagillin (**Fig. 23C**). As it is possible to see in **Fig. 23D**, RAW264.7 cells did not suffer any fumagillin concentration dependent effect.

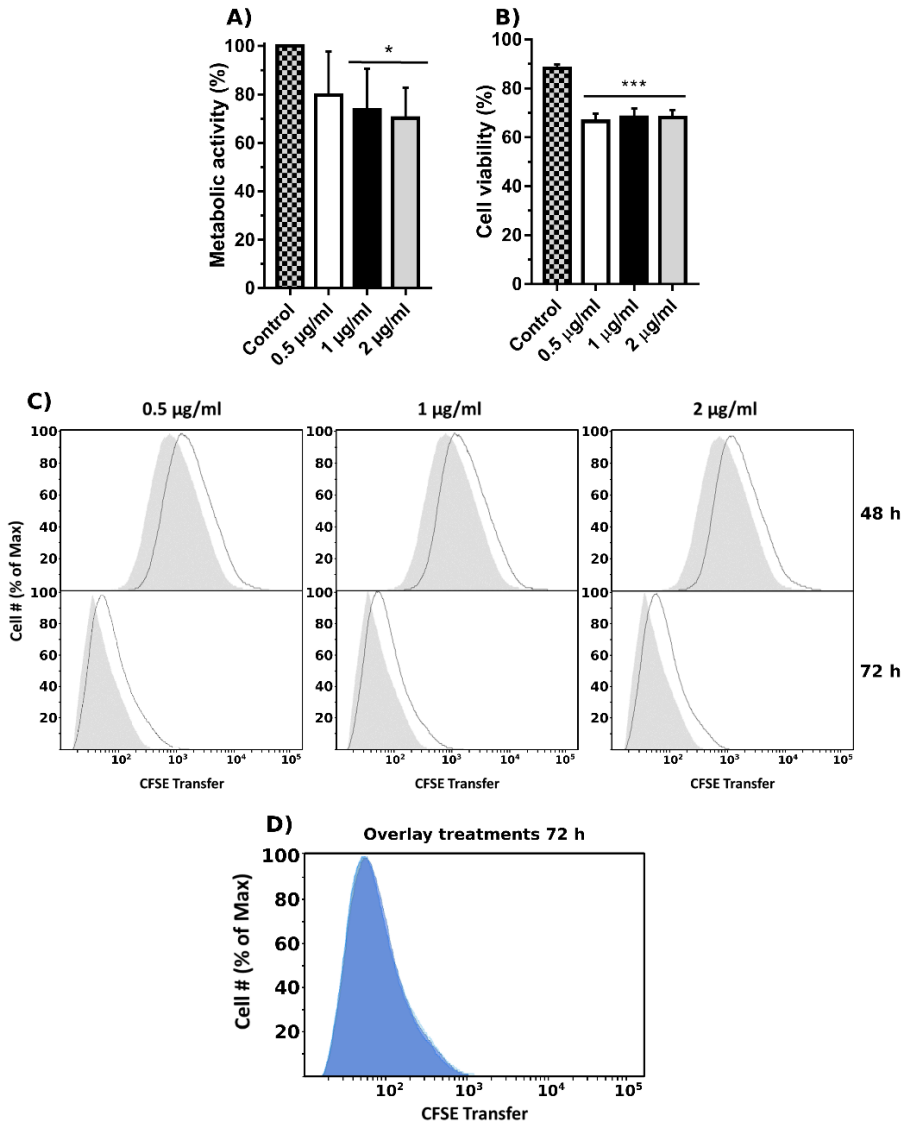


Figure 23. Fumagillin effect over RAW 264.7 cell line **A)** Cell activity of the cell cultures growing in presence of different fumagillin concentration during 24 hours. Results are expressed relative to the cells growing without fumagillin. **B)** Cell viability of the A549 cells measured by flow cytometry previous stain with propidium iodide. **C)** CFSE analysis of the A549 cell line in presence of 0.5, 1 and 2 µg/ml of fumagillin during 72 hours. The percentage of cells normalized versus the CFSE transferred at 48 hours and 72 hours is plot. Grey area represented the control cells without fumagillin while black line represent the results of the cells after exposition to the mycotoxin. **D)** Last panel shows the overlay results obtained at 72 hours with the three concentration of fumagillin tested. * $p < 0.05$ *** $p < 0.0001$

3.5 The inability to produce fumagillin affects *A. fumigatus* germination and phagocytosis

In order to understand if the ability to produce or not fumagillin can influence over the germination of the fungal strains in contact with phagocytes or even over the phagocytosis process, the contact of Wt, $\Delta fmaA$, and $\Delta fmaA::fmaA$ strains with a primary cell culture of BMMs and the RAW 264.7 cell line was studied. The culture controls (**Fig. 24A** and **24D**) showed no differences in the germination but the double branch hypha development of the mutant strain $\Delta fmaA$ was significant higher than the observed in the Wt. In contrast, although no differences in germination were found when the fungal strains were in contact with RAW 264.7 during 8 hours (**Fig. 24C**), in presence of the BMMs the $\Delta fmaA$ and $\Delta fmaA::fmaA$ strains germinated significantly higher than the Wt at 6 hours, reaching all the strains the same value at 8 hours (**Fig. 24B**).

Concerning double branch hypha development, the non-fumagillin producer strain formed a significant higher number of them than Wt in all conditions and than $\Delta fmaA::fmaA$ in contact with both cell types. This characteristic was observed in around the 20% of the $\Delta fmaA$ germinated conidia counted (**Fig. 24D** and **24E**).

The hyphae length was also studied, founding that the $\Delta fmaA$ and the $\Delta fmaA::fmaA$ strains produced significantly longer hyphae than the Wt when the fungus grew alone during 8 hours (**Fig. 24G**). The same effect was observed also in the co-culture of these strains with the BMMs (**Fig. 24H**). On the other hand, no differences in the hyphae length were found between strains when they grew with the RAW 264.7 macrophages (**Fig. 24I**).

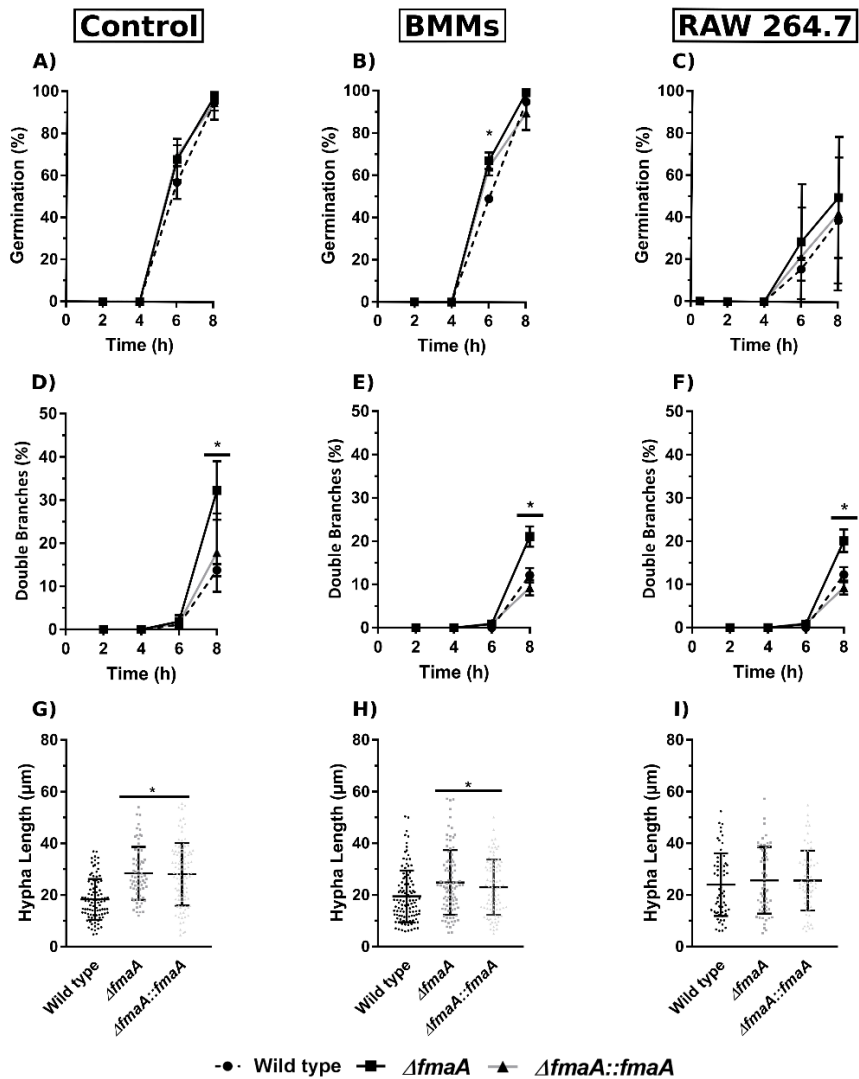


Figure 24. Fungal strains behaviour in co-incubation with macrophages and response of the immune cells during 8 hours. Data of fungal germination (%), double branches germination (%) and the length of the hyphae after 8 hours of incubation of the three fungal strains when they: **A, D and G**) growing alone (Control); **B, E and H**) growing in co-incubation with the BMMs; **C, F, I**) growing in co-incubation with the cell line RAW 264.7. * $p < 0.05$

Finally, the study of the phagocytosis during 8 hours showed that the $\Delta fmaA$ strain was significantly easier to be phagocytosed during the first 4 hours of contact with both BMMs and RAW 264.7. However, there were no differences in the phagocytosis at 6 and 8 hours (**Fig. 25A and 25B**). In addition, the phagocytosis study performed

using heat-inactivated conidia of the three strains did not show differences between these fungal strains (data not shown).

Specifically, the phagocytosis of $\Delta fmaA$ strain mediated by the BMMs was the most efficient in the 6 first hours. For that we studied the ability of this cells to response of the fungal strains measuring the production of TNF. The $\Delta fmaA$ strain seems to stimulate less the BMMs cells during all the time studied. The $\Delta fmaA$ and $\Delta fmaA::fmaA$ strains showed significantly lower TNF production by the BMMs than the Wt strain after 4 hours. Nevertheless, it is highlighting a significant higher production of TNF by the BMMs in contact with $\Delta fmaA::fmaA$ than the $\Delta fmaA$ strain after 8 h of coincubation (**Fig. 25C**). The great biological variability by the BMMs to produce TNF could conditioned the assay.

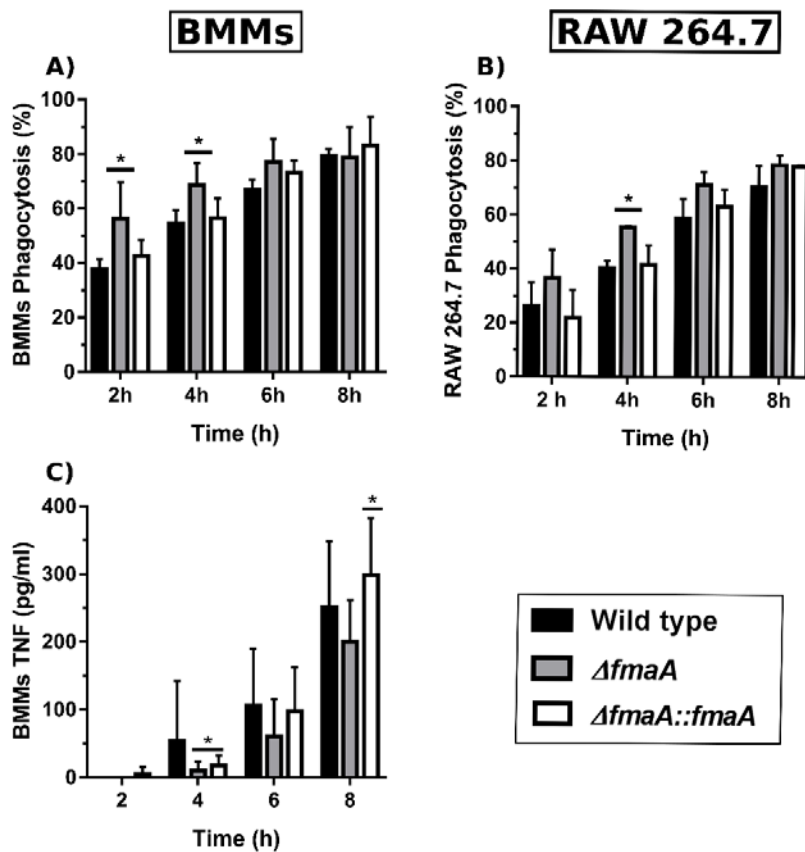


Figure 25. Phagocytosis results. A) Phagocytosis results of co-incubation between the three fungal strains and the BMMs. B) Phagocytosis results of co-incubation between the three fungal strains and the

macrophage cell line RAW 264.7. **C)** BMMs TNF production during co-incubation with the three fungal strains. * $p < 0.05$

3.6 The capacity to produce fumagillin increase mortality rate and fungal load in a mouse model of invasive aspergillosis

The three *A. fumigatus* strains (Wt, $\Delta fmaA$ and $\Delta fmaA::fmaA$) were administrated intranasally in a leukopenic mouse model of invasive aspergillosis (Guruceaga *et al.*, 2018b) to study the virulence and the mortality rate. **Fig. 26A** shows that the $\Delta fmaA$ strain induced a 50% mortality in the first 4 days post-infection, but the mice that survived this day stayed alive throughout all the experiment. In contrast, the mice infected with both the Wt and the $\Delta fmaA::fmaA$ strains showed a more progressive increase in mortality rate, reaching a 60% and 90% at the end of the experiment, respectively. The same conidia suspension used for the infections was at the same time studied to assay their specific ability to produced fumagillin by UHPLC. This result revealed that the $\Delta fmaA::fmaA$ conidia used in this infections was able to produced more fumagillin than the Wt strain and that the $\Delta fmaA$ strain used did not produced fumagillin, as expected.

The lung fungal burden in all animals infected was slightly higher in the group of mice infected with the $\Delta fmaA$ strain than in the other groups (**Fig. 26B**). However, the higher average data in this group of mice infected with $\Delta fmaA$ was consequence of the 50% of mice died during the first four days, which presented high CFUs values because, surprisingly, in the lungs of almost all the mice (4 out of 5) that survived the experiment, CFUs were not found. In contrast, mice infected with the Wt and the $\Delta fmaA::fmaA$ strains presented variable CFUs counts without a clear relationship between the day of the death and the fungal burden and, even survivor mice presented CFUs values, except for one.

To finish, the symptoms of the infected mice were monitored using a scale 0 to 10, showing that mice infected with the $\Delta fmaA::fmaA$ strain presented a symptomatology more severe that those infected with the Wt and the $\Delta fmaA$ strain (**Fig. 26C**). From day 16 to the end of the experiment this clinical score values were similar between all

the groups. In contrast to the clinical score, the evolution of the mice weight (**Fig. 26D**) was the same regardless of the fungal strain used to infect the mice.

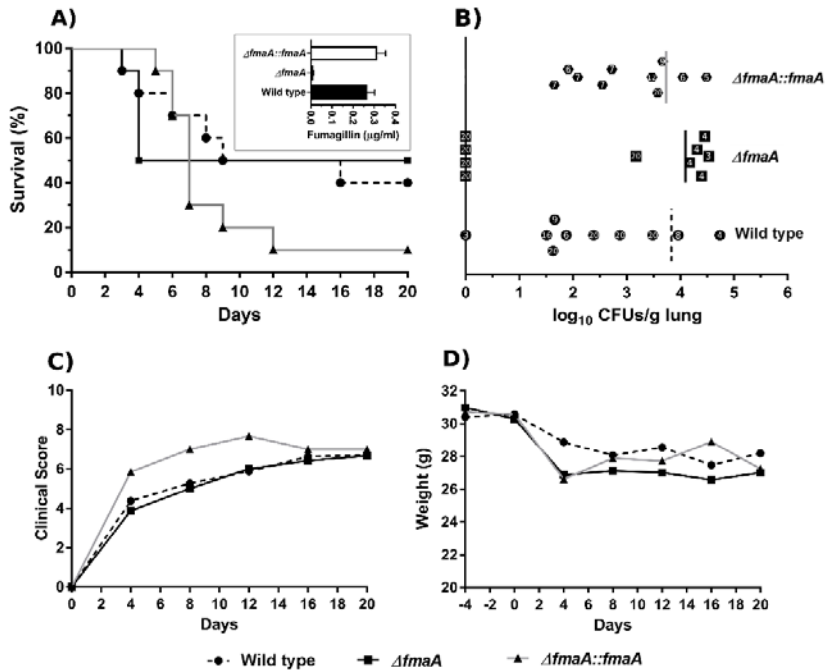


Figure 26. Results obtained after infected a leukopenic mice model intranasal with *A. fumigatus*. **A)** Kaplan-Meier analysis of the infected mice during 20 days post intranasal exposition to WT, $\Delta fmaA$ and $\Delta fmaA::fmaA$. The panel also shows the ability of the conidia used to infected mice to produced fumagillin. **B)** Fungal burden analysis of the lungs. The numbers inside the symbols represented the death day of each mouse. **C)** Graphical representation of the symptoms of each mice group annotated during all the experiment. **D)** Evolution of the mice weight during the experiment.

4. Discussion

The importance of some mycotoxins, as gliotoxin, for fungal virulence is widely described (Mullbacher and Eichner, 1984; Eichner *et al.*, 1986; Amitani *et al.*, 1995; Yamada, Kataoka and Nagai, 2000; Tsunawaki *et al.*, 2004; Watanabe *et al.*, 2004; Stanzani *et al.*, 2005; Orciuolo *et al.*, 2007) but, others, such as fumagillin, have not been deeply studied yet. Recent publications pointed out that fumagillin could induced lung epithelial cell damage both acting alone (Guruceaga *et al.*, 2018b) and in synergy with gliotoxin (Gayathri, Akbarsha and Ruckmani, 2020). Moreover, this mycotoxin is able to inhibit endothelial cell proliferation and angiogenesis process (Ingber *et al.*, 1990). However, little is known about its effect over other cell types such as epithelial cell lines or macrophages, or about its effect *in vivo* during the development of aspergillosis.

To shed light on this, we started by standardizing an UHPLC method for the detection of fumagillin in samples of RPMI obtained after *in vitro* assays. Fumagillin is a small sesquiterpene with an acidic portion responsible of a strong ultraviolet absorption (335-350 nm) that allows its chromatographic detection (Garret and Eble, 1954). Taking advantage of this property, we were able to detect a minimum of 0.1 µg/ml of fumagillin in a reliably way. In fact, the low variations found between replicates in the detection of the mycotoxin demonstrates the efficacy of the UHPLC method to detect the molecule quickly using supernatants.

Then, we studied the effect of synthetic fumagillin over both pneumocytes A549 and macrophages RAW 264.7, which are common cell lines to perform toxin/molecule/drug response studies (Guruceaga *et al.*, 2018b; Alex *et al.*, 2020; Gayathri, Akbarsha and Ruckmani, 2020). The time evolution study done incubating cell lines with a fix concentration of 1 µg/ml of fumagillin during 24 hours, demonstrated that each cell type absorbed the mycotoxin in a different way. The A549 cell line practically absorbed all the mycotoxin from the supernatant (93.5%) while macrophages RAW 264.7 only absorbed the 23.5% of the initial concentration. It is also possible that cells as consequence of their metabolism could degrade fumagillin

and the decreased observed was not only due to absorption process. Theoretically, fumagillin, due to its small size, could passively cross the cell membrane reaching the cell cytosol (Zhou *et al.*, 2013). In contrast, other authors point out that macrophages could have efflux pumps to expel macrolides from the cytosol (Seral *et al.*, 2003) and, as fumagillin has certain similarity with this family of antibiotics (Hamilton-Miller, 1973), efflux system in macrophages could be a plausible explanation of the effect observed. Finally, it is important to highlight that 10% of the fumagillin used as standard suffered some degradation maybe motivated by light and/or temperature (Eble and Garret, 1954; Garret, 1954; Garret and Eble, 1954).

A recent study demonstrated that A549 cell line suffered a dose dependent increase of cell cytotoxicity working with fumagillin (Gayathri, Akbarsha and Ruckmani, 2020), which do not seems to be in concordance with our results of the propidium iodide assay that show that exposition to fumagillin did not affect to the cell viability. However, these authors interpret the MTT assay as cell cytotoxicity while in our opinion it is more accurate to consider it as measure of the ETC activity. Taking into consideration this fact, the results obtained by Gayathri *et al.* (2020) as well as the ones obtained by Schulz *et al.* (Schulz, Senkpiel and Ohgke, 2004) and Bünger *et al.* (Bünger *et al.*, 2004) are according with ours although our highest fumagillin (2 µg/ml) concentration is the lowest of all the studies mentioned before.

Classically, the principal role of the ETC was the ATP synthesis, but Birsoy and coworkers (2015) demonstrated a new role on aspartate synthesis and the maintaining of cell proliferation (Birsoy *et al.*, 2015). In this line, our results support this idea, as both the wound healing assay and the CFSE analysis performed by flow cytometry demonstrated that the proliferation of A549 cells was affected after fumagillin exposition. Specifically, the covalent binding of fumagillin to its molecular target, MetAP2, results in an inhibition of all functions that MetAP2 orchestrate inside the cell (Guruceaga *et al.*, 2020). They include the membrane signaling pathway involving proteins such as Gi/o, Giβγ, PI3K, PLC, DAG or IP3 that arrange cell migration and proliferation (Neves, Ram and Iyengar, 2002; Gresset and Harden, 2012; Van Keulen and Rothlisberger, 2017).

On the other hand, the results obtained with the RAW 264.7 macrophages were slightly different since although they suffered a drop in the ETC activity and a delay in the cell proliferation motivated by exposition to fumagillin, the effect was less marked than the observed in A549 cells and not dependent of concentration. These results are apparently in contradiction with a non-cytotoxic effect of this toxin over rat alveolar macrophages described by Mitchell and coworkers (1997), but it may be due to they used trypan blue, a less sensible method, to measure cell viability (Mitchell, Slight and Donaldson, 1997).

The results previously described using other toxins are not useful to compare with the ones obtained in this study because, as we demonstrate in this paper, the effect of each toxin over the cells follows a toxin specific mechanism that could be different even depending of the cell types. In fact, our results have shown that fumagillin induces higher delay in pneumocytes proliferation than in macrophages but, in contrast, it only showed effect over the macrophages viability.

The second approach of the work was to study the influence of the *fmaA* gene absence for the fungus and its virulence using a mutant strain. The phenotypical study showed that the mutant strain $\Delta fmaA$ did not present any phenotypical difference comparing to Wt strain when they grew in presence of structural, osmotic and oxidative stresses. The results obtained related with ability to produced fumagillin corroborate the results obtained previously by Wiemann and coworkers (Wiemann *et al.*, 2013). Similar results are observed in the case of the $\Delta gliZ$ mutant strain, the essential transcription factor that dictates gliotoxin production, authors did not report any differences in phenotype (Bok *et al.*, 2006).

In the study of the microscopic fungal morphology and growth, it was possible to monitor that $\Delta fmaA$ strain was able to germinate before the other strains. It might be possible that the portion of energy that the $\Delta fmaA$ strain spends in the fumagillin biosynthesis is focused on promote the germination. If fumagillin is important to fungal fitness, the inability of $\Delta fmaA$ strain to produce the toxin must be compensated. An accelerated germination seems to be the strategy elected by the mutant strain to fulfill this purpose. Furthermore, the lack of *fmaA* gene encourage a

significant double branch germination of the hyphae, which could suggest the implication of the gene in some point of the hypha polarization process or even in the regulation of the polarization process. In other fungi such as *A. nidulans*, this kind of regulation use to be orchestrated by transcription factors such as FlbB (Etxebeste *et al.*, 2008, 2009) or proteins that interact with its transcription factor such as FlbE/FlbD (Otamendi *et al.*, 2019). The possible involvement of the *fmaA* gene in these hyphal polarization regulation processes in *A. fumigatus* as well as why the non-fumagillin producer strain promoted its germination should be examined in depth in future studies.

In addition, the *fmaA* gene seems to protect, at least in part, the fungus to be phagocytosed. The evidence that phagocytosis of the heat-inactivated conidia is similar in mutants and Wt strains points out that the reduced phagocytosis of the non-fumagillin producer strain is not due to the external composition of the conidia cell wall but to the *fmaA* gene activity. Furthermore, the phagocytosis rate made by the BMMs cells was higher than the one obtained using the RAW 264.7 cell line, similarly to the results obtained previously by other authors with *Lomentospora prolificans* and different macrophages (Pellon *et al.*, 2018). Moreover, the stimulation of BMMs to produce TNF, although not significantly except at 4 hours, was in general terms lower in $\Delta fmaA$ strain than in Wt and revertant.

To finish, the *in vivo* effect of the inability to produce fumagillin was studied, showing that the $\Delta fmaA::fmaA$ strain was significant more lethal than the Wt and $\Delta fmaA$ strain. These results are in congruence with the ability to produced fumagillin observed between conidia of strains used in these experiments. In fact, although on average only in the 25% of the measures done with the complemented strain produced higher concentration of fumagillin than the Wt, the $\Delta fmaA::fmaA$ conidia used for the two mice infections produced highest mycotoxin concentration.

In contrast, the lowest mortality rate (although not significant regarding with the other two strains used) was observed in those mice infected with the $\Delta fmaA$ strain. These mice died in the first four days of infection while the rest of mice infected with the others strains died more progressively. This correlate perfectly with CFUs analysis

in which it is possible to observed that all the mice that really presented large fungal burden in its lungs were the death mice of the first 96 hours post-infection while most of survival mice did not present CFUs in their lungs. A previous study performed with this same non-fumagillin producer strain also demonstrated that the non-producer fungal strain has less cytotoxicity over the A549 cell line doing the ⁵¹Cr release assays (Guruceaga et al., 2018).

In our knowledge this is the first research that study in depth the role of the fumagillin and its importance to *A. fumigatus* virulence. The research demonstrates that fumagillin is a molecule easily detected by UHPLC that can affect in different way the different the cell types used and the fungal strain non fumagillin producer seems to be less virulent. Those mice infected with the mutant strain non-fumagillin producer survived more and in better conditions than those infected with the wild type or even the complementary strain. This supposed the first evidence in the bibliography of the importance of a mycotoxin to the infection process.

Chapter 3

Association between *A.fumigatus* *maiA* gene, cell wall and virulence



1. Introduction

As indicated in the general introduction, melanins are secondary metabolites composed by phenolic polymers or indolic monomers that act as pigments (Bayry et al 2014). The saprophytic fungus *A. fumigatus* can produce two types of melanins. On the one hand, it can synthesize dihydroxynaphtalene melanin, also known as DHN-melanin, which is one of the principal components of the conidial cell wall (Latge & Chamilos, 2019) together with galactomannans, β -1,3-glucans, chitin and rodlet proteins. On the other hand, the fungus can produce pyomelanin that is an extracellular water-soluble pigment (reviewed by Perez-Cuesta *et al.*, 2020). This molecule is produced by spontaneous polymerization of homogentisate (HGA) during the L-phenylalanine/L-tyrosine (Phe/Tyr) degradation pathway. This HGA is accumulated and goes to benzoquinone acetate by oxidative transformation that polymerize to pyomelanin.

Among the biological functions that pyomelanin fulfills, it is highlighting that this molecule seems to protect the young hyphae against the oxidative stress (Schmaler-Ripcke *et al.*, 2009). This pyomelanin production is associated to conidia germinating and directly depends of three surface sensors (Wsc1, Wsc3 and MidA) that detect Phe or Tyr and send a signal to Rho GTPases and MAP kinases (Bck1, Mkk2 and MpkA) in order to produce the activation of the cluster of genes involved in L-Phe degradation pathway (Valiante *et al.*, 2009). Furthermore, there are studies that demonstrate an overexpression of the cluster of genes involved in Tyr degradation pathway when the fungus is exposed to both mechanical and chemical cell wall stresses (Valiante *et al.*, 2009; Jain *et al.*, 2011). Therefore, pyomelanin could be a cell wall protective factor in this conditions.

It has been also described in the general introduction that the Phe/Tyr degradation pathway is mediated by six genes located in chromosome 2 of *A. fumigatus* (*hppD*, *hmgX*, *hmgA*, *fahA*, *maiA* and *hmgR*). In addition, there are other two genes not included inside the cluster abovementioned, the *phhA* and *tat* genes, which codify for the phenylalanine hydroxylase and the tyrosine aminotransferase, respectively

(Heinekamp *et al.*, 2013), and are responsible for the first degradation steps of Phe and Tyr to 4-hydroxyphenylpyruvate. In the previous transcriptomic study performed during an intranasal animal infection by this fungus, the genes *hppD* and *maiA* have been detected as up-regulated (Guruceaga *et al.*, 2018) pointing out the importance of these genes for *A. fumigatus* virulence.

There are several studies published deepening in the function of the genes of the Phe/Tyr degradation gene cluster and their importance for the fungus based on deletion/disruption mutants. However, there are still two genes of the cluster not well-characterized because they have not been deleted yet (*fahA* and *maiA*). The *maiA* is a 696 bp gene located in the chromosome 2 of *A. fumigatus* (Afu2g04240). This gene does not show introns in its sequence and codifies a maleylacetoacetate isomerase involved in Phe/Tyr degradation pathway. Concretely, this enzyme orchestrates the isomerization of 4-maleylacetoacetate into 4-fumarylacetoacetate. Theoretically, the resulting phenotype of the mutant strain $\Delta maiA$ should be similar to the phenotype shown by $\Delta hmgA$, which is the gene that codifies the enzyme located just previous to *maiA* in this degradation pathway.

In this chapter, the *A. fumigatus* genes strongly over-expressed after co-cultures of the fungus with two different cellular models (murine macrophages and human lung epithelial cells) were studied using the microarray AWAFUGE. Taking into account the transcriptomic results obtained and those obtained previously in the mouse model (**Chapter 1**), the *maiA* gene was selected because its overexpression in the three experimental infection conditions. To study the role of *maiA* gene, both in the fungal biology and virulence, the $\Delta maiA$ mutant strain was performed. The results showed a strong involvement of *maiA* in the maintenance of the cell wall structure as well as in the virulence of the fungus using a neutropenic mice model.

2. Material & Methods

2.1 *Aspergillus fumigatus* strains, media and growth conditions

The *A. fumigatus* Af293 strain was used in this chapter as Wt strain. In addition, we have developed the $\Delta maiA$ mutant strain following the method described in the **Section 2.13** of this chapter. The maintenance of these strains and the collection of their conidia and the adjustment of their concentration for subsequent studies will be carried out as indicated in **Section 2.1** of chapter 1 of the previous chapter.

To study the ability of the fungal strains to grow with a sole carbon source the GMM was replaced by a GMM modification medium without glucose that we named Salt Agar.

2.2 Cell lines

The murine macrophage cell line known as RAW 264.7 and the human epithelium cell line A549, both obtained from the American Type Culture Collection (ATCC, Manassas; VA, USA), have been used in this study. The culture conditions as well as viability calculation and passage method were done following the method described in the **Section 2.4** of the chapter 2.

2.3 Phagocytosis assays and fungal behavior against RAW 264.7 cell line

To understand the behavior of the fungal strains (Wt and $\Delta maiA$) in contact with the murine macrophages cell line RAW 264.7 we followed the method described in the **Section 2.11** of the chapter 2.

2.4 Endocytosis assays and fungal behavior against A549 cell line

To study the fungal behavior in contact with the human alveolar epithelial cell line A549 we seeded 1×10^6 cells/ml in 500 μ l of RPMI complete using 24-well plates which

contained 12 mm-diameter cover slips. After an overnight incubation, the cells were co-culture with *A. fumigatus* conidia pre-stained with FITC (conidia were stained overnight at 4°C in an orbital shaker) at a multiplicity of infection of 5 (five conidia per cell). At each incubation time (2, 4, 6, 8 and 10 hours), we removed the coverslip to a new plate in order to calculate the percentage of endocytosis. For that, a minimum of 500 cell/conidia/hyphae were count in each replica of the experiment using the invert microscope Nikon Eclipse TE2000-U (Nikon, Minato, Tokio, Japan) in order to calculated endocytosis (%), fungal germination (%) and hyphal branching (%) both in contact with epithelial cell lines and *A. fumigatus* growing alone as control condition.

2.5 RAW 264.7 ability to produced Reactive Oxygen Species (ROS) and Reactive Nitrogen Species (RNS) against *A. fumigatus*

The RAW 264.7 ability study to produce ROS and RNS in response to the fungus *A. fumigatus* was done in 24-well plates using the same conditions and times described for the phagocytosis assay method.

For the detection of ROS a kit for detection of ROS (Life Technologies, C6827) was used following the manufacturer's instructions. Briefly, during co-incubation time, a vial of the kit for detection of ROS was reconstituted by adding 173 µL of DMSO. After that the vial was diluted 1:100 with sterile PBS and pre-heated in a water bath at 37°C until its use. At the end of the 8-hour infection period, the medium was removed from all wells, 2 washes were performed with sterile pre-heated PBS, and 500 µL of the pre-heated probe was added. Subsequently, it was incubated at 37°C, 5% CO₂ for 20 minutes to allow incorporation of the probe into the cells. Then, the solution with free probe was removed and replaced by 500 µL of sterile preheated PBS incubating again for another 20 minutes under the same conditions, allowing the cells to process the incorporated probe. Finally, the fluorescence of the processed probe was measured in a plate reader (Biotek, Synergy HT) at 492 nm.

The RNS production was performed by measuring the nitrite accumulated in the medium. Once the incubation time finished, 150 µl of the supernatant was mix with 130 µl of destiled water and 20 µl of a solution SFA-NED (1:1) in a 96-well plate. After

that, the plate was incubated at room temperature during 30 minutes in dark. Finally the absorbance was measured in a plate reader (Biotek, Synergy HT) at 548 nm.

All the experiments were done in three independent days using the ROS or RNS production of a cell culture that grew without presence of fungus as control.

2.6 Cellular electron transport chain activity

The fungal electron chain activity was done after the co-incubation with RAW 264.7 macrophages and A549 epithelial cell lines. For that, we followed the methodology described in **Section 2.8** of the chapter 2.

2.7 RNA isolation

For RNA isolation we collected the cells and fungus using a cell scraper after the incubation time selected in each case (6.5 hours with RAW 264.7 and 8.5 hours with A549). Then, the samples were centrifuged during 1 minute at 14.000 rpm and the pellet was suspended in 1 ml of pre-cold DEPC sterile destilated water in order to lyse the mouse/human cells. After that, the samples were centrifuged again in the same conditions abovementioned, the fungal pellet was suspend in 500 µl of pre-cold DEPC sterile destilated water and transferred to a 1.5 ml tube containing the equivalent of 200 µl of 0.5 mm glass beads (Sigma Aldrich). The samples were homogenized using the MillMix 20 beat-beater (Technica, Slovenia) at 30 Hz during 2 minutes. Finally, we centrifuged the samples as abovementioned and the supernatant was recovered and transferred to the extraction columns of the RNeasy Plant Mini Kit, also used in **Section 2.2.5**. The RNA isolation procedure was finished following the manufacturer's instructions and the RNA quantity and integrity was verified on a 2100 Bionalyzer (Agilent Technologies, Santa Clara, CA, USA). For microarray analysis and RT-qPCR confirmation, three independent RNA samples for each time point, each of them obtained from an independent co-incubation with cells assays, were studied.

2.8 Microarray selection and hybridization.

The fungal transcriptome was analyzed using the Agilent Whole *A. fumigatus* Genome Expression 44K v.1 (AWAFUGE) microarray following the methodology describe in **Section 2.6** of the chapter 1.

2.9 Microarray expression data analysis

The raw data obtained form each microarray was processed exactly as is described in **Section 2.7** of the chapter 1. With this analysis we determined the genes down-regulated or up-regulated if their expression was significantly lower or higher relative to the fungal growth alone.

2.10 Microarray data confirmation by reverse transcription quantitative PCR

We selected a subset of 22genes to verify by RT-qPCR the fungal expression profile against RAW 264.7 macrophages, and 22 genes against A549 pneumocytes. In bboth cases we used the same 4 referrece genes (**Table S4**). Specific *A. fumigatus* primers were designed using Primers Quest Tool (available at “<https://eu.idtdna.com/site>”) in order to avoid false positives due to mouse or human RNA remaining in the samples. RT-qPCR experimentes and analysis were done as is described in **Section 2.9** of the chapter 1, including the Housekeeping genes selection.

2.11 Gene ontology (GO) analysis

The GO enrichment of those DEGs that presented $\log FC > 1.5$ or $\log FC < -1.5$, was done using the method described in **Section 2.8** of the chapter 1.

2.12 Gene target selection criteria

The selection of *maiA* as an important *A. fumigatus* gene involved in fungal virulence was determined after analyzed previous transcriptomic studies. We classified the genes following their fold change values (FC). We only focused our attention in those genes highly down- or up-regulated ($FC < 1.5$ or $FC > 1.5$ respectively). After that, we

compared the common up-regulated DEGs of *A. fumigatus* genes in three different assays: **1)** Af293 *A. fumigatus* strain in co-incubation with lung epithelial cell line A549, **2)** Af293 *A. fumigatus* strain in co-incubation with macrophages RAW 264.7 and **3)** Af293 *A. fumigatus* strain infecting immunosuppressed mice (Guruceaga *et al.*, 2018) (**Chapter 1**).

2.13 Generation of the $\Delta maiA$ mutant strain using CRISPR-Cas9 technology

The *A. fumigatus* mutant strain used in this study was performed using the CRISPR-Cas9 protocol developed and published by the Dr. Fortwendel's research group (Al Abdhalla *et al.*, 2017). Although the $\Delta akuB$ *A. fumigatus* strain is the easiest strain to transform successfully, in this study we used the Wt genetic background Af293 strain in order to use the same strain used in the transcriptomic studies in which we selected *maiA* gene as interesting, avoiding bias interpretations. The list of used primers, their corresponding sequences and the objective by which we designed that primers are summarized in **Table 3**. Briefly, *A. fumigatus maiA* mutant strains were performed using hygromycin B (ThermoFisher, Waltham, MA, USA) as selected marker. For the disruption mutant strain ($\Delta maiA$), hygromycin resistant cassette (HygR) was PCR amplified from pUCGH plasmid using the primer set P1/P2 that included 40 bp of *maiA* microhomology sequence each (**Fig. 27A**).

For the *in vitro* assembly of the abovementioned cassettes, we used CAS9-gRNA ribonucleoprotein complexes (RNPs) strategy. The RNPs were composed of crRNA, tracrRNA and the Cas9 protein (IDT, Coraville, IA, USA) (Al Abdhalla *et al.*, 2017) To disrupt the *maiA* gene ($\Delta maiA$), the gRNA target and its corresponding Cas9 cut point were designed in order to delete initial methionine (iMet) of the *maiA* gene, thus performing a disruption of the target gene.

Transformation of *A. fumigatus* protoplasts was carried out following the classic protocols described in the **Section 2.2** of the **Chapter 1**.

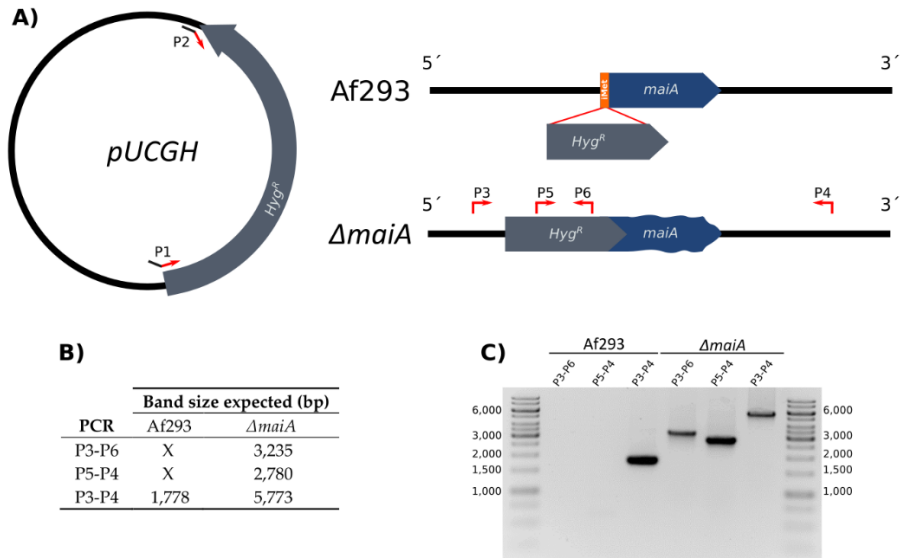


Figure 27. Scheme of the genetic strategy followed to develop the mutant strain $\Delta maiA$. **A)** Summary of the primers location used in this study as well as the disruption mechanism used to generate the disruption strain $\Delta maiA$. **B)** Table that summarizes the band size expected (in base pairs, bp) depending of the combination of primers used to validate the mutant colonies. **C)** Agarose gel showing the PCR confirmation of the $\Delta maiA$ mutant strain comparing with the wild type strain Af293.

Table 3. List of primers used and its utility in this study.

Primer name	Sequence (5' → 3')	Utility
P1	<u>TACCCAAGTGGCACTCTTTCATAATCAAAGT</u> <u>TAACATCGTGGCCAGTGCCAAGCTTGCAT</u>	Cassete construction
P2	<u>AAGAGCTGATATGCATTCCAAATGTGCACAA</u> <u>AGGAAGCCTAACATGAGAATTCATCGATG</u>	
P3	TCGGATGTTTGTAGCAGCGG	Screening
P4	CCATATCTTCGGCGTCGTAT	
P5	GCTCACGAGTTCGTACATT	
P6	TCGACTTCAGCAACATCTCC	

Underline nucleotides are the ones designed by microhomology. Bold nucleotides are the ones complementary to 5' and 3' regions of hygromycin resistant gene included in pUCGH plasmid.

2.14 Mutant strains PCR confirmation

All the strains capable to grow at least twice in GMM supplemented with 150 µg/ml of hygromycin B were confirmed by PCR, combining different primer sets (**Table 3**) as we showed in the **Fig. 27B**. First, we checked the presence of the HygR cassette in the expected genome site performing two screening PCRs. For the first one we used a forward primer located in the promoter combined with a reverse primer located inside the HygR (P3/P6). Conversely, for the second PCR we used a forward primer located inside the HygR and a reverse one in the terminator (P5/P4). Finally, we amplified the whole region using P3/P4 and we compared the product size with the obtained in the Wt strain after perform an electroforesis. For that we used an agarose gel (1%) that were run during 45 minutes at 90 v.

2.15 Determination of the pyomelanin production

Pyomelanin production was done following a published protocol (Schmaler-Ripcke *et al.*, 2009). Briefly, GMM broth (200ml) was inoculated with 1×10^7 conidia of each respective *A. fumigatus* strain. After 20 h of preincubation, Phe or Tyr was added to a final concentration of 10 mM. Aliquots of 500 µl of GMM broth were taken at 24, 48h and 72 hours. Pigment formation was analyzed by direct absorbance measurements at 405 nm of the alkaliized supernatants obtained by adding 20 µl of 5M NaOH per ml of sample and centrifuging them at 16,000 x g for 2 min. The experiment was carry out in three independent days.

2.16 Fungal susceptibility to H₂O₂ oxidative agent

The sensitivities of the *Af293* and *ΔmaiA* mutant strains to H₂O₂ were measured using GMM agar plate following the diffusion assay. Briefly, conidia of both strains (2×10^8) were seeded and expanded along all the surface of a GMM agar plate (Petri dishes of 90 mm). Once the fungus was seeded a central hole was done in the middle of the agar plate using a tip. Finally, 50 μl of a 200 mM solution of H₂O₂ was added to the central hole. After let drying the plates during 5 minutes, the plates were incubated at 37°C during 48 hours. Daily the diameter of the inhibition halo was measured. The experiment was carry out in three independent days.

2.17 Quantification of cell wall glucan content

Total β-glucan assay was performed following the methods previously described (Fortwendel et al., 2009; Koenig et al., 2017; Oliveira Souza et al., 2018). Briefly, 2×10^8 conidia were grown overnight into 100 ml of GMM broth at 37°C. After 14 hours of growing, hyphae were collected by filtration through Miracloth (SigmaAldrich, St. Louis, Mo, USA) and washed using 0.1 M NaOH solution. Washed fungal hyphae were lyophilized during 24 hours. Dry hyphae were weight and then samples were disrupted in a bead-beater three times (1 minute each) intercalating with 1 minute of ice incubation. Hyphal powder was resuspendend getting a final concentration of 20 mg/ml in 1 M NaOH and the solution was incubated at 52°C for 30 min. Fifty microliter of each sample were mixed with 185 μl of aniline blue staining solution (183 mM glycine, 229 mM NaOH, 130 mM HCl, and 618 mg/l aniline blue, pH 9.9) into a 96 well masked fluorescence plate (ThermoFisher, Waltham, MA, USA). A standard curve (from 160 μg/ml to 2.5 μg/ml) was added to the plate using Curdlan (a β-1.3-glucan analog). The sample containing plates were incubated at 52°C for 30 min followed by a cool down period of 30 min at room temperature. Fluorescence readings were performed using an excitation/emission wavelength of 405/460 nm respectively. All the experiments were performed by triplicate using three independent *A. fumigatus* cultures.

2.18 *A. fumigatus* stress response: spotting assay and radial growth.

The spotting assay of each strain (Wt and $\Delta maiA$) was done following the method described in the **Section 2.2** of the chapter 2 (**Fig. 20**). The stresses used are summarized in **Table 4**.

Furthermore we characterized the radial growth ability of the $\Delta maiA$ mutant strain in comparison with the Wt. For that, we seeded a 20 μ l drop containing a suspension of 10^8 fresh conidia in the middle of a GMM agar plate. The plates were incubated at 37°C during five days and the radial growth of the macroscopic colonies will be measured daily.

All the experiments were done in three independent days. In the results sections only the most representative pictures of each condition will be show.

Table 4. Summary of stressant compounds used in the spotting assay

Base Medium	Stress compound	Concentration	Aim	Figure
GMM	CR	40 µg/ml	Cell wall stress	Fig. 33
	CW	40 µg/ml		
	CR + Sorbitol	40 µg/ml + 1.3 M		
	CW + Sorbitol	40 µg/ml + 1.3 M		
	SDS	0.00625%	Osmotic stress	
	Sorbitol	1.3 M		
	NaCl	1.2 M		
Salt Agar	KCl	1.2 M	MAPK stress	Fig. 31
	Caffeine	5 mM		
	Tyr	0.5 M		
	Phe	0.5 M		
	Tyr + Phe	0.5 M + 0.5 M	sole carbon source	

(CR) Congo red, (CW) Calcofluor white, (SDS) Sodium dodecyl sulfate, (Phe) L-Phenilalanine, (Tyr) L- Tyrosine, (MAPK) Mitogen-activated protein kinases.

2.19 Scanning electron microscopy (SEM)

For the cell wall surface study 5×10^5 conidia/ml from the Af293 and $\Delta maiA$ strains were seeded in 1 ml of GMM in 24-well plates containing glass coverslips. The plates were incubated at 37°C, 5% CO₂ and 95% of humidity during 12 hours. The fungal surface of each strain was studied after 2, 4, 8 and 12 hours of incubation by SEM. After each time studied the GMM was removed and fixing solution was added to each well. Then the samples were dehydrated through increasing ethanol concentrations and hexamethyldisilazane. Finally, they were covered with gold under argon atmosphere, and visualized under the scanning electron microscope (Hitachi S-4800).

2.20 Murine model of invasive pulmonary aspergillosis

Groups of 8 female CD-1 mice (Charles River, Wilmington, MA, USA), weighing approximately 25 g, were immunosuppressed by intraperitoneal injections of 150 mg/kg of cyclophosphamide (Sigma-Aldrich) starting 3 days before the inoculation and every 3 days, and a single subcutaneous injection of triamcinolone acetonide (Kenalog, Bristol-Myers Squibb) (40 mg/kg) 24 hours before the infection.

On day 0, mice were slightly anesthetized with isoflurane and challenged via nasal instillation with 10^6 conidia in saline solution. Survival was monitored at least twice a day and those animals showing severe signs of distress were humanely euthanized by anoxia with CO₂. In order to prevent bacterial infections, mice were administered with a combination of sulfamethoxazole and trimethoprim in the drinking water, starting 3 days before the infection. Survival curves were compared using the log-rank test in GraphPad Prism v. 8.2.1 for Windows. The studies were performed in accordance to approved protocols by the LACU committee of the University of Tennessee Health Science Center.

3. Results

3.1 Different *A. fumigatus* behaviour against macrophages and lung epithelial cell lines

We performed a preliminary study of the interaction between *A. fumigatus* and two of the predominant cell types that the fungus can find during lung colonization, macrophages and lung epithelial cells, to characterize the process and select the optimal point to obtain the sample to transcriptomic analysis (around 30% of fungal germination).

3.1.1 Study of co-incubation between *A. fumigatus* and macrophages

The results obtained from the co-incubation with the murine macrophages RAW 264.7 showed a maximum of 80% of phagocytosis after 4 hours (**Fig. 28A**). Regarding fungal germination, the 30% was reached about 6 hours of incubation in all cases (**Fig. 28B**). Furthermore, the contact with the immune cells seems to stimulate this process, being the differences in germination between conditions statistically significant after 8 hour. On the contrary, we did not find any differences in the amount of fungal hyphal growth or their double branch germination (**Fig. 28C**).

In relation with *A. fumigatus* viability, a decreased in fungus viability was detected as the co-incubation time progressed (**Fig. 28D**). Finally, the production of reactive oxygen species (ROS) and nitrites by macrophages showed that while ROS production was progressively increasing during the time of co-incubation, reaching a maximum of production after 8 hours (47.88% more production than the macrophages alone) (**Fig. 28E**), the nitrite production presented the opposite pattern. Specifically, Nitrite showed the maximum production after only 5 minutes (71.93 μM), decreasing almost completely after 80 minutes (**Fig. 28F**).

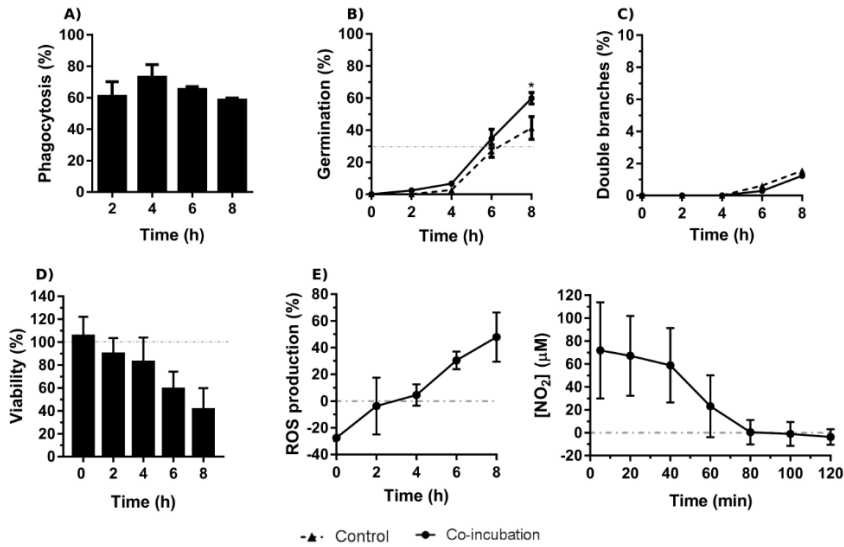


Figure 28. Characterization of the co-incubation between the fungal strain Af293 and the macrophage cell line RAW 264.7. **A)** Phagocytosis assay during 8 hours of co-incubation with Af293 fungal strain. **B)** Percentage of germination of the Af293 strain alone and in co-incubation with the macrophage cell line RAW 264.7. Grey dashed line means 30% of germination. **C)** Percentage of double branches of the Af293 strain alone and in co-incubation with the macrophage cell line RAW 264.7. **D)** Viability study of the Af293 strain after been incubated with the RAW 264.7 macrophages. The results are relative the fungal strain growing without macrophages. Grey dashed line means 100% of cellular viability. **E)** Reactive oxygen species (ROS) production of the cell line RAW 264.7 during the co-incubation with the Af293 fungal strain. Grey dashed line corresponds to ROS production by control macrophages. **F)** NO_2 production ability of the cell line RAW 264.7 in co- incubation with the Af293 fungal strain. Grey dashed line corresponds to RNS production by control macrophages. * $p < 0.05$

3.1.2 Study of co-incubation between *A. fumigatus* and epithelial cells

The co-incubation process between *A. fumigatus* and the lung epithelial cell line A549 showed a maximum of endocytosis of around 5% after 6 hours of co-incubation (**Fig. 29A**). In addition, an inhibition of the germination rate was observed when the fungus was growing in co-culture with this epithelial cell line. In fact, the 30% of germination was reached after 8 hours of co-incubation with the epithelial cells while the fungus growing alone reached this germination rate at 6 hours (**Fig. 29B**). However, in spite of this delay in germination, an increase of the double germination at 8 h was observed until reaching at least the double of the one observed in the controls when *A. fumigatus* grew alone (**Fig. 29C**).

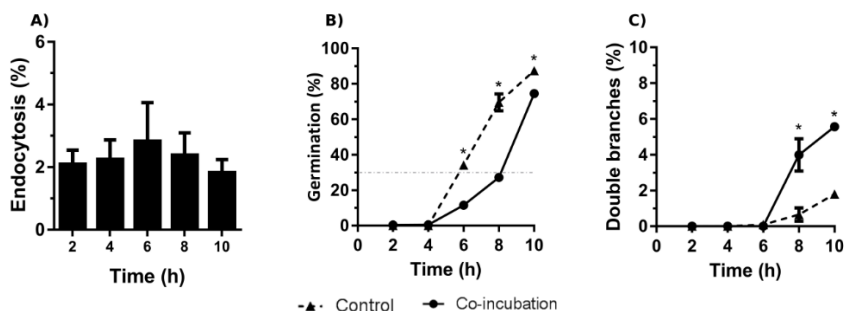


Figure 29. Characterization of the co-incubation between the fungal strain Af293 and the human epithelial cell line A549. A) Endocytosis assay during 10 hours of co-incubation with Af293 fungal strain. **B)** Percentage of germination of the Af293 strain in co-incubation with the lung epithelial cell line A549. Grey dashed line means 30 % of germination. **C)** Percentage of double branches of the Af293 strain in co-incubation with the lung epithelial cell line A549. *p< 0.05

3.2 *A. fumigatus* gene expression in response to the co-incubation with RAW 264.7 macrophages or A549 epithelial cell line

After the selection of 6 and 8 hours of co-incubation with macrophages and epithelial cells, respectively, as the time to obtain a 30% of germination, three samples of mRNA from each condition obtained in independent experiments, as well as their respective controls were hybridized with the microarray. Once analyzed and normalized the data, it was found that 2.137 were *A. fumigatus* DEGs when incubated with the macrophages and 5.325 with the human lung epithelial cells compared to the fungus growing alone during the same period of time.

Due to the great amount of DEGs, only those genes greater up- or down-regulated (fold change (FC) > 1.5 or < -1.5) were studied. Taking into account this consideration, during the co-incubation with the macrophages 235 *A. fumigatus* genes were down-regulated and 280 up-regulated (**Fig. 30A**), while 534 were down-regulated and 878 up-regulated during the contact with the epithelial cells(**Fig. 30B**).

The transcriptomic data obtained from the AWAFFUGE microarray were, then, confirmed by RT-qPCR (**Fig. 30C and 30D**), showing a good correlation results between both techniques. Specifically, a correlations of 70.79% and 90.03% were obtained between microarray and RT-qPCR verification in the co-incubation of *A. fumigatus* with macrophages, and with epithelial cells, respectively (**Fig. 30C and 30D**). In **Fig.**

30D and 30E FC values for each gene used for validation process are shown. All of them, except those marked in red, showed a similar expression in both techniques.

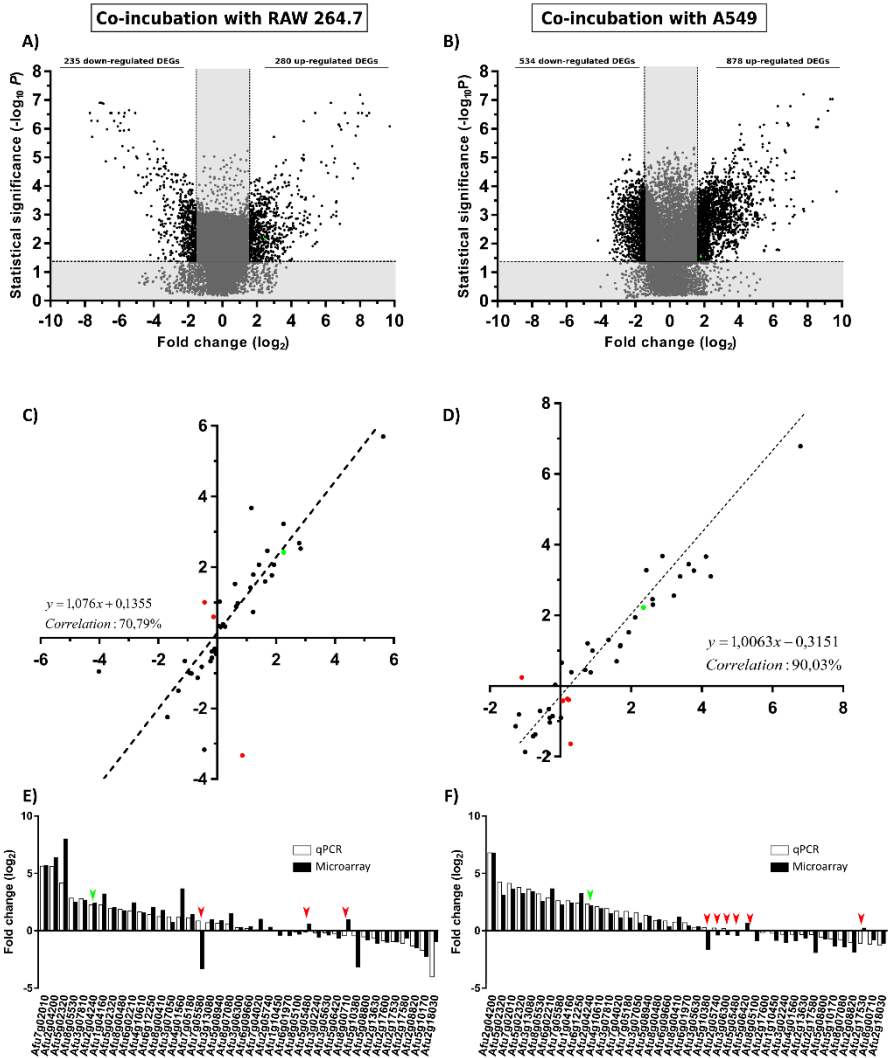


Figure 30. Gene expression analysis. **A** and **B**) Volcano plot showing *A. fumigatus* differentially (black) ($FC > 1.5$ or $FC < -1.5$) and non-differentially (grey) expressed genes in co-incubation with the murine macrophages cell line RAW 264.7 (**A**), and human lung epithelium cell line A549 (**B**). The x-axis values represent the fold change (\log_2) of microarray data and the y-axis values represent the statistical significance ($-\log_{10}P$). Spots with positive values indicate upregulation of the fungal genome during the co-incubation with the cell line abovementioned. **C** and **D**) Correlation analysis between microarray and RT-qPCR data. The x-axis values represent the fold change (\log_2) of microarray data and the y-axis values represent the fold change (\log_2) of RT-qPCR results of the selected fungal genes in co-incubation with the murine macrophages cell line RAW 264.7 (**C**), and human lung epithelium cell line A549 (**D**). Each point corresponds to the mean value from three independent samples. **E**) Comparative levels of fungal genes expression between the microarray and the RT-qPCR (*Af293* in co-incubation with the murine macrophages cell line RAW 264.7). **F**) Comparative levels of fungal genes expression between the microarray and the RT-qPCR (*Af293* in co-incubation with the human epithelium cell line A549). Green points in **A**, **B**, **C** and **D** and green arrows in **E** and **F** show the corresponding results obtained to *maiA* gene. Red spots in **C** and **D** and red arrows in **E** and **F** showed contradictory results in gene expression detected between microarrays and RT-qPCR results.

3.3 Go enrichment analysis of the most up/down-regulated DEGs and comparison between different infection models

A GO enrichment analysis of those genes that reached the cut-off point of $FC > 1.5$ (up-regulated) or $FC < -1.5$ (down-regulated) was performed to obtain a general idea of those process, components and functions of great relevance for *A. fumigatus* during the experimental procedure (The whole analysis of DEGs can be found in **Table S5**).

Among all these *A. fumigatus* genes, 227 (RAW 264.7 vs Control) and 592 (A549 vs Control) were adscript to a known biological process. The five most relevant process in this category are those related with the transport, the regulation, the response to stress, the sencodary metabolic process, and the lipid metabolic process.

In addition, 252 *A. fumigatus* genes (RAW 264.7 vs Control) and 605 genes (A549 vs Control) were adscript to a known molecular function. About the activities more relevant in this last section it is worth mentioning the oxidoreductase, hydrolase activity, and transporter and transferase activities

To finish with GO enrichment analysis, it is remarkable that 321 (RAW 264.7 vs Control) and 795 (A549 vs Control) have been previously described in any cellular location, being mebrane, mitochondrion, nucleus, cytosol, plasma membrane and the extracellular region, in this order, the locations that agrupated more genes.

To select the most important genes related to infection, among the great amount of overexpressed *A. fumigatus* genes found, those up-regulated with a $FC > 1.5$ in co-incubation with both the macrophages and the epithelial cells were selected. In this way, a total of 140 *A. fumigatus* genes were obtained (**Table S6**), which were also compared with those detected during mice infection model (**Chapter 1**). The results are 13 genes significantly up-regulated under the three experimental infection models and summarized in **Table 5**, of which the gene *Afu2g04240* was selected as a good candidate to study its implication for *A. fumigatus*. The expression pattern of this gene has been corroborated by qPCR (green spots in **Fig. 30C** and **30D** and green arrows in

Fig. 30E and 30F). This gene is an exonic small gene of 696 base pairs located in *A. fumigatus* chromosome 2. The gene is called *maiA* and codifies a maleylacetoacetate isomerase involved in the Phe/Tyr degradation pathway.

Table 5. Common overexpressed DEGs in the three experimental infection models.

ID	Product		Fold Change (log ₂)		
			RAW 264.7 vs Control	A549 vs Control	Intranasal infection (Day 4 vs Day 1)
Afu1g04160	Aspartate aminotransferase		3.22	2.45	3.22
Afu2g04200	4-hydroxyphenylpyruvate dioxygenase		6.38	6.78	4.21
Afu2g04240	Maleylacetoacetate isomerase	<i>maiA</i>	2.42	2.22	3.72
Afu3g07810	Succinate dehydrogenase subunit	<i>sdh1</i>	2.72	1.52	2.90
Afu4g10610	Stress responsive A/B barrel domain protein		1.59	1.94	4.39
Afu5g02320	Conserved hypothetical protein		2.07	3.27	3.33
Afu5g02330	Major allergen and cytotoxin Asp f 1	<i>aspf1</i>	3.00	3.10	4.64
Afu6g00430	IgE-binding protein		2.84	2.24	4.02
Afu6g02210	Cytochrome P450 monooxygenase		2.46	3.68	4.28
Afu6g03590	Citrate synthase	<i>cit1</i>	2.61	3.54	4.05
Afu6g12250	Succinyl-CoA:3-ketoacid-coenzyme A transferase putative		2.07	3.28	3.61
Afu7g02010	Indoleamine 2,3-dioxygenase family protein		5.70	3.66	5.72
Afu8g05530	Fumarate reductase	<i>osm1</i>	2.52	2.56	3.97

3.4 $\Delta maiA$ disruption mutant strain genetic manipulation strategy

The genetic manipulation strategy followed to construct the $\Delta maiA$ mutant strain is summarized in **Fig. 27A**. Briefly, a disruption mutant in which the initial methionine (iMet) was replaced by the hygromycin resistance gene was constructed. The resulting mutant strain ($\Delta maiA$) is resistant to hygromycin and has the target gene silenced due to the lack of the iMet.

To validate the mutation process of those fungal strains able to grow in presence of hygromycin after Af293 transformation, a PCR strategy was followed. In the **Fig. 27B**, it was shown the band size expected of WT and disruption mutant strains by use of each pair of primer. Using this strategy, of the two colonies obtained growing on the hygromycin media, only one was a correct $\Delta maiA$ mutant strain (50% of efficiency). The **Fig. 27C** shows the the PCR products resulting from the PCR confirmation migrated in an agarose gel.

3.5 The *maiA* gene is essential for Phe/Tyr degradation pathway

The behaviour of the wild type strain Af293 as well as the $\Delta maiA$ mutant strain when they grew during 72 hours in GMM broth (**Fig. 31B**), GMM broth supplemented with 10 mM of Phe (**Fig. 31C**) and GMM supplemented with 10 mM of Tyr was the expected. Indeed, when Phe or Tyr are added to the media, the $\Delta maiA$ mutant strain accumulated HGA and 4-MA and their subsequent spontaneous polymerization to pyomelanin (absorbance at 405 nm) was observed (**Fig. 31C** and **31D**). The production of pyomelanin was different when Phe or Tyr were used, indicating different ability to degrade both aminoacids, maybe produced because the Phe can be used in more metabolic pathways than the Tyr (**Fig. S2**).

It was also highlighting that when Salt Agar plates supplemented with 0.1 M of Phe, 0.1 M of Tyr or 0.1 M of both aminoacids as only carbon source were used, the $\Delta maiA$ strain was unable to growth (**Fig. 31E**).

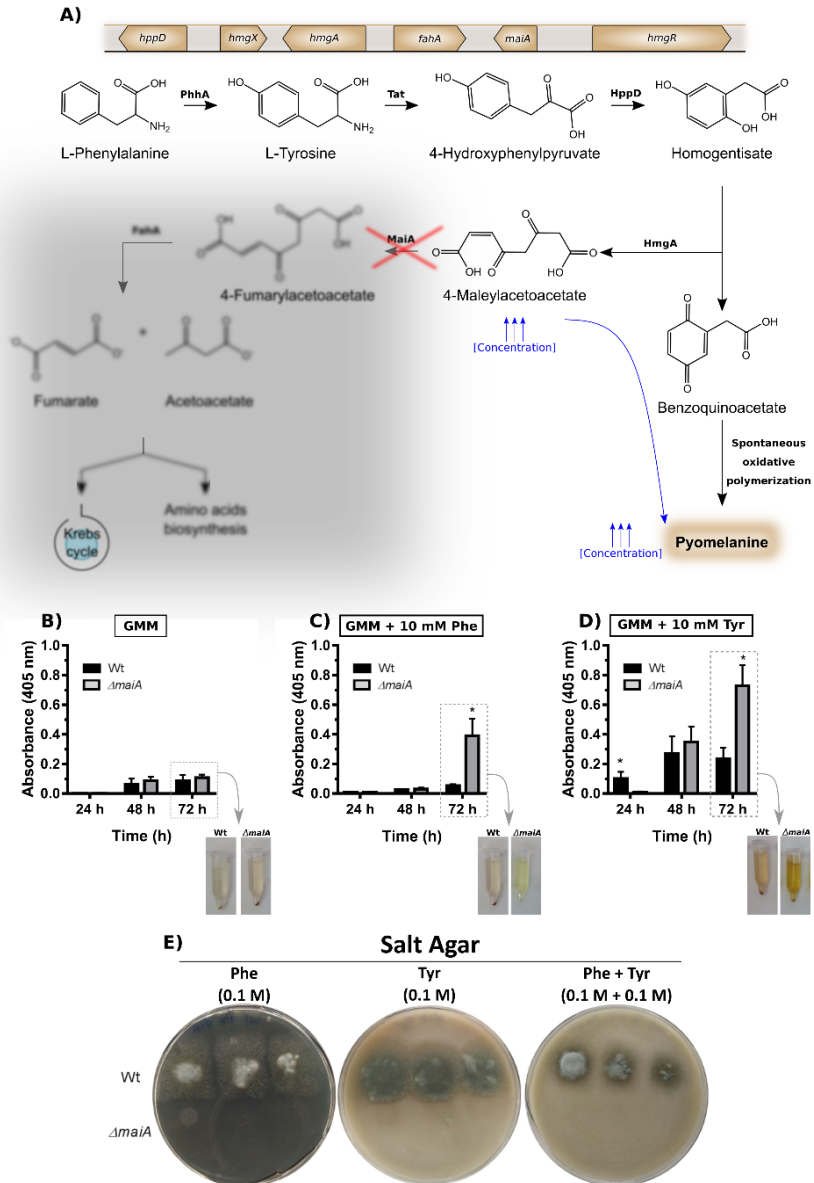


Figure 31. Fungal strains characterization results in relation with pyomelanin production and growth ability in presence of Phe and/or Tyr. A) Phe degradation pathway including the genetic cluster and the proteins involved in each step. The red cross means the point in which the pathway is disrupted due to the knock down mutation produced in $\Delta maiA$ strain. The diffused grey area indicate the part of the pathway that the $\Delta maiA$ strain cannot develop. Pyomelanin secretion ability of the fungal strains Af293 and $\Delta maiA$ growing in **B)** GMM broth, **C)** GMM broth supplemented with 10 mM of Phe and **D)** GMM broth supplemented with 10 mM of Tyr. The three panels (**B**, **C** and **D**) include photograph details of the samples measure to generate the graphs. **E)** Spotting assay after 72 hours of incubation of the Wt and $\Delta maiA$ strains in salt agar plates in which the only carbon source were Phe (0.1M), Tyr (0.1M) and a mix of Phe and Tyr (0.1M each).

3.6 The *maiA* gene affects germination, cell-wall composition and cellular homeostasis in *A. fumigatus*

The first step to understand the role and importance of the *maiA* gene for the fungus was to study the basic behaviour of the $\Delta maiA$ mutant strain. For that, first the germination ability of the mutant *versus* the Wt strain was compared. The **Fig. 32A** shows that the $\Delta maiA$ mutant strain presented a germination rate higher than the Wt, this difference being significant after 8 hours of incubation.

In contrast, there was not any difference in the radial growths of the macroscopy colonies in GMM agar plates (**Fig. 32B**). Neither were differences found between the strains in the H₂O₂ susceptibility assay since the diameter of inhibition in both strains was of around 20 mm (**Fig. 32C**).

A very interesting finding was that the $\Delta maiA$ mutant strain presented significant less glucans than the Wt strain (**Fig. 32D**). Specifically, while the Wt strain presented 4.95 μg of glucans per milligram of mycelia, the mutant had only 2.67 $\mu\text{g}/\text{mg}$. In some of the replicas, the amount of glucans measured in the Wt strain was more than twice of the amount of glucans quantified in the mutant strain.

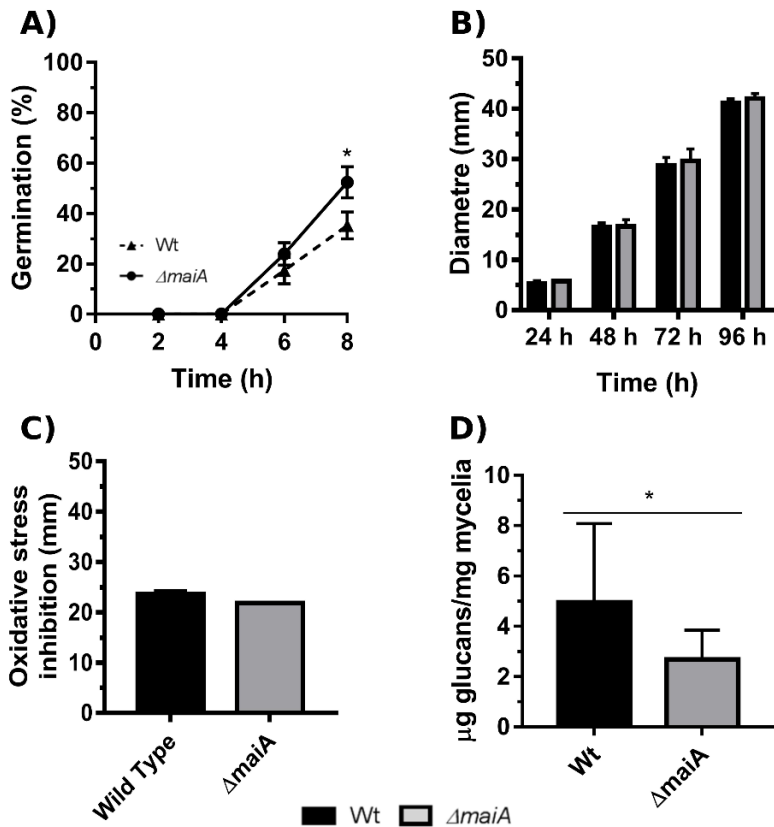


Figure 32. Cellular characterization results of the $\Delta maiA$ mutant strain. A) Percentage of germination during 8 hours of incubation in RPMI completed of the Af293 and $\Delta maiA$ strains. **B)** Diameter evolution of the colonies of both strains in GMM plates. **C)** Inhibition halo diameter of a culture of both fungal strains in GMM agar plates after 48 hours of incubation in presence of 200 mM H_2O_2 in a centre hole of the plate. **D)** Quantification of the amount of glucans present in the fungal strains (μg of glucans / mg of mycelia weight). * $p < 0.05$

Therefore, to deep into the role of *maiA* in the cell wall, a spotting assay using different stressor compounds was performed (Fig. 33). As it was expected due to the less amount of glucans in its cell wall, the mutant strain was hyper-susceptible to the cell wall stressors congo red (CR) and calcofluor white (CW). The ability of the mutant strain to grow in presence of both compounds was recovered by addition of sorbitol. In contrast, the mutant was more resistant than the Wt strain to ion stress produced by KCl, NaCl, Sorbitol and SDS.

Finally, we tested the fungal response using a Tor pathway stressor (Caffeine) to study MAPK functioning. The results obtained show that the $\Delta maiA$ strain grew slightly better than the Wt.

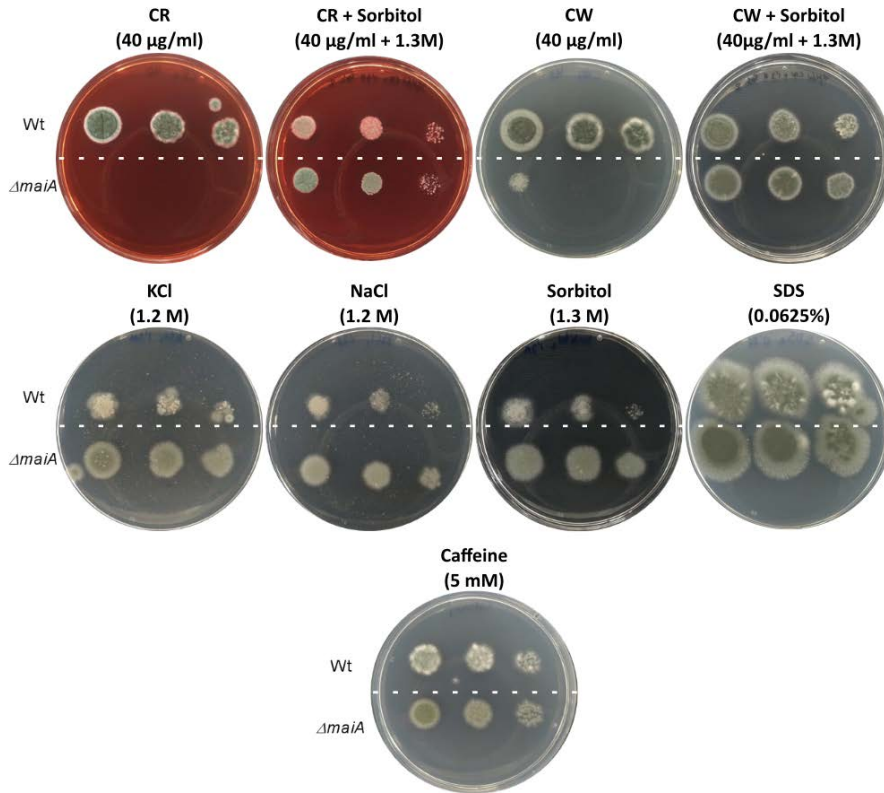


Figure 33. Phenotypic characterization spotting assay using GMM agar plates supplemented with the different agents indicated after 72 hours of incubation.

3.7 The $\Delta maiA$ hyphae present an unstructured morphology.

Scanning electron microscopy (SEM) analysis of the fungal appearance after growing 12 hours in GMM broth showed that while Wt strain maintained a perfect morphology of hyphae with its typical 45° branches and a general aspect of mycelial order well attached to the surface of the medium (**Fig. 34A**). On the contrary, the $\Delta maiA$ strain showed disorganized mycelium, which seemed to be more aerial and less attached to the medium. It was composed by thinner hyphae than Wt, with less ramifications and not dispersed at 45° angle (**Fig. 34B**).

In addition, analyzing in detail the images, the Wt hyphae were surrounded by an unknown matrix, which was more prevalent in the apex of the structure (**Fig. 34C**), while most of $\Delta maiA$ hyphae did not present it (**Fig. 34D**). Finally, it is also highlighting the differences between the hyphal surfaces, because $\Delta maiA$ hyphae surface revealed a composition more erratic and less turgid than the Wt, whose hyphae were appeared more consistent and organized. In general and from a subjective point of view, the $\Delta maiA$ hyphae presented a weakened aspect compared to the Wt strain.

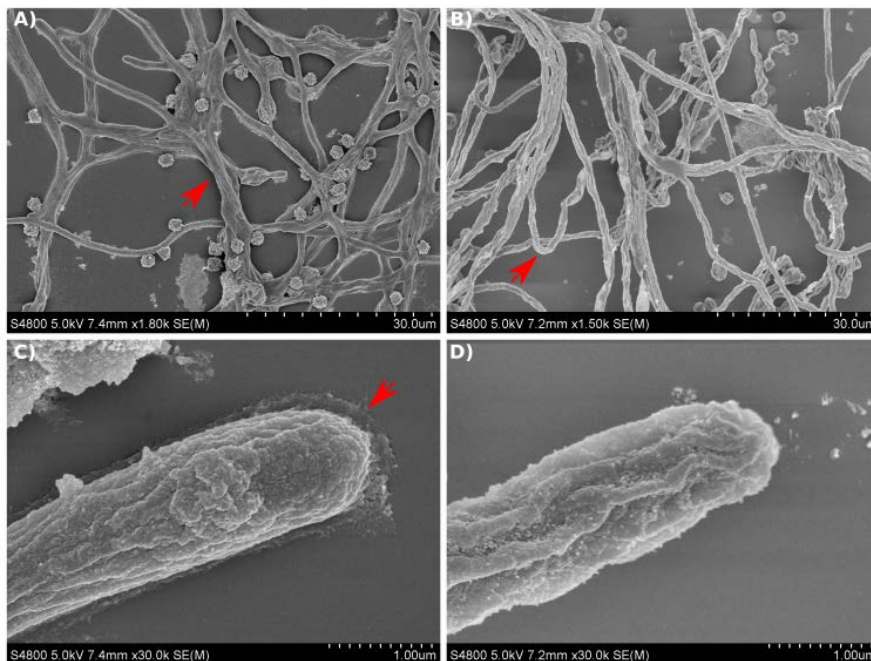


Figure 34. Scanning electron micrographs of *A. fumigatus* strains growing in GMM broth during 12 hours. **A and C)** SEM images of Af293 hyphae. **B and D)** SEM images of $\Delta maiA$ hyphae. Red arrows showed specific details described in text.

3.8 The *maiA* gene has a direct impact in the virulence of *A. fumigatus*

The last step in the characterization process was the evaluation of the infective ability of the mutant strain $\Delta maiA$. For that, the first experiment was a phagocytosis assay in which both fungal strains (Af293 and $\Delta maiA$) were co-incubated with macrophages. The results showed that, in general, during the 8 hours of the experiment, the mutant strain was more susceptible to phagocytosis than the Wt strain, this difference being statistically significant only at 2 hours of co-incubation (**Fig. 35A**).

In parallel, the germination ability of the fungal strains during the co-incubation was also studied. In this assay, it was observed that the germination of the $\Delta maiA$ was significant higher than that of the Wt (**Fig. 35B**). Although after 8 hours of co-incubation, the phagocytosis of both strains was equal, the mutant strain $\Delta maiA$ showed an average germination near to 80% against the 30% of the Af293 strain.

Finally, we wanted to study the impact of the absence of the *maiA* gene on virulence *in vivo*, using a neutropenic mouse model. The results revealed that while all mice infected with the Wt strain died from day 7 until day 10 post-infection. However, the mice began to die on day 8 post-infection (one day later) and, more significantly, 70% of the mice survived until the end of the experiment (day 15), showing a significant lower lethality than Wt strain (**Fig. 35C**).

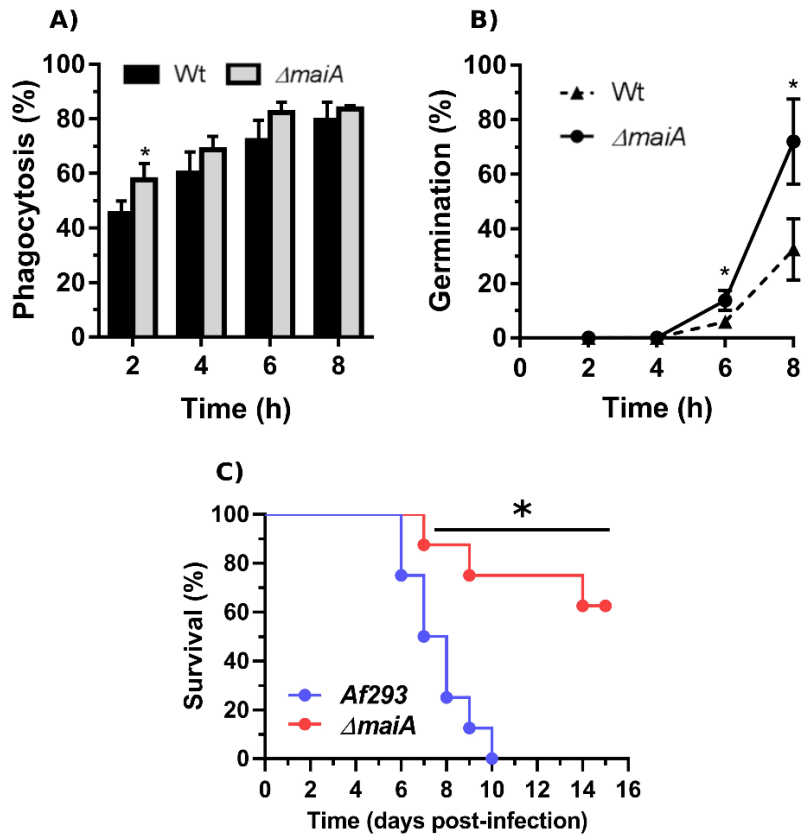


Figure 35. Characterization results of the $\Delta maiA$ mutant strain during infection process. A) Phagocytosis results after 8 hours of co-incubation between the two fungal strains and the macrophage cell line RAW 264.7. **B)** Percentage of germination of the Af293 and $\Delta maiA$ strains in co-incubation with the macrophage cell line RAW 264.7. **C)** Kaplan-Meier analysis of leukopenic infected mice during 15 days post intranasal exposition to Af293 and $\Delta maiA$ fungal strains. * $p < 0.05$

4. Discussion

The whole transcriptomic studies have been a great molecular strategy to understand, from a global point of view, the gene response of an organism to different conditions. In the case of *A. fumigatus*, there are several examples in the literature in which the whole gene expression pattern has been studied (McDonagh *et al.*, 2008; Sugi *et al.*, 2008; Bertuzzi *et al.*, 2014; Cairns *et al.*, 2010; Sueiro-Olivares *et al.*, 2015; Guruceaga *et al.*, 2018). Since some years ago, the combination of *A. fumigatus* transcriptomic studies with the generation of mutant strains has been consolidated as a suitable approach to clarify gene functions. However, the strategies to obtain *A. fumigatus* mutant strains has changed during the last years thanks to the molecular revolution caused by CRISPR-Cas9, which was applied for the first time on *A. fumigatus* in 2017 when Al Abdhalla and coworkers defined a new great efficiency protocol (Al abdhalla *et al.*, 2017).

In this chapter, two *A. fumigatus* transcriptomic studies in two different *in vitro* infection model assays were carried out followed by the generation of a mutant strain of a gene up-regulated in all experimental infections used in this Doctoral Thesis to define its role on fungal pathobiology.

For that, *A. fumigatus* Wt strain was co-cultured with two cell types usually found in lung: macrophages and lung epithelium cells. Concerning macrophages, it is important to highlight that the maximum of phagocytosis was reached after 4 hours of co-incubation (around 80%). Furthermore, the fungus germinated more in co-incubation with macrophages being the difference significant after 8 hours of co-incubation. Finally it should be highlight that the viability of the fungus decreased during the 8 hours of the assay in consequence of the response of the macrophages. This response consists in a combination of an initial NO₂ production during the first hour follow by a ROS production from the 2 hours of assay until the 8 hours. On the other hand, the lung epithelial cell line presented a maximum of endocytosis after 6 hours of co-incubation (5%). Furthermore, we observed an inhibition of the germination when the fungus was growing in co-culture with the epithelial cell line. However, a

significant greater amount of germinated conidia with double branches was detected in comparison to the ones counted when *A. fumigatus* grew alone, maybe in order to response against the endocytosis. We use the incubation time when *A. fumigatus* reached 30% of germination to obtain the total mRNA to hybridize with the AWAFUGE 1.0 microarray. After analyzed the transcriptomic of both *in vitro* experimental assays, 140 *A. fumigatus* genes were detected as up-regulated with FC values higher than 1.5 in the two models used. To reduce the number of genes of interes, these genes were compared with those detected as up-regulated during the mice intranasal infection carried out in **Chapter 1** (Guruceaga *et al.*, 2018). In this way, 13 genes were found to be up-regulated in the three abovementioned infection procedures. Some of them have been previously studied by other authors and related with the infection process or detected as expressed in the onset of the contact between cells or sera. Among them, it is important to highlight genes such as *aspf1* gene, which is a well-studied *A. fumigatus* and codify an allergen commonly found in diferent *A. fumigatus* proteomic/transcriptomic studies (Guruceaga *et al.*, 2018; Ramirez-Garcia *et al.*, 2018). In addition, the fumarate reductase Osm1 previously found as expressed during hypoxia process and during the first contact between the host and the dormant conidia (Teutschbein *et al.*, 2012; Vodisch *et al.*, 2011). Another enzyme detected by us, the succinate dehydrogenase Sdh1 has been previously described as expressed after human neutrophils exposition (Sugui *et al.*, 2008), during the exit of the dormancy (Lamarre *et al.*, 2008) as well as during hypoxia situations (Vodisch *et al.*, 2011). It was also detect the citrate synthase Cit1 that has been detected by other authors as expressed during the contact with sera (Asif *et al.*, 2010) and with airway epithelial cells (Oosthuizen *et al.*, 2011). Furhteremore, the *cit1* gene was also described as essential for AI manifestation (Ibrahim-Granet *et al.*, 2008).

Finally, we selected the gene *maiA* as a good candidate to study its role in *A. fumigatus* virulence because it is involved in pyomelanin synthesis as a consequence of the Phe/Tyr degradation pathway. The catabolic Phe/Tyr degradation pathway, in which *maiA* is involved, has the singularity to produce one type of soluble melanin, known as pyomelanin, when an accumulation of some of the intermediates metabolites, such as Homogentisate (HGA) or 4-Maleylacetoacetate (4-MA), happens. The mutation of

the *maiA* gene will imply the truncation of the final part of the pathway avoiding the correct degradation of Phe or Tyr to fumarate and acetoacetate, which are destined to the Krebs cycle or the biosynthesis of other aminoacids. As a consequence, there will be an accumulation of 4-MA and HGA and the subsequent production of pyomelanin.

The cluster of genes involved in the Phe/Tyr degradation pathway has been previously studied through the development of loss function mutant strains of some of the genes. Between them, the $\Delta hppD$ null mutant showed a lack of pyomelanin synthesis because HGA formation was avoided. Furthermore, the hyphae of this mutant show increased susceptibility to hydrogen peroxide and other oxidizing agents when compared with Wt (Schmaler-ripcke *et al.*, 2009). Moreover, although this gene has been detected as overexpressed at 96 hours post-intranasal infection in comparison with the first 24 hours in immunosuppressed mice (Guruceaga *et al.*, 2018), no differences in mortality rates were observed when the immunosuppressed mice were intravenously infected with the $\Delta hppD$ mutant strain (Keller *et al.*, 2011). Other authors have also detected by microarray the overexpression of the homologous gene in the *Penicillium marneffeii*, *hpdA*, obtained their deletion mutant and studied their growth and morphology under different conditions (Pasricha *et al.*, 2013; Boyce *et al.*, 2014).

In addition, when studying another of the genes in the cluster, *hmgX*, some authors observed that its null mutant showed similarities with $\Delta hppD$ strain (Keller *et al.* 2011). This $\Delta hmgX$ mutant was unable to produce HGA and, according to these authors, this means that HmgX could be a cofactor or mediator of HppD enzyme (Keller *et al.* 2011). On the other hand, the third gene studied was the *hmgA*, the mutant $\Delta hmgA$ showing an increase in pyomelanin owing to the accumulation of HGA and a less susceptibility to oxidizing agents than the $\Delta hppD$ (Schmaler-Ripcke *et al.* 2009). Finally, the last gene of the Phe/Tyr degradation pathway studied using mutants was the *hmgR*. In this case, the $\Delta hmgR$ mutant seemed to be incapable of using Tyr as the only source of carbon or nitrogen and, therefore, only a residual accumulation of pyomelanin was observed in cultures. Furthermore, the immunosuppressed mice infected with the $\Delta hmgR$ strain did not modify the mortality rate comparing to the Wt (Keller *et al.*, 2011). These

results may indicate that this gene is not the only transcription factor involved in Tyr degradation pathway (Keller et al. 2011).

Therefore, from the cluster of the Phe/Tyr degradation pathway, two genes (*fahA* and *maiA*) remain to be studied in depth through the development of mutant strains in *A. fumigatus*. The only study published concerning *maiA* in *A. fumigatus* demonstrated that this gene was overexpressed when the medium was supplemented with Tyr (Keller et al., 2011). In contrast, both genes have been silenced in *Aspergillus nidulans* and in *P. marneffeii* (Fernandez-Cañon & Peñalva 1995; Fernandez-Cañon & Peñalva 1998; Boyce 2014), obtaining similar phenotypic results in both fungus. Taking into account the overexpression in the three infection models studied in this doctoral thesis, the importance of the Phe/Tyr pathway and that its participation in virulence has been little studied, for that the study of the *maiA* gene results of great interest.

For these reasons, the mutant $\Delta maiA$ was constructed by CRISPR-Cas9 but, in this case, a disruptant mutant instead the classic deletion. This kind of gene inactivation seems to be enough considering that there is a lot of information about other genes of the cluster disposable. Moreover, although it is not the most common way to silence a gene, other authors have also developed a *maiA* mutant strain following a disruption strategy in *A. nidulans* (Fernandez-Cañon & Peñalva 1998)

The $\Delta maiA$ strain obtained showed the expected phenotype in response to Phe and Tyr. The mutation in the $\Delta maiA$ strain block the Phe/Tyr degradation pathway causing an accumulation of 4-MA and, probably, of the previous metabolites of the route. Specifically, the mutant strain started to produce pyomelanin when Phe but, above all, Tyr were added to the medium. Nevertheless, results obtained by other authors using the $\Delta hmgA$ mutant showed that this mutant produced more pyomelanin by the addition of Phe than by Tyr (Schmaler-Ripcke et al., 2009). In spite of this apparent inconsistency, it is highlighting that the $\Delta hmgA$ mutant accumulates HGA while $\Delta maiA$ strains could accumulate HGA and 4-MA. Furthermore, $\Delta maiA$ strain was no able to grow with Tyr as the sole carbon source and energy, while it did with Phe. Analyzing carefully the use of Phe and Tyr by *A. fumigatus*, it was detect that Phe can be

metabolized to obtain energy by other pathways while there is not still described any *A. fumigatus* alternative route to redirect Tyr (**Fig. S2**). In consequence, when $\Delta maiA$ strain grew in presence of Phe or Tyr, the Phe could be redirect to another metabolism, but as the only option to produce energy using Tyr is completing the Phe/tyr degradation pathway, the 4-MA is accumulated and the pyomelanin produced. With this data it is difficult to explain the inability of the fungus to grow when both aminoacids were added as a sole carbon source, but maybe an accumulation of toxic residued derived from Phe/Tyr degradation pathway secondary metabolites could happen. The results obtained by Schmalder-Ripcke working with *A. fumigatus* and the ones obtained by Boyce and coworkers studying *P. marneffeii* also support our hypothesis (Schmalder-ripcke *et al.*, 2009; Boyce *et al.*, 2014).

Regarding the behaviour of the mutant strain, the $\Delta maiA$ presented a germination rate higher than the Wt strain although no differences in the radial growth size of the macroscopic colony were found. The sensitivity to H₂O₂ was also similar in both $\Delta maiA$ and Wt strains, similar to what was previously described for the $\Delta hppD$ and $\Delta hmgA$ mutants (Schmalder-Ripcke *et al.*, 2009). These authors also showed that when the medium was supplemented with Tyr, the $\Delta hppD$ mutant strain was more sensible to the oxidative agent (Schmalder-Ripcke *et al.*, 2009). Boyce and coworkers, also performed the same experiment but in this case with *P. marneffeii*. They found that $\Delta hppA$ and $\Delta hmgA$ showed a very mild sensitivity to H₂O₂ (Boyce *et al.*, 2014). Therefore, in the future, the same experiment supplementing the medium with Tyr should be preformed with $\Delta maiA$ strain.

Another interesting result was that the mutant strain presented significant less glucans in the cell wall than the Wt strain. The relevance of this finding is that no one has previously described a phenotype similar with the mutants of the genes involved in Phe/Tyr degradation developed in *A. fumigatus*, *A. nidulans* and *P. marneffeii*. The cell wall is an essential structure for the fungi and can suffer variations in its molecular composition, organization and thickness depending on environmental conditions (Ram *et al.*, 2006). One way to study the integrity of the cell wall of a mutant strain is to subject the mutant and the Wt strains to cell wall stresses and compare their grow ability (Pellon *et al.*, 2017; Martin-vicente *et al.*, 2018; Souza *et al.*, 2019). The spotting

assay carried out here demonstrated that the $\Delta maiA$ strain suffers an alteration of the cell wall structure/composition, which make it unable to grow in presence of CR or CW. The ability to grow in presence of both compounds was recovered by osmotic stabilization using sorbitol. CR and CW are compounds with a chemical structure that can interact with β -linked glucans and, specifically, it is thought that both compounds interfere with cell wall assembly by binding to chitin. Conceivably, CW and CR act by binding to nascent chitin chains, thereby inhibiting the assembly enzymes that connect chitin to β -1,3-glucan and β -1,6-glucan (Wood 1980; Herth 1980; Pringle 1991).

In contrast, although the $\Delta maiA$ strain presented a phenotype compatible with a cell wall defect, it was more resistant to osmotic stresses such as KCl, NaCl, sorbitol and SDS than the Wt strain. These surprising results have never been described in any mutant involved in Phe/Tyr degradation pathway. In fact, other studies performed with mutant strains non-related with this pathway (*shoA*, *msbA*, *opyA*, *sakA* and *mpkC*) and reported with similar cell wall phenotype altered (more sensible to cell wall stress) were at the same time more sensitive to osmotic stresses (Mattos *et al.*, 2020; Silva Pereira *et al.*, 2020). In addition, these other mutants were also more sensitive to caspofungin, but our $\Delta maiA$ did not to any of the antifungal drugs tested (voriconazol, fluconazole, isavuconazol, caspofungin and micafungin) (data not shown). It is true that while *maiA* gene is involved in Phe/tyr degradation pathway, the other genes are involved in high-osmolarity glycerol response pathway and, therefore, the studies are not totally comparable.

The SEM analysis performed showed a general unstructured appearance of the $\Delta maiA$ mutant strain confirming the phenotype observed of the spotting assay. The Wt hyphae looked well similar to other SEM images presented by other authors previously (Gonzalez-Ramirez *et al.*, 2016; Wuren *et al.*, 2014; Joubert *et al.*, 2017). However, $\Delta maiA$ hyphae did not present the typical 45° angle ramification and in general terms their hyphae looked thinner and less turgid. Hyphae details also revealed difference in the external structure of the cell wall and also a lack of an unknown matrix that surrounded mainly the apex of Af293 hyphae.

To study whether the $\Delta maiA$ cell wall modifications were related to the mitogen-activated protein kinases (MAPK) an spotting assay using caffeine was used following previous published strategies (Valiante *et al.*, 2008; Valiante *et al.*, 2009). All the studies of these authors demonstrated that those mutant strains related with MAPK genes ($\Delta bck1$, $\Delta mkk2$, $\Delta mpkA$) were more sensible to cell wall stresses, even when they used sorbitol as osmoregulator agent alongside to caffeine. However, the $\Delta maiA$ strain was not affected by caffeine, ruling out the MAPK pathway as the cause of the alteration in the wall. Probably this effect could be caused as a consequence of the blockage in the Phe/Tyr degradation pathway since we are preventing that $\Delta maiA$ strain finish the catabolic process of Phe and Tyr by which the fungus can synthesize new aminoacids for structural purposes.

The last step of the research was to study the effect of the silencing of the *maiA* gene on the fungal virulence. The cell wall is the main fungal target recognized by the immune cells and, for that, an *in vitro* model of infection using with RAW 264.7 macrophages was performed. Phagocytosis results pointed out that $\Delta maiA$ strain was more easily phagocytosed than the Wt but its germination rate was higher.

To finish, an *in vivo* infection model was using immunosuppressed mice was conducted. The $\Delta maiA$ strain showed a significantly lower lethality than the Wt strain. These results obtained in mice are really novel and interesting because other mutant strains of the Phe/Tyr degradation pathway ($\Delta hmgR$ and $\Delta hppD$) did not show any difference in the mortality rate observed. It is highlighting that other studies used a corticosteroids instead of cyclophosphamide to immunosuppress mice, which could suggest that phagocytosis is essential to control the virulence caused by the mutant strain. The $\Delta maiA$ cell wall defect as well as the slight tendency to be easily phagocytosed could be the keys to understand the importance of macrophages against $\Delta maiA$ strain.

Summarizing, although there are still many questions to be clarified, in this chapter an involvement of *maiA* gene with fungal the cell wall, which is independent of the classical MAPK regulation, has been established. Furthermore, a new Phe/Tyr fitness theory by which the use of Phe as sole carbon source is energetically more beneficial

to *A. fumigatus* has been proposed. Finally, the role of *maiA* gene in fungal virulence has been evidenced using a neutropenic mice infection model. In fact, this is the first time in which a mutation of one of the genes involved in the Phe/Tyr degradation pathway is directly related to *A. fumigatus* virulence. The process by which $\Delta maiA$ strain suffers cell wall defects should be study in depth in future investigations, but the impossibility of this mutant strain to biosynthesize some new aminoacids could be involve in the phenotype observed both related with cell wall defects as well as the virulence.

5. Supplementary material

Table S4. List of primers used for the microarray verification process

Target ^a	Symbol ^b	Primer name ^c	Sequence (5'→3') ^d	Tm ^e
Aspartate aminotransferase	AFUA_1G0416 0	1g04160F	AGAGTCCCAAGTAACGAGC	59,10
		1g04160R	CGTTGTGCGCTCATAATCGA	59,08
Hypothetical protein	AFUA_1G1045 0	1g10450F	GACCAGAGAAACCATCGCAC	58,92
		1g10450R	AGGCCTCAAAGACTCTTCC	59,01
Maleylacetoacetate isomerase MaiA	AFUA_2G0424 0	2g04240F	AATCCTTCCGGTACAGTCCC	58,80
		2g04240R	GATGGTCACGGTTCTTTGG	58,83
Rho GTPase ModA	AFUA_2G0574 0	2g05740F	CCGCTGGTCAGGAGGATTAT	58,95
		2g05740R	GAGTTTCTCACGAACGGCAG	59,22
Hypothetical protein	AFUA_2G0882 0	2g08820F	TCCGATCTCATGGTCATCCC	58,66
		2g08820R	CGGTTTGACAGGATGCAGAG	58,92
Rho GTPase Rac	AFUA_3G0630 0	3g06300F	TGCCTACCCTCAAACCGAC	59,03
		3g06300R	GATACTTGTGCGCTCGGATC	58,87
WSC domain protein	AFUA_3G0705 0	3g07050F	TGAAATCCTGACAGCACCT	58,93
		3g07050R	AATGGAATGAAAACCGCCCC	59,10
Succinate dehydrogenase subunit Sdh1	AFUA_3G0781 0	3g07810F	CTTGAGGGACCAGAGACGTT	59,03
		3g07810R	CAGAGCAGCGTTGATACCAC	59,00
Hypothetical protein	AFUA_3G1308 0	3g13080F	CTCAACGAAGAACCACAGCC	59,13
		3g13080R	CAACCAGGTGAGAACGCAAA	58,98

MFS myo-inositol transporter	AFUA_4G0156	4g01560F	GATCAAACGTCTCGGACTGC	59,01
	0	4g01560R	AATGTAGAGGGGCTGGCAAT	59,07
Hypothetical protein	AFUA_5G0232	5g02320F	CTGCGAACCGTTCTGATGAG	59,01
	0	5g02320R	AGCAACGGTAAATCTCCCA	59,01
Rheb small monomeric GTPase RhbA	AFUA_5G0548	5g05480F	TCGCCACAGAGATCGTTGAT	59,18
	0	5g05480R	CTCTCGCCAATTGCCTAC	58,98
Hypothetical protein	AFUA_5G0880	5g08800F	CTTCGGTATCACAATGGGCG	59,06
	0	5g08800R	CGTTGGTGTGGAGTTGTTT	58,90
3-methylcrotonyl-CoA carboxylase, beta subunit (MccB)	AFUA_5G0894	5g08940F	GGAGCGCACTTCATTGAACT	58,84
	0	5g08940R	TTCGGACCCATAACACCAA	58,93
Pectin lyase	AFUA_5G1017	5g10170F	TGGACTIONCTCTCTCGG	59,45
	0	5g10170R	CAAAGTAGTTGCCCTCGAGC	58,92
Pectin lyase	AFUA_5G1038	5g10380F	GGAAATGCCTCCCTGTCTA	58,79
	0	5g10380R	CACGAGTTCTGGTTGATGGC	59,20
Succinyl-CoA:3-ketoacid-coenzyme A transferase (ScoT)	AFUA_6G1225	6g12250F	AAGGCTTTGGAGGTGCAATG	59,03
	0	6g12250R	CATGGGCTTGACATCATCCG	59,05
Lipase	AFUA_7G0402	7g04020F	TCGGAGCATTGCCTCCTTAA	59,09
	0	7g04020R	TGGAGCTTTGACCGGGTAAA	59,23
Methionine aminopeptidase type II (metAP)	AFUA_8G0041	8g00410F	TTCCGAACAACCTCTATCC	58,98
	0	8g00410R	TTGTCGAGGTGACGTTTCTC	58,85
Phytanoyl-CoA dioxygenase	AFUA_8G0048	8g00480F	TCTGGTTCCAACGTGACTGA	58,88
	0	8g00480R	CATGTGAGGCGCCGAATAAT	58,77

Secreted antimicrobial peptide	AFUA_8G0071	8g00710F	TGCTACCATCGTCTATCCCTAC	58,58
	0	8g00710R	TCTTGTAGTTGCCGCTCATG	58,27
Elastinolytic metalloproteinase Mep	AFUA_8G0708	8g07080F	TCCATGCTGTACGAGGTGTT	59,03
	0	8g07080R	CCTGGACAAAGTTGGGGTTG	58,96
4-Hydroxyphenylpyruvate dioxygenase	AFUA_2G0420	2g04200F	TATGCAGCGACGAACAATGG	58,99
	0	2g04200R	CTAAAGTGTGCGTGGTCTCG	58,94
Aromatic aminotransferase Aro8	AFUA_2G1363	2g13630F	TCCAGGTCTCATCTCGTTGG	58,81
	0	2g13630R	TCGGTATGCTCAGTCACGAA	58,83
Conidial pigment biosynthesis oxidase Arb2	AFUA_2G1753	2g17530F	GCTATCAGTCTGCTCCGA	59,25
	0	2g17530R	GAGCTTGCGGACTCAGAATG	58,99
Conidial pigment biosynthesis scytalone dehydratase Arp1	AFUA_2G1758	2g17580F	TGCGAAAGTGGGATGACATG	58,55
	0	2g17580R	GCGGTAGTAGTGCTCATTGG	58,43
Conidial pigment polyketide synthase PksP/Alb1	AFUA_2G1760	2g17600F	GGTCAATGGAGTGGCTTTAC	62,00
	0	2g17600R	CCCTGGTACTCTGGTTTGTATT T	62,00
Catalase Cat	AFUA_2G1803	2g18030F	GTCGAACAACCTGGCCTTCTC	58,85
	0	2g18030R	CGTCACGAAGAGTTGGGTTG	59,14
Aromatic-L-amino-acid decarboxylase	AFUA_3G0224	3g02240F	TTACATCACGCTTGCCATGG	58,91
	0	3g02240R	AAACTGTCAACACCTTCCGC	58,98
Phospholipase D1 (PLD1)	AFUA_3G0563	3g05630F	CGATCCAACCTCCAGTGCTTG	58,92
	0	3g05630R	CTCGCTGTCAGGCATAACAAC	59,00
Stress responsive A/B barrel domain protein	AFUA_4G1061	4g10610F	ACGCATCACTCTTTTCAACGT	58,79
	0	4g10610R	CGGCGCTGAGAATATACGGT	60,04

Allergen and cytotoxin AspF1	AFUA_5G0233	5g02330F	CACGCCCATCAAATTCGGAA	59,19
	0	5g02330R	TCCTTGGGTTTCTTCGAGTCA	58,96
Rheb small monomeric GTPase RhbA	AFUA_5G0548	5g05480F	TCGCCACAGAGATCGTTGAT	59,18
	0	5g05480R	CTCTTCGCCCAATTGCCTAC	58,98
MAP kinase kinase kinase SteC	AFUA_5G0642	5g06420F	AGTGTATTGGTGGCCGAAGA	59,02
	0	5g06420R	TGAGCTCTCCAGTGATTGCA	59,02
GATA transcriptional activator AreA	AFUA_6G0197	6g01970F	ACCCAAGCGATTTCCCTACA	59,01
	0	6g01970R	GGCGTTGTCATACCAAAGT	59,05
Cytochrome P450 monooxygenase	AFUA_6G0221	6g02210F	GGGTGTATCGGGAAGAGCAT	59,24
	0	6g02210R	TACTTGGCGCTCGTGAATG	58,92
Citrate synthase Cit1	AFUA_6G0359	6g03590F	TGTTTTGGCTGCTCTTGACG	59,34
	0	6g03590R	ACTTGATCAGGTCCAAAATAT GC	57,36
Nonribosomal peptide synthase GliP	AFUA_6G0966	6g09660F	GTTGGACTGGGAATGCGTTT	59,04
	0	6g09660R	GCTTTCGTGAGTGACCGTAC	58,94
Indoleamine 2,3-dioxygenase family protein	AFUA_7G0201	7g02010F	CCTGAAGAGTTCCCTCATATC	61
	0	7g02010R	GACGTGCAGTAGGGTAGAAA G	62
Defensin domain protein	AFUA_7G0518	7g05180F	ACAACCTCCATCTCCTGCATGA	59,09
	0	7g05180R	CCACGGTATCCTCCTCGATG	59,4
Phospholipase PldA	AFUA_7G0558	7g05580F	GCGACAAACACGAGGTCAAT	59,13
	0	7g05580R	TGCCTTTTCACTCTCCGGAT	59,02
Hypothetical protein	AFUA_8G0510	8g05100F	GTAGCCAGCAAGTCACATCG	59
	0	8g05100R	CCGGAATACTAGAGGGCCTG	59,03

Fumarate reductase Osm1	AFUA_8G0553 0	8g05530F	CCACAACATGCCCTTTGACA	58,96
		8g05530R	GCAAGTTCACCACAAGCGTA	59,06
Alpha/beta hydrolase	AFUA_2G0292 0	H_AlphBe_F	ACTGGTCGTGACACTGTTGG	59.62
		H_AlphBet_R	CGCATTGTGGATGCTAGACT	58.90
Mis12-Mtw1 family protein	AFUA_3G1395 0	H_Mis12_F	GCTCTCGAATTGGTTTGGAC	59.68
		H_Mis12_R	ATGTTTTTCGGGTTTCGGTTT	60.57
Isochorismatase family protein	AFUA_3G1450 0	H_Isochor_F	GAAGAACGACGGAGTGGTAA G	62
		H_Isochor_R	CTCAGGTAGGTCCAAGTCATA AAT	62
Molybdopterin synthase small subunit CnxG	AFUA_7G0158 0	H_Molybdop_F	ACCAGTCTTCCAATCCACTAC	62
		H_Molybdop_ R	TAGGAAATCAAAGAGCCTGGA C	62
Glucose-6-phosphate 1-dehydrogenase 2	NM_019468.2	MmF	CCTTTGGTACTGAGGGTCGT	59.03
		MmR	ATCCATTGGCAGCTTCTCCT	59.08

^aProduct description of the genes chosen to verificate the microarray data following RefSeq nomenclature.

^bSystematic name of the gene following AspGD nomenclature.

^cF: Forward; R: Reverse

^dSequence of each primer.

^eTm: Melting temperature of each primer.

Table S5. Go enrichment analysis of the *A. fumigatus* up-regulated genes (FC > 1.5) and down-regulated genes (FC < -1.5) in both *in vitro* experimental models of infection.

GO Slim Term	Number of Genes			
	RAW 264.7 vs Control		A549 vs Control	
	Up regulated	Down regulated	Up regulated	Down regulated
Biological process	126	101	403	189
Transport	35	34	89	40
Regulation of biological process	22	8	56	22
Response to stress	17	15	36	8
Secondary metabolic process	17	23	30	6
Response to chemical	14	17	40	11
Lipid metabolic process	13	8	30	3
RNA metabolic process	13	7	18	10
Developmental process	13	1	20	5
Cellular amino acid metabolic process	12	7	19	8
Transcription, DNA-templated	11	3	15	4
Cellular respiration	11	-	6	1
Carbohydrate metabolic process	10	20	49	23
Toxin metabolic process	9	2	12	-
Cellular homeostasis	7	18	9	7
Cell cycle	6	2	12	6
Filamentous growth	6	1	18	7
Sexual sporulation	6	1	7	2
Asexual sporulation	4	-	5	3
Organelle organization	3	1	16	11
Pathogenesis	3	7	12	4
Translation	2	-	1	2
Cellular protein modification process	2	-	9	10
Conjugation	1	-	3	-
DNA metabolic process	1	-	2	2
Vitamin metabolic process	1	2	1	2
Cell adhesion	1	-	3	-
Signal transduction	1	-	6	5
Transposition	1	-	-	-
Ribosome biogenesis	-	2	1	2
Cytokinesis	-	1	1	3
Protein catabolic process	-	1	2	4
Cytoskeleton organization	-	-	5	2
Vesicle-mediated transport	-	-	4	3
Protein folding	-	-	2	-
Other	35	34	105	52

Number of Genes

GO Slim Term	RAW 264.7 vs Control		A549 vs Control	
	Up regulated	Down mregulated	Up regulated	Down regulated
Cellular component	161	160	536	259
Membrane	55	33	112	49
Mitochondrion	32	4	28	5
Nucleus	27	8	37	18
Cytosol	20	3	10	5
Plasma membrane	17	8	32	7
Extracellular region	13	12	38	16
Vacuole	8	3	8	3
Endomembrane system	7	3	10	12
Cell wall	6	1	11	1
Peroxisome	6	3	9	-
Endoplasmic reticulum	5	-	2	6
Golgi apparatus	3	-	3	2
Site of polarized growth	1	-	7	3
Nucleolus	-	1	-	2
Cell cortex	-	-	6	1
Cytoskeleton	-	-	4	3
Chromosome	-	-	2	5
Actin cytoskeleton	-	-	1	1
Microtubule cytoskeleton	-	-	1	2
Ribosome	-	-	-	2
Other	11	11	41	9

GO Slim Term	Number of Genes			
	RAW 264.7 vs Control		A549 vs Control	
	Up regulated	Down regulated	Up regulated	Down regulated
Molecular function	146	106	407	198
Oxidoreductase activity	62	37	117	54
Hydrolase activity	24	32	89	40
Transporter activity	21	18	48	13
Transferase activity	21	20	47	28
DNA binding	8	7	21	8
Lyase activity	8	2	14	5
Peptidase activity	7	1	10	5
Protein binding	3	-	8	2
RNA binding	2	-	5	4
Isomerase activity	2	-	5	-
Protein kinase activity	1	-	5	-
Signal transducer activity	1	-	-	-
Structural molecule activity	1	-	-	-
Lipase activity	1	1	4	-
Phosphatase activity	1	-	10	1
Ligase activity	1	-	-	-
Enzyme regulator activity	1	1	-	-
Helicase activity	-	1	1	2
Ligase activity	-	-	3	2
Enzyme regulator activity	-	-	3	-

Nucleotidyltransferase activity	-	-	1	1
Structural molecule activity	-	-	1	1
Translation regulator activity	-	-	-	1
Other	17	20	54	16

Table S6. List of common *A. fumigatus* up-regulated DEGs during the co-incubation of the fungus with the macrophages RAW 264.7 and the human lung epithelium cell line A549.

ID	Product		Fold Change (log ₂)	
			RAW 264.7 vs Control	A549 vs Control
Afu1g01300	GPI anchored protein		4.663	2.609
Afu1g03570	Acid phosphatase PHOa	<i>phoA</i>	2.228	7.182
Afu1g04160	Aspartate aminotransferase		3.223	2.452
Afu1g06610	NADH-quinone oxidoreductase, 23 kDa subunit		2.774	3.180
Afu1g07380	Glutamate synthase Glt1		2.110	1.544
Afu1g13510	C6 transcription factor FacB/Cat8		2.392	2.545
Afu1g13750	C ₂ H ₂ transcription factor (Rpn4)		1.663	2.095
Afu1g14540	Oxidoreductase, short-chain dehydrogenase/reductase family		2.474	3.855
Afu1g14550	Mn superoxide dismutase MnSOD		4.439	5.605
Afu1g15590	Succinate dehydrogenase subunit CybS		2.927	1.708
Afu1g17070	FYVE domain protein		2.640	3.023
Afu1g17360	bZIP transcription factor (BACH2)		2.437	5.423
Afu2g00630	GDSL lipase/acylhydrolase family protein		1.751	2.509
Afu2g00890	Conserved hypothetical protein		1.553	2.057
Afu2g02180	Hypothetical protein		1.565	1.343
Afu2g02460	Hypothetical protein		2.462	4.392
Afu2g03730	Ctr copper transporter family protein		2.334	3.116
Afu2g04200	4-hydroxyphenylpyruvate dioxygenase		6.384	6.783
Afu2g04210	Hypothetical protein		3.843	4.234
Afu2g04220	Homogentisate 1,2-dioxygenase	<i>hmgA</i>	3.782	3.726

Afu2g04240	Maleylacetoacetate isomerase	<i>maiA</i>	2.416	2.219
Afu2g04262	C6 transcription factor		2.331	1.539
Afu2g05060	Alternative oxidase AlxA		4.657	5.252
Afu2g07720	Cytochrome b5		3.462	2.262
Afu2g07910	myo-inositol transporter		1.840	2.280
Afu2g09400	Cyclohexanone monooxygenase		1.643	2.002
Afu2g10540	Hypothetical protein		1.602	2.300
Afu2g12630	Allergenic cerato-platanin Asp f 13	<i>aspf13</i>	1.817	1.429
Afu2g12710	MFS monocarboxylate transporter. putative		4.852	2.753
Afu2g12780	von Willebrand domain protein		1.645	3.149
Afu2g13175	Hypothetical protein		2.093	3.159
Afu2g15860	TAM domain methyltransferase		3.356	1.866
Afu2g16180	Hypothetical protein		1.616	1.682
Afu2g16930	Succinate:fumarate antiporter (Acr1)		3.965	4.153
Afu2g17790	Amino acid transporter		1.924	5.138
Afu3g01150	GPI anchored cell wall protein, putative		3.154	2.034
Afu3g03040	Hypothetical protein		2.144	3.023
Afu3g03060	Cell wall protein PhiA		4.723	4.309
Afu3g03230	bZIP transcription factor		1.760	1.932
Afu3g03280	FAD binding monooxygenase		3.064	2.326
Afu3g03290	Hypothetical protein		2.595	3.634
Afu3g03310	RTA1 domain protein		3.383	4.797
Afu3g06730	MFS sugar transporter		1.696	3.086

Afu3g07810	Succinate dehydrogenase subunit	<i>sdh1</i>	2.721	1.519
Afu3g07990	GABA permease GabA		1.622	4.559
Afu3g08210	Hypothetical protein		1.729	2.506
Afu3g09220	P450 family fatty acid hydroxylase		1.936	2.563
Afu3g12920	Non-ribosomal peptide synthase GliP-like		2.194	2.061
Afu3g13640	Extracellular serine-rich protein		1.779	2.691
Afu3g13660	Ctr copper transporter family protein		5.135	4.005
Afu3g13670	Siderochrome-iron transporter		4.181	2.705
Afu3g13680	Hypothetical protein		4.238	3.022
Afu3g13690	Pyoverdine/dityrosine biosynthesis family protein, putative		3.119	1.698
Afu3g13700	Transferase family protein		6.523	5.245
Afu3g14665	Hypothetical protein		4.943	4.108
Afu3g14940	Hypothetical protein		2.490	2.713
Afu4g01270	Integral membrane protein		3.144	1.868
Afu4g01290	endo-chitosanase, pseudogene		3.606	3.776
Afu4g01470	C6 finger domain protein		2.026	2.629
Afu4g03240	Cell wall serine-threonine-rich galactomannoprotein Mp1		2.800	3.524
Afu4g03270	Epoxide hydrolase		1.535	2.714
Afu4g03410	Flavoheomprotein		4.829	3.099
Afu4g03920	MFS drug transporter		3.569	5.353
Afu4g03930	Cysteine synthase B		4.722	6.870
Afu4g03940	Ferric-chelate reductase		3.165	3.276
Afu4g04190	Hypothetical protein		3.355	4.413

Afu4g04530	Short chain dehydrogenase/reductase (Ayr1)	<i>ayr1</i>	1.535	2.467
Afu4g08490	acyl-CoA dehydrogenase		2.373	2.396
Afu4g09110	Cytochrome c peroxidase Ccp1		4.674	3.321
Afu4g09140	L-ornithine aminotransferase Car2		3.120	1.683
Afu4g09470	Cytochrome P450 monooxygenase		2.532	3.903
Afu4g09560	ZIP Zinc transporter		1.695	1.373
Afu4g09580	Major allergen Asp f 2	<i>aspf2</i>	2.676	2.452
Afu4g10610	Stress responsive A/B barrel domain protein		1.591	1.942
Afu4g10690	Iron-sulfur cluster assembly accessory protein Isa1, putative		3.122	2.066
Afu4g13510	Isocitrate lyase AcuD		4.034	4.707
Afu4g13540	Potassium uptake transporter		1.955	2.238
Afu4g13780	Polyphenol monooxygenase		2.289	4.003
Afu5g00300	Zinc-binding oxidoreductase		3.549	3.817
Afu5g00740	Hypothetical protein		1.908	2.496
Afu5g01030	Glyceraldehyde 3-phosphate dehydrogenase		1.927	3.091
Afu5g01200	Carboxypeptidase S1		2.858	2.204
Afu5g02320	Conserved hypothetical protein		2.068	3.266
Afu5g02330	Major allergen and cytotoxin Asp f 1 (MitF)	<i>aspf1</i>	3.001	3.102
Afu5g07480	Hypothetical protein		1.705	1.695
Afu5g07500	β -lactamase family protein		1.761	2.657
Afu5g09330	CipC-like antibiotic response protein		2.636	4.687
Afu5g10370	Iron-sulfur protein subunit of succinate dehydrogenase	<i>sdh2</i>	2.986	1.928
Afu5g11260	Siderophore transcription factor	<i>sreA</i>	2.104	2.095

Afu5g11290	D-amino acid oxidase		1.551	1.559
Afu5g12840	Hydroxyacylglutathione hydrolase		2.209	2.194
Afu5g13800	Transcriptional regulator		2.291	2.068
Afu5g13810	Transulfuration enzyme family protein		2.494	3.435
Afu5g14650	RING finger protein		1.662	3.628
Afu6g00290	Aminotransferase		1.678	1.504
Afu6g00430	IgE-binding protein		2.836	2.241
Afu6g00680	Conserved hypothetical protein		2.285	2.038
Afu6g00690	Conserved hypothetical protein		3.229	3.073
Afu6g00720	LysM domain protein		1.989	2.779
Afu6g00740	Conserved hypothetical protein		2.983	4.180
Afu6g02210	Cytochrome P450 monooxygenase		2.459	3.678
Afu6g02810	Ctr copper transporter		1.810	1.767
Afu6g02820	Metalloreductase		1.760	1.903
Afu6g03540	Malate synthase	<i>acuE</i>	2.848	3.706
Afu6g03590	Citrate synthase	<i>cit1</i>	2.610	3.541
Afu6g07710	Mitochondrial dicarboxylate carrier protein		1.858	3.376
Afu6g07720	Phosphoenolpyruvate carboxykinase	<i>acuF</i>	3.707	3.663
Afu6g07750	MFS phospholipid transporter	<i>git1</i>	2.105	2.506
Afu6g09200	Hypothetical protein		2.230	1.594
Afu6g10310	Hypothetical protein		2.313	3.249
Afu6g12250	Succinyl-CoA:3-ketoacid-coenzyme A transferase (ScoT), putative	<i>scoT</i>	2.072	3.276

Afu6g12930	Mitochondrial aconitate hydratase		2.077	2.090
Afu6g13750	Ferric-chelate reductase		2.445	1.820
Afu6g14010	GPI anchored protein		3.245	2.255
Afu7g00990	Transcriptional activator of ethanol catabolism AlcS		4.067	4.992
Afu7g01020	Hypothetical protein		2.092	1.221
Afu7g01050	Salicylate hydroxylase		2.203	2.215
Afu7g02010	Indoleamine 2,3-dioxygenase family protein		5.696	3.663
Afu7g02070	AIF-like mitochondrial oxidoreductase (NfrI)		2.957	3.208
Afu7g05490	Conserved hypothetical protein		3.083	3.841
Afu7g05500	Glutathione S-transferase		2.045	1.817
Afu7g06180	Hypothetical protein		2.220	3.612
Afu7g06380	Maltase		1.663	1.977
Afu7g06680	AAA family ATPase		1.735	2.200
Afu7g06820	Galactose oxidase		1.519	2.193
Afu7g07020	Hypothetical protein		2.404	4.156
Afu7g07060	Hypothetical protein		2.285	4.371
Afu7g08310	Hypothetical protein		2.245	4.523
Afu8g00790	Hypothetical protein		3.704	2.542
Afu8g01310	Ferric-chelate reductase	<i>fre2</i>	6.239	6.378
Afu8g01670	Bifunctional catalase-peroxidase	<i>cat2</i>	1.828	2.289
Afu8g02050	Conserved hypothetical protein		2.061	3.535
Afu8g02060	Glycan biosynthesis protein (PigL), putative		3.115	4.641
Afu8g02070	Glycosyl transferase		3.893	5.660

Afu8g02090	Nucleotide-sugar transporter		2.299	3.432
Afu8g02620	CobW domain protein		2.871	6.542
Afu8g05530	Fumarate reductase	<i>osm1</i>	2.522	2.555
Afu8g05730	β -glucosidase		2.191	3.195
Afu8g06080	Flavoheмоprotein		4.032	3.217

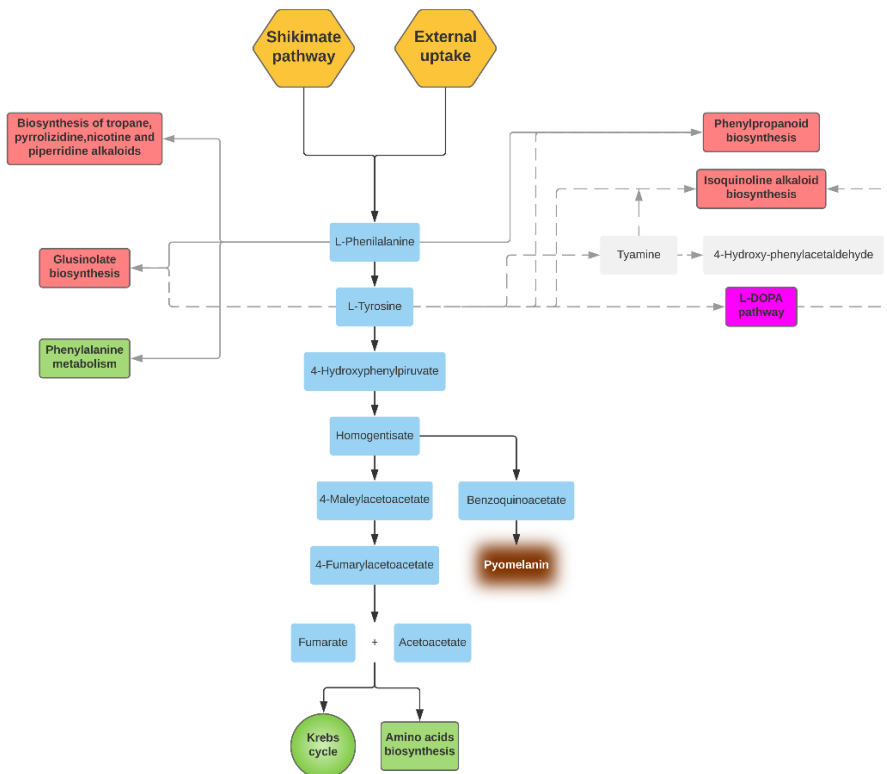


Figure S2. Schematic representation of the Phe/Tyr degradation pathway as well as the metabolic pathways in which Phe or Tyr take part. Red boxes mean those metabolic pathways still un-described in *A. fumigatus*. The pink box means that the pathway is described in *A. fumigatus* but not generates energy as consequence. Green boxes/circle are metabolic pathways by which *A. fumigatus* could obtained energy. Yellow boxes are the two mechanisms of *A. fumigatus* to obtain Phe. Grey boxes are steps described in other species but not in *A. fumigatus*. Grey boxes and discontinuous grey lines are related with Tyr while continuous grey lines are related with Phe.

Discusión general



4. Discusión general

Aspergillus fumigatus es un hongo saprófito que cuenta con una serie de características biológicas que le permiten ser un hongo distribuido en prácticamente todo el mundo, detectándose incluso en la Estación Espacial Internacional (Chazalet *et al.*, 1998; Pöggeler, 2002; Nierman *et al.*, 2005; Pringle *et al.*, 2005). Este hongo se dispersa mediante conidios cuyo pequeño tamaño, hidrofobicidad, termotolerancia y la presencia de melanina les dota de gran capacidad de resistencia a la desecación y a la temperatura, lo que permite explicar su ubicuidad (O’Gorman, 2011; Krijgsheld *et al.*, 2013; Latgé and Chamilos, 2019).

Se considera que *A. fumigatus* es un patógeno oportunista con capacidad para ocasionar un gran abanico de enfermedades que dependen del estado inmunológico del paciente. Sus conidios, gracias a las características anteriormente citadas, tienen la capacidad de mantenerse durante largos periodos de tiempos suspendidos en el aire y, al ser inhalados, alcanzar los alveolos pulmonares con facilidad (Hope, Walsh and Denning, 2005). En los paciente inmunodeprimidos que inhalan los conidios del hongo, estos pueden superar las barreras respiratorias pudiéndose establecer en el pulmón donde pueden germinar y, en consecuencia, colonizar e invadir el tejido pulmonar causando la patología más severa descrita para este hongo, conocida como IA (Osheroov, 2007; Dagenais and Keller, 2009).

El proceso de infección e invasión de los tejidos llevado a cabo por el hongo esta mediado por lo que se denominan factores de virulencia, pero la virulencia de este hongo parece ser multifactorial y todavía no está suficientemente aclarada. En la introducción general se han descrito algunos de los factores de virulencia más conocidos, como los relacionados con la termotolerancia, la composición de la pared celular de conidios y/o hifas, ó las toxinas. Por otra parte, hay que destacar que los hongos filamentosos cuentan con un complejo metabolismo secundario y, en consecuencia, son microorganismos con una capacidad de secreción de MS muy importante (Guruceaga *et al.*, 2020). Dentro de las funciones de estos MS, cabe destacar que intervienen en la mejora de la competitividad con otros

microorganismos en el nicho ecológico y durante el proceso de infección con la respuesta inmunológica (Bennett and Bentley, 1989; Raffa and Keller, 2019). Entre los MS más estudiados, se encuentran las toxinas, por ser claros factores de virulencia debido a su actividad tóxica (Kamei and Watanabe, 2005; Keller *et al.*, 2006; Arias *et al.*, 2018; Shankar *et al.*, 2018; Keller, 2019; Raffa and Keller, 2019; Raffa, Osheroov and Keller, 2019; Romsdahl and Wang, 2019). Dentro de la amplia variedad de toxinas producidas por *A. fumigatus*, cabe destacar la gliotoxina, ya que es una de las más estudiadas y posee efectos inhibitorios y citotóxicos sobre diferentes tipos celulares del sistema inmunológico como células T, monocitos o macrófagos (Mullbacher and Eichner, 1984; Eichner *et al.*, 1986; Amitani *et al.*, 1995; Yamada, Kataoka and Nagai, 2000; Tsunawaki *et al.*, 2004; Watanabe *et al.*, 2004; Stanzani *et al.*, 2005; Orciuolo *et al.*, 2007).

Como se puede apreciar, el estudio y descubrimiento de nuevos factores de virulencia es una labor esencial de investigación para comprender el proceso de infección que lleva a cabo *A. fumigatus* y poder así determinar nuevas dianas terapéuticas e incluso diagnósticas. La microbiología moderna tiende a realizar este tipo de estudios a través de la generación de cepas mutantes en los potenciales factores de virulencia. Es entonces cuando la selección de genes candidatos para elaborar mutaciones dirigidas sobre ellos cobra especial relevancia. ¿Cómo se determina que un gen es interesante para ser mutado? ¿En qué técnicas hay que basarse para poder seleccionar genes de manera correcta? Estas son preguntas clave para iniciar una investigación en este campo.

En el presente trabajo de investigación intentamos responder las anteriores preguntas utilizando un microarray de expresión de diseño propio (AWAFUGE vers. 1) con el cual se puede estudiar el patrón de expresión de todo el genoma de *A. fumigatus* en cualquier situación experimental. Este sistema fue utilizado por primera vez por nuestro grupo de investigación en 2015 para estudiar los cambios transcriptómicos que *A. fumigatus* sufre al crecer a dos temperaturas diferentes, 24 y 37°C (Sueiro-Olivares *et al.*, 2015). De manera similar, algunos autores han utilizado también técnicas de transcriptómica como microarrays de expresión para realizar estudios descriptivos de genes o grupos de genes sobre o infra expresados en determinadas

condiciones (Morton *et al.*, 2011; Fliesser *et al.*, 2015). Sin embargo, otros autores han profundizado en el estudio de algunos de los genes detectados con estos sistemas para encontrar un sentido biológico del patrón de expresión de los mismos en las condiciones ensayadas (Sugui *et al.*, 2008; Bertuzzi *et al.*, 2014; Scott *et al.*, 2020). En nuestro caso, el enfoque que plantea la investigación realizada en esta Tesis Doctoral busca utilizar esta potente herramienta para poder llevar a cabo un estudio de transcriptómica que permita seleccionar genes o grupos de genes de *A. fumigatus* por su patrón de sobreexpresión durante infecciones experimentales; tanto en ratones inmunosuprimidos infectados intranasalmente (**Capítulo 1**) como en infecciones *in vitro* utilizando tipos celulares presentes en el ambiente pulmonar (**Capítulo 3**).

En la primera parte de este trabajo, recogida en el **Capítulo 1**, se estudió la expresión génica de *A. fumigatus* en su relación huésped-patógeno (Guruceaga *et al.*, 2018). Para ello, se infectaron ratones inmunodeprimidos con conidios de *A. fumigatus* por vía intranasal, con el objetivo de observar la evolución de la expresión del hongo durante los primeros 4 días post-infección, o lo que correspondería con el inicio del establecimiento de la AI, evaluando diariamente la progresión de la misma mediante estudios histológicos de los pulmones y el estudio transcriptómico de la expresión génica.

La histopatología reveló una clara progresión de la infección en los pulmones a lo largo de las 96 horas de estudio, lo que resulta congruente con lo demostrado por otros autores (Ibrahim-Granet *et al.*, 2010). A partir de las 72-96 horas post-infección se pudieron observar síntomas evidentes de angioinvasión, quedando demostrado el comienzo del cuadro clínico de IA. En cuanto a la expresión génica del hongo, hay que destacar que el momento en el cual se detecta la angioinvasión (72-96 h) coincide con una sobreexpresión estadísticamente significativa de 103 genes de *A. fumigatus* utilizando como control la expresión del hongo en el día 1 de infección. En otras investigaciones transcriptómicas sobre el inicio de la AI, se detectaban muchos más genes diferencialmente expresados, hasta más de 1.000. Sin embargo, hay que destacar que en estos trabajos se comparaba el crecimiento del hongo *in vivo* (durante la infección) vs. *in vitro* (el hongo creciendo en medio de cultivo) utilizando esta condición como control (Mcdonagh *et al.*, 2008; Bertuzzi *et al.*, 2014), mientras que,

como hemos comentado, nuestro control es la expresión del hongo a las 24 horas de infección. De esta manera en este capítulo estamos estudiando los genes que son importantes para el hongo durante la invasión del tejido pulmonar pero no que genes del hongo son importantes para la adaptación y el establecimiento inicial de la infección.

Entre los genes diferencialmente expresados hay que destacar que se encuentran 14 perteneciente al *cluster* biosintético de fumagilina/pseurotina, lo cual supone la sobreexpresión del 67% de los genes de este *cluster* (14 genes de un total de 21) y un 10% de los genes diferencialmente detectados en el estudio. Cabe destacar la presencia del factor de transcripción esencial para la expresión de este *cluster*, el gen *fumR* (Afu8g00420). Por otra parte, además de los genes relacionados con este *cluster* se observó la sobreexpresión de diversas proteínas líticas que podrían estar tomando parte en el proceso de destrucción del parénquima pulmonar observada en la histología y permitir la progresión de la infección. De hecho, está bien descrito en la bibliografía que *A. fumigatus* es capaz de producir una amplia gama de enzimas líticas con los cuales puede degradar el tejido pulmonar durante el proceso de infección y liberar así nutrientes que favorezcan su crecimiento (Bertuzzi *et al.*, 2014; Krappmann 2016; van de Veerdonk *et al.*, 2017). No obstante, como han indicado otros autores, todavía no se ha aclarado cuales son las enzimas encargadas de llevar a cabo este proceso (van de Veerdonk *et al.*, 2017). Nuestros resultados muestran la sobreexpresión de dos genes que codifican lipasas (Afu5g02040 and Afu7g04020), de cuatro genes que codifican cuatro de las principales proteasas extracelulares del hongo (DppIV, DppV, Mep/Asp f 5 y Asp f 1) así como de un gen que codifica la quitinasa ChiB1 relacionada con funciones autolíticas (Jaques *et al.*, 2003; Alcazar-Fuoli *et al.*, 2011). Este último podría estar llevando a cabo una degradación parcial de la propia pared celular del hongo para favorecer la elongación de la hifa durante el proceso de infección.

Dada la sobreexpresión de una parte importante de los genes del *cluster* de biosíntesis de fumagilina/pseurotina (67%), nos propusimos estudiar cómo estas micotoxinas, y principalmente fumagilina, podrían favorecer la progresión de la infección. En los estudios realizados en el **Capítulo 1** se demostró que la cepa mutante no productora

de fumagilina y productora de pseurotina, *ΔpsoA*, no mostraba ningún efecto tóxico sobre células epiteliales pulmonares. Por ello, nuestro estudio se centró principalmente en el estudio de la fumagilina. A pesar de que otras micotoxinas como la gliotoxina (Dagenais *et al.*, 2009) o la endocrocina (Berthier *et al.*, 2013) habían sido previamente relacionados con la virulencia del hongo, nuestro estudio es el primero que ha detectado y relacionado la expresión de este *cluster* con la progresión del proceso de infección de *A. fumigatus*. Además, existían estudios previos con la fumagilina describiendo su capacidad anti-angiogénica (Laschke & Menger 2012; Kanno *et al.*, 2015), así como su capacidad para reducir la proliferación de las células endoteliales (Ingber *et al.*, 1990; Kusaka *et al.*, 1991; Yoshida *et al.*, 1997; Chiang *et al.*, 2008; Ito 2013). Por todo ello, vimos la necesidad de investigar el impacto real de esta toxina sobre el proceso de infección y sobre las células, para así intentar comprender cuál es el beneficio que *A. fumigatus* obtiene tras su biosíntesis y secreción durante la infección.

Lo primero que llevamos a cabo fue la estandarización de un método de detección de la toxina mediante UHPLC, en colaboración con el Departamento de Química Analítica de la UPV/EHU), que nos permitía detectar una concentración mínima de 0,1 µg/ml de toxina de una manera fiable y estable. Posteriormente, y utilizando fumagilina sintética comercial, nos dispusimos a estudiar el efecto de esta toxina sobre los macrófagos murinos RAW 264.7 y el epitelio alveolar humano A549. Los resultados mostraron que cuando se añadía una concentración fija de 1 µg/ml a los neumocitos durante 24 horas, prácticamente toda la toxina (93,5%) desaparecía del medio de cultivo mientras que en el caso de los macrófagos RAW 264.7 sólo se reducía el 23,5%. La desaparición de la toxina en el medio podría deberse, como indican otros autores, a un proceso de absorción en el cual la toxina cruza de manera pasiva la membrana celular debido a su pequeño tamaño (Zhou *et al.*, 2013) entrando en el interior celular donde se encuentra la proteína MetAP-2, que es su diana celular, a la cual se une de una manera covalente e irreversible (Sin *et al.*, 1997; Liu *et al.*, 1998). El diferente comportamiento de los macrófagos puede deberse a la existencia de bombas de expulsión de macrólidos en su membrana (Seral *et al.*, 2003), dada la similitud estructural entre la toxina y esta familia de antibióticos (Hamilton-Miller, 1973). A

pesar de no poderse descartar otras posibilidades como que las células puedan degradar la toxina, estos resultados parecen indicar por primera vez que la fumagilina parece comportarse de manera diferente sobre los dos tipos celulares estudiados.

Además, los resultados también mostraron que las células pulmonares sufrieron una disminución de la actividad de las ETCs en presencia de la toxina, pero que no se tradujo en un descenso de la viabilidad celular. La disminución del metabolismo energético que implica la inhibición provocada por la fumagilina sobre las ETCs puede relacionarse también con el claro efecto dosis dependiente de la toxina que se ha observado sobre la capacidad de proliferación de la línea celular. Estos resultados no son acordes con los publicados por otros autores que hablan de un efecto citotóxico de la fumagilina sobre las mismas células A549 (Bünger *et al.*, 2004; Schulz, Senkpiel and Ohgke, 2004; Gayathri, Akbarsha and Ruckmani, 2020). Sin embargo, esos trabajos consideran el ensayo MTT (que mide la actividad de las ETCs) como una medida de la citotoxicidad, mientras que nosotros, a pesar de detectar un efecto sobre ETCs, interpretamos esta técnica como una medida del metabolismo energético. Además, todos los trabajos anteriormente citados utilizan concentraciones de toxina más elevadas que las utilizadas en nuestra investigación y, por lo tanto, sus resultados puede que no sean del todo comparables a los nuestros.

Por otra parte, en los macrófagos además de inducir un descenso de la actividad de la ETC, la toxina tuvo un efecto citotóxico sobre ellos, y solo se detectó una leve inhibición de su proliferación celular que a diferencia de lo observado en neumocitos no fue dosis dependiente.

Una vez estudiado el efecto directo de la fumagilina sobre dos líneas celulares, en el **Capítulo 2** se realizó estudio en profundidad de la cepa mutante del hongo incapaz de producir fumagilina, la $\Delta fmaA$ y el efecto de la delección sobre la patobiología del hongo. Para ello, se comenzó por corroborar mediante la técnica UHPLC que la cepa $\Delta fmaA$ no era capaz de producir fumagilina y realizar su caracterización fenotípica.

Los ensayos de dilución de inóculo utilizando placas de agar donde se incluyeron estresores estructurales (CR, CW o SDS) y osmóticos (NaCl, KCl o Sorbitol) no revelaron

diferencias entre las tres cepas empleadas (Wt, $\Delta fmaA$ y $\Delta fmaA::fmaA$). Por otra parte, el estudio del crecimiento y la morfología de las cepas llevado a cabo por microscopía mostró que la cepa mutante germinaba antes que la cepa Wt y la cepa complementada y, además, producía un número significativamente mayor de conidios con hifas emergiendo de dos puntos de germinación diferentes. Este fenotipo podría deberse al uso de la energía que la cepa Wt invierte en la biosíntesis de la toxina y que la cepa mutante puede invertir en germinar, aunque esto debería ser comprobado en estudios posteriores. También podría existir una relación entre el gen *fmaA* y el proceso de polarización de los conidios para la germinación.

Por otra parte, cabe destacar que el gen *fmaA*, y la producción de fumagilina que ello implica, parece ofrecer una protección al hongo, al menos en parte, frente a la fagocitosis, dada la observación de una mayor fagocitosis por parte de macrófagos y BMMs de la cepa $\Delta fmaA$. En estas pruebas también se demuestra que la protección depende de que la viabilidad del conidio, ya que al utilizar conidios inactivados no se observaron diferencias significativas entre las cepas. A esto hay que sumar que la producción de TNF por parte de los BMMs fue menor cuando en presencia de la cepa $\Delta fmaA$, lo que implicaría una menor activación de estas células por la cepa mutante.

Una vez realizada la caracterización *in vitro* y observado que el gen *fmaA* cumple una función relevante para el hongo en la resistencia a los fagocitos, nos dispusimos a realizar un ensayo de infección intranasal en modelo de ratón inmunodeprimido. Los resultados mostraron que la cepa $\Delta fmaA::fmaA$ fue significativamente más letal que la Wt y, sobre todo, que la mutante ($\Delta fmaA$). Paralelamente, se estudió la capacidad de secretar fumagilina por los mismos conidios utilizados en cada una de las infecciones realizadas y se observó que, los conidios de la cepa $\Delta fmaA::fmaA$ utilizados en estas infecciones mostraron una capacidad de producción de toxina mayor que la Wt, lo que podría explicar las diferencias de mortalidad observadas. Así mismo, los ratones que murieron al ser infectados con la cepa mutante no productora de fumagilina lo hicieron todos en las primeras 96 horas de ensayo. Este hecho podría deberse a que en los ratones infectados con la cepa mutante se habría dado una germinación más rápida y con doble polarización, tal y como hemos descrito anteriormente en la cepa mutante. Esto pudo producir lesiones en los pulmones de

manera mecánica destruyendo el tejido antes de que la respuesta inmunológica residual de los animales inmunosuprimidos pudiera controlar la infección. Los datos de carga fúngica apoyan esta hipótesis, ya que solo aquellos ratones que murieron en las primeras 96 horas debido a la infección por este mutante presentaron UFCs en sus pulmones, mientras que no se aislaron colonias fúngicas de los pulmones de aquellos ratones que sobrevivieron a la infección por la cepa $\Delta fmaA$. Esto es una diferencia muy significativa frente a la wt y revertiente ya que, en ambos casos, los ratones supervivientes sí que mostraron una relativamente alta carga de UFCs.

De los resultados de estos dos primeros capítulos se puede concluir que el *cluster* de genes involucrados en la biosíntesis de la fumagilina se activa durante las primeras 96 horas de infección junto con otras proteasas y genes que pueden facilitar la colonización por parte del hongo del tejido pulmonar, así como la diseminación a otros órganos. Por otra parte, hay que destacar que la fumagilina es una toxina detectable de manera fiable mediante UHPLC y que ha presentado tener diferente efecto en función del tipo celular ya que para los neumocitos presentó un marcado efecto inhibitorio de la ETC, migración y proliferación, mientras que para los macrófagos además de inhibir la actividad de la ETC y la proliferación celular resulto ser citotóxica. Finalmente, destacar que la producción de la toxina es importante, al menos *in vitro*, para el hongo a la hora de defenderse contra la fagocitosis, mientras que *in vivo* aquellos ratones infectados con la cepa de hongo no productora de la toxina sobreviven en mejores condiciones que aquellos infectados con las cepas Wt y complementada.

En el **Capítulo 3** de esta Tesis doctoral el objetivo fue estudiar el patrón de expresión génica de *A. fumigatus* en contacto con dos tipos celulares presentes en el ambiente pulmonar durante lo que se podría considerar el inicio o establecimiento de la infección para detectar posibles genes implicados en la virulencia y seleccionar uno de ellos para su estudio en profundidad.

Para ello, se realizaron dos ensayos de infección *in vitro* donde se co-incubó la cepa Wt del hongo con la línea celular de macrófagos murinos RAW 264.7 y con los neumocitos humanos A549. Una vez el hongo alcanzó el 30% de germinación, se

realizó una extracción de ARN total para ser hibridado con el microarray AWAFLUGE y estudiar la expresión génica del hongo comparando los resultados con su control sin contacto con las líneas celulares. Los resultados obtenidos ofrecieron un número muy elevado de DEGs que hacía muy difícil continuar el estudio. Esto concuerda con los indicado por otros autores que estudiaban el transcriptoma completo durante estudios de infecciones cuando utilizaban los resultados de expresión en cultivos in vitro como control (>1.000 genes DEG). Por ello, con el objetivo de encontrar genes importantes durante el proceso de infección de manera más específica y rápida, centramos nuestra atención en aquellos genes sobreexpresados con un FC > 1.5 tanto en contacto con los macrófagos como en contacto con los neumocitos e incluimos sólo aquellos que también hubieran presentado un patrón de sobreexpresión durante la infección intranasal en el modelo de ratón realizada en el **Capítulo 1**.

Únicamente 13 genes de *A. fumigatus* cumplieron las estrictas condiciones de expresión impuestas. Entre ellos no se encontraba el *cluster* de fumagilina/pseurotina estudiado en los capítulos anteriores, lo que parece indicar que la producción de fumagilina se mantiene constante y sin cambios en estas condiciones. Entre los 13 genes que comparten sobreexpresión en los tres modelos de infección experimental utilizados, consideramos uno de ellos, el gen *maiA*, como interesante. Este gen codifica una enzima que forma parte de la ruta de degradación de Phe/Tyr. Esta ruta había sido relacionada con la virulencia, dada su relación con la producción de piomelanina. Además, otros genes de esta misma ruta metabólica ya habían sido previamente estudiados por otros grupos (Schmaler-ripcke *et al.*, 2009; Keller *et al.*, 2011) y, de antemano, podíamos esperar un fenotipo resultante donde las rutas afectadas ya estaban descritas. Esto era un punto de control importante para nosotros ya que este iba a ser el primer mutante realizado por nuestro grupo de investigación utilizando la técnica dirigida CRISPR/Cas.

La ruta de degradación de Phe/Tyr esta mediada por enzimas codificadas por 6 genes (*hppD*, *hmgX*, *hmgA*, *fahA*, *maiA* and *hmgR*) localizados en un *cluster* en el cromosoma 2 de *A. fumigatus* que está regulado por el factor de transcripción HmgR (Perez-Cuesta *et al.*, 2020). Como se ha mencionado anteriormente, algunos genes de este *cluster*, cuatro concretamente, han sido estudiados previamente mediante el desarrollo de

cepas mutantes y han ofrecido resultados interesantes: *hmgR*, *hppD*, *hmgX* y *hmgA*. El mutante en el gen regulador del *cluster*, $\Delta hmgR$, fue incapaz de utilizar Tyr como una fuente de carbono o nitrógeno y en consecuencia únicamente produce de manera residual piomelanina. En cuanto a su virulencia, los ratones inmunosuprimidos infectados por vía intravenosa con este mutante presentaron la misma tasa de mortalidad que los infectados con el Wt (Keller *et al.*, 2011). Por otro lado, el mutante $\Delta hppD$ también fue incapaz de sintetizar piomelanina y mostró sensibilidad a los estreses oxidativos (Schmaler-ripcke *et al.*, 2009). Además, tampoco mostraba diferencias en letalidad de los animales infectados en comparación con el Wt (Keller *et al.*, 2011). Sin embargo, en nuestro estudio de infección intranasal en ratones incluido en el **Capítulo 1**, este gen *hppD* ha sido detectado como sobre expresado (Guruceaga *et al.*, 2018), lo que puede ser sorprendente ya que implicaría que podría ser importante en el desarrollo de la infección invasiva. El mutante de otro de los genes del *cluster* estudiados, el $\Delta hmgX$, ofrecía resultados similares al $\Delta hppD$ en estudios de infección animal, lo cual llevó a pensar que HmgX podría actuar como mediador de HppD (Keller *et al.* 2011). Finalmente, el mutante del gen *hmgA*, presentaba la capacidad de sintetizar más piomelanina debido a que acumulaba HGA, pero no ha sido ensayado en una infección animal (Schmaler-Ripcke *et al.* 2009).

Para llevar a cabo el silenciamiento del gen *maiA* se utilizó la técnica CRISPR-Cas9 por su alta eficiencia (Al abdhalla *et al.*, 2017), pero en esta ocasión en vez de realizar una delección completa del gen se optó por una estrategia de disrupción, en donde la metionina inicial del gen *maiA* se reemplazó por el gen de resistencia a la higromicina B. Esta estrategia ya ha sido utilizada años atrás por otros investigadores para silenciar el gen *maiA* en *A. nidulans* con el objetivo de utilizar el hongo como modelo genético para estudiar el catabolismo humano de Phe (Fernandez-Cañon & Peñalva 1998).

Dado que $\Delta maiA$ tiene bloqueada la ruta de degradación de Phe y Tyr, en presencia de dichos aminoácidos se debería acumular piomelanina en el medio debido a una acumulación de 4-MA y de los metabolitos anteriores de la ruta. Como se esperaba, la producción de piomelanina en este mutante se estimuló cuando se añadió Phe al medio, pero este efecto fue mayor cuando se añadió Tyr. Otros investigadores describieron que el mutante $\Delta mhgA$, produce mayor concentración de piomelanina

en presencia de Phe que cuando se añade Tyr (Schmaler-Ripcke *et al.*, 2009) y, además, no fue capaz de crecer con Tyr como única fuente de carbono, pero sí con Phe. Esto nos hizo plantearnos como *A. fumigatus* puede utilizar la Phe y la Tyr en su metabolismo y, la realidad es que cuenta con genes que codifican proteínas que permiten que el hongo cuente con una alternativa metabólica para utilizar la Phe como fuente de carbono única y derivarla a otras rutas metabólicas de obtención energía, pero no cuenta con ninguno, al menos aún descrito, para derivar la Tyr a otras rutas alternativas. Este hecho podría explicar la falta de crecimiento de la cepa $\Delta maiA$ cuando la Tyr era la única fuente de carbono y energía.

En cuanto a otras características fenotípicas de la cepa $\Delta maiA$, hay que destacar la significativamente menor cantidad de glucanos detectados en su pared en comparación con la cepa Wt. Esto es un dato relevante ya que hasta lo que se conoce, ninguno de los mutantes de genes relacionados con la degradación de Phe/Tyr generados, tanto en *A. fumigatus* como en *A. nidulans* o *P. marneffe*, han presentado esta característica (Fernandez-Cañón & Peñalva 1995; Fernandez-Cañón & Peñalva 1998; Keller *et al.*, 2011; Boyce 2014). La pared celular es una estructura esencial para mantener la homeostasis de la célula y muestra una gran plasticidad, variando su composición, grosor u organización dependiendo de las condiciones ambientales (Ram *et al.*, 2006) permitiendo la adaptación del hongo a diferentes condiciones. Para estudiar el efecto de la menor cantidad de glucanos en la pared del $\Delta maiA$, se expuso al hongo tanto a estreses de pared (CR y CW) como a estreses osmóticos (NaCl, KCl, sorbitol y SDS). Como era de esperar, la cepa mutante no fue capaz de crecer en presencia de CR y CW, en cambio cuando el medio se estabilizó osmóticamente con sorbitol la cepa mutante recuperó la capacidad de crecimiento. Se cree que la estabilización osmótica, en este caso con un azúcar, puede interactuar con el enlace β de los glucanos e incluso interferir en el proceso de ensamblaje de la pared celular (Wood 1980; Herth 1980; Pringle 1991). Por otra parte, el uso de sorbitol como estabilizador de la pared o incluso de células sin pared (protoplastos) es ampliamente conocido ya que se usa de rutina durante el proceso de transformación de *A. fumigatus*.

Por el contrario, a pesar de que la cepa mutante presentó un fenotipo compatible con el de un hongo con deficiencias en su pared celular, fue ligeramente más resistente que el Wt cuando se sometió a presión osmótica. Estudios con otras cepas mutantes, como *shoA*, *msbA*, *opyA*, *sakA* y *mpkC*, que presentaron sensibilidad a estreses de pared no mostraban estos patrones de resistencia a estreses osmóticos ya que eran sensibles a los mismos y además fueron más sensibles a caspofungina (Mattos *et al.*, 2020; Silva Pereira *et al.*, 2020). A pesar de que los resultados de sensibilidad a antifúngicos no se han mostrado en esta Tesis Doctoral, el mutante $\Delta maiA$ presentó el mismo patrón de sensibilidad que la cepa Wt en presencia de voriconazol, fluconazol, isavuconazol, caspofungina y micafungina. Sin embargo, estos otros estudios realizados con mutantes no son comparables al nuestro, dado que *maiA* es un gen relacionado con la degradación de aminoácidos mientras que el resto de genes mencionados anteriormente están relacionados con HOG (*high-osmolarity glycerol response pathway* por sus siglas en inglés), una ruta metabólica implicada en la osmolaridad.

Para terminar con la pared celular de nuestro mutante, hay que destacar que la microscopía electrónica de barrido confirmó de manera visual una desestructuración general de las hifas de la cepa mutante $\Delta maiA$ que mostraron un aspecto menos turgente, más aéreo y algo más estrecho que la morfología normal presentada por la cepa Wt y que se puede observar en estudios previamente publicados por otros autores (Gonzalez-Ramirez *et al.*, 2016; Wuren *et al.*, 2014; Joubert *et al.*, 2017). Además, las hifas de la cepa mutante no mostraron las ramificaciones típicas en ángulo de 45°, ni la matriz aparentemente secretada por el hongo y que si se pudo observar rodeando las hifas de la cepa Wt.

Los estudios de Valiante y colaboradores en los cuales realizaron mutaciones de las MAPK (*bck1*, *mkk2* y *mpk*) también demostraron que todos los mutantes generados fueron más sensibles a los estreses de pared celular, incluso utilizando sorbitol como agente osmoregulador, y a cafeína (Valiante *et al.*, 2008; Valiante *et al.*, 2009). Por ello y en un intento de relacionar el gen *maiA* con los fenotipos detectados por estos autores, la cepa $\Delta maiA$ fue crecida en presencia de cafeína que resulta ser un agente estresante de MAPKs. Los resultados mostraron que la cepa mutante no se veía

afectada, y por tanto los defectos de la pared celular no están relacionados con las rutas de activación por MAPKs. Por ello, una posible explicación de nuestros resultados sería que la cepa mutante al tener bloqueado el catabolismo de Phe/Tyr no es capaz de llegar a sintetizar algunos aminoácidos que podrían formar parte de la pared celular. Esto debería demostrarse en estudios posteriores a realizar.

Finalmente, se estudió la virulencia de la cepa mutante utilizando dos modelos de infección experimental *in vivo* e *in vitro*. Inicialmente utilizamos un modelo *in vitro* de co-incubación con macrófagos murinos, donde se observó que la cepa mutante $\Delta maiA$ fue más susceptible de ser fagocitada que la Wt a pesar de que presentó una mayor capacidad de germinación. Posteriormente se realizó una infección intranasal utilizando un modelo de ratón inmunosuprimido. Los resultados obtenidos demostraron que la cepa mutante $\Delta maiA$ fue significativamente menos letal que la Wt, ya que el 70 % de los ratones infectados por ella sobrevivieron. Estos datos son realmente interesantes y novedosos ya que, hasta la fecha, ninguno de los mutantes obtenidos y relacionados con la degradación de Phe/Tyr ($\Delta hmgR$ y $\Delta hppD$) mostraron variación en su mortalidad durante infecciones animales (Keller *et al.*, 2011). Hay que destacar que los estudios realizados por estos autores utilizaron un modelo de ratón inmunosuprimido con corticoesteroides y no con ciclofosfamida como hemos utilizado nosotros, lo que podría afectar a la respuesta del animal a la infección y a la diferencia de resultados obtenidos. Los defectos de la pared celular de la cepa $\Delta maiA$, así como la ligera tendencia a ser más fácilmente fagocitado pueden ser las claves por las cuales se observa una supervivencia tan elevada en los ratones infectados por nuestro mutante.

De este tercer capítulo se puede concluir que el gen *maiA* es un gen de *A. fumigatus* que se ha detectado diferencialmente sobre-expresado tanto en los modelos de infección *in vitro* como *in vivo* ensayados. La disrupción de este gen mediante el sistema CRISPR-Cas9 ha resultado una manera muy efectiva de estudiar la implicación de *maiA* tanto en el fenotipo del hongo como en la virulencia del mismo. Los resultados obtenidos apuntan a una relación aún desconocida entre el gen *maiA* implicado en el catabolismo de Phe y Tyr con la pared celular del hongo, ya que la cepa mutante mostro evidentes deficiencias estructurales de la misma, así como a una

implicación en la virulencia, ya que la cepa mutante inducía menor mortalidad en los ratones infectados con ella en comparación de los ratones infectados con la cepa Wt.

En resumen, podemos decir que este trabajo de investigación sigue un planteamiento donde hemos utilizado una técnica de estudio de transcriptoma completo (microarray de expresión) para detectar patrones de expresión diferencial de genes o rutas metabólicas de *A. fumigatus* tras ser sometido a modelos de infección tanto *in vitro* como *in vivo*. Los resultados se recogen en 3 capítulos. En el primero de ellos tras estudiar el transcriptoma del hongo durante una infección intranasal en ratones inmunosuprimidos, se detectó la sobreexpresión de un *cluster* de genes involucrado en la biosíntesis de fumagilina. En el segundo se profundizó en el estudio de los efectos que esta toxina tiene sobre dos tipos celulares presentes en el ambiente pulmonar, así como en la implicación que la producción de la toxina tiene para el hongo mediante la elaboración de una cepa mutante no productora de la misma. Esta toxina podría ser un factor de virulencia del hongo ya que produce diferente daño según el tipo celular y parece importante para el proceso de infección ya que ratones infectado con la cepa no productora sobreviven en mejores condiciones. Finalmente, en el tercer capítulo se recogen los resultados obtenidos tras detectar el gen *maiA* de *A. fumigatus* sobreexpresado en los tres modelos de infección diferentes utilizados en esta Tesis Doctoral. Tras el desarrollo de una cepa mutante para este gen mediante la técnica CRISPR-Cas9, podemos concluir que este gen, además de estar involucrado en la ruta de degradación de Phe/Tyr, tiene relación con el correcto desarrollo de la pared celular y su silenciamiento supone una alteración grave de la capacidad de infección del hongo.

Conclusiones



5. Conclusiones / Conclusions

1. Entre los genes que son importantes para el desarrollo, la invasión del tejido pulmonar y la angioinvasión en las infecciones animales causadas por *A. fumigatus* se encuentran los del cluster de biosíntesis de la fumagilina, así como genes que codifican proteasas y enzimas líticos (*aspf1*, *aspf5*, *chib1*, *dpp IV*, *dppV*...) y otros genes involucrados en rutas metabólicas del hongo (*hppD*, *maiA*, *idoC*, *nosA*...).

Among the genes that are important for development, lung tissue invasion and angioinvasion in animal infections caused by *A. fumigatus* are those of the fumagillin biosynthetic cluster, as well as genes that encode proteases and lytic enzymes (*aspf1*, *aspf5*, *chib1*, *dppIV*, *dppV*...) and other genes involved in fungal metabolic pathways (*hppD*, *maiA*, *idoC*, *nosA*...).

2. La fumagilina es una micotoxina que afecta de forma importante a la actividad metabólica y proliferación de los dos tipos celulares estudiados, neumocitos A549 y macrófagos RAW 264.7, causando, además, en los primeros inhibición de la migración celular y en los segundos un aumento de la mortalidad.

Fumagillin is a mycotoxin that significantly affects the metabolic activity and proliferation of the two cell types studied, A549 pneumocytes and RAW 264.7 macrophages, also causing inhibition of cell migration in the former and increased mortality in the latter.

3. La producción de fumagilina por *A. fumigatus* es un mecanismo de virulencia que utiliza en la invasión tisular de los pulmones, a tenor de la sobreexpresión del cluster de genes de su biosíntesis detectada durante el proceso infeccioso. Además, su producción protege *in vitro* a *A. fumigatus* de los mecanismos de defensa fagocíticos. Por otro lado, la incapacidad para producir fumagilina del mutante $\Delta fmaA$ desregula la germinación, generando una despolarización que se traduce en un aumento de la producción de dobles hifas. Este mutante origina

infecciones menos letales, además de observarse mejores condiciones y menor carga fúngica final en los animales supervivientes.

The production of fumagillin by *A. fumigatus* is a virulence mechanism that it uses in the tissue invasion of the lungs, based on the overexpression of the cluster of genes of its biosynthesis detected during the infectious process. Moreover, its production protects *A. fumigatus* from phagocytic defense mechanisms *in vitro*. On the other hand, the inability of the $\Delta fmaA$ to produce fumagillin deregulates the germination, causing a depolarization that results in an increase in the production of double branch hyphae. This mutant strain causes less lethal infections, in addition to better conditions and lower fungal burden in the survival animals.

4. Únicamente 13 genes de *A. fumigatus* (Afu1g04160, Afu2g04200, *maiA*, *sdh1*, Afu4g10610, Afu5g02320, *aspf1*, Afu6g00430, Afu6g02210, *cit1*, Afu6g12250, *idoC* y *osm1*) presentaron una importante sobreexpresión, con un valor de fold change superior a 1,5, en las tres condiciones de infección ensayadas en esta Tesis Doctoral por lo que pueden ser considerados importantes para el crecimiento en condiciones de infección y en la virulencia de este hongo.

Only 13 genes of *A. fumigatus* (Afu1g04160, Afu2g04200, *maiA*, *sdh1*, Afu4g10610, Afu5g02320, *aspf1*, Afu6g00430, Afu6g02210, *cit1*, Afu6g12250, *idoC* y *osm1*) showed a significant overexpression, with fold change values greater than 1.5, in the three infection models used in this Doctoral Thesis. For that, they can be considered important for the fungal growth under infection conditions and for virulence.

5. El gen *maiA* de *A. fumigatus* no es esencial para el hongo dado que la disrupción del gen solo impide el crecimiento de la cepa mutante $\Delta maiA$ con L-tirosina y dificultades para crecer con L-fenilalanina como únicas fuentes de carbono.

The *maiA* gene of *A. fumigatus* is not essential for the fungus since the disruption of the gene only prevents the growth of the $\Delta maiA$ mutant strain with L-tyrosine and difficulties to grow with L-phenylalanine as the only carbon sources.

6. El gen *maiA* tiene una relación aún desconocida con la biosíntesis de la pared celular, ya que la cepa mutante $\Delta maiA$ presenta menor resistencia a los estreses de pared, defectos evidentes en su estructura y una menor concentración de β -glucanos en la misma respecto a la cepa Wt.

The *maiA* gene has an unknown link with cell wall biosynthesis, since the mutant strain $\Delta maiA$ shows lower resistance to cell wall stresses, evident defects in its structure and a lower concentration of β -glucans in the cell wall compared to the Wt strain.

7. El gen *maiA* parece ser un nuevo factor de virulencia de *A. fumigatus* dado que su disrupción origina una cepa mutante ($\Delta maiA$) que produce más piomelanina, es más susceptible a la fagocitosis y, además, presenta una letalidad significativamente menor que la cepa Wt en las infecciones animales.

The *maiA* gene seems to be a novel virulence factor of *A. fumigatus* since its disruption leads a mutant strain ($\Delta maiA$) that produces more pyomelanin, is more susceptible to phagocytosis, and has significantly lower lethality than the Wt strain in animal infections.

Bibliografia / References



6. Referencias / Reference

Abad, A., Victoria Fernández-Molina, J., Bikandi, J., Ramírez, A., Margareto, J., Sendino, J., ... Rementeria, A. (2010). ¿Qué hace que *Aspergillus fumigatus* sea un patógeno de éxito? Genes y moléculas involucrados en la aspergilosis invasora. *Revista Iberoamericana de Micología*, 27(4), 155–182. <https://doi.org/10.1016/j.riam.2010.10.003>

Agarwal, R., Chakrabarti, A., Shah, A., Gupta, D., Meis, J. F., Guleria, R., ... Denning, D. W. (2013). Allergic bronchopulmonary aspergillosis: review of literature and proposal of new diagnostic and classification criteria. *Clinical and Experimental Allergy*, 43(8), 850–873. <https://doi.org/10.1111/cea.12141>

Aguado, J. M., Ruiz-Camps, I., Muñoz, P., Mensa, J., Almirante, B., Vázquez, L., ... Cuenca-Estrella, M. (2011). Guidelines for the treatment of invasive candidiasis and other yeasts. Spanish Society of Infectious Diseases and Clinical Microbiology (SEIMC). 2010 Update. *Enfermedades Infecciosas y Microbiología Clínica*, 29(5), 345–361. <https://doi.org/10.1016/j.eimc.2011.01.008>

Aimanianda, V., Bayry, J., Bozza, S., Knemeyer, O., Perruccio, K., Elluru, S. R., ... Latgé, J. P. (2009). Surface hydrophobin prevents immune recognition of airborne fungal spores. *Nature*, 460(7259), 1117–1121. <https://doi.org/10.1038/nature08264>

Al Abdallah, Q., Ge, W., & Fortwendel, J. R. (2017). A simple and universal system for gene manipulation in *Aspergillus fumigatus*: in vitro-assembled Cas9-guide RNA ribonucleoproteins coupled with microhomology repair templates. *mSphere*, 2, e00446-17. <https://doi.org/10.1128/msphere.00446-17>

Alastruey-Izquierdo, A., Mellado, E., Peláez, T., Pemán, J., Zapico, S., Alvarez, M., ... Cuenca-Estrella, M. (2013). Population-based survey of filamentous fungi and antifungal resistance in Spain (FILPOP study). *Antimicrobial Agents and Chemotherapy*, 57(7), 3380–3387. <https://doi.org/10.1128/AAC.00383-13>

Alastruey-Izquierdo, Ana, Cadranet, J., Flick, H., Godet, C., Hennequin, C., Hoenigl, M., ... Salzer, H. J. F. (2018). Treatment of chronic pulmonary Aspergillosis: current standards and future perspectives. *Respiration*, 96(2), 159–170. <https://doi.org/10.1159/000489474>

Alcazar-Fuoli, L., Clavaud, C., Lamarre, C., Aimanianda, V., Seidl-Seiboth, V., Mellado, E., & Latgé, J. P. (2011). Functional analysis of the fungal/plant class chitinase family in *Aspergillus fumigatus*. *Fungal Genetics and Biology*, 48, 418–429. <https://doi.org/10.1016/j.fgb.2010.12.007>

Alex, J., González, K., Kindel, T., Bellstedt, P., Weber, C., Heinekamp, T., ... Brakhage, A. A. (2020). Caspofungin functionalized polymethacrylates with antifungal

properties. *Biomacromolecules*, 21(6), 2104–2115.
<https://doi.org/10.1021/acs.biomac.0c00096>

Alker, A. P., Mwapasa, V., & Meshnick, S. R. (2004). Rapid real-time PCR genotyping of mutations associated with sulfadoxine-pyrimethamine resistance in *Plasmodium falciparum*. *Antimicrobial Agents and Chemotherapy*, 48(8), 2924–2929.
<https://doi.org/10.1128/AAC.48.8.2924-2929.2004>

Amaiike, S., & Keller, N. P. (2009). Distinct roles for VeA and LaeA in development and pathogenesis of *Aspergillus flavus*. *Eukaryotic Cell*, 8(7), 1051–1060.
<https://doi.org/10.1128/EC.00088-09>

Amitani, R., Taylor, G., Elezis, E. N., Llewellyn-Jones, C., Mitchell, J., Kuze, F., ... Wilson, R. (1995). Purification and characterization of factors produced by *Aspergillus fumigatus* which affect human ciliated respiratory epithelium. *Infection and Immunity*, 63(9), 3266–3271. <https://doi.org/10.1128/iai.63.9.3266-3271.1995>

Ankrah, A. O., Span, L. F. R., Klein, H. C., de Jong, P. A., Dierckx, R. A. J. O., Kwee, T. C., ... Glaudemans, A. W. J. M. (2019). Role of FDG PET/CT in monitoring treatment response in patients with invasive fungal infections. *European Journal of Nuclear Medicine and Molecular Imaging*, 46(1), 174–183. <https://doi.org/10.1007/s00259-018-4192-z>

Arfin, S. M., Kendall, R. L., Hall, L., Weaver, L. H., Stewart, A. E., Matthews, B. W., & Bradshaw, R. A. (1995). Eukaryotic methionyl aminopeptidases: two classes of cobalt-dependent enzymes. *Proceedings of the National Academy of Sciences of the United States of America*, 92(17), 7714–7718. <https://doi.org/10.1073/pnas.92.17.7714>

Arias, M., Santiago, L., Vidal-García, M., Redrado, S., Lanuza, P., Comas, L., ... Gálvez, E. M. (2018). Preparations for invasion: Modulation of host lung immunity during pulmonary aspergillosis by gliotoxin and other fungal secondary metabolites. *Frontiers in Immunology*, 9, 1–12. <https://doi.org/10.3389/fimmu.2018.02549>

Arruda, L. K., Mann, B. J., & Chapman, M. D. (1992). Selective expression of a major allergen and cytotoxin, Asp f I, in *Aspergillus fumigatus*. Implications for the immunopathogenesis of Aspergillus-related diseases. *The Journal of Immunology*, 149(10), 3354–3359.

Arruda, L. K., Platts-Mills, T. A. E., Fox, J. W., & Chapman, M. D. (1990). *Aspergillus fumigatus* allergen I, a Major IgE-binding protein, is a member of the mitogillin family of cytotoxins. *Journal of Experimental Medicine*, 172(5), 1529–1532.
<https://doi.org/10.1084/jem.172.5.1529>

Ascioglu, S., Rex, J. H., De Pauw, B., Bennett, J. E., Bille, J., Crokaert, F., ... Walsh, T. J. (2002). Defining opportunistic invasive fungal infections in immunocompromised patients with cancer and hematopoietic stem cell transplants: An international consensus. *Clinical Infectious Diseases*, 34(1), 7–14. <https://doi.org/10.1086/323335>

- Asif, A. R., Oellerich, M., Armstrong, V. W., Riemenschneider, B., Monod, M., & Reichard, U. (2006). Proteome of conidial surface associated proteins of *Aspergillus fumigatus* reflecting potential vaccine candidates and allergens. *Journal of Proteome Research*, 5(4), 954–962. <https://doi.org/10.1021/pr0504586>
- Askew, D. S. (2008). *Aspergillus fumigatus*: virulence genes in a street-smart mold. *Bone*, 11(4), 331–337. <https://doi.org/10.1016/j.mib.2008.05.009>.
- Azie, N., Neofytos, D., Pfaller, M., Meier-Kriesche, H. U., Quan, S. P., & Horn, D. (2012). The PATH (Prospective Antifungal Therapy) Alliance® registry and invasive fungal infections: Update 2012. *Diagnostic Microbiology and Infectious Disease*, 73(4), 293–300. <https://doi.org/10.1016/j.diagmicrobio.2012.06.012>
- Bailey, L. (1953). Effect of fumagillin upon *Nosema apis* (Zander). *Nature*, 171, 212–213.
- Baillie, G. S., & Douglas, L. J. (1999). Role of dimorphism in the development of *Candida albicans* biofilms. *Journal of Medical Microbiology*, 48(7), 671–679. <https://doi.org/10.1099/00222615-48-7-671>
- Banerjee, B., & Kurup, V. P. (2003). Molecular biology of *Aspergillus* allergens. *BioScience*, 8, 128–139.
- Barhoom, S., & Sharon, A. (2004). cAMP regulation of “pathogenic” and “saprophytic” fungal spore germination. *Fungal Genetics and Biology*, 41, 317–326. <https://doi.org/10.1016/j.fgb.2003.11.011>
- Barker, B. M., Kroll, K., Vödisch, M., Mazurie, A., Kniemeyer, O., & Cramer, R. a. (2012). Transcriptomic and proteomic analyses of the *Aspergillus fumigatus* hypoxia response using an oxygen-controlled fermenter. *BMC Genomics*, 13, 62. <https://doi.org/10.1186/1471-2164-13-62>
- Barnes, P. D., & Marr, K. A. (2006). Aspergillosis: spectrum of disease, diagnosis and treatment. *Infectious Disease Clinics of North America*, 20, 545–561. <https://doi.org/10.1016/j.idc.2006.06.001>
- Barnes, R. A., White, P. L., Morton, C. O., Rogers, T. R., Cruciani, M., Loeffler, J., & Donnelly, J. P. (2018). Diagnosis of aspergillosis by PCR: Clinical considerations and technical tips. *Medical Mycology*, 56, S60–S72. <https://doi.org/10.1093/mmy/myx091>
- Barrangou, R., Fremaux, C., Deveau, H., Melissa, R., Boyaval, P., Moineau, S., ... Horvath, P. (2007). CRISPR provides acquired resistance against viruses in prokaryotes. *Science*, 315, 1709–1712.
- Bassett, A. R., Tibbit, C., Ponting, C. P., & Liu, J. L. (2013). Highly Efficient targeted mutagenesis of *Drosophila* with the CRISPR/Cas9 system. *Cell Reports*, 4, 220–228. <https://doi.org/10.1016/j.celrep.2013.06.020>

Bayram, Ö., Krappmann, S., Ni, M., Jin, W. B., Helmstaedt, K., Valerius, O., ... Braus, G. H. (2008). VelB/VeA/LaeA complex coordinates light signal with fungal development and secondary metabolism. *Science*, 320, 1504–1506. <https://doi.org/10.1126/science.1155888>

Bayry, J., Beaussart, A., Dufrêne, Y. F., Sharma, M., Bansal, K., Kniemeyer, O., ... Beauvais, A. (2014). Surface structure characterization of *Aspergillus fumigatus* conidia mutated in the melanin synthesis pathway and their human cellular immune response. *Infection and Immunity*, 82(8), 3141–3153. <https://doi.org/10.1128/IAI.01726-14>

Beauvais, A., & Latgé, J. (2015). *Aspergillus* biofilm *in vitro* and *in vivo*. *Microbiology Spectrum*, 3(4), MB-0017-2015. <https://doi.org/10.1128/microbiolspec.MB-0017-2015.f1>

Beauvais, A., Schmidt, C., Guadagnini, S., Roux, P., Perret, E., Henry, C., ... Latgé, J. P. (2007). An extracellular matrix glues together the aerial-grown hyphae of *Aspergillus fumigatus*. *Cellular Microbiology*, 9(6), 1588–1600. <https://doi.org/10.1111/j.1462-5822.2007.00895.x>

Beffa, T., Staib, F., Lott Fischer, J., Lyon, P. F., Gumowski, P., Marfenina, O. E., ... Latgé, J. P. (1998). Mycological control and surveillance of biological waste and compost. *Medical Mycology*, Supplement, 36(suppl.1), 137–145.

Bell, M., Johnson, J., Wildi, B., & Woodward, R. B. (1958). The structure of gliotoxin. *The Journal of the American Chemical Society*, 80(4), 1001–1001.

Ben-Ami, R. (2013). Angiogenesis at the mold-host interface: A potential key to understanding and treating invasive aspergillosis. *Future Microbiology*, 8(11), 1453–1462. <https://doi.org/10.2217/fmb.13.114>

Bennett, J. W., & Bentley, R. (1989). What's in a Name?-Microbial Secondary Metabolism. *Advances in Applied Microbiology*, 34, 1–28. [https://doi.org/10.1016/S0065-2164\(08\)70316-2](https://doi.org/10.1016/S0065-2164(08)70316-2)

Berthier, E., Lim, F. Y., Deng, Q., Guo, C. J., Kontoyiannis, D. P., Wang, C. C. C., ... Keller, N. P. (2013). Low-Volume toolbox for the discovery of immunosuppressive fungal secondary metabolites. *PLoS Pathogens*, 9(4), e1003289. <https://doi.org/10.1371/journal.ppat.1003289>

Bertuzzi, M., Schrettl, M., Alcazar-Fuoli, L., Cairns, T. C., Muñoz, A., Walker, L. A., ... Bignell, E. M. (2014). The pH-Responsive PacC transcription factor of *Aspergillus fumigatus* governs epithelial entry and tissue invasion during pulmonary aspergillosis. *PLoS Pathogens*, 10(10), e1004413. <https://doi.org/10.1371/journal.ppat.1004413>

Bhabhra, R., & Askew, D. S. (2005). Thermotolerance and virulence of *Aspergillus fumigatus*: role of the fungal nucleolus. *Medical Mycology*, 43(SUPPL.1), 87–93. <https://doi.org/10.1080/13693780400029486>

- Bignell, E., Cairns, T. C., Throckmorton, K., Nierman, W. C., & Keller, N. P. (2016). Secondary metabolite arsenal of an opportunistic pathogenic fungus. *Philosophical Transactions of the Royal Society Biological Sciences*, 371, 1–9. <https://doi.org/10.1098/rstb.2016.0023>
- Birsoy, K., Wang, T., Chen, W. W., Freinkman, E., Abu-Remaileh, M., & Sabatini, D. M. (2015). An essential role of the mitochondrial electron transport chain in cell proliferation is to enable aspartate synthesis. *Cell*, 162(3), 540–551. <https://doi.org/10.1016/j.cell.2015.07.016>
- Bok, J. W., & Keller, N. P. (2004). LaeA, a regulator of secondary metabolism in *Aspergillus spp.* *Eukaryotic Cell*, 3(2), 527–535. <https://doi.org/10.1128/EC.3.2.527-535.2004>
- Bok, J. W., Chung, D. W., Balajee, S. A., Marr, K. A., Andes, D., Nielsen, K. F., ... Keller, N. P. (2006). GliZ, a transcriptional regulator of gliotoxin biosynthesis, contributes to *Aspergillus fumigatus* virulence. *Infection and Immunity*, 74(12), 6761–6768. <https://doi.org/10.1128/IAI.00780-06>
- Boyce, K. J., McLauchlan, A., Schreider, L., & Andrianopoulos, A. (2015). Intracellular growth is dependent on tyrosine catabolism in the dimorphic fungal pathogen *Penicillium marneffeii*. *PLoS Pathogens*, 11(3), 1–30. <https://doi.org/10.1371/journal.ppat.1004790>
- Bradshaw, R. A., Brickey, W. W., & Walker, K. W. (1998). N-terminal processing: the methionine aminopeptidase and N(α)-acetyl transferase families. *Trends in Biochemical Sciences*, 23, 263–267. [https://doi.org/10.1016/S0968-0004\(98\)01227-4](https://doi.org/10.1016/S0968-0004(98)01227-4)
- Braga, G. U. L., Rangel, D. E. N., Fernandes, É. K. K., Flint, S. D., & Roberts, D. W. (2015). Molecular and physiological effects of environmental UV radiation on fungal conidia. *Current Genetics*, 61, 405–425. <https://doi.org/10.1007/s00294-015-0483-0>
- Brakhage, A. A., & Langfelder, K. (2002). Menacing mold: the molecular biology of *Aspergillus fumigatus*. *Annual Review of Microbiology*, 56, 433–455. <https://doi.org/10.1146/annurev.micro.56.012302.160625>
- Brazma, A., & Vilo, J. (2000). Gene expression data analysis. *Microbes and Infection*, 480, 17–24. [https://doi.org/10.1016/S1286-4579\(01\)01440-X](https://doi.org/10.1016/S1286-4579(01)01440-X)
- Breakspear, A., & Momany, M. (2007). The first fifty microarray studies in filamentous fungi. *Microbiology*, 153, 7–15. <https://doi.org/10.1099/mic.0.2006/002592-0>
- Briard, B., Mislin, G. L. A., Latgé, J., & Beauvais, A. (2019). Interactions between *Aspergillus fumigatus* and pulmonary bacteria: current state of the field, new data and future perspective. *Journal of Fungi*, 5(48), 1–20. <https://doi.org/10.3390/jof5020048>
- Brown, G. D., & Gordon, S. (2001). A new receptor for B-glucans. *Nature*, 413(6851), 36–37. <https://doi.org/10.1038/35092617>

Brown, Gordon D., Denning, D. W., Gow, N. A. R., Levitz, S. M., Netea, M. G., & White, T. C. (2012). Hidden killers: human fungal infections. *Science Translational Medicine*, 4(165), 1–10. <https://doi.org/10.1126/scitranslmed.3004404>

Bryant, A. S., & Cerfolio, R. J. (2006). The maximum standardized uptake values on integrated FDG-PET/CT is useful in differentiating benign from malignant pulmonary nodules. *Annals of Thoracic Surgery*, 82(3), 1016–1020. <https://doi.org/10.1016/j.athoracsur.2006.03.095>

Bukreyeva, I., Angoulvant, A., Bendib, I., Gagnard, J. C., Bourhis, J. H., Dargère, S., ... Wyplosz, B. (2017). *Enterocytozoon bieneusi* microsporidiosis in stem cell transplant recipients treated with fumagillin. *Emerging Infectious Diseases*, 23(6), 1039–1041. <https://doi.org/10.3201/eid2306.161825>

Bünger, J., Westphal, G., Mönnich, A., Hinnendahl, B., Hallier, E., & Müller, M. (2004). Cytotoxicity of occupationally and environmentally relevant mycotoxins. *Toxicology*, 202(3), 199–211. <https://doi.org/10.1016/j.tox.2004.05.007>

Caillot, D., Casanovas, O., Bernard, A., Couaillier, J. F., Durand, C., Cuisenier, B., ... Guy, H. (1997). Improved management of invasive pulmonary aspergillosis in neutropenic patients using early thoracic computed tomographic scan and surgery. *Journal of Clinical Oncology*, 15(1), 139–147. <https://doi.org/10.1200/JCO.1997.15.1.139>

Caillot, D., Mannone, L., Cuisener, B., & Couaillier, J. F. (2001). Role of early diagnosis and aggressive surgery in the management of invasive pulmonary aspergillosis in neutropenic patients. *Clinical Microbiology and Infection*, 7, 54–61. <https://doi.org/10.1111/j.1469-0691.2001.tb00010.x>

Cairns, T., Minuzzi, F., & Bignell, E. (2010). The host-infecting fungal transcriptome. *FEMS Microbiology Letters*, 307, 1–11. <https://doi.org/10.1111/j.1574-6968.2010.01961.x>

Calera, J. A., Paris, S., Monod, M., Hamilton, A. J., Debeaupuis, J. P., Diaquin, M., ... Latgé, J. P. (1997). Cloning and disruption of the antigenic catalase gene of *Aspergillus fumigatus*. *Infection and Immunity*, 65(11), 4718–4724. <https://doi.org/10.1128/iai.65.11.4718-4724.1997>

Cao, Y. (2007). Angiogenesis modulates adipogenesis and obesity. *Journal of Clinical Investigation*, 117(9), 2362–2368. <https://doi.org/10.1172/JCI32239.2362>

Carlile M.J., Watkinson S.C., Gooday G. 2001. *The Fungi*. 2^a ed. Academic Press, San Diego, California, Estados Unidos.

Catalano, A., Romano, M., Robuffo, I., Strizzi, L., & Procopio, A. (2001). Methionine aminopeptidase-2 regulates human mesothelioma cell survival: role of Bcl-2 expression and telomerase activity. *American Journal of Pathology*, 159(2), 721–731. [https://doi.org/10.1016/S0002-9440\(10\)61743-9](https://doi.org/10.1016/S0002-9440(10)61743-9)

Cerqueira, G. C., Arnaud, M. B., Inglis, D. O., Skrzypek, M. S., Binkley, G., Simison, M., ... Wortman, J. R. (2014). The *Aspergillus* genome database: multispecies curation and incorporation of RNA-Seq data to improve structural gene annotations. *Nucleic Acids Research*, 42, 705–710. <https://doi.org/10.1093/nar/gkt1029>

Chamilos, G., Macapinlac, H. A., & Kontoyiannis, D. P. (2008). The use of 18F-fluorodeoxyglucose positron emission tomography for the diagnosis and management of invasive mould infections. *Medical Mycology*, 46, 23–29. <https://doi.org/10.1080/13693780701639546>

Champion, L., Durrbach, A., Lang, P., Delahousse, M., Chauvet, C., Sarfati, C., ... Molina, J. M. (2010). Fumagillin for treatment of intestinal microsporidiosis in renal transplant recipients. *American Journal of Transplantation*, 10, 1925–1930. <https://doi.org/10.1111/j.1600-6143.2010.03166.x>

Chang, Y. H., Teichert, U., & Smith, J. A. (1992). Molecular cloning, sequencing, deletion, and overexpression of a methionine aminopeptidase gene from *Saccharomyces cerevisiae*. *Journal of Biological Chemistry*, 267(12), 8007–8011. [https://doi.org/10.1016/S0021-9258\(18\)42400-3](https://doi.org/10.1016/S0021-9258(18)42400-3)

Charpentier, E., & Marraffini, L. A. (2014). Harnessing CRISPR-Cas9 immunity for genetic engineering. *Current Opinion in Microbiology*, 19, 114–119. <https://doi.org/10.1016/j.mib.2014.07.001>

Chaudhuri, R., Ansari, F. A., Raghunandan, M. V., & Ramachandran, S. (2011). FungalRV: adhesin prediction and immunoinformatics portal for human fungal pathogens. *BMC Genomics*, 12(192), 1–14. <https://doi.org/10.1186/1471-2164-12-192>

Chazalet, V., Debeaupuis, J. P., Sarfati, J., Lortholary, J., Ribaud, P., Shah, P., ... Latgé, J. P. (1998). Molecular typing of environmental and patient isolates of *Aspergillus fumigatus* from various hospital settings. *Journal of Clinical Microbiology*, 36(6), 1494–1500. <https://doi.org/10.1128/jcm.36.6.1494-1500.1998>

Chen, S., Vetro, J. A., & Chang, Y. H. (2002). The specificity in vivo of two distinct methionine aminopeptidases in *Saccharomyces cerevisiae*. *Archives of Biochemistry and Biophysics*, 398(1), 87–93. <https://doi.org/10.1006/abbi.2001.2675>

Cheng, J., Zhang, Y., & Li, Q. (2004). Real-time PCR genotyping using displacing probes. *Nucleic Acids Research*, 32(7), 1–10. <https://doi.org/10.1093/nar/gnh055>

Chong, G. L. M., Van De Sande, W. W. J., Dingemans, G. J. H., Gaajetaan, G. R., Vonk, A. G., Hayette, M. P., ... Rijnders, B. J. A. (2015). Validation of a new *Aspergillus* real-time PCR assay for direct detection of *Aspergillus* and azole resistance of *Aspergillus fumigatus* on bronchoalveolar lavage fluid. *Journal of Clinical Microbiology*, 53, 868–874. <https://doi.org/10.1128/JCM.03216-14>

Cong, L., Ran, F. A., Cox, D., Lin, S., Barretto, R., Hsu, P. D., ... Marraffini, L. a. (2013). Multiplex genome engineering using CRISPR/Cas Systems. *Science*, 339(6121), 819–823. <https://doi.org/10.1126/science.1231143>.

Conteas, C. N., Berlin, O. G. W., Ash, L. R., & Pruthi, J. S. (2000). Therapy for human gastrointestinal microsporidiosis. *American Journal of Tropical Medicine and Hygiene*, 63, 121–127. <https://doi.org/10.4269/ajtmh.2000.63.121>

Cornely, O. A., Maertens, J., Winston, D. J., Perfect, J., Ullmann, A. J., Walsh, T. J., ... Angulo-Gonzalez, D. (2007). Posaconazole vs. fluconazole or itraconazole in pediatric patients with neutropenia. *The New England Journal of Medicine*, 34(6), 348–359. <https://doi.org/10.1007/s10096-015-2340-y>

Cornely, Oliver A., Maertens, J., Bresnik, M., Ebrahimi, R., Dellow, E., Herbrecht, R., & Donnelly, J. P. (2010). Efficacy outcomes in a randomised trial of liposomal amphotericin B based on revised EORTC/MSG 2008 definitions of invasive mould disease. *Mycoses*, 54, 449–455. <https://doi.org/10.1111/j.1439-0507.2010.01947.x>

Cruciani, M., Mengoli, C., Barnes, R., Peter Donnelly, J., Loeffler, J., Jones, B. L., ... White, L. P. (2019). Polymerase chain reaction blood tests for the diagnosis of invasive aspergillosis in immunocompromised people. *Cochrane Database of Systematic Reviews*, 9, 1–84. <https://doi.org/10.1002/14651858.CD009551.pub4>.

D'Enfert, C. (1997). Fungal spore germination: Insights from the molecular genetics of *Aspergillus nidulans* and *Neurospora crassa*. *Fungal Genetics and Biology*, 21(2), 163–172. <https://doi.org/10.1006/fgbi.1997.0975>

da Silva Ferreira, M. E., Malavazi, I., Savoldi, M., Brakhage, A. A., Goldman, M. H. S., Kim, H. S., ... Goldman, G. H. (2006). Transcriptome analysis of *Aspergillus fumigatus* exposed to voriconazole. *Current Genetics*, 50(1), 32–44. <https://doi.org/10.1007/s00294-006-0073-2>

Dagenais, T. R. T., & Keller, N. P. (2009). Pathogenesis of *Aspergillus fumigatus* in invasive aspergillosis. *Clinical Microbiology Reviews*, 22(3), 447–465. <https://doi.org/10.1128/CMR.00055-08>

Datta, B., Ray, M. K., Chakrabarti, D., Wylie, D. E., & Gupta, N. K. (1989). Glycosylation of eukaryotic peptide chain initiation factor 2 (eIF-2)-associated 67-kDa polypeptide (p67) and its possible role in the inhibition of eIF-2 kinase-catalyzed phosphorylation of the eIF-2 α -subunit. *Journal of Biological Chemistry*, 264(34), 20620–20624. [https://doi.org/10.1016/S0021-9258\(19\)47108-1](https://doi.org/10.1016/S0021-9258(19)47108-1)

Debeaupuis, J. P., Sarfati, J., Chazalet, V., & Latgé, J. P. (1997). Genetic diversity among clinical and environmental isolates of *Aspergillus fumigatus*. *Infection and Immunity*, 65(8), 3080–3085. <https://doi.org/10.1128/iai.65.8.3080-3085.1997>

- Del Bono, V., Mikulska, M., & Viscoli, C. (2008). Invasive aspergillosis: Diagnosis, prophylaxis and treatment. *Current Opinion in Hematology*, 15, 586–593. <https://doi.org/10.1097/MOH.0b013e328311890c>
- Denis, J., Forouzanfar, F., Herbrecht, R., Toussaint, E., Kessler, R., Sabou, M., & Candol, E. (2018). Evaluation of two commercial Real-Time PCR Kits for *Aspergillus* DNA detection in bronchoalveolar lavage fluid in patients with invasive pulmonary aspergillosis. *The Journal of Molecular Diagnosis*, 20, 298–306. <https://doi.org/10.1016/j.jmoldx.2017.12.005>.
- Denning, D. W., Lee, J. Y., Hostetler, J. S., Pappas, P., Kauffman, C. A., Dewsnap, D. H., ... Stevens, D. A. (1994). NIAID mycoses study group multicenter trial of oral itraconazole therapy for invasive aspergillosis. *American Journal of Medicine*, 97, 135–144. [https://doi.org/10.1016/0002-9343\(94\)90341-7](https://doi.org/10.1016/0002-9343(94)90341-7)
- Denning, D.W. (2001). Chronic forms of pulmonary aspergillosis. *Clinical Microbiology and Infection*, 7, 25–31. <https://doi.org/10.1111/j.1469-0691.2001.tb00006.x>
- Denning, David W. (1998). Invasive Aspergillosis. *Clinical Infectious Diseases*, 26, 781–805. Retrieved from <http://www.jstor.org/stable/pdf/4481476.pdf>
- Denning, David W., Cadranet, J., Beigelman-Aubry, C., Ader, F., Chakrabarti, A., Blot, S., ... Lange, C. (2015). Chronic pulmonary aspergillosis: rationale and clinical guidelines for diagnosis and management. *European Respiratory Journal*, 47, 45–68. <https://doi.org/10.1183/13993003.00583-2015>
- Dhingra, S., Lind, A. L., Lin, H. C., Tang, Y., Rokas, A., & Calvo, A. M. (2013). The fumagillin gene cluster, an example of hundreds of genes under *veA* control in *Aspergillus fumigatus*. *PLoS ONE*, 8(10), e77147. <https://doi.org/10.1371/journal.pone.0077147>
- Diamond, R. D., & Clark, R. A. (1982). Damage to *Aspergillus fumigatus* and *Rhizopus oryzae* hyphae by oxidative and nonoxidative microbicidal products of human neutrophils *in vitro*. *Infection and Immunity*, 38(2), 487–495. <https://doi.org/10.1128/iai.38.2.487-495.1982>
- Drott, M. T., Bastos, R. W., Rokas, A., Ries, L. N. A., Gabaldón, T., Goldman, G. H., ... Greco, C. (2020). Diversity of Secondary metabolism in *Aspergillus nidulans* clinical isolates. *mSphere*, 5(2), e00156-20. <https://doi.org/10.1128/mSphere.00156-20>
- Eble, T. E., & Garret, E. R. (1954). Studies on the stability of fumagillin: II. Photolytic degradation of crystalline funagillin. *Journal of the American Pharmacists Association*, 26(5), 800–805. <https://doi.org/10.1002/jps.3030430906>
- Eichner, R. D., Al Salami, M., Wood, P. R., & Müllbacher, A. (1986). The effect of gliotoxin upon macrophage function. *International Journal of Immunopharmacology*, 8(7), 789–797. [https://doi.org/10.1016/0192-0561\(86\)90016-0](https://doi.org/10.1016/0192-0561(86)90016-0)

Eisenman, H. C., & Casadevall, A. (2012). Synthesis and assembly of fungal melanin. *Applied Microbiology and Biotechnology*, 93(3), 931–940. <https://doi.org/10.1007/s00253-011-3777-2>.

Endo, H., Takenaga, K., Kanno, T., Satoh, H., & Mori, S. (2002). Methionine aminopeptidase 2 is a new target for the metastasis-associated protein, S100A4*. *Journal of Biological Chemistry*, 277(29), 26396–26402. <https://doi.org/10.1074/jbc.M202244200>

Escobar, N., Ordonez, S. R., Wösten, H. A. B., & Haas, P. A. (2016). Hide, keep quiet, and keep low : Properties that make *Aspergillus fumigatus* a successful lung pathogen. *Frontiers in Microbiology*, 7(438). <https://doi.org/10.3389/fmicb.2016.00438>

Etxebeste, O., Herrero-García, E., Araújo-Bazán, L., Rodríguez-Urra, A. B., Garzia, A., Ugalde, U., & Espeso, E. A. (2009). The bZIP-type transcription factor FlbB regulates distinct morphogenetic stages of colony formation in *Aspergillus nidulans*. *Molecular Microbiology*, 73(5), 775–789. <https://doi.org/10.1111/j.1365-2958.2009.06804.x>

Etxebeste, O., Ni, M., Garzia, A., Kwon, N. J., Fischer, R., Yu, J. H., ... Ugalde, U. (2008). Basic-zipper-type transcription factor FlbB controls asexual development in *Aspergillus nidulans*. *Eukaryotic Cell*, 7(1), 38–48. <https://doi.org/10.1128/EC.00207-07>

Fallon, J. P., Reeves, E. P., & Kavanagh, K. (2011). The *Aspergillus fumigatus* toxin fumagillin suppresses the immune response of *Galleria mellonella* larvae by inhibiting the action of haemocytes. *Microbiology*, 157(5), 1481–1488. <https://doi.org/10.1099/mic.0.043786-0>

Fernández-Cañón, José M., & Peñalva, M. A. (1995). Fungal metabolic model for human type I hereditary tyrosinaemia. *Proceedings of the National Academy of Sciences of the United States of America*, 92(20), 9132–9136. <https://doi.org/10.1073/pnas.92.20.9132>

Fernández-Cañón, José Manuel, & Peñalva, M. A. (1998). Characterization of a fungal maleylacetoacetate isomerase gene and identification of its human homologue. *Journal of Biological Chemistry*, 273(1), 329–337. <https://doi.org/10.1074/jbc.273.1.329>

Fliesser, M., Morton, C. O., Bonin, M., Ebel, F., Hünninger, K., Kurzai, O., ... Löffler, J. (2015). Hypoxia-inducible factor 1 α modulates metabolic activity and cytokine release in anti-*Aspergillus fumigatus* immune responses initiated by human dendritic cells. *International Journal of Medical Microbiology*, 305(8), 865–873. <https://doi.org/10.1016/j.ijmm.2015.08.036>

Fontaine, T., Simenel, C., Dubreucq, G., Adam, O., Delepierre, M., Lemoine, J., ... Latgé, J. P. (2000). Molecular organization of the alkali-insoluble fraction of *Aspergillus fumigatus* cell wall. *Journal of Biological Chemistry*, 275(36), 27594–27607. <https://doi.org/10.1074/jbc.M909975199>.

Fortwendel, J. R., Juvvadi, P. R., Pinchai, N., Perfect, B. Z., Alspaugh, J. A., Perfect, J. R., & Steinbach, W. J. (2009). Differential effects of inhibiting chitin and 1,3- β -D-glucan synthesis in Ras and calcineurin mutants of *Aspergillus fumigatus*. *Antimicrobial Agents and Chemotherapy*, 53(2), 476–482. <https://doi.org/10.1128/AAC.01154-08>

Fries, I. (1993). *Nosema apis*, a parasite in the honeybee colony. *Bee World*, 74(1), 5–19. <https://doi.org/10.1080/0005772X.1993.11099149>

Frisvad, J. C., Rank, C., Nielsen, K. F., & Larsen, T. O. (2009). Metabolomics of *Aspergillus fumigatus*. *Medical Mycology*, 47, 53–71. <https://doi.org/10.1080/13693780802307720>

Froel, A. R., Jung, V., Engers, R., Müller, M., Schulz, W. A., & Wullich, B. (2005). Application of a modified Real-Time PCR technique for relative gene copy number quantification to the determination of the relationship between NKX3.1 Loss and MYC gain in prostate cancer. *Clinical Chemistry*, 51(3), 649–652. <https://doi.org/10.1373/clinchem.2004.045930>

Fuller, K. K., Chen, S., Loros, J. J., & Dunlap, J. C. (2015). Development of the CRISPR/Cas9 system for targeted gene disruption in *Aspergillus fumigatus*. *Eukaryotic Cell*, 14(11), 1073–1080. <https://doi.org/10.1128/EC.00107-15>

Furukawa, T., van Rhijn, N., Fraczek, M., Gsaller, F., Davies, E., Carr, P., ... Bromley, M. J. (2020). The negative cofactor 2 complex is a key regulator of drug resistance in *Aspergillus fumigatus*. *Nature Communications*, 11(427), 1–16. <https://doi.org/10.1038/s41467-019-14191-1>

Gams W., Christensen M., Onions A.H., Pitt J.I., Samson R.A. 1985. Infrageneric taxa of *Aspergillus*. p.55-62. In: *Advances in Penicillium and Aspergillus Systematics*. Samson R.A.,

Garret, E. R. (1954). Studies on the stability of fumagillin: III. Thermal degradation in the presence and absence of air. *Journal of the American Pharmaceutical Association. American Pharmaceutical Association*, 43(9), 539–543.

Garret, E. R., & Eble, T. E. (1954). Studies on the Stability of Furnagillin: I. Photolytic degradation in alcohol solution. *Journal of the American Pharmaceutical Association. American Pharmaceutical Association*, 43(7), 385–390.

Gastebois, A., Clavaud, C., Aïmanianda, V., & Latgé, J. P. (2009). *Aspergillus fumigatus*: cell wall polysaccharides, their biosynthesis and organization. *Future Microbiology*, 4(5), 583–595. <https://doi.org/10.2217/fmb.09.29>

Gayathri, L., Akbarsha, M. A., & Ruckmani, K. (2020). In vitro study on aspects of molecular mechanisms underlying invasive aspergillosis caused by gliotoxin and fumagillin, alone and in combination. *Scientific Reports*, 10(14473), 1–20. <https://doi.org/10.1038/s41598-020-71367-2>

Gibson, J. (2006). The use of real-time PCR methods in DNA sequence variation analysis. *Clinica Chimica Acta*, 363, 32–37. <https://doi.org/10.1016/j.cccn.2005.06.022>

Glass, N. L., Rasmussen, C., Roca, M. G., & Read, N. D. (2004). Hyphal homing, fusion and mycelial interconnectedness. *Trends in Microbiology*, 12(3), 135–141. <https://doi.org/10.1016/j.tim.2004.01.007>

González-Ramírez, A. I., Ramírez-Granillo, A., Medina-Canales, M. G., Rodríguez-Tovar, A. V., & Martínez-Rivera, M. A. (2016). Analysis and description of the stages of *Aspergillus fumigatus* biofilm formation using scanning electron microscopy. *BMC Microbiology*, 16(243), 1–13. <https://doi.org/10.1186/s12866-016-0859-4>

Gow, N. A. R., Latgé, J.-P., & Munro, C. A. (2017). The fungal cell wall: structure, biosynthesis and function. *Microbiology Spectrum*, 5(3), 1–25. <https://doi.org/10.1128/9781555819583.ch12>

Gravelat, F. N., Doedt, T., Chiang, L. Y., Liu, H., Filler, S. G., Patterson, T. F., & Sheppard, D. C. (2008). *In vivo* analysis of *Aspergillus fumigatus* developmental gene expression determined by real-time reverse transcription-PCR. *Infection and Immunity*, 76(8), 3632–3639. <https://doi.org/10.1128/IAI.01483-07>

Gresset, A., & Harden, T. K. (2012). The phospholipase C isoenzymes and their regulation. *Sub-Cellular Biochemistry* (Vol. 58). <https://doi.org/10.1007/978-94-007-3012-0>

Grosjean, P., & Weber, R. (2007). Fungus balls of the paranasal sinuses: A review. *European Archives of Oto-Rhinolaryngology*, 264, 461–470. <https://doi.org/10.1007/s00405-007-0281-5>

Guarro J., Orzechowski X., Severo L.C. 2010. Differences and similarities amongst Pathogenic *Aspergillus* species. In: *Aspergillosis: from diagnosis to prevention*. Pasqualotto AC (ed). Springer.

Guruceaga, X., Ezpeleta, G., Mayayo, E., Sueiro-Olivares, M., Abad-Diaz-De-Cerio, A., Urizar, J. M. A., ... Rementeria, A. (2018). A possible role for fumagillin in cellular damage during host infection by *Aspergillus fumigatus*. *Virulence*, 9(1), 1548–1561. <https://doi.org/10.1080/21505594.2018.1526528>

Guruceaga, X., Perez-Cuesta, U., De Cerio, A. A. D., Gonzalez, O., Alonso, R. M., Hernando, F. L., ... Rementeria, A. (2020). Fumagillin, a mycotoxin of *Aspergillus fumigatus*: biosynthesis, biological activities, detection, and applications. *Toxins*, 12(7), 1–26. <https://doi.org/10.3390/toxins12010007>

Guruceaga, X., Sierra, A., Marino, D., Santin, I., Nieto-Garai, J. A., Bilbao, J. R., ... Mayor, U. (2020). Fast SARS-CoV-2 detection protocol based on RNA precipitation and RT-qPCR in nasopharyngeal swab samples. *MedRxiv*, 1–22. <https://doi.org/10.1101/2020.04.26.20081307>

- Hamilton Miller, J. M. T. (1973). Chemistry and biology of the polyene macrolide antibiotics. *Bacteriological Reviews*, 37(2), 166–196. <https://doi.org/10.1128/membr.37.3.166-196.1973>
- Hanson, F. R. ., & Eble, T. E. (1949). An antiphage agent isolated from *Aspergillus* spp. *Journal of Bacteriology*, 58(4), 527–529. <https://doi.org/10.1128/jb.58.4.527-529.1949>
- Harris, S. D. (2006). Cell polarity in filamentous fungi: shaping the mold. *International Review of Cytology*, 251, 41–76. [https://doi.org/10.1016/S0074-7696\(06\)51002-2](https://doi.org/10.1016/S0074-7696(06)51002-2)
- Harris, S. D., & Momany, M. (2004). Polarity in filamentous fungi: moving beyond the yeast paradigm. *Fungal Genetics and Biology*, 41, 391–400. <https://doi.org/10.1016/j.fgb.2003.11.007>
- Hartwig, A. (1971). Nucleic acids in intestine of *Apis mellifica* infected with *Nosema apis* and treated with fumagillin DCH: cytochemical and autoradiographic studies. *Journal of Invertebrate Pathology*, 18, 331–336.
- Hawksworth, D. L., Crous, P. W., Redhead, S. A., Reynolds, D. R., Samson, R. A., Seifert, K. A., ... Zhang, N. (2011). The Amsterdam declaration on fungal nomenclature. *IMA Fungus*, 2(1), 105–112. <https://doi.org/10.5598/imafungus.2011.02.01.14>
- Heinekamp, T., Thywißen, A., Macheleidt, J., Keller, S., Valiante, V., & Brakhage, A. A. (2013). *Aspergillus fumigatus* melanins: interference with the host endocytosis pathway and impact on virulence. *Frontiers in Microbiology*, 3(440), 1–7. <https://doi.org/10.3389/fmicb.2012.00440>
- Henry, C., Latgé, J. P., & Beauvais, A. (2012). α 1,3 glucans are dispensable in *Aspergillus fumigatus*. *Eukaryotic Cell*, 11(1), 26–29. <https://doi.org/10.1128/EC.05270-11>
- Herbrecht, R., Denning, D. W., Patterson, T. F., Bennett, J. E., Greene, R. E., Oestmann, J. W., ... De Pauw, B. (2002). Voriconazole versus amphotericin B for primary therapy of invasive aspergillosis. *The New England Journal of Medicine*, 347(6), 408–415. <https://doi.org/10.1056/NEJMoa020191>
- Herbrecht, R., Maertens, J., Baila, L., Aoun, M., Heinz, W., Martino, R., ... Viscoli, C. (2010). Caspofungin first-line therapy for invasive aspergillosis in allogeneic hematopoietic stem cell transplant patients: An European Organisation for Research and Treatment of Cancer study. *Bone Marrow Transplantation*, 45, 1227–1233. <https://doi.org/10.1038/bmt.2009.334>
- Herbrecht, Raoul, Patterson, T. F., Slavin, M. A., Marchetti, O., Maertens, J., Johnson, E. M., ... Pappas, P. G. (2015). Application of the 2008 definitions for invasive fungal diseases to the trial comparing voriconazole versus amphotericin B for therapy of invasive aspergillosis: A Collaborative Study of the Mycoses Study Group (MSG 05) and the European Organization for R. *Clinical Infectious Diseases*, 60(5), 713–720. <https://doi.org/10.1093/cid/ciu911>

- Herth, W. (1980). Calcofluor white and congo red inhibit chitin microfibril assembly of *Poteroiochromonas*: Evidence for a gap between polymerization and microfibril formation. *Journal of Cell Biology*, 87, 442–450. <https://doi.org/10.1083/jcb.87.2.442>
- Hillmann, F., Novohradská, S., Mattern, D. J., Forberger, T., Heinekamp, T., Westermann, M., ... Brakhage, A. A. (2015). Virulence determinants of the human pathogenic fungus *Aspergillus fumigatus* protect against soil amoeba predation. *Environmental Microbiology*, 17(8), 2858–2869. <https://doi.org/10.1111/1462-2920.12808>
- Hohl, T. M., & Feldmesser, M. (2007). *Aspergillus fumigatus*: principles of pathogenesis and host defense. *Eukaryotic Cell*, 6(11), 1953–1963. <https://doi.org/10.1128/EC.00274-07>
- Honda, A., Hirose, M., Sankai, T., Yasmin, L., Yuzawa, K., Honsho, K., ... Ogura, A. (2015). Single-step generation of rabbits carrying a targeted allele of the tyrosinase gene using CRISPR/Cas9. *Experimental Animals*, 64(1), 31–37. <https://doi.org/10.1538/expanim.14-0034>
- Hope, W. W., Walsh, T. J., & Denning, D. W. (2005). The invasive and saprophytic syndromes due to *Aspergillus* spp. *Medical Mycology*, 43, 207–238. <https://doi.org/10.1080/13693780400025179>
- Hot, A., Maunoury, C., Poiree, S., Lanternier, F., Viard, J. P., Loulergue, P., ... Lortholary, O. (2011). Diagnostic contribution of positron emission tomography with [¹⁸F]fluorodeoxyglucose for invasive fungal infections. *Clinical Microbiology and Infection*, 17(3), 409–417. <https://doi.org/10.1111/j.1469-0691.2010.03301.x>
- Hou, L., Mori, D., Takase, Y., Meihua, P., Kai, K., & Tokunaga, O. (2009). Fumagillin inhibits colorectal cancer growth and metastasis in mice: *in vivo* and *in vitro* study of anti-angiogenesis. *Pathology International*, 59, 448–461. <https://doi.org/10.1111/j.1440-1827.2009.02393.x>
- Houbraken, J., de Vries, R. P., & Samson, R. A. (2014). Modern taxonomy of biotechnologically important *Aspergillus* and *Penicillium* species. *Advances in Applied Microbiology* (1st ed., Vol. 86). Copyright © 2014 Elsevier Inc. All rights reserved. <https://doi.org/10.1016/B978-0-12-800262-9.00004-4>
- Huang, W. F., Solter, L. F., Yau, P. M., & Imai, B. S. (2013). *Nosema ceranae* escapes fumagillin control in honeybees. *PLoS Pathogens*, 9(3), e1003185. <https://doi.org/10.1371/journal.ppat.1003185>
- Hubka, V., Nováková, A., Kolařík, M., Jurjević, Ž., & Peterson, S. W. (2015). Revision of *Aspergillus* section *Flavipedes*: seven new species and proposal of section *Jani* sect. nov. *Mycologia*, 107(1), 169–208. <https://doi.org/10.3852/14-059>
- Ibrahim-Granet, O., Jouvion, G., Hohl, T. M., Droin-Bergère, S., Philippart, F., Kim, O. Y., ... Brock, M. (2010). *In vivo* bioluminescence imaging and histopathologic

analysis reveal distinct roles for resident and recruited immune effector cells in defense against invasive aspergillosis. *BMC Microbiology*, 10, 105. <https://doi.org/10.1186/1471-2180-10-105>

Ingber, D., Fujita, T., Kishimoto, S., Sudo, K., Kanamaru, T., Brem, H., & Folkman, J. (1990). Synthetic analogues of fumagillin that inhibit angiogenesis and suppress tumour growth. *Nature*, 348, 555–557. <https://doi.org/10.1038/348555a0>

Irmer, H., Tarazona, S., Sasse, C., Olbermann, P., Loeffler, J., Krappmann, S., ... Braus, G. H. (2015). RNAseq analysis of *Aspergillus fumigatus* in blood reveals a just wait and see resting stage behavior. *BMC Genomics*, 16, 640. <https://doi.org/10.1186/s12864-015-1853-1>

Ito, J. I. (2013). Enhancing Angiogenesis in Invasive Aspergillosis : A novel therapeutic approach. *The Journal of Infectious Diseases*, 207(7), 1031–1033. <https://doi.org/10.1093/infdis/jis944>

Jahn, B., Langfelder, K., Schneider, U., Schindel, C., & Brakhage, A. A. (2002). PKSP-dependent reduction of phagolysosome fusion and intracellular kill of *Aspergillus fumigatus* conidia by human monocyte-derived macrophages. *Cellular Microbiology*, 4(12), 793–803. <https://doi.org/10.1046/j.1462-5822.2002.00228.x>

Jain, R., Valiante, V., Remme, N., Docimo, T., Heinekamp, T., Hertweck, C., ... Brakhage, A. A. (2011). The MAP kinase MpkA controls cell wall integrity, oxidative stress response, gliotoxin production and iron adaptation in *Aspergillus fumigatus*. *Molecular Microbiology*, 82(1), 39–53. <https://doi.org/10.1111/j.1365-2958.2011.07778.x>

Jaques, A. K., Fukamizo, T., Hall, D., Barton, R. C., Escott, G. M., Parkinson, T., ... Adams, D. J. (2003). Disruption of the gene encoding the ChiB1 chitinase of *Aspergillus fumigatus* and characterization of a recombinant gene product. *Microbiology*, 149(10), 2931–2939. <https://doi.org/10.1099/mic.0.26476-0>

Jean-Michel Molina, Muriel Tourneur, Claudine Sarfati, Sylvie Chevret, Amaury de Gouvello, Jean-Gérard Gobert, S. B. and F. D. (2016). Fumagillin treatment of intestinal microsporidiosis. *New England Journal of Medicine*, 346(25), 1963–1969. <https://doi.org/10.1056/NEJMoa012924>

Jiang, W., Zhou, H., Bi, H., Fromm, M., Yang, B., & Weeks, D. P. (2013). Demonstration of CRISPR/Cas9/sgRNA-mediated targeted gene modification in *Arabidopsis*, tobacco, sorghum and rice. *Nucleic Acids Research*, 41(20), 1–12. <https://doi.org/10.1093/nar/gkt780>

Jin, W. B., Balajee, S. A., Marr, K. A., Andes, D., Nielsen, K. F., Frisvad, J. C., & Keller, N. P. (2005). LaeA, a regulator of morphogenetic fungal virulence factors. *Eukaryotic Cell*, 4(9), 1574–1582. <https://doi.org/10.1128/EC.4.9.1574-1582.2005>

- Jinek, M., Chylinski, K., Fonfara, I., Hauer, M., Doudna, J. A., & Charpentier, E. (2012). A programmable dual RNA-guided DNA endonuclease in adaptive bacterial immunity. *Science*, 337(6096), 816–821. <https://doi.org/10.1126/science.1225829>
- Jinek, M., East, A., Cheng, A., Lin, S., Ma, E., & Doudna, J. (2013). RNA-programmed genome editing in human cells. *eLife*, e00471, 1–9. <https://doi.org/10.7554/eLife.00471>
- Joubert, L. M., Ferreira, J. A., Stevens, D. A., Nazik, H., & Cegelski, L. (2017). Visualization of *Aspergillus fumigatus* biofilms with scanning electron microscopy and variable pressure-scanning electron microscopy: a comparison of processing techniques. *Journal of Microbiological Methods*, 132, 46–55. <https://doi.org/10.1016/j.mimet.2016.11.002>
- Kamei, K., & Watanabe, A. (2005). *Aspergillus* mycotoxins and their effect on the host. *Medical Mycology*, 43, 95–99. <https://doi.org/10.1080/13693780500051547>
- Kanno, T., Uehara, T., Osawa, M., Fukumoto, H., Mine, S., Ueda, K., ... Katano, H. (2015). Fumagillin, a potent angiogenesis inhibitor, induces Kaposi sarcoma-associated herpesvirus replication in primary effusion lymphoma cells. *Biochemical and Biophysical Research Communications*, 463(4), 1267–1272. <https://doi.org/10.1016/j.bbrc.2015.06.100>
- Kao, R., & Davies, J. (1995). Fungal ribotoxins: a family of naturally engineered targeted toxins? *Biochemistry and Cell Biology*, 73, 1151–1159. <https://doi.org/10.1139/o95-124>
- Kao, Richard, & Davies, J. (1999). Molecular dissection of mitogillin reveals that the fungal ribotoxins are a family of natural genetically engineered ribonucleases. *Journal of Biological Chemistry*, 274(18), 12576–12582. <https://doi.org/10.1074/jbc.274.18.12576>
- Katznelson, H., & Jamieson, C. A. (1952). Control of *Nosema* disease of honeybees with fumagillin. *Science*, 115(2977), 71–72. <https://doi.org/10.1126/science.115.2977.71>
- Keller, N. P. (2019). Fungal secondary metabolism: regulation, function and drug discovery. *Nature Reviews Microbiology*, 17(3), 167–180. <https://doi.org/10.1038/s41579-018-0121-1>
- Keller, N., Bok, J., Chung, D., Perrin, R. M., & Keats Shwab, E. (2006). LaeA, a global regulator of *Aspergillus* toxins. *Medical Mycology*, 44, 83–85. <https://doi.org/10.1080/13693780600835773>
- Keller, S., Macheleidt, J., Scherlach, K., Schmalzer-Ripcke, J., Jacobsen, I. D., Heinekamp, T., & Brakhage, A. A. (2011). Pyomelanin formation in *Aspergillus fumigatus* requires HmgX and the transcriptional activator HmgR but is dispensable for virulence. *PLoS ONE*, 6(10), e26604. <https://doi.org/10.1371/journal.pone.0026604>

- Kenneth, B., Dorothy, R. and, & Fennell, I. (1965). The fungi the genus *Aspergillus*. *Science*, 150, 736–737.
- Kernien, J. F., Snarr, B. D., Sheppard, D. C., & Nett, J. E. (2018). The interface between fungal biofilms and innate immunity. *Frontiers in Immunology*, 8, 1–10. <https://doi.org/10.3389/fimmu.2017.01968>
- Kidoikhammouan, S., Seubwai, W., Silsirivanit, A., Wongkham, S., Sawanyawisuth, K., & Wongkham, C. (2019). Blocking of methionine aminopeptidase-2 by TNP-470 induces apoptosis and increases chemosensitivity of cholangiocarcinoma. *Journal of Cancer Research and Therapeutics*, 15(1), 148-152. https://doi.org/10.4103/jcrt.JCRT_250_17
- Killough, J. H., Magill, G. B., & Smith, R. C. (1952). The treatment of amebiasis with fumagillin. *Science*, 115(2977), 71–72. <https://doi.org/10.1126/science.115.2977.71>
- Klont, R. R., Mennink-Kersten, M. A. S. H., & Verweij, P. E. (2004). Utility of *Aspergillus* antigen detection in specimens other than serum specimens. *Clinical Infectious Diseases*, 39, 1467–1474. <https://doi.org/10.1086/425317>
- Koenig, S., Rühmann, B., Sieber, V., & Schmid, J. (2017). Quantitative assay of β -(1,3)- β -(1,6)-glucans from fermentation broth using aniline blue. *Carbohydrate Polymers*, 174, 57–64. <https://doi.org/10.1016/j.carbpol.2017.06.047>
- Köhli, M., Galati, V., Boudier, K., Roberson, R. W., & Philippsen, P. (2008). Growth-speed-correlated localization of exocyst and polarisome components in growth zones of *Ashbya gossypii* hyphal tips. *Journal of Cell Science*, 121(23), 3878–3889. <https://doi.org/10.1242/jcs.033852>
- Kosmidis, C., & Denning, D. W. (2015). The clinical spectrum of pulmonary aspergillosis. *Thorax*, 70, 270–277. <https://doi.org/10.1136/thoraxjnl-2014-206291>
- Kousha, M., Tadi, R., & Soubani, A. O. (2011). Pulmonary aspergillosis: a clinical review. *European Respiratory Review*, 20(121), 156–174. <https://doi.org/10.1183/09059180.00001011>
- Krappmann, S. (2016). How to invade a susceptible host: cellular aspects of aspergillosis. *Current Opinion in Microbiology*, 34, 136–146. <https://doi.org/10.1016/j.mib.2016.10.002>
- Krijghsheld, P., Bleichrodt, R., van Veluw, G. J., Wang, F., Müller, W. H., Dijksterhuis, J., & Wösten, H. A. B. (2013). Development in *Aspergillus*. *Studies in Mycology*, 74, 1–29. <https://doi.org/10.3114/sim0006>
- Kuhlman, J. E., Fishman, E. K., & Siegelman, S. S. (1985). Invasive pulmonary aspergillosis in acute leukemia: Characteristic findings on CT, the CT halo sign, and the role of CT in early diagnosis. *Radiology*, 157(3), 611–614. <https://doi.org/10.1148/radiology.157.3.3864189>

Kuhn, D. M., Chandra, J., Mukherjee, P. K., & Ghannoum, M. A. (2002). Comparison of biofilms formed by *Candida albicans* and *Candida parapsilosis* on bioprosthetic surfaces. *Infection and Immunity*, 70(2), 878–888. <https://doi.org/10.1128/IAI.70.2.878-888.2002>

Kumar, A., Ahmed, R., Singh, P. K., & Shukla, P. K. (2011). Identification of virulence factors and diagnostic markers using immunosecretome of *Aspergillus fumigatus*. *Journal of Proteomics*, 74(7), 1104–1112. <https://doi.org/10.1016/j.jprot.2011.04.004> [doi]

Kumar, A., Reddy, L. V., Sochanik, A., & Kurup, V. P. (1993). Allergens, IgE, mediators, inflammatory mechanisms Isolation and characterization of a recombinant heat shock protein of *Aspergillus fumigatus*. *The Journal of Allergy and Clinical Immunology*, 91(5), 1024–1030. [https://doi.org/10.1016/0091-6749\(93\)90215-2](https://doi.org/10.1016/0091-6749(93)90215-2)

Kusaka, M., Sudo, K., Fujita, T., Marui, S., Itoh, F., Ingber, D., & Folkman, J. (1991). Potent anti-angiogenic action of AGM-1470: comparison to the fumagillin parent. *Biochemical and Biophysical Research Communications*, 174(3), 1070–1076. [https://doi.org/10.1016/0006-291X\(91\)91529-L](https://doi.org/10.1016/0006-291X(91)91529-L)

Kwon-Chung, K. J., & Sugui, J. A. (2013). *Aspergillus fumigatus*-What makes the species a ubiquitous human fungal pathogen? *PLoS Pathogens*, 9(12), e1003743. <https://doi.org/10.1371/journal.ppat.1003743>

L. Mauriz, J., Martin-Renedo, J., Garcia-Palomo, A., J. Tunon, M., & Gonzalez-Gallego, J. (2010). Methionine Aminopeptidases as Potential Targets for Treatment of Gastrointestinal Cancers and other Tumours. *Current Drug Targets*. <https://doi.org/10.2174/1389210205839704501>

Langfelder, K., Jahn, B., Gehringer, H., Schmidt, A., Wanner, G., & Brakhage, A. A. (1998). Identification of a polyketide synthase gene (pksP) of *Aspergillus fumigatus* involved in conidial pigment biosynthesis and virulence. *Medical Microbiology and Immunology*, 187, 79–89. <https://doi.org/10.1007/s004300050077>

Laschke, M. W., & Menger, M. D. (2012). Anti-angiogenic treatment strategies for the therapy of endometriosis. *Human Reproduction Update*, 18(6), 682–702. <https://doi.org/10.1093/humupd/dms026>

Latgé, J. P. (1999). *Aspergillus fumigatus* and aspergillosis. *Clinical Microbiology Reviews*, 33(1), 310–350. <https://doi.org/10.1128/CMR.00140-18>

Latgé, J. P., & Beauvais, A. (2014). Functional duality of the cell wall. *Current Opinion in Microbiology*, 20, 111–117. <https://doi.org/10.1016/j.mib.2014.05.009>

Latgé, J., & Chamilos, G. (2019). *Aspergillus fumigatus* and aspergillosis in 2019. *Clinical Microbiology Reviews*, 33, e00140-18. <https://doi.org/10.1128/CMR.00140-18>.

- Ledoux, M. P., Guffroy, B., Nivoix, Y., Simand, C., & Herbrecht, R. (2020). Invasive pulmonary aspergillosis. *Seminars in Respiratory and Critical Care Medicine*, 41(1), 80–98. <https://doi.org/10.1055/s-0039-3401990>
- Lee, M. J., & Sheppard, D. C. (2016). Recent advances in the understanding of the *Aspergillus fumigatus* cell wall. *Journal of Microbiology*, 54(3), 232–242. <https://doi.org/10.1007/s12275-016-6045-4>
- Lewis, R. E., Wiederhold, N. P., Chi, J., Han, X. Y., Komanduri, K. V., Kontoyiannis, D. P., & Prince, R. A. (2005). Detection of gliotoxin in experimental and human aspergillosis. *Infection and Immunity*, 73(1), 635–637. <https://doi.org/10.1128/IAI.73.1.635-637.2005>
- Liang, P., Xu, Y., Zhang, X., Ding, C., Huang, R., Zhang, Z., ... Huang, J. (2015). CRISPR/Cas9-mediated gene editing in human tripronuclear zygotes. *Protein and Cell*, 6(5), 363–372. <https://doi.org/10.1007/s13238-015-0153-5>
- Lijnen, H. R., Frederix, L., & Van Hoef, B. (2010). Fumagillin reduces adipose tissue formation in murine models of nutritionally induced obesity. *Obesity*, 18, 2241–2246. <https://doi.org/10.1038/oby.2009.503>
- Lin, H. C., Chooi, Y. H., Dhingra, S., Xu, W., Calvo, A. M., & Tang, Y. (2013). The fumagillin biosynthetic gene cluster in *Aspergillus fumigatus* encodes a cryptic terpene cyclase involved in the formation of β -trans-bergamotene. *Journal of the American Chemical Society*, 135(12), 4616–4619. <https://doi.org/10.1021/ja312503y>
- Lin, H. C., Tsunematsu, Y., Dhingra, S., Xu, W., Fukutomi, M., Chooi, Y. H., ... Tang, Y. (2014). Generation of complexity in fungal terpene biosynthesis: Discovery of a multifunctional cytochrome P450 in the fumagillin pathway. *Journal of the American Chemical Society*, 136(11), 4426–4436. <https://doi.org/10.1021/ja500881e>
- Lind, A. L., Lim, F. Y., Soukup, A. A., Keller, N. P., & Rokas, A. (2018). An LaeA- and BrIA-dependent cellular network governs tissue-specific secondary metabolism in the human pathogen *Aspergillus fumigatus*. *mSphere*, 3(2), e0050-18. <https://doi.org/10.1128/mSphere.00050-18>.
- Lind, Abigail L., Smith, T. D., Saterlee, T., Calvo, A. M., & Rokas, A. (2016). Regulation of secondary metabolism by the velvet complex is temperature-responsive in *Aspergillus*. *G3: Genes, Genomes, Genetics*, 6(12), 4023–4033. <https://doi.org/10.1534/g3.116.033084/-/DC1>.
- Lind, Abigail L., Wisecaver, J. H., Lameiras, C., Wiemann, P., Palmer, J. M., Keller, N. P., ... Rokas, A. (2017). Drivers of genetic diversity in secondary metabolic gene clusters within a fungal species. *PloS Biology*, 15(11), e2003583. <https://doi.org/10.1371/journal.pbio.2003583>

- Linder, M. B., Szilvay, G. R., Nakari-Setälä, T., & Penttilä, M. E. (2005). Hydrophobins: the protein-amphiphiles of filamentous fungi. *FEMS Microbiology Reviews*, 29(5), 877–896. <https://doi.org/10.1016/j.femsre.2005.01.004>
- Liu, J., Yang, Z. J., & Meng, Z. H. (1996). The isolation, purification and identification of fumitremorgin B produced by *Aspergillus fumigatus*. *Biomedical and Environmental Sciences*, 9(1), 1–11.
- Liu, S., Widom, J., Kemp, C. W., Crews, C. M., & Clardy, J. (1998). Structure of human methionine aminopeptidase-2 complexed with fumagillin. *Science*, 282(5392), 1324–1327. <https://doi.org/10.1126/science.282.5392.1324>
- Lortholary, O., Gangneux, J. P., Sitbon, K., Lebeau, B., de Monbrison, F., Le Strat, Y., ... Bretagne, S. (2011). Epidemiological trends in invasive aspergillosis in France: The SAIF network (2005–2007). *Clinical Microbiology and Infection*, 17, 1882–1889. <https://doi.org/10.1111/j.1469-0691.2011.03548.x>
- Loussert, C., Schmitt, C., Prevost, M. C., Balloy, V., Fadel, E., Philippe, B., ... Beauvais, A. (2010). *In vivo* biofilm composition of *Aspergillus fumigatus*. *Cellular Microbiology*, 12(3), 405–410. <https://doi.org/10.1111/j.1462-5822.2009.01409.x>
- Lowther, W. T., & Matthews, B. W. (2000). Structure and function of the methionine aminopeptidases. *Biochimica et Biophysica Acta*, 1477, 157–167. [https://doi.org/10.1016/S0167-4838\(99\)00271-X](https://doi.org/10.1016/S0167-4838(99)00271-X)
- Lumbreras, C., & Gavaldà, J. (2003). Aspergilosis invasora: manifestaciones clínicas y tratamiento. *Revista Iberoamericana de Micología*, 20, 79–89.
- Maertens, J. A., Raad, I. I., Marr, K. A., Patterson, T. F., Kontoyiannis, D. P., Cornely, O. A., ... Ullmann, A. J. (2016). Isavuconazole versus voriconazole for primary treatment of invasive mould disease caused by *Aspergillus* and other filamentous fungi (SECURE): A phase 3, randomised-controlled, non-inferiority trial. *The Lancet*, 387(10020), 760–769. [https://doi.org/10.1016/S0140-6736\(15\)01159-9](https://doi.org/10.1016/S0140-6736(15)01159-9)
- Mardis, E. R. (2008). Next-generation DNA sequencing methods. *Annual Review of Genomics and Human Genetics*, 9, 387–402. <https://doi.org/10.1146/annurev.genom.9.081307.164359>
- Marioni, J. C., Mason, C. E., Mane, S. M., Stephens, M., & Gilad, Y. (2008). RNA-seq: an assessment of technical reproducibility and comparison with gene expression arrays. *Genome Research*, 18(9), 1509–1517. <https://doi.org/10.1101/gr.079558.108>
- Marr, K. A., Schlamm, H. T., Herbrecht, R., Rottinghaus, S. T., Bow, E. J., Cornely, O. A., ... Maertens, J. A. (2015). Combination antifungal therapy for invasive aspergillosis. *Annals of Internal Medicine*, 162(2), 81–89. <https://doi.org/10.7326/M13-2508>
- Martin-Vicente, A., Souza, A. C. O., Al Abdallah, Q., Ge, W., & Fortwendel, J. R. (2018). SH3-class Ras guanine nucleotide exchange factors are essential for *Aspergillus*

fumigatus invasive growth. *Cellular Microbiology*, 21, e13013. <https://doi.org/10.1111/cmi.13013>

Martin-Vicente, A., Souza, A. C. O., Nywening, A. V., Ge, W., & Fortwendel, J. R. (2020). Overexpression of the *Aspergillus fumigatus* small GTPase, RsrA, promotes polarity establishment during germination. *Journal of Fungi*, 6(4), 1–19. <https://doi.org/10.3390/jof6040285>

Maschmeyer, G., Haas, A., & Cornely, O. A. (2007). Invasive aspergillosis: epidemiology, diagnosis and management in immunocompromised patients. *Indian Journal of Radiology and Imaging*, 67(11), 1597–1601. <https://doi.org/10.2165/00003495-200767110-00004>

Mattos, E. C., Silva, P., Valero, C., Castro, A. De, Taft, C. A., Al-furaiji, N., ... Brown, A. (2020). The *Aspergillus fumigatus* phosphoproteome reveals roles of high-osmolarity glycerol mitogen-activated protein kinases in promoting cell wall damage and caspofungin tolerance. *mBio*, 11, e02962-19. <https://doi.org/10.1128/mBio.02962-19>

McDonagh, A., Fedorova, N. D., Crabtree, J., Yu, Y., Kim, S., Chen, D., ... Bignell, E. (2008). Sub-telomere directed gene expression during initiation of invasive aspergillosis. *PLoS Pathogens*, 4(9), e10000154. <https://doi.org/10.1371/journal.ppat.1000154>

Miceli, M. H., & Maertens, J. (2015). Role of non-culture-based tests, with an emphasis on galactomannan testing for the diagnosis of invasive aspergillosis. *Seminars in Respiratory and Critical Care Medicine*, 36(5), 650–661. <https://doi.org/10.1055/s-0035-1562892>

Mirkes, P. E. (1974). Polysomes, ribonucleic acids, and protein synthesis during germination of *Neurospora crassa* conidia. *Journal of Bacteriology*, 117(1), 196–202. <https://doi.org/10.1128/JB.117.1.196-202.1974>.

Mitchell, C. G., Slight, J., & Donaldson, K. (1997). Diffusible component from the spore surface of the fungus *Aspergillus fumigatus* which inhibits the macrophage oxidative burst is distinct from gliotoxin and other hyphal toxins. *Thorax*, 52(9), 796–801. <https://doi.org/10.1136/thx.52.9.796>

Mojica, F. J.M., Díez-Villaseñor, C., García-Martínez, J., & Almendros, C. (2009). Short motif sequences determine the targets of the prokaryotic CRISPR defence system. *Microbiology*, 155(3), 733–740. <https://doi.org/10.1099/mic.0.023960-0>

Mojica, Francisco J.M., Díez-Villaseñor, C., García-Martínez, J., & Soria, E. (2005). Intervening sequences of regularly spaced prokaryotic repeats derive from foreign genetic elements. *Journal of Molecular Evolution*, 60(2), 174–182. <https://doi.org/10.1007/s00239-004-0046-3>

Momany, M. (2002). Polarity in filamentous fungi: establishment, maintenance and new axes. *Current Opinion in Microbiology*, 5(6), 580–585. [https://doi.org/10.1016/S1369-5274\(02\)00368-5](https://doi.org/10.1016/S1369-5274(02)00368-5)

Montagna, M. T., Lovero, G., Coretti, C., Martinelli, D., Delia, M., De Giglio, O., ... Pagano, L. (2014). SIMIFF study: Italian fungal registry of mold infections in hematological and non-hematological patients. *Infection*, 42(1), 141–151. <https://doi.org/10.1007/s15010-013-0539-3>

Montejo, M., (2002) Invasive infection by *Aspergillus* and other filamentous fungi in solid organ trasplant recipients. *Revista Iberoamericana de Micología*, 19(1), 9-12.

Morton, C. O., Varga, J. J., Hornbach, A., Mezger, M., Sennefelder, H., Kneitz, S., ... Loeffler, J. (2011). The temporal dynamics of differential gene expression in *Aspergillus fumigatus* interacting with human immature dendritic cells *in vitro*. *PLoS ONE*, 6(1), e16016. <https://doi.org/10.1371/journal.pone.0016016>

Moura, S., Cerqueira, L., & Almeida, A. (2018). Invasive pulmonary aspergillosis: current diagnostic methodologies and a new molecular approach. *European Journal of Clinical Microbiology and Infectious Diseases*, 37(8), 1393–1403. <https://doi.org/10.1007/s10096-018-3251-5>

Mullbacher, A., & Eichner, R. D. (1984). Immunosuppression *in vitro* by a metabolite of a human pathogenic fungus. *Proceedings of the National Academy of Sciences of the United States of America*, 81(12), 3835–3837. <https://doi.org/10.1073/pnas.81.12.3835>

Muñoz, P., Guinea, J., & Bouza, E. (2006). Update on invasive aspergillosis: clinical and diagnostic aspects. *Clinical Microbiology and Infection*, 12, 24–39. <https://doi.org/10.1111/j.1469-0691.2006.01603.x>

Neves, S. R., Ram, P. T., & Iyengar, R. (2002). G protein pathways. *Science*, 296(5573), 1636–1639. <https://doi.org/10.1126/science.1071550>

Nicolle, M. C., Benet, T., & Vanhems, P. (2011). Aspergillosis: nosocomial or community-acquired? *Medical Mycology*, 49, 29–34. <https://doi.org/10.3109/13693786.2010.509335>

Nierman, W. C., Pain, A., Anderson, M. J., Wortman, J. R., Kim, H. S., Arroyo, J., ... Denning, D. W. (2005). Genomic sequence of the pathogenic and allergenic filamentous fungus *Aspergillus fumigatus*. *Nature*, 438(7071), 1151–1156. <https://doi.org/10.1038/nature04332>

Niu, Y., Shen, B., Cui, Y., Chen, Y., Wang, J., Wang, L., ... Sha, J. (2014). Generation of gene-modified cynomolgus monkey via Cas9/RNA-mediated gene targeting in one-cell embryos. *Cell*, 156(4), 836–843. <https://doi.org/10.1016/j.cell.2014.01.027>

Nosanchuk, J. D., Stark, R. E., & Casadevall, A. (2015). Fungal melanin: what do we know about structure? *Frontiers in Microbiology*, 6(1463), 1–7. <https://doi.org/10.3389/fmicb.2015.01463>

O’Gorman, C. M. (2011). Airborne *Aspergillus fumigatus* conidia: a risk factor for aspergillosis. *Fungal Biology Reviews*, 25(3), 151–157. <https://doi.org/10.1016/j.fbr.2011.07.002>

O’Gorman, C. M., Fuller, H. T., & Dyer, P. S. (2009). Discovery of a sexual cycle in the opportunistic fungal pathogen *Aspergillus fumigatus*. *Nature*, 457(7228), 471–474. <https://doi.org/10.1038/nature07528>

Obayashi, T., Negishi, K., Suzuki, T., & Funata, N. (2008). Reappraisal of the serum (1→3)- β -D-glucan assay for the diagnosis of invasive fungal infections - a study based on autopsy cases from 6 years. *Clinical Infectious Diseases*, 46(12), 1864–1870. <https://doi.org/10.1086/588295>

Oda, K., Bignell, E., Kang, S. E., & Momany, M. (2016). Transcript levels of the *Aspergillus fumigatus* Cdc42 module, polarisome, and septin genes show little change from dormancy to polarity establishment. *Medical Mycology*, 55(4), 1-8. <https://doi.org/10.1093/mmy/myw085>

Oosthuizen, J. L., Gomez, P., Ruan, J., Hackett, T. L., Moore, M. M., Knight, D. A., & Tebbutt, S. J. (2011). Dual organism transcriptomics of airway epithelial cells interacting with conidia of *Aspergillus fumigatus*. *PLoS ONE*, 6(5), e20527. <https://doi.org/10.1371/journal.pone.0020527>

Orciuolo, E., Stanzani, M., Canestraro, M., Galimberti, S., Carulli, G., Lewis, R., ... Komanduri, K. V. (2007). Effects of *Aspergillus fumigatus* gliotoxin and methylprednisolone on human neutrophils: implications for the pathogenesis of invasive aspergillosis. *Journal of Leukocyte Biology*, 82(4), 839–848. <https://doi.org/10.1189/jlb.0207090>

Oshero N. 2007. The virulence of *Aspergillus fumigatus*. In *New insights in medical mycology*. Kavanagh K. (ed.). Springer, Países Bajos. p.1852-12.

Oshero, N., & May, G. S. (2001). The molecular mechanisms of conidial germination. *FEMS Microbiology Letters*, 199(2), 153–160. [https://doi.org/10.1016/S0378-1097\(01\)00178-1](https://doi.org/10.1016/S0378-1097(01)00178-1)

Otamendi, A., Perez-de-Nanclares-Arregi, E., Oiartzabal-Arano, E., Cortese, M. S., Espeso, E. A., & Etxebeste, O. (2019). Developmental regulators FlbE/D orchestrate the polarity site-to-nucleus dynamics of the fungal bZIP transcription factor FlbB. *Cellular and Molecular Life Sciences*, 76(21), 4369–4390. <https://doi.org/10.1007/s00018-019-03121-5>

Pagani, J., & Libshitz, H. I. (1981). Opportunistic fungal pneumonias in cancer patients. *American Journal of Roentgenology*, 137(5), 1033–1039. <https://doi.org/10.2214/ajr.137.5.1033>

Pagella, F., Matti, E., Bernardi, F. De, Semino, L., Cavanna, C., Marone, P., ... Castelnuovo, P. (2007). Paranasal sinus fungus ball: diagnosis and management. *Mycoses*, 50(6), 451–456. <https://doi.org/10.1111/j.1439-0507.2007.01416.x>

Pappas, P. G., Kauffman, C. A., Andes, D. R., Clancy, C. J., Marr, K. A., Ostrosky-Zeichner, L., ... Sobel, J. D. (2016). Clinical practice guideline for the management of candidiasis: 2016 update by the infectious diseases society of America. *Clinical Infectious Diseases*, 62(4), e1-50. <https://doi.org/10.1093/cid/civ933>

Paris, S., Debeaupuis, J., Cramer, R., Carey, M., Charle, F., Pre, M. C., ... Latge, J. P. (2003). Conidial Hydrophobins of *Aspergillus fumigatus*. *Applied and Environmental Microbiology*, 69(3), 1581–1588. <https://doi.org/10.1128/AEM.69.3.1581>

Paris, S., Wysong, D., Debeaupuis, J. P., Shibuya, K., Philippe, B., Diamond, R. D., & Latgé, J. P. (2003). Catalases of *Aspergillus fumigatus*. *Infection and Immunity*, 71(6), 3551–3562. <https://doi.org/10.1128/IAI.71.6.3551-3562.2003>.

Pasricha, S., Payne, M., Canovas, D., Pase, L., Ngaosuwan, N., Beard, S., ... Andrianopoulos, A. (2013). Cell-type-specific transcriptional profiles of the dimorphic pathogen *Penicillium marneffe* reflect distinct reproductive, morphological, and environmental demands. *G3: Genes, Genomes, Genetics*, 3(11), 1997–2014. <https://doi.org/10.1534/g3.113.006809>

Patterson, T. F., & Donnelly, J. P. (2019). New concepts in diagnostics for invasive mycoses: non-culture-based methodologies. *Journal of Fungi*, 5(1). <https://doi.org/10.3390/jof5010009>

Patterson, T. F., Thompson, G. R., Denning, D. W., Fishman, J. A., Hadley, S., Herbrecht, R., ... Bennett, J. E. (2016). Practice guidelines for the diagnosis and management of aspergillosis: 2016 update by the infectious diseases society of America. *Clinical Infectious Diseases*, 63(4), 1–60. <https://doi.org/10.1093/cid/ciw326>

Pellon, A., Andoni, R. G., Idoia, B., Aitziber, A., Aitor, R., & Fernando, L. H. (2017). Molecular and cellular responses of the pathogenic fungus *Lomentospora prolificans* to the antifungal drug voriconazole. *PLoS ONE*, 12(3), e0174885. <https://doi.org/10.1371/journal.pone.0174885>

Pellon, A., Ramirez-Garcia, A., Guruceaga, X., Zabala, A., Buldain, I., Antoran, A., ... Hernando, F. L. (2018). Microglial immune response is impaired against the neurotropic fungus *Lomentospora prolificans*. *Cellular Microbiology*, 20(8), e12847. <https://doi.org/10.1111/cmi.12847>

- Pepeljnjak, S., Slobodnjak, Z., Šegvić, M., Peraica, M., & Pavlović, M. (2004). The ability of fungal isolates from human lung aspergilloma to produce mycotoxins. *Human and Experimental Toxicology*, 23(1), 15–19. <https://doi.org/10.1191/0960327104ht409oa>
- Perez-Cuesta, U., Aparicio-Fernandez, L., Guruceaga, X., Martin-Souto, L., Abad-Diaz-de-Cerio, A., Antoran, A., ... Rementeria, A. (2020). Melanin and pyomelanin in *Aspergillus fumigatus*: from its genetics to host interaction. *International Microbiology*, 23, 55–63. <https://doi.org/10.1007/s10123-019-00078-0>
- Perrin, R. M., Fedorova, N. D., Jin, W. B., Cramer, R. A., Wortman, J. R., Kim, H. S., ... Keller, N. P. (2007). Transcriptional regulation of chemical diversity in *Aspergillus fumigatus* by LaeA. *PLoS Pathogens*, 3(4), e50. <https://doi.org/10.1371/journal.ppat.0030050>
- Pierce, C. G., Srinivasan, A., Uppuluri, P., Ramasubramanian, A. K., & López-Ribot, J. L. (2013). Antifungal therapy with an emphasis on biofilms. *Current Opinion in Pharmacology*, 13(5), 726–730. <https://doi.org/10.1016/j.coph.2013.08.008>
- Pihet, M., Vandeputte, P., Tronchin, G., Renier, G., Saulnier, P., Georgeault, S., ... Bouchara, J. P. (2009). Melanin is an essential component for the integrity of the cell wall of *Aspergillus fumigatus* conidia. *BMC Microbiology*, 9(177), 1–11. <https://doi.org/10.1186/1471-2180-9-177>
- Pitt J.I. (eds). Plenum Press, New York.
- Pöggeler, S. (2002). Genomic evidence for mating abilities in the asexual pathogen *Aspergillus fumigatus*. *Current Genetics*, 42(3), 153–160. <https://doi.org/10.1007/s00294-002-0338-3>
- Price, T. H., Boeckh, M., Harrison, R. W., McCullough, J., Ness, P. M., Strauss, R. G., ... Assmann, S. F. (2015). Efficacy of transfusion with granulocytes from G-CSF/dexamethasone-treated donors in neutropenic patients with infection. *Blood*, 126(18), 2153–2161. <https://doi.org/10.1182/blood-2015-05-645986>
- Pringle, A., Baker, D. M., Platt, J. L., Wares, J. P., Latgé, J. P., & Taylor, J. W. (2005). Cryptic speciation in the cosmopolitan and clonal human pathogenic fungus *Aspergillus fumigatus*. *Evolution*, 59(9), 1886–1899. <https://doi.org/10.1111/j.0014-3820.2005.tb01059.x>
- Pringle, J. R. (1991). Staining of bud scars and other cell wall chitin with Calcofluor. *Methods in Enzymology*, 194, 732–735. [https://doi.org/10.1016/0076-6879\(91\)94055-H](https://doi.org/10.1016/0076-6879(91)94055-H)
- Raffa, N., & Keller, N. P. (2019). A call to arms: mustering secondary metabolites for success and survival of an opportunistic pathogen. *PLoS Pathogens*, 15(4), e1007606. <https://doi.org/10.1371/journal.ppat.1007606>

- Raffa, N., Osherov, N., & Keller, N. P. (2019). Copper utilization, regulation, and acquisition by *Aspergillus fumigatus*. *International Journal of Molecular Sciences*, 20(8), 1980. <https://doi.org/10.3390/ijms20081980>
- Ramage, G., Rajendran, R., Sherry, L., & Williams, C. (2012). Fungal biofilm resistance. *International Journal of Microbiology*, 2012(528521), 1–14. <https://doi.org/10.1155/2012/528521>
- Ramirez-Garcia, A., Pellon, A., Buldain, I., Antoran, A., Arbizu-Delgado, A., Guruceaga, X., ... Hernando, F. L. (2018). Proteomics as a Tool to Identify New Targets Against *Aspergillus* and *Scedosporium* in the Context of Cystic Fibrosis. *Mycopathologia*, 183(1), 273–289. <https://doi.org/10.1007/s11046-017-0139-3>
- Rath, P. M., & Steinmann, J. (2018). Overview of commercially available PCR assays for the detection of *Aspergillus spp.* DNA in patient samples. *Frontiers in Microbiology*, 9(740), 1–6. <https://doi.org/10.3389/fmicb.2018.00740>
- Ray, M. K., Datta, B., Chakraborty, A., Chattopadhyay, A., Meza-Keuthen, S., & Gupta, N. K. (1992). The eukaryotic initiation factor 2-associated 67-kDa polypeptide (p67) plays a critical role in regulation of protein synthesis initiation in animal cells. *Proceedings of the National Academy of Sciences of the United States of America*, 89(2), 539–543. <https://doi.org/10.1073/pnas.89.2.539>
- Rementeria, A., López-Molina, N., Ludwig, A., Vivanco, A. B., Bikandi, J., Pontón, J., & Garaizar, J. (2005). Genes and molecules involved in *Aspergillus fumigatus* virulence. *Revista Iberoamericana de Micología*, 22(1), 1–23. [https://doi.org/10.1016/S1130-1406\(05\)70001-2](https://doi.org/10.1016/S1130-1406(05)70001-2)
- Richard, J. L., Dvorak, T. J., & Ross, P. F. (1996). Natural occurrences of gliotoxin in turkeys infected with *Aspergillus fumigatus*, Fresenius. *Mycopathologia*, 134(3), 167–170. <https://doi.org/10.1007/BF00436725>
- Robin, C., Cordonnier, C., Sitbon, K., Raus, N., Lortholary, O., Maury, S., ... Bastuji-Garin, S. (2019). Mainly post-transplant factors are associated with invasive Aspergillosis after allogeneic stem cell transplantation: a study from the surveillance des Aspergilloses invasives en France and société francophone de greffe de moelle et de thérapie cellulaire. *Biology of Blood and Marrow Transplantation*, 25(2), 354–361. <https://doi.org/10.1016/j.bbmt.2018.09.028>
- Rokas, A., Gibbons, J. G., Zhou, X., Beauvais, A., & Latgé, J. P. (2012). The diverse applications of RNA-seq for functional genomic studies in *Aspergillus fumigatus*. *Annals of the New York Academy of Sciences*, 1273(1), 25–34. <https://doi.org/10.1111/j.1749-6632.2012.06755.x>
- Romsdahl, J., & Wang, C. C. C. (2019). Recent advances in the genome mining of: *Aspergillus* secondary metabolites (covering 2012-2018). *MedChemComm*, 10(6), 840–866. <https://doi.org/10.1039/c9md00054b>

Ryckeboer, J., Mergaert, J., Coosemans, J., Deprins, K., & Swings, J. (2003). Microbiological aspects of biowaste during composting in a monitored compost bin. *Journal of Applied Microbiology*, 94(1), 127–137. <https://doi.org/10.1046/j.1365-2672.2003.01800.x>

Salehi, E., Hedayati, M. T., Zoll, J., Rafati, H., Ghasemi, M., Doroudinia, A., ... Fusarium, S. (2016). Discrimination of aspergillosis, mucormycosis, fusariosis, and scedosporiosis in formalin-fixed paraffin-embedded tissue specimens by use of multiple Real-time quantitative PCR assays. *Journal of Clinical Microbiology*, 54(11), 2798–2803. <https://doi.org/10.1128/JCM.01185-16>.

Sambrook, J., & Russell, D. (2001). *Molecular cloning: a laboratory manual*. Cold Spring Harbor (Vol. 1–3).

Samson R., Varga J. 2012. Molecular Systematics of *Aspergillus* and its Teleomorphs. In: *Aspergillus: Molecular Biology and Genomics*. Machida M. & Gomi K (eds). Caister Academic Press. Wymondham, UK. p. 19-40..

Samson, R. A., Hong, S., Peterson, S. W., Frisvad, J. C., & Varga, J. (2007). Polyphasic taxonomy of *Aspergillus* section Fumigati and its teleomorph *Neosartorya*. *Studies in Mycology*, 59, 147–203. <https://doi.org/10.3114/sim.2007.59.14>

Samson, R. A., Visagie, C. M., Houbraken, J., Hong, S. B., Hubka, V., Klaassen, C. H. W., ... Frisvad, J. C. (2014). Phylogeny, identification and nomenclature of the genus *Aspergillus*. *Studies in Mycology*, 78(1), 141–173. <https://doi.org/10.1016/j.simyco.2014.07.004>

Sawanyawisuth, K., Wongkham, C., Pairojkul, C., Saeseow, O. T., Riggins, G. J., Araki, N., & Wongkham, S. (2007). Methionine aminopeptidase 2 over-expressed in cholangiocarcinoma: Potential for drug target. *Acta Oncologica*, 46(3), 378–385. <https://doi.org/10.1080/02841860600871061>

Schaffner, A., Douglas, H., & Braude, A. (1982). Selective protection against conidia by mononuclear and against mycelia by polymorphonuclear phagocytes in resistance to *Aspergillus*. Observations on these two lines of defense in vivo and in vitro with human and mouse phagocytes. *Journal of Clinical Investigation*, 69(3), 617–631. <https://doi.org/10.1172/JCI110489>

Scharf, D. H., Heinekamp, T., Remme, N., Hortschansky, P., Brakhage, A. A., & Hertweck, C. (2012). Biosynthesis and function of gliotoxin in *Aspergillus fumigatus*. *Applied Microbiology and Biotechnology*, 93(2), 467–472. <https://doi.org/10.1007/s00253-011-3689-1>

Schmalzer-Ripcke, J., Sugareva, V., Gebhardt, P., Winkler, R., Kniemeyer, O., Heinekamp, T., & Brakhage, A. A. (2009). Production of pyomelanin, a second type of melanin, via the tyrosine degradation pathway in *Aspergillus fumigatus*. *Applied and Environmental Microbiology*, 75(2), 493–503. <https://doi.org/10.1128/AEM.02077-08>

Schulz, T., Senkpiel, K., & Ohgke, H. (2004). Comparison of the toxicity of reference mycotoxins and spore extracts of common indoor moulds. *International Journal of Hygiene and Environmental Health*, 207, 267–277. <https://doi.org/10.1078/1438-4639-00282>

Scott, J., Sueiro-Olivares, M., Thornton, B. P., Owens, R. A., Muhamadali, H., Fortune-Grant, R., ... Amich, J. (2020). Targeting methionine synthase in a fungal pathogen causes a metabolic imbalance that impacts cell energetics, growth and virulence. *mBio*, 11(5), e01985-20. <https://doi.org/10.1128/mBio.01985-20>.

Scroyen, I., Christiaens, V., & Lijnen, H. R. (2010). Effect of fumagillin on adipocyte differentiation and adipogenesis. *Biochimica et Biophysica Acta - General Subjects*, 1800(4), 425–429. <https://doi.org/10.1016/j.bbagen.2009.11.015>

Seidler, M. J., Salvenmoser, S., & Müller, F. M. C. (2008). *Aspergillus fumigatus* forms biofilms with reduced antifungal drug susceptibility on bronchial epithelial cells. *Antimicrobial Agents and Chemotherapy*, 52(11), 4130–4136. <https://doi.org/10.1128/AAC.00234-08>

Senn, L., Robinson, J. O., Schmidt, S., Knaup, M., Asahi, N., Satomura, S., ... Marchetti, O. (2008). 1,3- β -D-glucan antigenemia for early diagnosis of invasive fungal infections in neutropenic patients with acute leukemia. *Clinical Infectious Diseases*, 46(6), 878–885. <https://doi.org/10.1086/527382>

Seral, C., Michot, J. M., Chanteux, H., Mingeot-Leclercq, M. P., Tulkens, P. M., & Van Bambeke, F. (2003). Influence of p-glycoprotein inhibitors on accumulation of macrolides in J774 murine macrophages. *Antimicrobial Agents and Chemotherapy*, 47(3), 1047–1051. <https://doi.org/10.1128/AAC.47.3.1047-1051.2003>

Seruggia, D., Fernández, A., Cantero, M., Pelczar, P., & Montoliu, L. (2015). Functional validation of mouse tyrosinase non-coding regulatory DNA elements by CRISPR-Cas9-mediated mutagenesis. *Nucleic Acids Research*, 43(10), 4855–4867. <https://doi.org/10.1093/nar/gkv375>

Shankar, J., Tiwari, S., Shishodia, S. K., Gangwar, M., Hoda, S., Thakur, R., & Vijayaraghavan, P. (2018). Molecular insights into development and virulence determinants of *Aspergilli*: a proteomic perspective. *Frontiers in Cellular and Infection Microbiology*, 8(180), 1–15. <https://doi.org/10.3389/fcimb.2018.00180>

Shi, Y. S., Zhang, Y., Chen, X. Z., Zhang, N., & Liu, Y. B. (2015). Metabolites produced by the endophytic fungus *Aspergillus fumigatus* from the stem of *Erythrophloeum fordii* *oliv.* *Molecules*, 20(6), 10793–10799. <https://doi.org/10.3390/molecules200610793>

Shinohara, C., Hasumi, K., & Endo, A. (1993). Inhibition of oxidized low-density lipoprotein metabolism in macrophage J774 by helvolic acid. *Biochimica et Biophysica Acta (BBA)/Lipids and Lipid Metabolism*, 1167(3), 303–306. [https://doi.org/10.1016/0005-2760\(93\)90233-Y](https://doi.org/10.1016/0005-2760(93)90233-Y)

Silva, L. P., Frawley, D., Assis, L. J. de, Tierney, C., Fleming, A. B., Bayram, O., & Goldman, G. H. (2020). Putative membrane receptors contribute to activation and efficient signaling of mitogen-activated protein kinase cascades during adaptation of *Aspergillus fumigatus* to different stressors and carbon sources. *mSphere*, 5, e00818-20. <https://doi.org/10.1128/msphere.00818-20>

Sin, N., Meng, L., Wang, M. Q. W., Wen, J. J., Bornmann, W. G., & Crews, C. M. (1997). The anti-angiogenic agent fumagillin covalently binds and inhibits the methionine aminopeptidase, MetAP-2. *Proceedings of the National Academy of Sciences of the United States of America*, 94(12), 6099–6103. <https://doi.org/10.1073/pnas.94.12.6099>

Singh, B., Oellerich, M., Kumar, R., Kumar, M., Bhadoria, D. P., Reichard, U., ... Asif, A. R. (2010). Immuno-reactive molecules identified from the secreted proteome of *Aspergillus fumigatus*. *Journal of Proteome Research*, 9(11), 5517–5529. <https://doi.org/10.1021/pr100604x>

Singh, N., & Paterson, D. L. (2005). *Aspergillus* infections in transplant recipients. *Clinical Microbiology Reviews*, 18(1), 44–69. <https://doi.org/10.1128/CMR.18.1.44-69.2005>

Slesiona, S., Gressler, M., Mihlan, M., Zaehle, C., Schaller, M., Barz, D., ... Brock, M. (2012). Persistence versus escape: *Aspergillus terreus* and *Aspergillus fumigatus* employ different strategies during interactions with macrophages. *PLoS ONE*, 7(2), e31223. <https://doi.org/10.1371/journal.pone.0031223>

Souza, A. C. O., Al Abdallah, Q., DeJarnette, K., Martin-Vicente, A., Nywening, A. V., DeJarnette, C., ... Fortwendel, J. R. (2019). Differential requirements of protein geranylgeranylation for the virulence of human pathogenic fungi. *Virulence*, 10(1), 511–526. <https://doi.org/10.1080/21505594.2019.1620063>

Stanzani, M., Orciuolo, E., Lewis, R., Kontoyiannis, D. P., Martins, S. L. R., St. John, L. S., & Komanduri, K. V. (2005). *Aspergillus fumigatus* suppresses the human cellular immune response via gliotoxin-mediated apoptosis of monocytes. *Blood*, 105(6), 2258–2265. <https://doi.org/10.1182/blood-2004-09-3421>

Sueiro-Olivares, M., Fernandez-Molina, J. V., Abad-Diaz-De-Cerio, A., Gorospe, E., Pascual, E., Gुरुceaga, X., ... Rementeria, A. (2015). *Aspergillus fumigatus* transcriptome response to a higher temperature during the earliest steps of germination monitored using a new customized expression microarray. *Microbiology*, 161(3), 490–502. <https://doi.org/10.1099/mic.0.000021>

Sugui, J. A., Kim, H. S., Zarembek, K. A., Chang, Y. C., Gallin, J. I., Nierman, W. C., & Kwon-Chung, K. J. (2008). Genes differentially expressed in conidia and hyphae of *Aspergillus fumigatus* upon exposure to human neutrophils. *PLoS ONE*, 3(7), e2655. <https://doi.org/10.1371/journal.pone.0002655>

Swilaiman, S. S., O'gorman, C. M., Du, W., Sugui, J. A., Del Buono, J., Brock, M., ... Dyer, P. S. (2020). Global sexual fertility in the opportunistic pathogen *Aspergillus fumigatus* and identification of new supermater strains. *Journal of Fungi*, 6(4), 1–17. <https://doi.org/10.3390/jof6040258>

Taheri-Talesh, N., Horio, T., Araujo-Bazám, L., Dou, X., Espeso, E. A., Peñalva, M. A., ... Oakley, B. R. (2008). The tip growth apparatus of *Aspergillus nidulans*. *Molecular Biology of the Cell*, 19(4), 1439–1449. <https://doi.org/10.1091/mbc.E07-05-0464>

Taylor, J. W. (2011). One Fungus = One Name: DNA and fungal nomenclature twenty years after PCR. *IMA Fungus*, 2(2), 113–120. <https://doi.org/10.5598/imafungus.2011.02.02.01>

Tekaia, F., & Latgé, J. P. (2005). *Aspergillus fumigatus*: saprophyte or pathogen? *Current Opinion in Microbiology*, 8(4), 385–392. <https://doi.org/10.1016/j.mib.2005.06.017>

Thanh, N. V., Rombouts, F. M., & Nout, M. J. R. (2005). Effect of individual amino acids and glucose on activation and germination of *Rhizopus oligosporus* sporangiospores in tempe starter. *Journal of Applied Microbiology*, 99(5), 1204–1214. <https://doi.org/10.1111/j.1365-2672.2005.02692.x>

Thau, N., Monod, M., Crestani, B., Rolland, C., Tronchin, G., Latge, J. P., & Paris, S. (1994). Rodletless mutants of *Aspergillus fumigatus*. *Infection and Immunity*, 62(10), 4380–4388. <https://doi.org/10.1128/iai.62.10.4380-4388.1994>

Toledo, A. V., Emilio, M., Franco, E., Marianela, S., Lopez, Y., Troncozo, M. I., ... Balatti, P. A. (2017). Melanins in fungi: Types, localization and putative biological roles. *Physiological and Molecular Plant Pathology*, 99, 2–6. <https://doi.org/10.1016/j.pmpp.2017.04.004>

Torelli, R., Sanguinetti, M., Moody, A., Pagano, L., Caira, M., De Carolis, E., ... Posteraro, B. (2011). Diagnosis of invasive aspergillosis by a commercial real-time PCR assay for *Aspergillus* DNA in bronchoalveolar lavage fluid samples from high-risk patients compared to a galactomannan enzyme immunoassay. *Journal of Clinical Microbiology*, 49(12), 4273–4278. <https://doi.org/10.1128/JCM.05026-11>

Tsai, H. F., Chang, Y. C., Washburn, R. G., Wheeler, M. H., & Kwon-Chung, K. J. (1998). The developmentally regulated *alb1* gene of *Aspergillus fumigatus*: its role in modulation of conidial morphology and virulence. *Journal of Bacteriology*, 180(12), 3031–3038. <https://doi.org/10.1128/jb.180.12.3031-3038.1998>

Tsai, H. F., Washburn, R. G., Chang, Y. C., & Kwon-Chung, K. J. (1997). *Aspergillus fumigatus* *arp1* modulates conidial pigmentation and complement deposition. *Molecular Microbiology*, 26(1), 175–183. <https://doi.org/10.1046/j.1365-2958.1997.5681921.x>

- Tsunawaki, S., Yoshida, L. S., Nishida, S., Kobayashi, T., & Shimoyama, T. (2004). Fungal metabolite gliotoxin inhibits assembly of the human respiratory burst NADPH oxidase. *Infection and Immunity*, 72(6), 3373–3382. <https://doi.org/10.1128/IAI.72.6.3373-3382.2004>
- Ullmann, A. J., Lipton, J. H., Vesole, D. H., Chadrusekar, P., Langston, A., Tarantolo, S. R., ... Durrant, S. (2007). Posaconazole or fluconazole for prophylaxis in severe graft-versus-host disease. *The New England Journal of Medicine*, 356(4), 335–347. <https://doi.org/10.1056/NEJMoa1513614>
- Umeyama, T., Hayashi, Y., Shimosaka, H., Inukai, T., Yamagoe, S., Takatsuka, S., ... Miyazaki, Y. (2018). CRISPR/Cas9 genome editing to demonstrate the contribution of Cyp51A Gly138Ser to azole resistance in *Aspergillus fumigatus*. *Antimicrobial Agents and Chemotherapy*, 62(9), 1–16. <https://doi.org/10.1128/AAC.00894-18>
- Vacher, G., Niculita-Hirzel, H., & Roger, T. (2015). Immune responses to airborne fungi and non-invasive airway diseases. *Seminars in Immunopathology*, 37(2), 83–96. <https://doi.org/10.1007/s00281-014-0471-3>
- Valiante, V., Heinekamp, T., Jain, R., Härtl, A., & Brakhage, A. A. (2008). The mitogen-activated protein kinase MpkA of *Aspergillus fumigatus* regulates cell wall signaling and oxidative stress response. *Fungal Genetics and Biology*, 45, 618–627. <https://doi.org/10.1016/j.fgb.2007.09.006>
- Valiante, V., Jain, R., Heinekamp, T., & Brakhage, A. A. (2009). The MpkA MAP kinase module regulates cell wall integrity signaling and pyomelanin formation in *Aspergillus fumigatus*. *Fungal Genetics and Biology*, 46, 909–918. <https://doi.org/10.1016/j.fgb.2009.08.005>
- Valsecchi, I., Dupres, V., Stephen-Victor, E., Guijarro, J. I., Gibbons, J., Beau, R., ... Beauvais, A. (2017). Role of hydrophobins in *Aspergillus fumigatus*. *Journal of Fungi*, 4(2), 1–19. <https://doi.org/10.3390/jof4010002>
- Valsecchi, I., Lai, J. I., Stephen-Victor, E., Pillé, A., Beaussart, A., Lo, V., ... Latgé, J. P. (2019). Assembly and disassembly of *Aspergillus fumigatus* conidial rodlets. *The Cell Surface*, 6(5), 100023. <https://doi.org/10.1016/j.tcs.2019.100023>
- Valsecchi, I., Stephen-Victor, E., Wong, S. S. W., Karnam, A., Sunde, M., Guijarro, J. I., ... Aïmanianda, V. (2020). The role of RodA-conserved cysteine residues in the *Aspergillus fumigatus* conidial surface organization. *Journal of Fungi*, 6(3), 151. <https://doi.org/10.3390/jof6030151>
- Van De Veerdonk, F. L., Gresnigt, M. S., Romani, L., Netea, M. G., & Latgé, J. P. (2017). *Aspergillus fumigatus* morphology and dynamic host interactions. *Nature Reviews Microbiology*, 15(11), 661–674. <https://doi.org/10.1038/nrmicro.2017.90>

Van Keulen, S. C., & Rothlisberger, U. (2017). Effect of N-terminal myristoylation on the active conformation of Gai1-GTP. *Biochemistry*, 56(1), 271–280. <https://doi.org/10.1021/acs.biochem.6b00388>

Van Leeuwen, M. R., Smant, W., de Boer, W., & Dijksterhuis, J. (2008). Filipin is a reliable in situ marker of ergosterol in the plasma membrane of germinating conidia (spores) of *Penicillium discolor* and stains intensively at the site of germ tube formation. *Journal of Microbiological Methods*, 74(2–3), 64–73. <https://doi.org/10.1016/j.mimet.2008.04.001>

Van Leeuwen, M. R., Van Doorn, T. M., Golovina, E. A., Stark, J., & Dijksterhuis, J. (2010). Water- and air-distributed conidia differ in sterol content and cytoplasmic microviscosity. *Applied and Environmental Microbiology*, 76(1), 366–369. <https://doi.org/10.1128/AEM.01632-09>

Venkatesh, N., & Keller, N. P. (2019). Mycotoxins in conversation with bacteria and fungi. *Frontiers in Microbiology*, 10, 1–10. <https://doi.org/10.3389/fmicb.2019.00403>

Vetro, J.A.; Dummitt, B.; Chang, Y.H. (2004) Methionine-aminopeptidase: Emerging role in angiogenesis. In *Aminopeptidases in Biology and Disease*; Hooper, N.M., Lendeckel, U., Eds.; Kluwer Academic/Plenum Publishers: New York, NY, USA; pp. 17–44

Vidal-Acuña, M. R., Ruiz, M., Torres, M. J., & Aznar, J. (2018). Prevalence and in vitro antifungal susceptibility of cryptic species of the genus *Aspergillus* isolated in clinical samples. *Enfermedades Infecciosas y Microbiología Clínica*, 37(5), 296–300. <https://doi.org/10.1016/j.eimc.2018.07.010>

Virginio, E. D., Kubitschek-Barreira, P. H., Vieira Batista, M., Schirmer, M. R., Abdelhay, E., Shikanai-Yasuda, M. A., & Lopes-Bezerra, L. M. (2014). Immunoproteome of *Aspergillus fumigatus* using sera of patients with Invasive Aspergillosis. *International Journal Molecular Sciences*, 15(8), 14505–14530. <https://doi.org/10.3390/ijms150814505>

Viscoli, C., Herbrecht, R., Akan, H., Baila, L., Sonet, A., Gallamini, A., ... Maertens, J. (2009). An EORTC phase II study of caspofungin as first-line therapy of invasive aspergillosis in haematological patients. *Journal of Antimicrobial Chemotherapy*, 64(6), 1274–1281. <https://doi.org/10.1093/jac/dkp355>

Voltersen, V., Blango, M. G., Herrmann, S., Schmidt, F., Heinekamp, T., Strassburger, M., ... Brakhage, A. A. (2018). Proteome analysis reveals the conidial surface protein CcpA essential for virulence of the pathogenic fungus *Aspergillus fumigatus*. *mBio*, 9(5), e01557-18. <https://doi.org/10.1128/mBio.01557-18>

Walker, K. W., & Bradshaw, R. A. (1999). Yeast methionine aminopeptidase I Alterations of substrate specificity by site-directed mutagenesis. *Journal of Biological Chemistry*, 274(19), 13403–13409. <https://doi.org/10.1074/jbc.274.19.13403>

Wallwey, C., Matuschek, M., & Li, S. M. (2010). Ergot alkaloid biosynthesis in *Aspergillus fumigatus*: Conversion of chanoclavine-I to chanoclavine-I aldehyde catalyzed by a short-chain alcohol dehydrogenase FgaDH. *Archives of Microbiology*, 192(2), 127–134. <https://doi.org/10.1007/s00203-009-0536-1>

Wang, Z., Gerstein, M., & Snyder, M. (2009). RNA-Seq: a revolutionary tool for transcriptomics. *Nature Reviews*, 10(1), 57–63. <https://doi.org/10.1038/nrg2484>.

Ward, C. L., Dempsey, M. H., Ring, C. J. A., Kempson, R. E., Zhang, L., Gor, D., ... Tisdale, M. (2004). Design and performance testing of quantitative real time PCR assays for *Influenza A* and *B* viral load measurement. *Journal of Clinical Virology*, 29(3), 179–188. [https://doi.org/10.1016/S1386-6532\(03\)00122-7](https://doi.org/10.1016/S1386-6532(03)00122-7)

Watanabe, A., Kamei, K., Sekine, T., Waku, M., Nishimura, K., Miyaji, M., ... Kuriyama, T. (2004). Effect of aeration on gliotoxin production by *Aspergillus fumigatus* in its culture filtrate. *Mycopathologia*, 157(1), 245–254. <https://doi.org/10.1023/B:MYCO.0000012224.49131.dd>

Watanabe, N., Nishihara, Y., Yamaguchi, T., Koito, A., Miyoshi, H., Kakeya, H., & Osada, H. (2006). Fumagillin suppresses HIV-1 infection of macrophages through the inhibition of Vpr activity. *FEBS Letters*, 580(11), 2598–2602. <https://doi.org/10.1016/j.febslet.2006.04.007>

Webster, T. C. (1994). Fumagillin affects *Nosema apis* and honey bees (*Hymenoptera: Apidae*). *Journal of Economic Entomology*, 87(3), 601–604. <https://doi.org/10.1093/jee/87.3.601>

Wéry, N. (2014). Bioaerosols from composting facilities—a review. *Frontiers in Cellular and Infection Microbiology*, 4(42), 1–9. <https://doi.org/10.3389/fcimb.2014.00042>

Wheat, L. J., & Walsh, T. J. (2008). Diagnosis of invasive aspergillosis by galactomannan antigenemia detection using an enzyme immunoassay. *European Journal of Clinical Microbiology and Infectious Diseases*, 27(4), 245–251. <https://doi.org/10.1007/s10096-007-0437-7>

White, P. L., Barnes, R. A., Springer, J., Klingspor, L., Cuenca-Estrella, M., Morton, C. O., ... Loeffler, J. (2015). Clinical performance of *Aspergillus* PCR for testing serum and plasma: a study by the European *Aspergillus* PCR initiative. *Journal of Clinical Microbiology*, 53, 2832–2837. <https://doi.org/10.1128/JCM.00905-15>

Whitworth, K. M., Lee, K., Benne, J. A., Beaton, B. P., Spate, L. D., Murphy, S. L., ... Prather, R. S. (2014). Use of the CRISPR/Cas9 system to produce genetically engineered pigs from *in vitro*-derived oocytes and embryos. *Biology of Reproduction*, 91(3), 1–13. <https://doi.org/10.1095/biolreprod.114.121723>

Wiemann, P., Guo, C. J., Palmer, J. M., Sekonyela, R., Wang, C. C. C., & Keller, N. P. (2013). Prototype of an intertwined secondary-metabolite supercluster. *Proceedings*

of the National Academy of Sciences of the United States of America, 110(42), 17065–17070. <https://doi.org/10.1073/pnas.1313258110>

Wiemann, P., Lechner, B. E., Baccile, J. A., Velk, T. A., Yin, W. B., Bok, J. W., ... Keller, N. P. (2014). Perturbations in small molecule synthesis uncovers an iron-responsive secondary metabolite network in *Aspergillus fumigatus*. *Frontiers in Microbiology*, 5(530), 1-16. <https://doi.org/10.3389/fmicb.2014.00530>

Williams, G. R., Sampson, M. A., Shutler, D., & Rogers, R. E. L. (2008). Does fumagillin control the recently detected invasive parasite *Nosema ceranae* in western honeybees (*Apis mellifera*)? *Journal of Invertebrate Pathology*, 99(3), 342–344. <https://doi.org/10.1016/j.jip.2008.04.005>

Wood, P. J. (1980). Specificity in the interaction of direct dyes with polysaccharides. *Carbohydrate Research*, 85, 271–287. [https://doi.org/10.1016/S0008-6215\(00\)84676-5](https://doi.org/10.1016/S0008-6215(00)84676-5)

Wuren, T., Toyotome, T., Yamaguchi, M., Takahashi-Nakaguchi, A., Muraosa, Y., Yahiro, M., ... Kamei, K. (2014). Effect of serum components on biofilm formation by *Aspergillus fumigatus* and other *Aspergillus* species. *Japanese Journal of Infectious Diseases*, 67, 172–179. <https://doi.org/10.7883/yoken.67.172>

Yamada, A., Kataoka, T., & Nagai, K. (2000). The fungal metabolite gliotoxin: immunosuppressive activity on CTL-mediated cytotoxicity. *Immunology Letters*, 71(1), 27–32. [https://doi.org/10.1016/S0165-2478\(99\)00155-8](https://doi.org/10.1016/S0165-2478(99)00155-8)

Yamazaki, M., Fujimoto, H., & Kawasaki, T. (1980). Chemistry of tremorogenic metabolites: I. Fumitremorgin A from *Aspergillus fumigatus*. *Chemical Pharmaceutical Bulletin*, 28(43), 2091.

Yokota, K., Kamaguchi, A., & Sakaguchi, O. (1977). Studies on the toxin of *Aspergillus fumigatus*. VII Purification and some properties of hemolytic toxin (Asp-Hemolysin) from culture filtrates and mycelia. *Microbiology and Immunology*, 21(1), 11–22. <https://doi.org/10.1111/j.1348-0421.1977.tb02803.x>

Yoshida, S., Ono, M., Shono, T., Izumi, H., Ishibashi, T., Suzuki, H., & Kuwano, M. (1997). Involvement of Interleukin-8, vascular endothelial growth factor, and basic fibroblast growth factor in tumor necrosis factor alpha-dependent angiogenesis. *Molecular and Cellular Biology*, 17(7), 4015–4023. <https://doi.org/10.1128/MCB.17.7.4015>

Youngchim, S., Hay, R. J., & Hamilton, A. J. (2005). Melanization of *Penicillium marneffeii* in vitro and in vivo. *Microbiology*, 151(1), 291–299. <https://doi.org/10.1099/mic.0.27433-0>

Zaas, A. K. and B. D. Alexander, (2009) Invasive Pulmonary Aspergillosis. In: *Aspergillus fumigatus* and aspergillosis. J.P. Latgé and Steinbach, W.J. (eds). Washington DC: ASM press, p. 293-299.

Zhang, P., Nicholson, D. E., Bujnicki, J. M., Su, X., Brendle, J. J., Ferdig, M., ... Chiang, P. K. (2002). Angiogenesis inhibitors specific for methionine aminopeptidase 2 as drugs for malaria and leishmaniasis. *Journal of Biomedical Science*, 9(1), 34–40. <https://doi.org/10.1159/000048197>

Zhou, G. C., Liu, F., Wan, J., Wang, J., Wang, D., Wei, P., & Ouyang, P. (2013). Design, synthesis and evaluation of a cellular stable and detectable biotinylated fumagillin probe and investigation of cell permeability of fumagillin and its analogs to endothelial and cancer cells. *European Journal of Medicinal Chemistry*, 70, 631–639. <https://doi.org/10.1016/j.ejmech.2013.10.033>

Zmeili, O. S., & Soubani, A. O. (2007). Pulmonary aspergillosis: a clinical update. *QJM an International Journal of Medicine*, 100(6), 317–334. <https://doi.org/10.1093/qjmed/hcm035>